UNIVERSITAT
RAMON LLULL

Biotechnological production of polyunsaturated fatty acids omega-3 by heterotrophic microalgae

Sergi Abad Sánchez

http://hdl.handle.net/10803/400556

UNIVERSITAT
RAMON LLULL

DOCTORAL THESIS

Title	**Biotechnological production of omega-3 polyunsaturated fatty acids by heterotrophic microalgae.**
Presented by	**Sergi Abad Sánchez**
Centre	**IQS School of Engineering**
Department	**Bioengineering**
Directed by	**Dr. Xavier Turon Casalprim and Dr. Antoni Planas Sauter**

To all my family, especially

Yolanda, Agustí, Albert and Gabriela.

It is during our darkest moments

that we must focus to see the light.

Aristo Onassis

Abstract

This dissertation describes the development of a biotechnological process to obtain polyunsaturated fatty acids (PUFA) by heterotrophic microalgae. The selected heterotrophic microorganism was *Aurantiochytrium limacinum* SR21 due to its capacity to produce PUFA, grow with different carbon sources and tolerate high salinity. During the thesis investigation diverse analytical methods have been developed in order to monitor *A. limacinum* growth. Moreover, different experimental design strategies/tools, such us Taguchi orthogonal matrices, Artificial neural network, Response surface methodology, etc. have been used to develop a growth medium specifically optimized for *A. limacinum*. Instead of using traditional carbon sources, the process has been developed to grow *A. limacinum* with crude glycerol, an industrial by-product.

The same experimental design tools served to find the best oxygen supply conditions to stimulate either biomass or DHA production. Batch, fed-batch, continuous and multi-stage continuous bioreactors have been studied to find the most prolific strategy. Batch and Fed-batch reactor generated the highest DHA yields. However, continuous cultivations produced higher DHA productivity values, especially the multi-stage strategy. In a multi-stage continuous bioreactor, the first tank/s were dedicated to biomass production whereas the following tanks were set to stimulate DHA production.

DHA products currently in market are formulated as DHA methyl esters or re-esterified triglycerides, but not as unmodified triglycerides. In this thesis, an approach for preparative and process scale chromatography purification of unmodified triglycerides containing DHA has been developed.

Preface

This thesis marks the completion of 4 years of research, which included more than 7000 hours of cultivation and several litres of an artificial seawater medium, all for the sake of Biotechnology. This report will explain the full development of bioprocess engineering, including the development of analytical chemistry, the production process and the purification steps required. The knowledge recorded in the following pages will explain the very best way (to the best knowledge of the author), to produce a common bioproduct while seeking sustainability at every step. Sustainability is not a new idea; however, it is necessary for future generations who will require individual complex solutions such as the one presented in this dissertation. Although this may not be a definitive solution, it is hoped that this work will stimulate further research that will produce even better solutions in biotechnology and similar fields.

This thesis has been written not only to document the research but also to help new bioprocess engineering students/researchers in the *bioengineering department*, of *Institut Químic de Sarrià*. The chapters of this thesis will explain many different tools, modelling and statistical techniques that have been applied during different phases of the research process. Conducting this research and writing this thesis has also offered the author many opportunities for professional and personal scientific growth. Every important technique has been introduced in the correspondingly applied chapter. Therefore, it might be advisable to read this thesis as a linear story for better understanding.

Table of contents

8

List of tables

List of figures

13

14

15

Acknowledgements

Firstly, I would like to express my sincere gratitude to my advisors Dr. Xavier Turon and Dr. Antoni Planas for the continuous support of my Ph.D study and related research, for their patience, motivation, and immense knowledge. Their guidance helped me in all the time of research and writing of this thesis. Thank you for believing in me and accepting me as a Ph.D student.

Besides my advisor, I would like to thank Dr. Gary Gilleskie for the opportunity to work in BTEC, for encouraging my research and for allowing me to grow as a research scientist during my days in North Caroline. I would specially like to thank Dr. Nathaniel Henz and Mr. Brian Mosley for a very great time in your laboratory. Thank you all for showing me all the "goodies" from Raleigh.

I thank my fellow labmates and TFM/Master students from Bioengineering department. In particular, to Cristina, Victoria, Carles, Hugo, Javi and Estela for the stimulating discussions, for the long days we were working together before deadlines, and for all the fun we have had in the last four years. Also I thank my friends from Caldes and Sant Feliu.

My sincere thanks also goes to Josep M Minguell, Jaume Lope, Gustau Garcia and all my colleagues from BIOCON. After more than one year working in BIOCON, I keep learning from you every single day.

Last but not the least, I would like to thank my family: my parents, my brother and Gabriela for supporting me spiritually throughout writing this thesis and my life in general. You mean everything to me. Mom thank you, with your fight you gave me the most valuable lesson. Never give up. I would like to express my sincere gratitude to Carol and her family, for helping me during my mom long fight and giving me some time to finish this work.

Finally, thanks to you, reader. If you are reading this line after the others, you have at least read one page of my thesis. Thank You.

This page intentionally left blank

Chapter 1: Introducing to a New Biotechnological Process

Bioprocess Engineering and bioseparation

1.1   Introduction to a bioprocess

The role of bioprocess engineering in biotechnology

Biotechnology involves environmental resource adaptation to meet human needs, involving food, beverages and medicines. Biotechnology has been used for millennia to make bread and beer, and mouldy soybean curd was used 5000 years ago to treat skin infections in China [1]. It is currently a science that is full of potential and that embodies the future of mankind. Biotechnology has faced the deadliest illnesses, it is used in the fight to satisfy the world's food demands and it has offered innovation for countless industrial processes. However, the benefits of biotechnology could not be a reality without bioprocess engineering and bioseparation engineering. These disciplines define the two main blocks of productive biotechnology, without which the creation and purification of biotechnologically derived products would not be possible on a large scale (Box 1 shows an historical example). The aforementioned, derived products can be classified as biopharmaceuticals; including all molecules with therapeutic value and bioproducts; including non-pharmaceutical products such as nutritional supplements, biofuels, biocatalysts for industry, building blocks for biodegradable products, etc. In this thesis, an innovative, biotechnological production of an existing bioproduct will be proposed.

> **Box 1.1. Human insulin production**
>
> The discovery of the insulin potential, and the expression of the insulin gene in bacteria is an historical achievement of general biotechnology. The first marketed recombinant human insulin was marketed by Lilly in 1982. It required 31 major processing steps. Bioprocess engineering allows this process to be done in 10 steps making it more cost effective and accessible to patients around the world.

21

With nine calories per gram compared to proteins and carbohydrates that have four calories per gram, lipids were traditionally considered to have a negative impact on human health. Currently, lipids are seen as compounds that are essential for human health but it is now known that they are more intricate than simply good vs. bad. Although omega fatty acids families are a small part of the complex world of lipids, they are an important asset for the human diet and are only abundant in certain foods. With omega-3, omega-6 and omega-9 variations, only 3 and 6 are essential. Omega-9 can be produced by the human body[2]. On the other hand, omega-6 fatty acids are present in many vegetable-based foods and omega-3 is only available from flaxseed, walnuts and fish. Nevertheless, long chain polyunsaturated fatty acids omega-3s (n-3 long chain PUFA) such as docosahexaenoic (DHA) and eicosapentaenoic (EPA) acid are mainly introduced into the diet through fish [3]. Being among the scarcer fatty acids in nature, their health benefits are claimed to be diverse and orientated against many human disorders. Omega-3 fatty acid supplement products are obtained from a diverse range of sources, with fish oil as the traditional commercial source.

However, fish oil is susceptible to contamination with lipophilic organic chemicals that are now ubiquitous contaminants of marine ecosystems [4]. The increasing market demand for contaminant-free and concentrated omega-3 products has led to the search for new sources and development of new processes for the production of omega-3 fatty acids. Marine microorganisms and transgenic plants are potential sustainable sources of contaminant-free n-3

long chain PUFA [5–8]. It is for this reason that bioprocess engineering must find a cost effective and ecologically responsible way to produce contaminant-free, concentrated n-3 long chain PUFA. Currently, the most productive of these alternative options is the use of heterotrophic marine microorganisms as a source of n-3 long chain PUFA [8,9], which offer the potential for increased productivity. The fish oil industry is well developed with lower costs than the aforementioned alternatives but the purification from contaminants has a negative impact on the cost of the process. Despite purification, commercial products are still highly contaminated [10,11] and may not be suitable for long-term human consumption.

Supplementation with fish oils may impair a person's subsequent metabolic ability to convert α-linolenic acid (ALA) to EPA [4,12]. ALA is present in many vegetable oils and is more abundant than EPA and DHA. In light of this fact, DHA is considered the most valued and scarcer of the n-3 PUFA, which can be produced by marine microorganisms. In general, heterotrophic microorganisms offer increased productivity due to higher growth rates when compared to autotrophic microalgae. *Thraustochytrids*, a cluster of eukaryotic heterotrophic marine microorganisms, have a fatty acid profile that is rich in DHA commonly accounting for 20 to 40% of total fatty acids. Depending on the strain, they might accumulate low amounts of arachidonic acid (AA), EPA [13] and other PUFA [14–17]. Thraustochytrids allow the substitution of a traditional carbon source (glucose), for cheaper sources (i.e. glycerol, crude glycerol, molasses, whey and food waste, etc.), which would have a positive impact on the economics of the bioprocess. Cost reduction for growth media with minimal undesired effects is crucial for a potential industrial implementation.

A complete bioprocess for the production and purification of DHA through *A. limacinum* cultures using glycerol as a carbon source will be described in this dissertation. This process has been fully developed, taking into consideration the large-scale production implications, and has established the basic knowledge regarding Thraustochytrids cultivation. New analytical methodologies have been designed to carry out the upstream and downstream steps of this process. Researchers in this dissertation put forth significant effort to develop a cost effective media and adjust culture parameters while maintaining productivity. The main bioprocess strategies (batch, fed-batch and continuous) have been investigated to elucidate the most prolific operation mode. The fully developed biotechnological process can serve as an approach for the production of other added-value metabolites such as natural pigments, organic acids and squalene. In fact, part of the presented research was focused on the purification of these other molecules.

Bioprocess engineering allows the production of DHA, other fatty acids, pigments, organic acids and squalene in an alternative biotechnological way, avoiding lipophilic contaminants. Products obtained through the developed process are not dependent on the seasons or the annual fluctuations of fish oil production. In addition, photosynthetic equipment is not required. On the other hand, bioseparation technologies allow the purification of DHA and astaxanthin on a large scale as described in many procedures, as either ethyl esters, phospholipids or re-esterified

triglycerides. Moreover, in the work presented here, an approach to purify unmodified triglycerides[1] directly from thraustochytrids is presented.

1.2 Motivation for the project
Valorisation of crude glycerol while avoiding Omega-3 contaminants

This project originally sought a way to valorise the crude glycerol excess that was experienced during 2008-2011. Glycerol is the main by-product of the conversion of vegetable oils (generally) into biodiesel. The progressive increase of biodiesel production has in turn caused a sudden increase in crude glycerol. After the transesterification reaction that is performed to produce biodiesel[2], roughly 10% of the feedstock was converted into glycerol [18–20]. The total EU27 biodiesel production for 2010 was over 21 million metric tons. Between 2009 and 2010, a production increase of 233% was achieved. The steady annual increase of biodiesel production in Europe, as well as in America and Asia, caused a sudden increase in the generation of crude glycerol. Between 2003 and 2010, biodiesel experienced a dramatic, worldwide annual growth in consumption as well. Studies showed an increase of 39% per year, as illustrated in Figure 1.1. Thus, any possible valorisation of crude glycerol, raising the value of the current biodiesel product, might have a notable contribution. The viability of biodiesel without subsidies is doubtful with the current world economic situation [21].

23

Traditionally glycerol was purified to a technical grade or pharma-grade (pure) glycerol depending to the contaminants removed. However, according to the feedstock and the process used to produce biodiesel, crude glycerol has different compounds that are considered
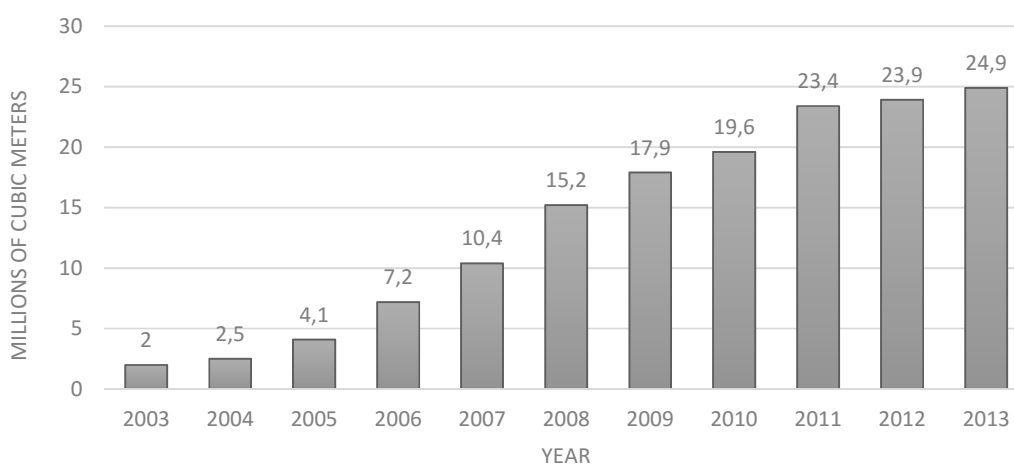
Figure 1.1. Evolution of world consumption of biodiesel in millions of cubic meters.

---

[1] Currently marketed Triglycerides (TG) are in fact re-esterified triglycerides. Their moieties were previously modified to be purified, and were then enzymatically re-esterified into TGs.
[2] Reaction performed to produce biodiesel from natural residues.

contaminants. The most common contaminants are methanol and soap [20,21], but a high salinity content is also typically present due to the catalyst used in the process. Purified glycerol was primarily used in the pharmaceutical, food or cosmetic industries, however the cost of purification at such a large scale makes its utilization economically unviable [22,23]. As a consequence, tons of raw glycerol needed to be valorised, which lowered the production costs of different transformation opportunities due to its low cost per Kg.

Since purified glycerol is a commercially available chemical that has thousands of potential uses, crude glycerol presents great opportunities for new applications. Recently, the possibility of using crude glycerol in feed has been investigated because of the increase in the price of corn [24]. Nevertheless, **chemicals produced via biological conversion** or through conventional catalytic conversion offer the largest number of potential applications.

For example, Himmi *et al. (1998)* [25] studied batch fermentations using *Clostridium butyricum* to produce 1,3-propanediol. *C. butyricum* F2b was found to be suitable for waste glycerol conversion; yielding 0.50 g of 1,3-propanediol per gram of glycerol. Later, studies using *Klebsiella pneumoniae* obtained a yield of 0.86 g 1,3-propanediol per gram of glycerol. Additionally, Cardona *et al.* [26] observed a 1,3- propanediol production by *K. pneumoniae* in aerobic and anaerobic conditions yielding 0.51 g/g and 0.52 g/g, respectively. 1,3-propanediol is used in composite materials, adhesives, laminates, powder and UV-cured coatings, mouldings, novel aliphatic polyesters, co-polyesters, solvents, and anti-freeze [27]. Therefore, it has a great potential to absorb a large amount of the crude glycerol. Another example includes dihydroxyacetone, which is a simple three-carbon sugar that is non-toxic, and is used in the cosmetics industry. Immobilized *Acetobacter xylinum* A-9 is used to oxidize glycerol to dihydroxyacetone [28]. This added-value metabolite is synthesized by *Gluconobacter oxydans* using glycerol as the carbon source [29,30]. Another possibility is the production of succinic acid. It is typically used to obtain synthetic resins, biodegradable polymers and as an intermediate for chemical synthesis. This could be produced by the fermentation of *Actinobacillus succinogenes, Basfia succinoproducens* and *Anaerobiospirillum* sp. in which a maximum yield of 1.33 g of succinic acid per gram of glycerol is obtained [31]. Citric acid was satisfactorily produced by acetate mutants of *Yarrowia lipolytica* reaching concentrations of 139 g/L of product. Crude-glycerol growth media has also been used to produce pigments such as β-carotene. For example, *Blakeslea trispora* [32] showed a yield of 15 mg β-carotene per gram of biomass. Another widely used food supplement is the cyanobacteria *Spirulina platensis*[3], which has been shown to successfully grow on crude glycerol based media [33]. Polyhydroxyalkanoates are the last example. They represent a complex class of naturally occurring bacterial polyesters that have been recognized as good substitutes for non-biodegradable petroleum derived polymers. *Cupriavidus necator* DSM 545 was used to accumulate poly (3-hydroxybutyrate) (P(3HB)) with a final productivity of 0.84 gPHB / L· h.

---

[3] This is a cyanobacteria that can be consumed by animals and humans either as a dietary supplement or as a whole food.

Table 1.1 shows products that have been obtained via the biological conversion of crude glycerol and their market values. Undoubtedly, PUFA are the most valuable molecules derived from crude glycerol and could be the key to biodiesel viability. There are many works that discuss the production of different PUFA by using diverse microorganisms growing on crude glycerol as carbon sources. *Crypthecodinium cohnii* and *Nitzschia closterium* are known for their ability to accumulate lipids, especially DHA [13,34–36]. Other strong PUFA producer microorganisms are *Skelotema costatum*, *Pythium ultimum*, *Pythium irregulare*, *Mortiriella alpine*, *Nannochloropsis salina* and various species of *Codium* sp. [35,37–44], among many other marine microorganisms. However, there is a family of marine eukaryotic microorganisms with an extraordinary PUFA accumulation capacity, eclipsing all others.

In 1969, the special fingerprint of a marine microorganism cluster in terms of the fatty acid profile and DHA content had already been highlighted by Ellenbogen *et al*. (1969) [45]. This cluster was

Table 1.1 Summary of all components produced by biological transformation of crude glycerol. Price calculations are made from Sigma-Aldrich considering the same purity (97 % - 98%) and the smallest quantity for each product between 2009 and 2011.It is evident that the prices shown are not representative of large scale suppliers. However, it shows the difference of value between each

Product	Price (€/g)
1,3-propanediol	0.302
dihydroxyacetone	55.3
Succinic acid	0.1648
Citric acid	5.8
ß-carotene	16.92
EPA	1860
DHA	1670
poly (3-hydroxybutyrate)	10.5

the Thraustochytrids family. It belongs to Labyrinthumycetes, of the kingdom of Chromista (also known as Straminopila). Thraustochytrids are heterotrophic marine protists phylogenetically considered microalgae. In the last decade, researchers have become aware of its potential to lead to new biotechnological applications [34,46–48].

Thraustochytrids produce significant amounts of DHA. Their high ratio of DHA, combined with lower amounts of structurally related PUFA (compared to other species) simplifies the separation and purification processes [49,50]. The potential for PUFA production, especially n-3 PUFA, with this family of microorganisms was incontestable. Many thraustochytrid strains accumulate considerable amounts of triacylglycerides with a high proportion of long chain PUFA, particularly DHA and docosapentanoic acid (DPA)[4]. DHA commonly accounts for 20 to 50% of total fatty acids. Depending on the strain, they might also accumulate lower amounts of AA[5] , EPA [13] and other

---

[4] Docosapentanoic acid is an n-3 PUFA with 5 double bonds: *22:5 7, 10,13,16,19* n-3.
[5] Arachidonic acid is another interesting PUFA for human health: *20:4 5, 8, 11, 14* n-6

PUFA [14–16]. *Thraustochytrium, Schizochytrium* and *Aurantiochytrium* are the species with the highest DHA productivity [9,48,49,51–56]. Comparing results of different strains (detailed in section 1.3, table 4), it is clear that *Aurantiochytrium* shows the largest production values of DHA; specifically, *Aurantiochytrium limacinum*.

With the aim of establishing the **knowledge base of thraustochytrid cultivation** and PUFA production, the objective of this project is to produce DHA through a specific strain of this family using industrial byproducts as a substrate (i.e crude glycerol). The process must be robust, allowing other strains of thraustochytrids to grow and produce either PUFA or other added-value metabolites. Moreover, the substitution of a traditional carbon source for cheaper sources has a positive impact on the economics of a bioprocess with minimal undesired effects.

Producing DHA in a controlled culture opens an opportunity to overcome lipophilic contamination of n-3 PUFA from fish oil, sustainable, season independent and invariable source of DHA. As mentioned above, fish oil is susceptible to contamination with lipophilic organic chemicals that are now ubiquitous contaminants of marine ecosystems [4,57,58]. There are many types of lipophilic contaminants that are bio cumulated in fish. These contaminants, together with dangerous heavy metals, represent the current concern about fish oil (comprehensively explained in section 1.3.2). In addition to contamination, the usage of fish oil has become unpopular due to its unpleasant smell and taste, poor oxidative stability and expensive purification process.

Thraustochytrids are a powerful tool for valorising industrial byproducts (e.g. crude glycerol) while producing added-value metabolites in a biotechnological way as an alternative to overcoming current problems (Figure 1.2). This solution offers new perspectives on **waste**
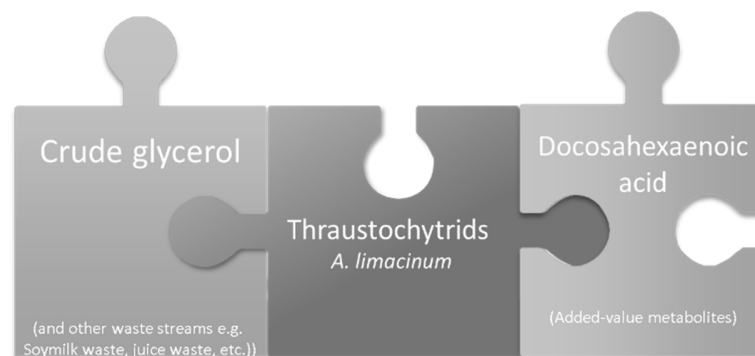
Figure 1.2. Thraustochytrids can provide a clean PUFA source as well as grow with industrial byproducts as a carbon source.

minimization and cost reduction. Thus, competing with fish oil traditional production. It is done by using a cheap carbon source, while offering a highly concentrated[6] and contaminant free DHA.

1.3 Polyunsaturated fatty acids omega-3
Basic definitions

Lipids[7] of all higher organisms contain appreciable quantities of polyunsaturated fatty acids (PUFA) with two or more double bonds of the *cis*-configuration separated by a single methylene group. PUFA are less abundant than other unsaturated varieties, but they are especially important conferring distinctive properties to microorganisms and higher organisms, which will be discussed in upcoming sections.

Box 1.2 . PUFA nomenclature

In 1964, Holman RT proposed a new numbering system for the unsaturation of fatty acids, the "omega nomenclature". In this system, the double bonds are counted from the methyl group, determining the metabolic family, noted by n-x (n for the total number of carbon, x being the position of the distal double bond). Based on this, IUPAC defined a simplified nomenclature specifies the chain length, number of double bonds and position of double bonds. The molecule shown below is docosahexaenoic acid or DHA, 22:6, with 22 carbons and 6 double bonds. Positions of double bonds are indicated by   and the number of the first carbon atom that form the double bond, counting from the carboxyl group carbon as number one. The 6 double bonds in DHA are located at the 4th, 7th, 10th, 13th, 16th and 19th carbons, so one simplified nomenclature is 22:6 4,7,10,13,16,19. Double bonds of the most abundant unsaturated fatty acids are in *cis* configuration and contain double bonds at three carbon intervals. Therefore, double bonds are separated by a methylene group. Because of this organisation, most common polyunsaturated fatty acids can also be described simply by indicating the number of double bonds closest to the terminal methyl group. With this nomenclature, DHA is termed 22:6n3. Once the bond closest to the omega carbon is identified, the remainder of the double bond can be inferred.

22:6 Δ4,7,10,13,16,19
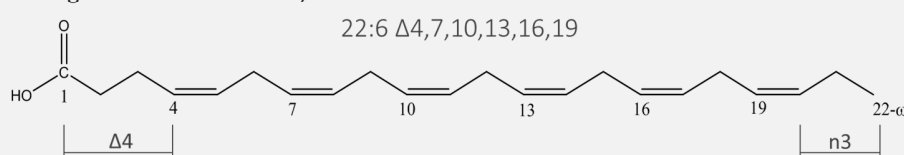
Adapted from
Wallis et al. (2002)
[233]

Fatty acids are compounds that are synthesized in nature via the condensation of malonyl co-A units with a fatty acid synthase complex. They are carboxylic acids with a long aliphatic tail (chain) usually containing even numbers of carbon atoms in straight chains (commonly C_4 to C_{24} according to IUPAC, but can be both shorter and longer). Odd-numbered fatty acids are mostly frequently found in bacteria and lower plants or animals but are significantly less abundant [59]. When a PUFA has a chain length from 2 to 6 it is called short-chain, from 8 to 12 it is a medium-chain, from 12 to 22 it is considered a long-chain fatty acid, and above 22 it is called a very long

---

[6] Some thraustochytrids have a high specificity in DHA and contains a 50% of lipids, generating a huge amount of DHA.
[7] Any substance of biological origin that is soluble in nonpolar solvents [232].

chain. Several hundreds of forms have been identified, but the number occurring frequently in the common lipids is much fewer; from 10 in plants to approximately 20 in animal tissues.

Fatty acids (FA) can be subdivided into well-defined families whose physical and biological properties are related.

☐ The simplest are referred to as **saturated fatty acids** (SFA). These have no unsaturated linkages and cannot be altered by hydrogenation or halogenation.

☐ When double bonds are present, fatty acids are said to be **unsaturated** or **monounsaturated** (monounsaturated fatty acids, MUFA) if only one double bond is present and **polyunsaturated** (polyunsaturated fatty acids, **PUFA**) if they have two or more double bonds generally separated by a single methylene group (methylene-interrupted fatty acids).

☐ Some uncommon polyunsaturated fatty acids have two adjacent double bonds separated by more than one methylene group. When this occurs, they are called **polymethylene-interrupted fatty acids**.

Table 1.2. List of omega-3 polyunsaturated fatty acids found in nature.

Common name	Lipid name	Chemical name
Hexadecatrienoic acid (HTA)	16:3 (*n*-3)	*16:3* 7,10,13
α-Linolenic acid (ALA)	18:3 (*n*-3)	*18:3* 9,12,15
Stearidonic acid (SDA)	18:4 (*n*-3)	*18:4* 6,9,12,15
Eicosatrienoic acid (ETE)	20:3 (*n*-3)	*20:3* 11,14,17
Eicosatetraenoic acid (ETA)	20:4 (*n*-3)	*20:4* 8,11,14,17
Eicosapentaenoic acid (EPA)	20:5 (*n*-3)	*20:5* 5,8,11,14,17
Heneicosapentaenoic acid (HPA)	21:5 (*n*-3)	*21:5* 6,9,12,15,18
Docosapentaenoic acid (DPA)	22:5 (*n*-3)	*22:5* 7,10,13,16,19
Docosahexaenoic acid (DHA)	22:6 (*n*-3)	*22:6* 4,7,10,13,16,19
Tetracosapentaenoic acid (TCA)	24:5 (*n*-3)	*24:5* 9,12,15,18,21
Tetracosahexaenoic acid (THA)	24:6 (*n*-3)	*24:6* 6,9,12,15,18,21

SFA components make up 40% of the total fatty acids in most natural lipids. the most common SFA in animal and plant tissues are Myristic (14:0, M) Palmitic (16:0, P) and Stearic (18:0, S) acid, but all of the possible odd and even-numbered homologues with 2 to 36 carbon atoms have been found in nature in an esterified form. PUFA constitute a large group of FAs and are generally synthesized by the modification of SFA precursors (explained in section 1.4.3). In higher plants, the number of double bonds in FA only rarely exceeds three, but in algae and animals, this can be up to six. Two principal families of PUFA occur in nature that are derived biosynthetically from linoleic acid (18:2 9, 12) and ALA. A PUFA cluster contains both omega-3 (Table 1.2), omega-6, omega-9 and conjugated components. Unique structural characteristics of PUFA are distinguished by their functions not only in regulating cell physiology but also in modulating the expression of certain genes, and their deficiencies lead to abnormalities [60]. Specifically, some members of the omega-3 family (listed in Table 1.2) are essential for humans due to their functions in the brain and the retina [61,62] (See section 1.3.1 for more information).

28

DHA and EPA (Table 1.2) are the most important components of the omega-3 family whereas ALA is the most abundant. Algae, marine microorganisms are primary producers of both DHA and EPA. These n-3 PUFA are more abundant in cold ecosystems where omega-3s help to fluidize living systems, due to its lower solidification temperature compared to SFAs [63]. They are derived biosynthetically by the elongation of the C20 and C22 polyunsaturated precursors. DHA is considered the most valued and scarcer of n-3 PUFA from an industrial standpoint. AA, ALA, and EPA can be obtained from different sources, but DHA can only be absorbed through the diet. DPA can also be decomposed into EPA or synthesized from ALA [3].

1.3.1 Health benefits of long chain n-3 PUFA
Truth and lies

Studies of fish oil effects in human serum cholesterol concentration were first performed in the 1950s, but they were not given the attention they deserved. Before the 1970s, omega-3 fatty acids were not adequately investigated. In 1972 when Bang and Dyerberg [64] reported their findings about Eskimos who had low rates of cardiovascular disorders or cancer, despite their high-fat diet. Many studies demonstrating that n-3 PUFA had a positive effect on human health were published shortly after Band and Dyeberg's work [65]. In the 1980s, knowledge about the benefits of omega-3s increased dramatically. In 1985, a conference called *Health Effects of Polyunsaturated Fatty Acids in Seafoods* established the fact that n-3 PUFA of marine origin, EPA and DHA play important roles in prostaglandins[8] metabolism, thrombosis and atherosclerosis, immunology and inflammation, and membrane function. Since this statement, the number of studies on n-3 PUFA has increased dramatically. Currently, the interest in omega-3s, as either ingredients or supplements has exploded, creating a major market with products of different sources.

29

Omega-3 supplementation offers a number of potentially heart-healthy effects, including reducing triglyceride levels, slightly raising levels of HDL cholesterol[9], reducing levels of homocysteine[10] and reducing blood pressure. There is strong evidence of blood pressure reduction when a patient is supplemented with n-3 PUFA and they are considered a complement to the fight against hypertension disorders [65]. Any other potential cardiovascular benefit of supplementation may be limited to people who do not regularly consume fish in their diets and who do not take other medications for heart disease. Interestingly, contrary to common belief, research does not support fish oil supplementation for preventing heart attacks or strokes in people who have heart disease or who are at risk for heart disease. Moreover, there is no reliable

---

[8] Prostaglandins are a group of physiologically active lipid compounds that have diverse hormone-like effects in animals. They sustain homeostatic functions and mediate pathogenic mechanisms, including the inflammatory response.

[9] High-density lipoproteins acting as cholesterol scavengers, picking up excess cholesterol in the blood and taking it back to the liver where it is broken down.

[10] A high level of homocysteine in the blood makes a person more prone to endothelial cell injury, which leads to inflammation in the blood vessels

evidence that fish oil supplements prevent heart disease in healthy people who are not at risk [66–72].

Increased intake of the n-3 PUFA stimulates the production of substances known as prostaglandins, and consequently reduce some forms of inflammation. On the basis of this, EPA and DHA have been tried in the treatment of symptoms of rheumatoid arthritis with considerable success. A study of several thousand women in Sweden found that, consistent long-term intake (averaging more than 210 mg per day of n-3 PUFA) from eating fish was associated with a 52% lower risk of developing rheumatoid arthritis compared with lower intake over the period of the study (7.5 years) [73]. The anti-inflammatory effects of EPA and DHA have also caused researchers to investigate the possible benefits of fish oil for the treatment of menstrual cramps, inflammatory bowel disease, lupus, and IgA nephropathy[11]. For each of these conditions, at least one double-blind study has obtained positive results. A large European study [66] showed that people with the highest consumption of DHA had a 77% reduction in the risk of developing ulcerative colitis, over an average period of four years than those consuming the lowest amount.

The number of publications regarding the use of n-3 PUFA in cancer studies in animals has increased exponentially in recent years. A positive relation between omega-3 supplementation and cancer reduction has been found for specific type of cancers [74]. Use of fish oil is associated with a 32% reduction in the risk of breast cancer. However, supplementation cannot be recommended for breast cancer prevention if the patient is undergoing chemotherapy. Omega-3s may interfere with chemotherapy by enhancing white blood cells leading to a resistance to chemotherapy [75]. Results of other studies have shown that n-3 PUFA delayed tumour appearance and decreased both the rate of growth and the size and number of tumours. In these models, calorie restriction potentiated the effect of n-3 PUFA whereas n-6 PUFA in the form of corn oil increased tumour formation, size, and number [65]. Therefore, n-3 PUFA supplementation can be considered a preventive support for cancer treatments unless the patient is undergoing chemotherapy.

Analyses of dietary intakes of n-3 PUFA show that participants who reported the highest intake of EPA and DHA were 30% less likely to develop diseases of the retina[12] compared to those with the lowest intake [76]. A study of over 30,000 female health professionals show that those consuming at least one serving per week of fish had a 42% reduction in risk of developing a disease of the retina compared to those eating less than one serving per month [76].

For reasons that are less clear, n-3 PUFA seem to help with depression, bipolar disorder, and schizophrenia, according to a number of double-blind trials. A recent study shows that participants who took a high dose of n-3 PUFA had a remission of depression compared to 16.7% of those taking a placebo [77]. It has been shown that when omega-3 supplementation is given

---

[11] Disease related to a deposition of immunoglobulin A in the kidneys, causing inflammation and malfunction of these organs.
[12] Neovascular age-related macular degeneration (AMD) and central geographic atrophy (CGA)

to participants suffering from severe to moderate depression, but not mild depression, the patient has shown a significant improvement. This was also evident with elderly patients whose depression was characterized by a very low levels of n-3 PUFA [78]. Furthermore, an analysis of blood samples from 1600 military personnel showed that those who committed suicide had significantly lower blood levels of DHA than personnel who did not commit suicide [79]. Other studies showed a 20% reduction in anxiety, stress and epilepsy episodes. Many other studies have investigated the benefits of omega-3 supplementation for memory-enhancement, strength training, muscle pain and inflammation after training, acne, etc.

Moreover, DHA is very important for normal brain and retina development as well as overall development of the fetus and infants. For this reason, it is thought that pregnant or nursing mothers may benefit from supplementation. It is recommended that pregnant women should consume 200 mg of DHA per day, from either a supplement or low-mercury fish, but the benefit of higher intake remains unclear. This is why the present study is so important; it is essential that a highly pure and non-contaminated source of DHA can be created for very susceptible patients or receptors. The effects of a PUFA deficiency on the developing brain have been widely documented. After 30 weeks of gestation, there is a preferential desaturation of the long chain n-3 PUFA in the brain. In the retina, the proportion of n-3 PUFA increase whereas that of n-6 PUFA decrease throughout development. Postnatally malnourished infants show an unusual concentration of DPA in the retina, as a compensatory mechanism of DHA deficiency [65].

31
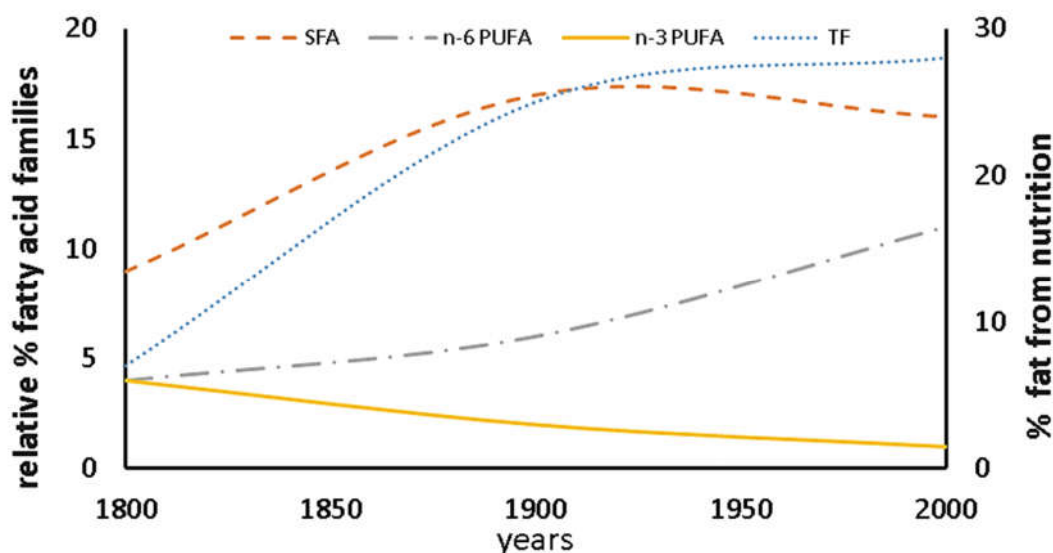
Figure 1.3. Fatty acid composition of the human diet over the years; adapted from Leaf and Weber *[80]*. TF=total fats in human nutrition indicated as % fats from nutrition.

Some current common health disorders might be caused or influenced by the changes in the human diet, as illustrated in Figure 1.3. Recent studies indicate that modern agriculture and aquaculture, as well as the industrial revolution, have led to changes in the production of both

plants and animals. This has caused changes in the composition of the food supply in Western societies. Interestingly, the amount of n-6 PUFA intake has increased, due to new trends regarding vegetable oils nutrition. Conversely, n-3 PUFA consumption has decreased. During human evolution there has been a change in ratio of 1:1 (n-6:n-3) to 20:1 [65]. Humans survived for one hundred thousand years on a diet that was much lower in SFE than is today's diet (Figure 1.3). The SFA content of industrial foods was dramatically increased due to modern food processing, as was predicted by Leaf and Weber [80]. In relation to this incidence, new studies are investigating whether the ratios between different omega families of PUFA are as important as the presence of n-3 PUFA. The use of an incorrect or non-evolutionary 1:1 (n-6:n3) ratio may be the cause of some contradictions in different n-3 PUFA supplementation studies.

Considering all the benefits potentially provided by n-3 PUFA a contaminant-free source of DHA and n-3 PUFA is needed. It is equally important to maintain a regular intake of these nutrients throughout life.

1.3.2 Current issues with n-3 PUFA supplementation products
A lipophilic contaminant vector and the negative effect on human health

Fisheries byproducts are one of the major sources of n-3 PUFA for marketed omega-3 supplements. This is a limited source with a substantial variability in composition and quality. Such fish oil can present relatively high concentrations of persistent organic pollutants (POPs)[13], such as polychlorodibenzodioxins (PCDDs) and polychlorodibenzofurans (PCDFs) commonly named dioxins or **PCDD/Fs**, polychlorinated biphenyls (PCBs), polychlorinated naphthalenes (PCNs), polybrominated diphenyl ethers (PDBDEs) organochlorine pesticides (OCPs) commonly named **PCBs**, and heavy metals, such as mercury, arsenic, cadmium and lead [4,10,11,58,81,82]. Dietary intake of fish is the major contributor of human exposure to these contaminants and omega-3 supplementation from the same source is an unnecessary risk [83,84]. In contrast, such contaminants are minimal/absent in vegetable oils [4]. Therefore, this is an oceanic environmental problem.

The negative impact that PCBs have on human health has been demonstrated [85]. In addition to contamination, the usage of fish oil has become unpopular due to the unpleasant smell and taste, poor oxidative stability and expensive purification. Furthermore, the price of fish oil has been rapidly increasing due to a flat supply and increased global demand for this commodity. Contaminant purification can cause a significant increase in the price. The Food and Agriculture Organization (FAO, United Nations) predicts that the demand for fish oil will reach 145% of the historical global production capacity by next year. Such a situation establishes the need for an alternative source to obtain PUFA. The search for new methods of production is a new field to explore.

---

[13] In some publications this is called Persistent Environmental Pollutants (PEPs)

PCBs, PCDDs and PCDFs are three families of organo-halogenated pollutants (Box 1.3), which cause a great deal of concern. They are classified as part of the twelve toxic POPs that where targeted by the Stockholm Convention in 2001 for reduction and eventual elimination [86]. While the risk level varies from one compound to another, they share the following properties: persistence, ubiquity, bioaccumulation, biomagnification and most importantly, toxicity. Their toxicity resides in a biochemical process that implies the union of the POP to a protein cytoplasmic receptor [87]. POP are present in very low concentration, but only a fraction of the large number of compounds that exist for each family is toxic. Because of this complexity, their determination is subjected to a long analytical method that must be performed on every batch. This increases the cost of the decontamination process for a fish oil supplement (and the procedure is not always performed properly). For example, Nevado *et al.* (2010) [11] reported that marketed products contain significant amounts of contaminants, that in some cases exceed EU legislation.

The main problem with PCDD/Fs is that the bioaccumulation and biomagnification in aquatic organisms is comparatively higher than in terrestrial organisms. Such process causes the contaminants to be transported and transferred throughout the food chain. Even though the poison is first dispersed widely and thinly, it gradually concentrates up to the highest trophic levels (bioaccumulation and biomagnification). Some fish can concentrate PCDD/Fs up to 10000 times the level of their surrounding environment. These contaminants are accumulated in fatty tissues due to their lipophilic character, their low solubility in water, and their resistance to degradation. In contrast, seals, higher marine organisms, apparently possess a biodegradative mechanism, which limits the amount of PCDD/F they accumulate in comparison with their

33

Box 1.3. PCDD/Fs and PCBs basic definitions

PCDDs/Fs are constituted by two benzene rings linked by two oxygen atoms, for PCDDs, or by one oxygen atom and a carbon-carbon bond as for PCDFs, which provides them with a quasi-planar configuration. Each ring may present a maximum chlorination degree of 8. According to the US-EPA nomenclature, a congener is each compound belonging to the same determined class of substances: there are 75 congeners of PCDD and 135 congeners of PCDF. A homologue refers to the compounds having the same degree of chlorination, and, within the same homologue group, isomers differ from the positions at which chlorine atoms are bonded to the molecular body. One specific congener is named after the number of chlorine atoms and their position along the body molecule, name of the homologue group and the class of compound to which this congener belongs. Another nomenclature gives a systematic number to each structure, which was proposed by Bacher and Ballschmiter in 1992 similar to the PCB nomenclature [234].

PCBs are a family of halogenated aromatic hydrocarbons that comprises 209 compounds. They can have a different chlorination grade, from 1 to 10 chlorine atoms, where the chlorine atoms can be in different positions. The most common nomenclature for them consists of giving a PCB number to each structure in a systematic way, according to Bacher and Ballschmiter (1992). Contrary to PCDD/Fs, PCBs are not strictly planar molecules, as the simple bond between the rings can rotate. Due to the specific substituted positions of the aromatic rings, PCBs can adopt a more planar configuration. This is the case with PCBs that have no chlorine atoms in ortopositions, and chlorine-substituted in both para- and at least one meta- position (PCB 77, PCB 81, PCB 126 and PCB 169) [234].
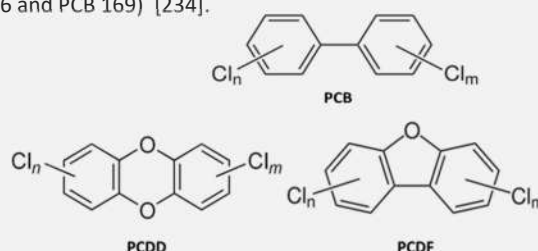
expected dietary intake of contaminated fish. As for plants, PCDD/Fs have been found due to superficial contamination by particle deposition on the leaves.

The effects of dioxin-like compounds are thought to be mediated by the cytosolic receptor Ah (Aryl hydrocarbon receptor)[14] [88–90]. The Ah receptor is an intracellular protein that acts as a signal transducer and a transcription factor, similar to steroid hormones. It binds to lipophilic chemicals (exogens) known as ligands, such as plants flavonoids and polyphenols. Unfortunately, PCDD/Fs and PCBs acts as ligands as well. The result of its activation with those undesired ligands, is a modification of the genetic transcription. Dioxin exposure arises with the induction of cytochrome P450 1A1 (CYP1A1), which belongs to a protein family that serves as detoxifier or activator of endogenic or exogenic chemicals.

The binding affinity to the Ah receptor and the potency of a chemical to induce CYP1A1T serves as an indicator (how harmful it is). Actually, the term Toxic Equivalency Factor (TEF) is basically a measurement of such affinity. For example, the most potent dioxin is the 2,3,7,8-TCDD. Other dioxins may cause the same effects as 2,3,7,8-TCDD but they require higher doses due to their lower affinity to the Ah receptor [91]. The proposed alternative n-3 PUFA source will allow infants and pregnant women to have daily safe intake of these nutrients. This could be used for other kind of patients as well.

1.3.3 Omega-3 Market
Future and new applications

It is important to establish the economic impact of n-3 PUFA in the world market. The rise in recognition and popularity of it has led to their introduction in a multitude of functional foods and beverages. Consumers are seeking additional supplementation through forms such as fish and flax seed oil. Fish oil sales increased by 8.1 percent in 2012. Products supplemented with fish oil are growing thanks to a number of scientific studies that have indicated their effectiveness for reducing health risks, as explained in section 1.3.1. *Euromonitor* reports that from 2011 to 2016, global retail value sales for the combined categories of fish oils and n-3 PUFA supplements are expected to increase by 5 percent annually up to $3.9 billion worldwide.

When marketing to vegetarians, flax seed is an alternative to fish oil, although it is much less efficient and requires a larger dosing (in terms of health benefits). Flax seed and fish oil are also already included in many fortified foods and beverages, resulting in a greater number of consumers being able to incorporate n-3 PUFA into their diets. Interestingly, n-3 PUFA from microalgae could be a satisfactory substitute for flax seed products (regarding n-3 PUFA supplementation). It even surpasses productivity values.

Algae and non-algae n-3 PUFA products are expected to experience an increasing in use, and sales could reach 7.32 billion USD by 2020, according to a new study by *Grand View Research,*

---

[14] The aryl hydrocarbon receptor is a ligand-activated (protein) transcription factor involved in the regulation of biological responses to planar aromatic hydrocarbons.

Inc. The Marine Ingredients Organization reported that Europe was the largest consumer of omega-3 ingredients in 2013, which accounts for over 60% of global consumption and is expected to maintain that leadership position until 2020. Consumer perception regarding fish oil smell, and the lack of standardization of this product in terms of labelling and registration, are expected to be key challenges for market participants in the future.

1.4   Thraustochytrids: The perfect tool for PUFA production
Prolific linage of PUFA producers

Several established works [9,38,47,92–109] have reported a wide range of photosynthetic (autotrophic) and heterotrophic microorganisms that would be a potential commercial source of EPA and DHA. As can be seen in Figure 1.4, there are many photosynthetic microorganisms that produce important amount of PUFA and n-3 PUFA. *Pavlova* sp. is widely used due to its capacity to produce both EPA and DHA. On the other hand, *Eustigmatophytes* is a good candidate for ARA and EPA production. However, autotrophic microorganism growth rates are certainly low which results in low productivity for industrial processes.
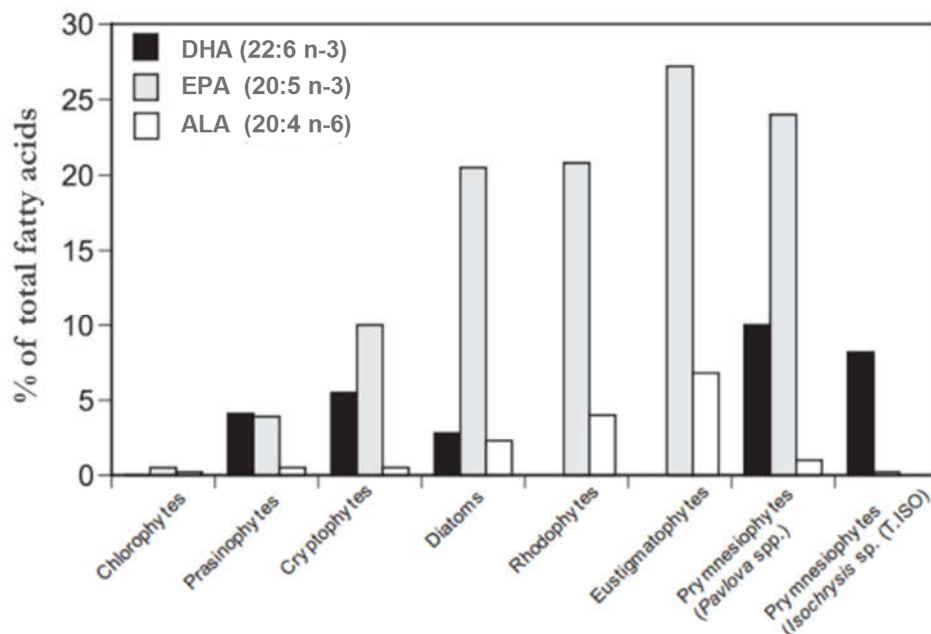
Figure 1.4. PUFA production of different photosynthetic microalgae *[107]*. AA is equal to ARA in the present thesis nomenclature.

For this reason, particular attention has been given to the thraustochytrids, due to their capacity to accumulate lipid and proportionately large quantities of DHA [108,109]. These properties indicate an important industrial potential. For example, some *Aurantiochytrium* strains are able to accumulate DHA for over 30% of the total FA [110]. In addition, the content of C18 and C20 (precursors of n-3 PUFA) in *Aurantiochytrium* were much lower than those in the genera

Thraustochytrium and *Schizochytrium* [111], while maintaining the greatest production of DHA. This makes *Aurantiochytrium* very special for the specific production of DHA which follows a different synthesis pathway than the traditional eukaryote biosynthesis pathway [112] (extensively explained in section 1.4.3).

In addition, the oil content of *Schizochytrium* sp. shown in Table 1.3, reveals the real potential of thraustochytrids to produce lipids compared to any other microorganism. Moreover, thraustochytrids do not require photosynthetic equipment, they can grow in regular bioreactors. And most importantly, they have an important specificity for ARA, EPA and DHA [56], and a basal capacity to accumulate lipids. Those three characteristics made the thraustochytrids family the perfect n-3 PUFA cell factories to establish a biotechnological production.

1.4.1 The place of thraustochytrids in the tree of life
Controversial heterotrophic microalgae

The family of thraustochytrids was established by Sparrow (1943) [113] for chytrid-like[15], eucarpic[16] and epi[17] and endobiotic[18] marine fungi attached to a substrate by an ectoplasmic net (see Box 1.3) while producing biflagellate zoospores (extensively explained in Chapter 2). Thraustochytrids belong to the phylogenic group of labyrinthulomicetes [114], which are marine heterotrophic fungus-like protists and belong to the eukaryotic kingdom of Stramenopiles [115]. Labyrinthulomicetes are important in nutrient recycling in different marine ecosystems. Recent studies have revealed their potential for squalene and carotenoid production in addition to PUFA [47,116–119]. The Stramenopiles kingdom accommodates the photosynthetic ochrophytes[19], along with the non-photosynthetic bioeceans and oomycetes[20], which are well known as plant pathogens. Labyrinthulomicetes share the stramenopile characteristics of having a cell wall of thin scales, tubular mitochondria, and biflagellate zoospores. Together with the alveolate relatives, which includes the apicomplexan[21], ciliates[22] and dinoflagellates[23] form the super-kingdom of Chromalveolata [120]. The ancestors of this super-kingdom were mixotrophic (photosynthetic and pathogenic) [121,122]. Therefore, photosynthesis capacity was lost in the common ancestor to labyrinthulomicetes and other non-photosynthetic organisms of Chromalveolata. Furthermore, phagotrophy is conserved in labyrinthulomicetes and may have preceded the development of an ectoplasm (see section 1.3.2) and cell wall. It is well established that plastids of all photosynthetic Stramenopiles were originated from a single common ancestor.

---

[15] Any of the simple, algae-like fungi constituting the class of aquatic and soil environments, having flagellated zoospores and little or no mycelium.

[16] Part of the cell becomes a sporangium.

[17] Relating to an organism that lives, usually parasitically, both on the surface and within the body of its host.

[18] Relating to an organism that exists as a parasite or symbiont entirely within the tissues of a host organism.

[19] Ochrophytes are the class of photosynthetic heterokonts.

[20] Filamentous fungus-like eukaryotic microorganisms. Most of oomycetes produced zoospores.

[21] Large phylum of parasitic protists.

[22] Any protozoan of the phylum Ciliophora. Ciliates are probably the best known and the most frequently observed of the microscopic unicellular marine microorganisms.

[23] Large group of photosynthetic and phagotrophic of flagellate protists.

Table 1.3. The oil of some microalgae species used for FA production. Harun et al. (2010) [235]

Microalgae	Oil content (% dry wt)
Botryococcus braunii	25–75
Chlorella sp.	28–32
Crypthecodinium cohnii	20
Cylindrotheca sp.	16–37
Dunaliella primolecta	23
Isochrysis sp.	25–33
Monallanthus salina	20
Nannochloris sp.	20–35
Nannochloropsis sp.	31–68
Neochloris oleoabundans	35–54
Nitzschia sp.	45–47
Phaeodactylum tricornutum	20–30
Schizochytrium sp.	50–77

The identification of a plastid derived gene in a photosynthetic algae of the kingdom, supports the idea of the photosynthetic ancestor [123].

Many thraustochytrids produce n-3 PUFA using desaturases and elongases. This process generally take place in chloroplasts in normal algae. A few members of labyrinthulomicetes have been described as phototactic and some present an eyespot[24], which may mark the remains of an ancestral chloroplast. These are believed to be derived from a chloroplast that underwent evolutionary reduction. Interestingly, in some zoospores the eyespots are located near the base of flagella, which could be related to current phototactic behavior [124–126]. As will be fully explained in Chapter 2, these eyespots store TG containing DHA, which supports the idea of an evolutionary reduction of chloroplasts.

Depending on the interest of the investigator, thraustochytrids were commonly called microalgae or marine fungae. Currently it is known as just one thing or the other. Figure 1.5 shows the heterogeneity of the kingdom, which is believed to be caused by a lack of knowledge about this kingdom of marine microorganisms.

Future discoveries could generate a new taxonomic rearrangement. By now, it is currently established that Stramenopiles include autotrophic species (ochrophytes and dinoflagellates) that are phylogenetically related to labyrinthulomycetes. Together with other photosynthetic related evidence explained above, it is not wrong to consider labyrintulomycetes as microalgae.

---

[24] An eyespot, also called stigma, is a heavily pigmented region in certain one-celled organisms that apparently functions in light reception.

Although the basic definition of algae includes autotrophy as the main characteristic, modern definitions already include non-autotrophic organisms.
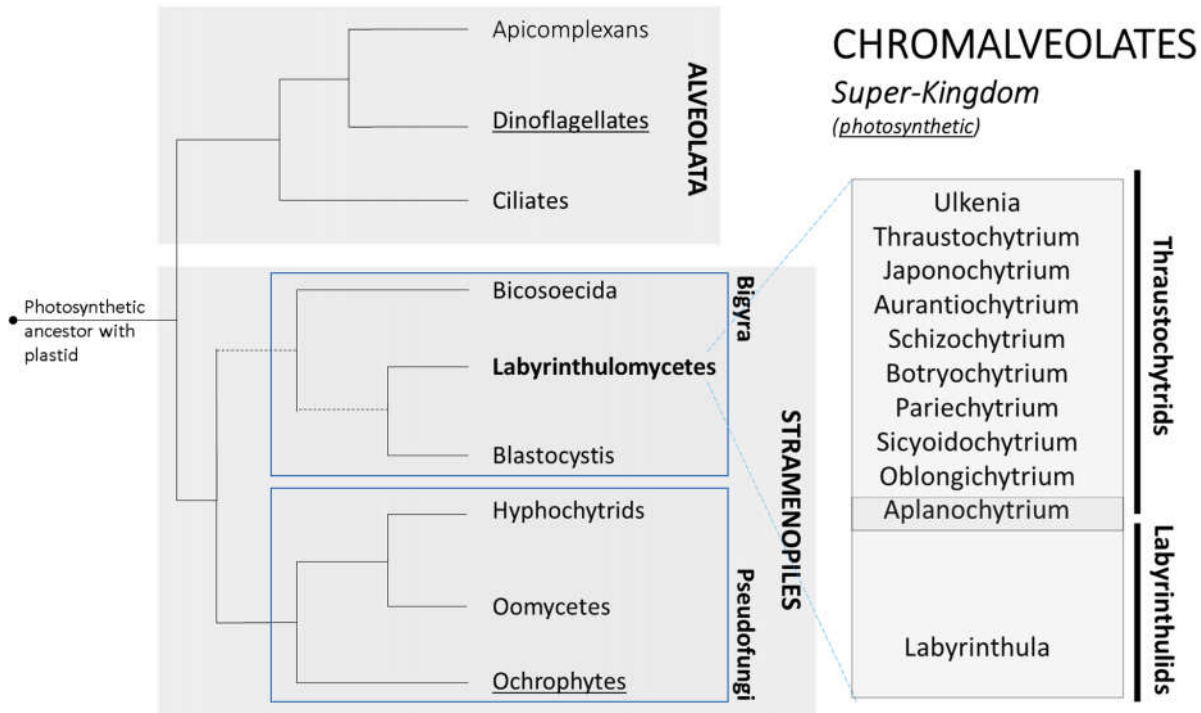
Figure 1.5. A schematic summary of Chromalveolata super-kingdom based on Riisberg et al. Riisberg (2009), Tsui et al. (2009) and Yokoyama et al. (2007) [110,125,127,236]. Aplanochytrium is included in both major linages.

1.4.2 Morphological and life cycle stage classification

Phylogenetic relationship within labyrinthulomycetes

As indicated in Figure 1.5, labyrinthulomycetes are composed of two main linages, thraustochytrids and labyrinthulids. Thraustochytrids are composed of nine genera: Aurantiochytrium, *Thraustochytrium*, *Schizochytrium*, *Ulkenia*, *Parietichytrium*, *Aplanochytrium*, *Sicyoidochytrium, Oblongichytrium, Japonochytrium* and *Botryochytrium*. Initially, they were only composed of two generas; *Schizochytrium* and *Ulkenia* [110,127]. For this reason, some genera of the linage may be confused in old publications (e.g., Aurantiochytrium was formerly called Schizochytrium, however both genera currently coexist independently). Different genera can be distinguished by a combination of morphological characteristics, profiles of polyunsaturated fatty acids and carotenoid pigments (as well as by the multi-staged life cycles).

Both linages are known for generating an **ectoplasmic net** from an organelle called sagenogenetosome (Box 1.3). Labyrinthulids can glide and move along the ectoplasmic net while thraustochytrids do not use an ectoplasmic net to glide. Labyrinthulomycetes share a life cycle phase with **vegetative cells** despite presenting important differences within linages. Labyrinthulids form single-shaped vegetative cells that glide inside the ectoplasmic net, whereas the thraustochytrid's vegetative stages for most of the genera consist of granular cells, which are globose to subglobose, measuring 4–20 µm in diameter [110,127,128], and in specific situations even more. *Aplanochytrium,* which is shared for both linages (Box 1.3) presents the greatest divergences. All labyrinthulomycetes produce **zoospores**[25] while *Aplanochytrium* produce

---

Box 1.3 . Sagenogenetosome or bothrosome

Almost all species of thraustochytrids develop ectoplasmic extensions from one (sometimes more) points on the cell. This branched network of plasma membrane extensions is generated by an organelle named sagenogenetosome or bothrosome, which is located at the periphery of the cell. It is **a unique organelle of thraustochytrids** that is capable of secreting a rizhoid membrane outside their cells. The ectoplasmic network appears to help cells to adhere to and penetrate substrates, and secrete digestive enzymes that are required to solubilize nutrients that can be absorbed by the cells [15,163,237,238].

A (left): Image of *A. limacinum* SR21 vegetative cells obtained at IQS. Optical microscope (x1000) with violet staining.

B (below): Common structure of thraustochytrids with electron microscope image of a sagenoegenetosome of *Aplanochytrium* sp. SEK 349
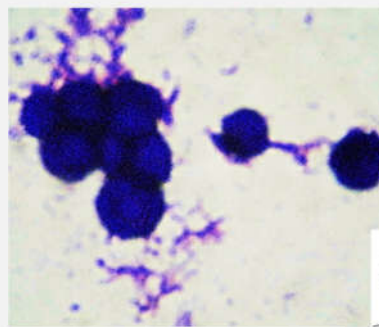
This study   Porter 2001 and Porter 1991

39

aplanospores[26]. On the other hand, *Aplanochytrium* vegetative cells are solitary contrary to what occurs with other labyrinthulomycetes, where vegetative cells are organized in **settlements** or colonies. When vegetative cells are grouped in a location, it is commonly called settlement.

From an eco-physiological standpoint, when labyrinthulomycetes are in a vegetative stage, wether generating an ectoplasmic net or not, it is because the environment is rich in nutrients. When relocation is needed to find a new source of nutrition, zoospores are produced. In this way, zoospores move along the marine ecosystem until they find a potential source of substrate, which is the beginning of a new settlement. In general, to enhance nutrient absorption, an ectoplasmic net is created despite the fact that some species of thraustochytrids do not create well-developed nets. Thraustochytrids multiply by mitotic division in the vegetative stage and reproduce by forming zoosporangium. When a zoosporangium is mature, it releases biflagellate zoospores, possessing a long anterior tinsel flagellum along with a short posterior whiplash flagellum [128,129].

The flagellum, which consists of lateral hair-like projections along its length, is called a **tinsel flagellum**. These hair-like projections are called fimmers or mastigonemes. These filaments change the flagellar action so that a wave coming down the filament towards the tip propels the

---

[25] An asexual spore produced by certain algae and some fungi, capable of moving about by means of flagella.
[26] A non-motile, asexual spore formed within a cell, the wall of which is distinct from that of the parent cell.

cell instead of pushing it. The naked flagellum is referred to as **whiplash flagellum**. It consists of two parts, a long lower portion and a short and flexible upper portion. The mode of zoospore production is part of the basis for genus differentiation within thraustochytrids. The cytoplasmic content of a vegetative cell develops into a zoosporangium, and then divides directly into zoospores in the genus *thraustochytrium*. The cytoplasm escapes as an amoeboid mass, prior to the zoospore division in *Ulkenia*. Interestingly, *Schizochytrium* is characterized by the successive bipartition of a vegetative cell resulting in the formation of the stages called the diad, tetrad and sometimes triad[27]. Then, the cells in these symmetrical structures become an individual zoosporangium. This zoosporangium phenomenon is shared with *Aurantiochytrium.* However, this last genera had been separated from the Schizochytrium species due to significant differences in PUFA profile and organelles organization [127]. These types of characteristics are used for complex thraustochytrids classification.

1.4.3 The secret pathway
Marine bacteria heritage

Two different n-3 PUFA biosynthetic pathways are the secret feature of thraustochytrids. There is a great deal of evidence to suggest that the presence of two synthetic pathways for PUFA in thraustochytrids, i.e. **polyketide synthase (PKS)-like** and the desaturase/elongase based **standard pathway** [112]. Matsuda *et al.* (2012) [112] clearly showed that both the standard pathway to produce PUFA and the PKS-like are present in thraustochytrids. In Matsuda *et al.* work, a gene encoding a putative   12-fatty acid desaturase from *Thraustochytrium aureum* was investigated. When this gene was introduced into a Yeast genome, oleic acid was converted into ALA. On the other hand, when this gene was disrupted in T.*aureum,* oleic acid was accumulated, whereas the content of the DHA increased. These data indicate that the mechanism responsible for DHA production in thraustochytrids might be a different pathway from the eukaryotic standard one. Hence, the PKS-like pathway may be causing the characteristic DHA specificity of some thraustochytrids (such as Aurantiochytrium strains).

Figure 1.6 shows the biosynthetic pathway of eukaryote microorganisms as well as the PKS-like pathway. The second pathway is still not well known. Interestingly, the standard pathway is oxygen dependent while the PSK-like can function without oxygen (as studied in Chapter 4). This difference can be a powerful tool to trigger DHA production in thraustochytrids. However, every

---

[27] Symmetrical structure of two cells (diad), three cells (triad) and four cells (tetrad). Triad is much less common.

genus in thraustochytrids have very different FA profiles and the parameters to trigger n-3 PUFA production might be different as well.
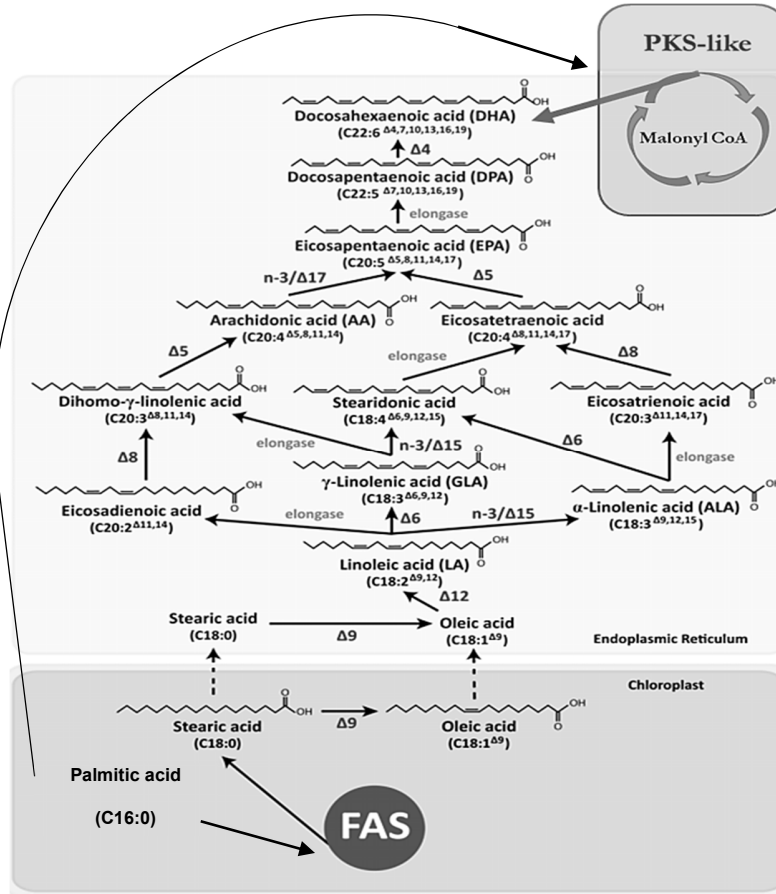
Figure 1.6. Biosynthetic pathway of PUFA from eukaryote microorganisms in chloroplast and Endoplasmic reticulum. At the upper right, the PKS-like pathway directly produces DHA & DPA. Adapted from Martin et al. (2013) and Matsuda et al. (2012) *[103.112]*

1.4.4 Aurantiochytrium limacinum SR21
Industrial candidate for DHA production

After a review regarding thraustochytrids that produce DHA (Table 1.4), *A. limacinum SR21*[28] and *mh0186, Aurantiochytrium* sp T66 and *Schizochytrium* sp. are clearly the most prolific producers (reported) of n-3 PUFA. These strains have great growth rates compared to other large, unicellular heterotrophic microorganisms, which benefits n-3 PUFA productivity. As published in the review of Advanced Biotechnology in 2012, Table 1.4 offers a list of different thraustochytrid strains and their DHA productivity and yield. These works include cultures based on glycerol, crude glycerol and glucose as a carbon source. There is a consistent evidence of the DHA

---

[28] *A. limacinum* SR21 and ATCC MYA-1381 are the same strain.

production potential of *A. limacinum* strain. Either SR21 or mh0186 show positive productivities. For this reason, this has been the most or one of the most investigated thraustochytrids.

Table 1.4. Overview of growth and DHA yields according to the microorganism used as published in the review of Advanced Biotechnology 2012 *[8]*. Literature works based on glycerol, crude glycerol and glucose cultures.

Microorganism		Time (h)	X (g/l)	P (mg DHA/l)	Calculated $Y_{P/X}$ mg/g [a]	Reference
Unknown *Thraustochytridae*	NIOS-1	120	–	–	128	Jain et al., 2007
	NIOS-2	120	–	–	6	Jain et al., 2007
	NIOS-4	120	–	–	8	Jain et al., 2007
	NIOS-10	120	–	–	8	Jain et al., 2007
	12B	72	31	6800	219	Perveen et al., 2006
	AS4-A1	–	8.1	580	72	Quilodran et al., 2010
Thraustochytrium	sp. (ATCC 20892)	120	2.7	67.6	25	Singh et al., 1996
	sp. (ATCC 20891)	120	1.9	1.8	0.9	Singh et al., 1996
	sp. (ATCC 20890)	120	1.2	0	0	Singh et al., 1996
	sp. (ATCC 34304)	69	5.7	0	0	Singh et al., 1996
	roseum sp. (ATCC 28210)	120	17.1	2100	122	Singh and Ward, 1996
	aureum ATCC 34304	96	4.9	500	102	Bajpai and Ward, 1991
	aureum ATCC 34304	69	5.7	182	32	Iida et al., 1996
	aureum ATCC 34304	168	–	–	280	Hur et al., 2002
	ONC–T18	96	28	4600	164	Burja et al., 2006
	stratium KF9	52	0.9	13.6	15	Fan et al., 2001
Schizochytrium	sp. (ATCC 20889)	120	5	10.8	2	Singh et al., 1996
	sp. HX-308	160	92.72	17700	190	Qu et al., 2010
	sp.	96	71	17500	246	Ren et al., 2010
	sp. (ATCC 20888)	120	2.6	10.7	4	Singh et al., 1996
	sp. G13/2S	48	68	7650	112	Ganuza et al., 2008
	limacinum SR21	96	48	1330	277	Yaguchi et al., 1997
	limacinum SR21	120	38	4200	110	Yokochi et al., 1998
	limacinum SR21	168	22.1	4900	222	Chi et al., 2009
	KH105	96	30	3400	113	Yamasaki et al., 2006
	sp. KF1	96	4.6	1700	37	Fan et al., 2001
	mangrovei KF2	96	13.3	2800	210	Fan et al., 2001
	mangrovei KF4	96	8.8	1500	170	Fan et al., 2001
	mangrovei KF5	96	7.9	1200	152	Fan et al., 2001
	mangrovei KF6	96	13.5	2800	207	Fan et al., 2001
	mangrovei KF7	96	6.6	70	10	Fan et al., 2001
	mangrovei KF14	96	8.1	1800	222	Fan et al., 2001
	mangrovei SK2	96	28	6000	214	Unagul et al., 2007
	sp. KK17-3	72	7.1	300	42	Huang et al., 2001
Aurantiochytrium [b]	*limacinum* ATCC MYA-1381	168	44.95	9750	217	Rosa et al., 2010
	limacinum ATCC MYA-1381	192	9	4950	550	Pooksawang et al., 2009
	limacinum ATCC MYA-1381	130	22.1	5000	226	Pyle et al., 2008a
	limacinum mh0186	56	21	4700	223	Nagano et al., 2009
	sp. T66	168	100	15600	156	Jakobsen et al., 2008

It might seem that glycerol cultivations should give lower productivities in terms of biomass and DHA. However, the usage of glycerol is not a handicap for such bioprocesses as shown in Table 1.5 that list some *Aurantiochytrium* and *Schizochytrium* cultivations using both glycerol types. Therefore, according to the current state of the art, glycerol and glucose can lead to comparable yields (Investigated in Chapter 3). DHA concentrations and yields obtained from crude glycerol cultures were comparable or higher than pure glycerol [93,130,131]. The final biomass concentration is typically higher in studies using pure glycerol, with similar fermentation times. This might indicate that harvesting time have a greater impact on DHA yields than the carbon source used (investigated in Chapter 2).

The great performance when growing thraustochytrids in crude glycerol is very unique. Other microorganisms are generally affected by the high salinity and other impurities such as soap and methanol (which crude glycerol contains). However, **thraustochytrids are well adapted to a wide range of salinities**. A good example of this, are *A. mangrove* strains. These strains have been

isolated from environments where salinity and temperature levels fluctuate daily, monthly and seasonally. A series of ecological and physiological investigations have been conducted with various isolates of thraustochytrids, found in subtropical mangroves, where salinity levels could vary between 5 and 35 ‰ in summer and winter[132]. Interestingly, Shabala *et al.* (2009) provided the proof of the thraustochytrids' osmotic adjustment capacity, and demonstrated the importance of the plasma membrane ion transport activity, for this process, under hypoosmotic conditions [133]. When cells are affected by hypoosmotic stress, they are subject to substantial inward flows of water. A decrease in the external solute concentration from 250 mM to nearly zero would increase the intracellular pressure by more than six atmospheres. These drastic forces will cause the cell rupture.

Table 1.5. Summary of studies using pure and crude glycerol to be transformed into DHA, by A. limacinum. X stands for dry cell weight. P – Concentration of DHA. Data presented as published in the review of Advance Biotechnology 2012 *[8]*.

Carbon source	Microorganism	Time (h)	X (g/l)	P (mg DHA/l)	Calculated $Y_{P/X}$ (mg/g)	Reference
Pure glycerol	S. limacinum SR21	120	38	4,200	110	Yokochi et al., 1998
	A. Limacinum MYA-1381	168	44.9	9,750	217	Rosa et al., 2010
	A. limacinum mh0186	56	21	4,700	223	Nagano et al., 2009
	A. Sp. T66	168	100	15,600	156	Jakobsen et al., 2008
	S. limacinum SR21	168	37.9	6,560	173.1	Chi et al., 2009
Crude glycerol	A. limacinum MYA-1381	192	9	4,950	550	Pooksawang et al., 2009
	A. limacinum MYA-1381	130	22.1	5,000	226	Pyle et al., 2008a
	S. limacinum	72	12	2,000	166.6	Ethier et al., 2011

In a study by Shabala *et al.*, it was verified that thraustochytrids can grow in a wide range (0-500 Mm) of NaCl concentrations in certain conditions. It was shown that using a **sugar alcohol** (i.e mannitol, glycerol, etc.) in the media helps to prevent osmotic stress allowing thraustochytrids to grow normally, as shown in Figure 1.7. These results also suggest the possibility of cultivation using low NaCl concentration. This would be beneficial for industrialization of the culture, because higher salinities lead to corrosion of steel bioreactors.

Salinity adaptability of thraustochytrids opens a potential opportunity to develop an industrial biotechnological production of n-3 PUFA using crude glycerol.
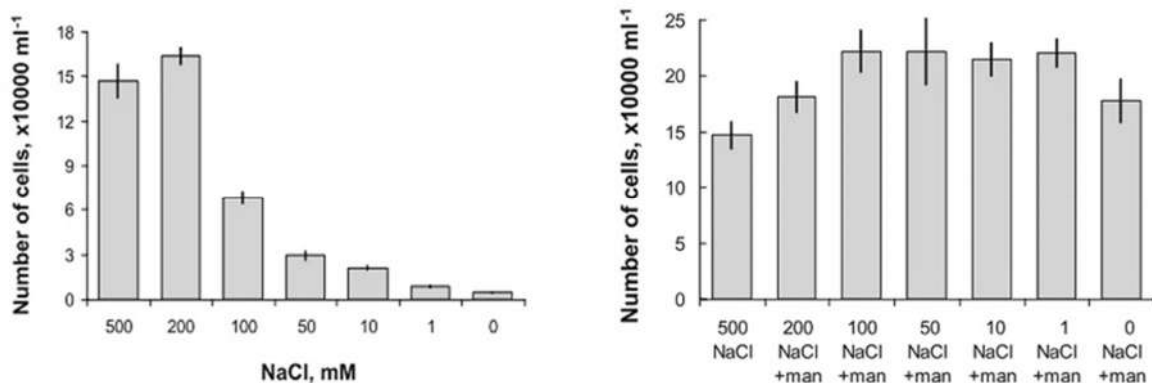
Figure 1.7. Left- The performance of a thraustochytrium culture using different salinities in the media. Right – The same experiment with mannitol. Data from Shabala et al. (2009) *[133]*.

1.5   Crude glycerol as a carbon source

Make DHA biotechnological production cost effective

Although several factors impact a bioprocess upstream cost (e.g. oxygen supply, power, etc.), the carbon source could typically represent more than 50% of the total direct cost of production. In other words, the yield of a process (g product/g substrate) is "a strong driver of cost". Industrial R&D efforts often aim at the optimization of the product yield (part of the objectives of this work, detailed in chapter 3 and 4). According to the bibliography, a maximum (theoretical) yield of 0.20 – 0.24 g DHA / g glycerol[29] could be obtained in bioreactors. In flask cultures the yield might be much higher as reported in Table 1.4.

Almost equally important is the ability of a microorganism to utilize different carbon sources. While corn syrup is still the major carbon source for industrial processes in the United States, carbon sources elsewhere are sucrose from sugar cane, sugar beet, or molasses. Alternatives such as whey from the soymilk industry or **crude glycerol** from biodiesel productions currently complete the list. At the same time, adaptability to carbon sources opens the possibility of changing the feedstock depending on different renewable feedstock values in the market. This adaptability gives a singular robustness to the DHA production process as well as a reduced cost, which would help for an industrial implementation.

Further efforts to lower carbon source costs play an important role in the overall development of the biorefinery concept[30]. Much knowledge has been gained, and significant progress has been made on the saccharification of cellulosic biomass to fermentable sugars for their subsequent bioconversion to chemicals. As a result, such processes are coming closer to commercial reality, which will provide a new, renewable feedstock for bioprocess.

Crude glycerol can be used directly as it comes out of the production plant, or after a simple purification step to eliminate soap and methanol as reported in different works [131] (explained in Chapter 3). Although it has been described in this introduction and in many bibliographic works [8], that crude glycerol can support the growth and DHA production using *A. limacinum* (12). In general, the composition of crude glycerol varies from plant to plant. Although the biodiesel manufacturing process does not involve any heavy metals, the oil feedstock may contain trace amounts of heavy metals, which may eventually end up in algal cells [93].

44

---

[29] According to bibliography, 0.3 g of DHA / g of biomass represents a natural limit. On the other hand, and a maximum yield of 0.8 g biomass / g glycerol leads to 0.24 g DHA / g glycerol as a theoretical limit.

[30] Biorefining refers to fractionating biomass into various separated products that possibly undergo a further biological, (bio)chemical, physical and/or thermal chemical processing and separation. By means of co-producing relatively (high) value chemicals (e.g. fine chemicals, pharmaceuticals, polymers) the production costs of secondary energy carriers (e.g. transport fuels, heat, power) potentially could become market competitive

1.5.1.1 Effects of impurities in waste glycerol

Crude-glycerol as a model to face of industrial waste stream valorization.

Crude glycerol is synthesized as a by-product of biodiesel production. The main impurities of crude glycerol are methanol, soap, salts and free fatty acids. Biodiesel refineries typically use an excess of methanol as a co-reactant, resulting in higher transesterification reaction productivity in terms of methyl esters (biodiesel). Soap is commonly generated due to a side reaction involving the free fatty acids in the feedstock [134,135]. Salts represent another common contaminant in crude glycerol. Many monovalent salts coming from the catalyst are accumulated in the crude glycerol. When used for cultivations, it decreases van der Waals force in lipid membranes and cause swelling of the cell membrane [136]. Other contaminants might be found in waste-glycerol, but in lower amounts or traces **depending on the feedstock** used [20,93,131]. Calcium, potassium, magnesium, phosphorous, sulfur and sodium are common examples. The remaining free fatty acids present in the crude glycerol are normally absorbed by thraustochytrids. Biodiesel obtained from vegetable oils generates a waste-glycerol that is rich in palmitic, oleic and linoleic acid. Some microorganisms can use such long fatty acids as a substrate to ultimately obtain longer polyunsaturated fatty acids such as DHA [137,138].

In some cases, crude glycerol is contaminated with ethanol. Surprisingly, it was found to be beneficial, stimulating the growth of some microalgae dedicated to PUFA production [139]. Nevertheless, biodiesel production using ethanol as a co-reactant is less efficient than methanol. Unfortunately, methanol negatively affects both microalgae growth and PUFA production. When methanol effects were investigated, the maximum dry cell weight, biomass productivity and cell yield decreased as the alcohol concentration was increased. However, the fatty acids profile or DHA/total fatty acids ratio remained constant [131]. Therefore, it is strongly recommended to eliminate methanol from the media. It is possible to evaporate methanol when autoclaving the media at lab scales. In large-scale production, methanol could also be evaporated during the sterilization process conveniently venting the reactor. Soap impurities have been shown to significantly impact cell growth and fatty acid composition, which has been observed by comparing soap-containing and soap-free cultures. However, soap impurities can be potentially removed with the addition of a strong acid during the media preparation coupled with a filtration process (as described in Chapter 2).

1.6   General objectives

The aim of this thesis was to develop a biotechnological process to provide contaminant-free n-3 PUFA through *Auranitochytrium limacinum cultivation*, while using industrial byproducts as carbon source. Four stages compose the thesis that are grouped in chapters.

The first stage included the procurement of basic knowledge and the development of tools for thraustochytrids bioprocess development (Described in Chapter 2). Establishing the knowledge base for the heterotrophic microorganisms handling and its cultivation. Moreover, the identification of cell cycle characteristics of *Aurantiochytrium limacinum* SR21 in bench scale bioreactors was an important requirement. According to bibliography, thraustochytrids can produce other added-value metabolites and in this thesis it was investigated.

Monitoring tools are very important in order to develop any bioprocess. Therefore, the second part of the first stage consisted in:

➢ Developing and validating a high throughput screening like methodology to quantify DHA production from large amounts of samples.

➢ Developing and validating a fast and cheap method for glycerol consumption monitoring.

Once the basic tools and knowledge was set up, next objective was to develop a DHA prolific production and cost effective medium for thraustochytrids (Described in Chapter 3). The medium had to be suitable for large scale production. The medium development includes:

➢ Comparing different carbon sources with crude glycerol.

➢ Modeling and optimization of carbon / nitrogen ratio considering cost and DHA productivity.

➢ Investigation of vitamin requirements.

➢ Substitution of TRIS by an affordable buffer at industrial scale.

➢ Adjustment of salt composition considering cost and DHA productivity, while maintaining scalability and viability of the process.

When the media was established, developing the upstream bioprocess was the next step – Batch and Continuous production of DHA and its implications using *Aurantiochytrium limacinum* SR21 (Described in Chapter 4). This stage included the following objectives:

➢ Exploring different bioprocess strategies to find the most prolific operating system: Batch, Fed-batch, continuous or multi-stage continuous.

➢ Modeling best agitation and aeration parameters for biomass and DHA production.

➢ Determination of proper temperature and pH cultivation.

➢ Determination of *Aurantiochytrium limacinum* SR21 implications for a better production of DHA.

DHA purification was the last step. The objective was to establish an approach for a green-like process scale purification process of unmodified triglycerides containing DHA. Thus, representing a source of a novel unmodified DHA-TG (Described in Chapter 5). This stage is composed of the following objectives:

➢ Developing a purification method for unmodified TG (containing DHA) purification, in order to produce the very first standard of those TG.
➢ Developing a scalable downstream approach of process chromatography for DHA purification.
➢ Comparison of *A. limacinum* extracted oil and commercial oil contaminants content.

This page intentionally left blank

Chapter 2: Knowledge base for thraustochytrids bioprocess development

Thraustochytrids handling and analytical methodology

2.1   Introduction

Only a few labs in the world have ever worked and investigated thraustochytrids. Even now, long after many references have certified their potential as cell factories, thraustochytrids are still not well characterized. Only a few countries have laboratories in which the investigation of thraustochytrids industrialization is currently taking place. The United States and China are strongly active in this regard. Some companies in these countries have already started marketing omega-3 oils that are made from *Schizochytrium* sp. and *Ulkenia* sp. [103].

Chapter 1 of this paper described the specific capacity of thraustochytrids to produce n-3 PUFA and revalorize crude glycerol, specifically *A. limacinum*. However, the cultivation of thraustochytrids brings new challenges. Thraustochytrids are marine eukaryotic microorganisms, which means that cultivation requirements are drastically different from typical bacteria and yeast cultures. Slower growth rates, significant medium requirements, different parameters, different morphology; everything was new for a laboratory that was used to working only with yeasts and bacteria.

In the early phases of the research for this study, it was not possible to find anyone in the area who was familiar with these types of microorganisms. It was necessary to investigate basic procedures and equipment that was discussed in the literature, to maintain, grow and work with thraustochytrids. Once the equipment had been acquired and prepared and a basic procedure established, six different thraustochytrids were purchased*; Thraustochytrium aureaum, Aurantiochytrium limacinum, Aurantiochytrium mangrovei, Ulkenia amoeboide, Sicyoidochytrium minutum and Botryochytrium radiatum*. These thraustochytrids were selected as potential producers of added-value metabolites such as PUFA, pigments and squalene. As discussed in Chapter 1, *A. limacinum* was selected because it appears to be the most prolific producer of DHA, which is the main objective of this thesis.

Basic analytical methodologies are essential for proper bioprocess development. Analytical chemistry allows the evaluation and monitoring of any investigation. Like many other bioprocess engineering developments, this study required the measurement of substrate consumption, product formation and the analysis of microorganism morphology and behavior. In the literature, many classical methodologies can be found regarding substrate consumption monitoring, none of which referred to a saline medium, or offered quick methods to process several samples simultaneously. Therefore, analytical methodology was needed to quantify glycerol consumption during cultures.

Monitoring substrates help the kinetic characterization of the microorganisms, but the product is what governs the entire development. Therefore, FA and DHA quantification methods were needed. Almost all of the documented methodologies about FA quantification, are based on old and unsuitable methods such as the Bligh and Dyer lipid extraction procedure [16,44,49,51,140–146]. Many other methods only refer to FA as a percentage of the gas chromatography signal[31],

50

---

[31] Not considering that the method might not be sensitive enough for all FA species in the profile.

without quantification. Because the biotechnological process developed in this study requires a very precise and reliable method to quantify DHA, a new and customized technique has been developed.

Thraustochytrids certainly have a complex life cycle that needs to be considered for an industrial process. In order to learn, monitor and investigate *A. limacinum* life cycles during bioreactor cultivations, certain basic microbiology procedures (i.e. microscopy) have been combined with image processing techniques. A Matlab®® algorithm has been adapted to analyze the cell phenotypes of *A. limacinum* as well as to measure cell dimensions.

The main objective of this thesis is to document a bioprocess development. The present work provides information about different optimization techniques such as general DoE, Taguchi methods, artificial neural networks (ANN) and response surface methodology (RSM). These techniques are detailed in Appendix A.

2.1.1 Glycerol quantification and monitoring

Thraustochytrids growth kinetics are substrate-dependent, therefore the calculation of growth related parameters that are essential for bioprocess engineering require a carbon source quantification. Currently, many labs and companies determine glycerol concentrations using techniques based on separation (liquid chromatography), enzymatic techniques and potentiometric methods [147]. When developing a bioprocess, monitoring carbon source requires reliable, inexpensive and particularly rapid methodologies to quantify the residual glycerol. A large number of samples are typically generated, and monitoring is crucial to the decision-making process during batch, fed-batch or continuous operations.

High performance liquid chromatography (HPLC) is widely used to analyse glycerol content in fermentation media because it offers high accuracy. Enzymatic based kits are also popular in glycerol based fermentations [38,52,93,148]. Enzymatic kits might offer less accuracy compared to HPLC, and could result in a direct cost per sample analysed. Both methods are time consuming with a delayed response. Current HPLC methodologies take approximately 30 minutes, from sample preparation injection to peak analysis. Depending on the column, the time can be reduced from 30 minutes down to 15 minutes per sample. Enzymatic kits work faster than HPLC methods, but the cost per each assay is relatively high. Cost might discourage an exhaustive monitoring due to the number of samples. Potentiometric methodologies are simple and cheaper than HPLC and enzymatic kits. However, these methodologies require sample volumes and would not be suitable for simultaneous monitoring of different cultures. The nature of the samples to be analysed can be crucial when selecting the method. Medium composition (e.g. high salinity and organic compounds) or metabolites that are generated may introduce errors or invalidate the methodology. For the specific case of enzymatic kits, the interference of the metals present in the medium could also mislead the determination. Potentiometric methods would not be applicable in the presence of organic compounds (e.g. yeast extract or metabolites produced) containing more than two hydroxyl groups on adjacent carbon atoms [149].

51

This dissertation introduces a method that was developed to monitor either pure or crude glycerol residual concentration from thraustochytrids cultivation samples. This method relies on a **Dot Blot** assay **(DB)**[32] coupled with image processing algorithms using Matlab®® R2011a (The MathWorks Inc., Natick, MA, 2000). The method was reported to quantify residual glycerol in biodiesel samples, using Thin Layer Chromatography (TLC), presenting several analogies [150]. In this study, the simple DB developed assay had specific staining adapted and validated for a bioprocess development in an aqueous medium with high salinity. Subsequent image processing and analysis has the advantage of rapid output with enough accuracy for bioprocess monitoring with a short response time. The new method was proofed during crude glycerol fermentations, comparing the three methods (HPLC, enzymatic kit and DB coupled with image processing method).

2.1.2   Fatty acids determination and quantification

There is a large number of bibliographic references describing fatty acids profile determination and the DHA quantification. Despite this, the development of an adapted analytical method is critical. It is essential to have an exhaustive, reliable, efficient and precise analysis. In this case, the method needed to be reliable in all of the steps, starting with the sample preparation and its posterior analysis. As a new method, every initial assumption was made based on the literature, such as the estimated product concentration, extraction, FA derivatization[33] and analysis process. There are many well-documented procedures to extract and analyse fatty acids from different matrices, but only a few focused on microalgae. Indeed, it was not possible to find any well documented procedures to extract fatty acids from thraustochytrids. Some of the methods were based on Bligh and Dyer [151], but imprecise. The developed method is used exclusively for thraustochytrid analysis and its validation will be thoroughly discussed in this chapter.

52

The most extensive, straightforward and well-documented FA analysis procedures are based on gas chromatography (GC). FA are not volatile enough to be analyzed by GC, and require a derivatization, which includes a transesterification. Transesterification is the general term used to describe the important class of organic reactions in which an ester is transformed into another through the interchange of the alkoxy moiety[34]. When working with TG in a transesterification reaction, FA react with an alcohol in the presence of a strong acid or base, producing a mixture of fatty acids, alkyl esters and glycerol. The overall process is a sequence of three consecutive and reversible reactions, in which diglycerides and monoglycerides are formed as intermediates. The stoichiometric reaction requires 1 mol of a triglyceride and 3 mols of the alcohol. Generally, an excess of the alcohol is used to increase the yields of the alkyl esters, and to allow a phase separation from the glycerol formed. In this thesis, Fischer-Speier esterification was selected, due to its relative simplicity Box 2.4.

---

[32] Dot Blot Is a technique that is used to detect biomolecules with a single sample droplet. In a Dot Blot, the biomolecules to be detected are not first separated by chromatography, such as in a TLC.

[33] The transesterification of fatty acids to fatty acid methyl esters is using an alkylation derivatization reagent.

[34] An alkyl (carbon and hydrogen chain) group singularly bonded to oxygen.

> ### *Box 2.4. Fischer-Speier esterification*
>
> Fischer-Speier esterification commonly called Fischer reaction is a special type of esterification by refluxing a carboxylic acid and an alcohol in the presence of an acid catalyst. The reaction was first described by Emil Fischer and Arthur Speier in 1985 [239]. Most carboxylic acids are suitable for the reaction, but the alcohol should generally be a primary or secondary alkyl. Methanol and ethanol are more commonly used than any other alcohol for PUFA esterification. Sulphuric and tosylic acids are commonly used as catalysts. The reaction is commonly carried out without a solvent but for the application of the work described here, a non-polar solvent is used to facilitate subsequent steps. The figure below shows generic reaction performed in this work, for analytical purposes.
>
>
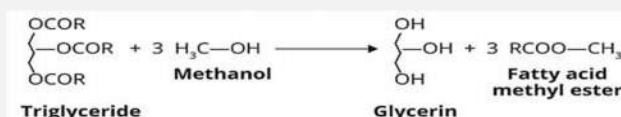
During bioprocess development, a large number of samples are generated, and rapid monitoring is crucial to decision-making in the upstream. In the case of fatty acids determination (which will be discussed in upcoming sections in this chapter), a minimum of steps are required due to the intracellular condition of major FA in thraustochytrids and the derivatization required to analyse them by chromatography. The initial development steps were based on work from Indarti *et al.* (2005) [152]. Indarti *et al.* reported a method that was used to quantify every FA from fish samples. This also included the extraction of FA and its derivatization using glass balloons in a silicon oil bath. After this step, the resultant derivatized sample needed to be purified using a decantation funnel. This method, which is based on glassware, requires a whole process cycle per sample. In other words, all of the steps must be performed to process a single sample, which becomes a very time consuming method.

In this thesis, a "4 steps in 1" method has been developed. It includes cell disruption, release of TG, release of fatty acids from TG, derivatization of released fatty acids into methyl esters and the purification from the sample matrix. All this steps are performed in the same recipient. This is a significant improvement on the initial Indarti *et al.* method. More importantly, this new method can handle several samples at the same time. This allows the analysis of "all samples" from a bioreactor to be performed under the exact same conditions. Moreover, it was developed for a HTS-like procedure. Instead of large volume glassware, the method uses 1.5 mL vials per sample. In order to find near-optimal conditions to perform the whole sample preparation process, different Taguchi methods (see Appendix A) were applied.

2.1.3 Life cycle characterization in batch cultures

Generally, a bioprocess implies the production of biopharmaceuticals or bioproducts by using microorganisms with simple and plain life cycles. The most widely used microorganisms are *E. coli* (many different strains) and *S. cerevisae* together with *CHO* mammalian cells, which do not require life cycle biology. The new interest in complex microorganisms such as *thraustochytrids* requires a deeper investigation on their life cycle during batch and continuous reactors, thus adding to the basic knowledge of thraustochytrids. Moreover, every life cycle stage can serve as an indicator of alterations during the bioprocess. In this chapter, the characterization of *A.*

limacinum will be discussed (section 2.2.3), focusing on growth rates and the stage with the highest amount of accumulated DHA.

2.1.3.1 Matlab® image processing as a tool to assist bioprocess development

MATLAB®® is a high-level language and interactive environment that is used by millions of engineers and scientists worldwide. It allows researchers to explore and visualize ideas across many disciplines including image processing. Matlab® has been used during this study as a support tool to precisely analyse Dot Blot and microscopy images. Matlab® that is applied to Dot Blot allows researchers to perform a precise and rapid calculation of glycerol consumption during a bioreactor [147] Appendix B. A second Matlab® script has been used to measure cell dimensions from microscope observations Appendix C.

2.1.4 Other added-value metabolites produced by A. limacinum

Thraustochytrids are known for having a great capacity to produce n-3PUFA in general. However, this family of microorganisms have the capacity to produce other added-value metabolites such as squalene, astaxanthin and carboxylic acids.

Squalene (2,6,10,15,19,23-hexamethyltetracosa-2,6,10,14,18,-22-hexane; C30H50) is a biosynthesized triterpene hydrocarbon and a precursor for all steroids in animals and plants[118]. Squalene is an important intermediate in the endogenous synthesis of cholesterol, and it is known to be a natural antioxidant and possesses cancer-preventive properties [153]. It is currently used as an important ingredient in the cosmetic industry because of its effectiveness. Squalene is also used in the pharmaceutical and medical industry because it increases cellular and non-specific immune functions, decreases serum cholesterol levels, protects against gamma rays, and suppresses tumour proliferation [118]. Liver oils of deep-sea sharks represent the richest source of squalene and are still the major commercial source of this product. The continuous supply and availability of the liver oils, however, are in doubt because of the concerns over the preservation of marine wildlife and fishery. Therefore, thraustochytrids offer a new opportunity for a clean and sustainable source of squalene.

Astaxanthin (3,3'-dihydroxy-β,β-carotene-4,4'dione) is a carotenoid that is specifically found in marine crustaceans (absorbed through microalgae). Astaxanthin is a natural antioxidant, which prevents the oxidation of surrounding molecules. It is generally added to food products and is the preferred pigment that is used in the feed for salmonid fish such as trout and salmon. *Schizochytrium aggregatum* and *Thraustochytrium CHN-1*, have both been found to contain this pigment [47]. However, this study has demonstrated that *A. limacinum* SR21 can produce astaxanthin under specific culture conditions. Other microorganisms, such as *Haematococcus pluvialis* produce massive amounts of astaxanthin in well-established industrial processes [154,155].

Carboxylic acids such as **Pyruvic** acid and **Oxalic** acid production was detected when *A. limacinum* is grown in continuous bioreactors (see section 2.3.4). These organic acids have different industrial applications. Oxalic acid has many applications such as for beekeeping [156] and

54

extractive metallurgy [157]. Pyruvic acid has not yet been applied on a large scale. However, a derivative bromopyruvic acid is being studied for potential cancer treatment applications by researchers at Johns Hopkins [158].

2.2   Results and discussion

2.2.1   Quantification and rapid monitoring of glycerol/crude-glycerol in *A. limacinum* cultures

A general method to analyse residual free glycerol in harsh conditions (artificial seawater and usage of byproducts) has not been documented. In this work, a Dot Blot methodology that enables glycerol detection and quantification has been developed and compared to conventional HPLC and enzymatic methods [147]. The results from the sample and reagents preparation, as well as sample processing were evaluated in terms of assay attributes as explained in Appendix A. Initially, an artificial sea water medium with known crude glycerol concentrations was tested to validate the methods. Then, the three methods were simultaneously used to monitor the residual crude glycerol concentration from a culture using an artificial seawater medium in a benchscale bioreactor.

2.2.1.1   Glycerol determination using HPLC

A typical chromatogram corresponding to a known concentration of crude glycerol in an artificial sea water medium (without cells), has a peak at a retention time of 11.2 minutes, which can be attributed to salts and other compounds in the artificial seawater medium. The peak appearing at 20.8 minutes corresponds to glycerol (see supplementary material S1). The glycerol peak is separated with near-baseline resolution, without any interference from other components of the medium. Therefore, this is a specific and selective method of identifying crude glycerol. Then, in order to evaluate specificity and selectivity, samples were compared in terms of the recovery % (*Table 2.6*). No significant interference was detected. Thus, the method could be considered specific and selective for glycerol regardless of the source and medium composition.

Table 2.6. Specificity and selectivity of HPLC-RID for glycerol determination, comparing recovery values (%) with different conditions.

	%Recovery	StD	%CV	
Commercial glycerol + H_2O	99.8	0.6	0.6	HPLC-RID
Crude glycerol + H_2O	97.6	1.1	1.1	
Commercial glycerol + Medium	98.3	0.9	0.9	
Crude glycerol + Medium	96.9	1.5	1.5	

To evaluate the linearity, accuracy and repeatability of the entire sample processing and HPLC-RID analysis, a calibration curve of eight different glycerol concentrations (triplicates) was performed. Artificial sea water medium with crude glycerol samples where quantified and found

55

to be linear (R^2>0.999). Table 2.7 summarizes the results of Response Units (RIU) vs. glycerol concentration (g/l) calibration curve. The slope ± standard error was found 171259 ± 2150 and the intercept ± standard error 54940 ± 12059. The method is linear in the range of 0.68 g/L to 12.5 g/L. In order to evaluate its accuracy, the mean bias (%RE) was calculated. %RE corresponds to the percentage difference between the value determined with the analytical method and the known concentration (weighted) of the standard used. The mean bias was between 1.2% and 11.6%. The repeatability was examined by measuring the variation between 6 replicas at each

Table 2.7 Precision and accuracy for glycerol quantification by HPLC-RID.

Glycerol (g/L)	Mean response	SD	%CV	Concentration found g/L	Mean bias %RE
0.5	1.57E+05	2.15E+03	1.4	0.56	11.60
1.0	2.30E+05	5.32E+03	2.3	0.99	1.27
2.5	4.76E+05	2.12E+03	0.4	2.43	2.83
5	8.93E+05	6.36E+03	0.7	4.88	2.46
7.5	1.33E+06	7.07E+03	0.5	7.42	1.12
10	1.79E+06	7.07E+03	0.4	10.14	1.36
	Mean (%)		0.9	Mean (%)	3.44

concentration (Table 2.7). Repeatability ranged between 0.4 and 2.3% (CV) at low and high glycerol concentrations respectively. The detection limit was found to be 0.2 g/L and the quantification limit 0.68 g/L of crude glycerol. Consequently, this method can detect and quantify minimal glycerol concentrations from a culture and detect the complete depletion of the carbon source.

HPLC is an excellent technique in terms of precision and accuracy. However, it requires considerable time to analyse each sample. The HPLC-RID methodology that has been discussed in this study, typically takes 30 minutes per sample. When monitoring cultures that might last several days, many samples need to be collected and analysed, which delays the outcome when quick decision-making is required. The chromatographic time can be reduced to 15 minutes using a different stationary phase (not available for this work). The HPLC-RID method showed suitable performance when analysing high salinity samples. Additionally, the contaminants present in crude glycerol did not interfere with the analysis.

2.2.1.2 Glycerol determination using an enzymatic kit

Many labs currently prefer to use a glycerol detection kit, which is based on enzymatic reactions. These kits offer faster quantifications than those based on HPLC methods. In this work, a K-GCROL (Megazyme International) kit was used. In approximately 20 minutes, the residual glycerol concentration of a cultivation sample can be determined. In order to compare the results obtained with HPLC determinations, the enzymatic method was validated in the same manner.

The results from sample and reagent preparation, as well as sample processing were evaluated in terms of assay attributes as described in section 2.1.1.2.2.

Specificity and selectivity were evaluated by comparing the results of the same concentration of crude and pure glycerol diluted (dilution factor 1:100) in Milli-Q water. A positive agreement was observed in the results (Table 2.9), which showed good recovery values. The method was found to be linear in the range of 0.01 g/L to 0.1 g/L of crude glycerol ($R^2 > 0.998$). Therefore, cultivation samples needed to be conveniently diluted in order to fall into this range. The slope ± standard error was found 0.0101 ± 0.0003 and the intercept ± standard error was -0.0003 ± 0.0018

Table 2.9 Specificity and selectivity of the enzymatic kit for glycerol determination, comparing recovery values (%) with different conditions.

	%Recovery	StD	%CV	
Commercial glycerol + H_2O	100.1	0.4	0.4	Enzymatic kit
Crude glycerol + H_2O	99.8	0.5	0.5	
Commercial glycerol + Medium	99.2	0.4	0.4	
Crude glycerol + Medium	99.7	0.6	0.6	

Absorbance Units (AU) vs. glycerol concentration (g/l). The enzymatic kit was found to be specific for glycerol, but it was not originally conceived to test high salinity media samples. However, the dilution required to fall into the analysis range allows acceptable conditions to host the enzymatic process and no evidence of interference with the enzymatic reactions was detected (Table 2.8).

Table 2.8. Precision and accuracy for glycerol quantification using a commercial kit.

Crude Glycerol g/L	Mean Response	SD	%CV	Concentration found g/L	Mean bias %RE
1	3.8	0.08	2.11	0.77	23.2
2.5	4.6	0.29	6.30	2.63	5.4
5	5.7	0.11	1.93	5.20	4.0
7.5	6.7	0.12	1.79	7.53	0.4
10	7.7	0.40	5.19	9.87	1.3
		Mean (%)	3.5	Mean (%)	6.9

Accuracy and repeatability were also evaluated. The %RE was always ≤ 4.58. The maximum variability was found to be 0.71%. This corresponds to a variation of 0.008 g/L for the most diluted samples. The detection limit was set to 0.008 g/L, and the limit of quantification to 0.1 g/L. Thus, the enzymatic kit could be considered as an accurate and precise method under the conditions assayed.

While offering similar performance, enzymatic kits work faster than HPLC methodologies and do not require special equipment. Nevertheless, considerable manual sample processing is required, which dissuades the usage of kits when a large number of samples need to be analysed. The kits

are a good option for punctual glycerol determination, but have drawbacks for bioprocess development and fermentation monitoring. The cost of enzymatic kits for glycerol determination might represent an additional drawback. This is especially true for studies that are focused on media, strains screening, or bioprocess development, in which sampling and analysis are extensive.

2.2.1.3 DotBlot assay validation

As an alternative, a thin silica gel layer was used as a support to perform a DotBlot assay. In a DotBlot, the typical TLC[35] elution is not performed due to the absence of unsaturated compounds or alcohols secreted by the microorganisms used. To visualize the spots, a permanganate solution was chosen, which oxidized glycerol and formed yellow spots (Table 2.10). In order to accelerate the reaction, the spots were heated to 100ºC.The intensity and size of the spot was found to be proportional to the glycerol concentration.

Table 2.10. Specificity and selectivity of the DotBlot assay for glycerol determination, comparing recovery values (%) with different conditions.

	%Recovery	StD	%CV	
Commercial glycerol + H_2O	98.7	0.9	0.9	
Crude glycerol + H_2O	97.8	1.2	1.2	DotBlot assay
Commercial glycerol + Medium	97.5	1.4	1.4	
Crude glycerol + Medium	97.1	1.1	1.1	

Once the DotBlot was stained, it was scanned and the image obtained was analysed using Matlab®® (script can be found in Appendix B). The analysis of the image f(x,y) was divided into three differentiated stages: normalization, segmentation and calculation. Normalization prepares the image for the segmentation process over the spots and guarantees repeatability to the method. The normalization results are strongly dependent on the quality of the staining process. Therefore, it is important to use the same permanganate solution in every batch. For this reason, the same permanganate solution was used and preserved using potassium carbonate to ensure freshness until the end of the culture. Once the normalization was done, a segmentation was performed. Segmentation is typically needed to apply the suitable Matlab®® function to calculate the area and intensity of each spot. The segmentation process differentiates the spots from the background of the image f(x,y) (Equation 1.1) based on a global threshold (T value).

$$f'(x,y) = \begin{cases} 1 \ if \ f(x,y) \ \geq T \\ 0 \ if \ f(x,y) \ < T \end{cases} \qquad\qquad \text{Equation 1.1}$$

---

[35] Thin layer chromatography
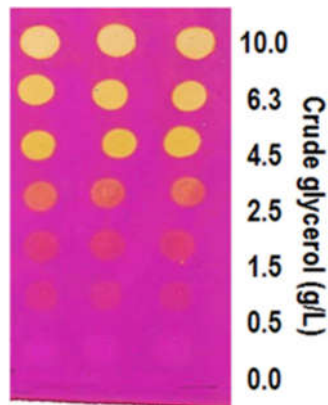
Figure 2.8 Dot Blot assay of crude glycerol standards (triplicates), stained with sodium

Finally, the calculation step determines the area and intensity values of each labelled spot. The method needed to be experimentally calibrated and validated using known concentrations of glycerol (using standard samples such as those in Figure 2.8).

The **validation** was performed with crude glycerol. As seen in Figure 2.8, the first row belongs to samples of 10 g/L glycerol, generating the brightest spots. The next rows of spots correspond to the decreasing concentrations of glycerol. The last row of spots corresponds to samples of artificial seawater in which the glycerol was already depleted (no colour change). Consequently, the methodology could be considered specific for glycerol, without interference from other components of the growth media. The results are detailed in Table 2.11. Furthermore, the specificity was evaluated by comparing the samples using pure glycerol and purified crude glycerol diluted in water or medium. The recovery % (Table 2.6,Table 2.9 and Table 2.10) values were stable for all samples, which confirms the specificity and selectivity of the methodology.

Table 2.11 Precision and accuracy for glycerol quantification using a commercial Kit.

Crude Glycerol g/L	Mean Response	SD	%CV	Concentration found g/L	Mean bias %RE
1	3.8	0.08	2.11	0.77	23.2
2.5	4.6	0.29	6.30	2.63	5.4
5	5.7	0.11	1.93	5.20	4.0
7.5	6.7	0.12	1.79	7.53	0.4
10	7.7	0.40	5.19	9.87	1.3
		Mean (%)	3.5	Mean (%)	6.9

The DotBlot assay was found to be linear from 1.5 g/L to 10 g/L ($R^2>0.998$). The slope ± standard error was 0.428 ± 0.012 and the intercept ± standard error was 3.471 ± 0.075 in response to arbitrary units vs. glycerol concentration (g/l). Table 2.11 summarises the results by evaluating the repeatability and accuracy between replicas and the calculated mean bias. The maximum variability among samples was below 7% (e.g. variation for the most diluted samples would be equal to 0.141 g/L). The %RE was ≤ 5.3% for samples above 2.5 g/L glycerol. The limit of detection was 0.5 g/L and the quantification limit was 1.5 g/L of glycerol. Below the threshold of 1.5 g/L, the method became less accurate in terms of quantification, but it was still sufficient to monitor glycerol during a fermentation.

2.2.1.4 Method comparison using fermentation broth

In order to evaluate whether the DotBlot capabilities were the same as the HPLC and the kit methodologies, *A. limacinum* crude glycerol consumption was monitored during the
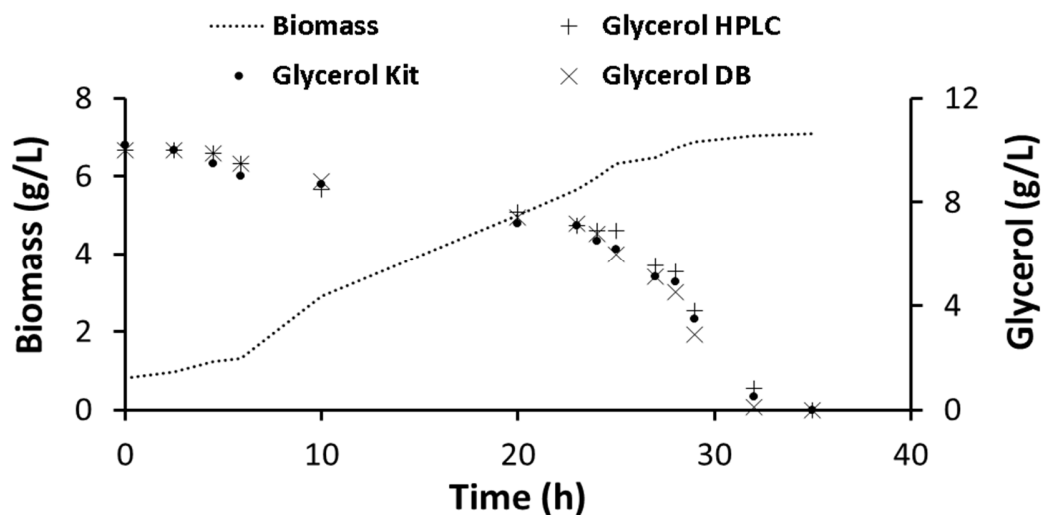
Figure 2.9 Substrate consumption measurements using three different methods. HPLC-RID, enzymatic kit and Dot Blot assay.

fermentation process. Several samples were taken at different times during the cultivation. Samples were analysed independently using each methodology. All samples were processed at the same time to reduce the variability.

As can be seen in Figure 2.9, all methods resulted in similar values of residual glycerol. The DotBlot assay gave slightly lower values towards the end of the culture, compared to the HPLC-RID and the kit. The total time needed to analyse all of the samples with HPLC-RID was 6 hours, 3 hours were needed using the enzymatic kits, whereas the DotBlot method required only 15 minutes. Thus, the three methods offer similar results, but the Dotblot offers faster and cheaper determinations and reduces sample manipulation.

2.2.2 Fatty acid determination and DHA quantification with High Resolution Gas Chromatography (HRGC)

For the development of this specific bioprocess a DHA quantification capacity was considered essential. Every improvement that will be applied in the successive chapters of this thesis, is mainly based on biomass and DHA measurements. For this reason, it is of vital importance that **a fast, reliable and precise** method is developed to quantify one of the most important PUFA.

2.2.2.1 Initial method: single sample per run

The first step was to determine the basic conditions needed to extract and transesterificate fatty acids contained in *A. limacinum* biomass. Indarti *et al.* (2005) [152] was chosen as the basis for this development, because their method was able to extract TG and transesterificate FA from fish samples. Therefore, a similar performance could be expected with microalgae biomass. The main feature of Indarti et al's work is the transesterification mixture (1.7:0.3:2.0 v/v/v) together with the heating process. For this study, different ranges of time and temperature were chosen. To
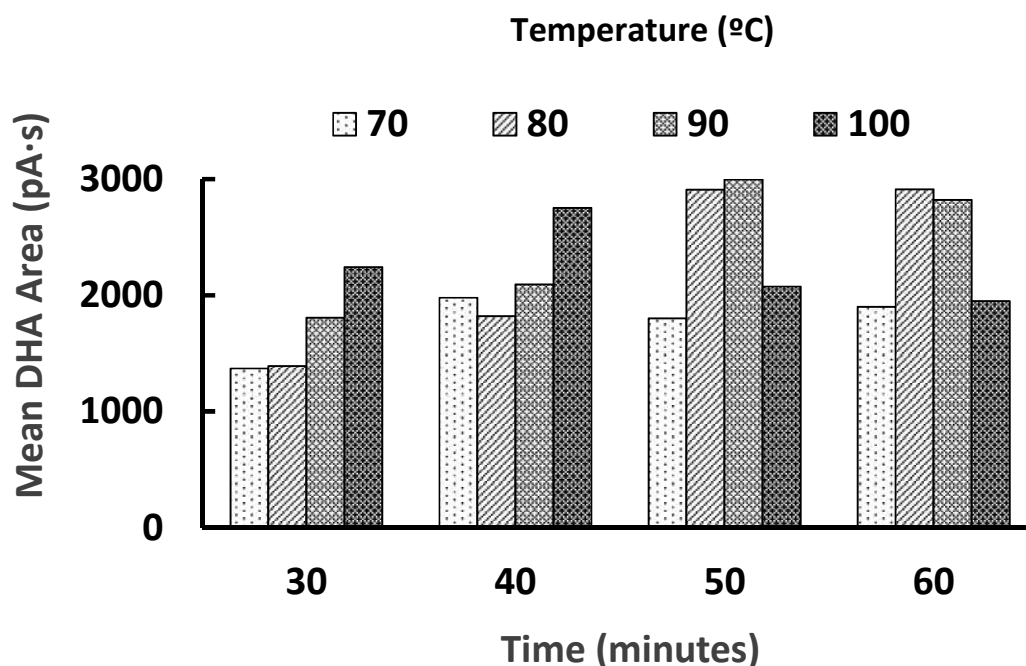
Figure 2.10 Summary of the results obtained in the full factorial experiment. The table shows the experimental table, with different times and temperatures. The response is equivalent to the mean value of 48 experiments (3 replicates). The plot above shows the values of every mean response among the time of reaction. Each set of data corresponds to a reaction temperature.

complete this study, a full factorial DoE was performed. The range of the investigated temperatures was from 70 to 100 °C during 30, 40, 50 and 60 minutes. The responses used corresponded to the relative abundance[36] of DHA as measured by the FID detector. Every sample was processed equally and injected using the same volume. This way, the difference in concentrations could only be attributed to the investigated factors. The retention time of DHA was previously determined using a methyl ester standard (Sigma-Aldrich, ref. 05832). The standard was analysed with the same method. Results are depicted in Figure 2.10.

As can be seen in Figure 2.10, there is a positive correlation between the amounts of DHA detected (response) and the time of reaction. This value reached a plateau after 50 minutes of reaction, which indicates that the optimal time of reaction is near 50 minutes; somewhere between 40

---

[36] Refers to the area of the DHA peak compared to other extractions.

and 60 minutes. The optimum temperature appears to be around 80 - 90 °C. These results are in concordance with the data found in the study by Indarti *et al.* [152] in which the optimum values are approximately 50 minutes of reaction with a temperature of 90 °C. On the other hand, there was a reduction in the values after 50 minutes if the reaction temperature was above 90 °C. This might indicate that some FAME experienced a process of degradation. In the research from Indarti *et. al.,* a similar phenomenon was reported. There was a reduction in the recovery of FAME. As suggested by the results indicated in Figure 2.10, the samples needed to be processed at 90 °C for 50 minutes.

At this point in the research, the sample preparation and analysis method of FA and DHA were sufficiently precise (but not fast) for the initial bioprocess development. This included the preliminary flask cultures and other bench scale investigations. Because the derivatization reaction was conducted in a 10 mL glass balloon with exhaust refrigeration, it only allowed one sample to be processed per run. This appeared to be a significant problem because *A. limacinum* culture experiments began to generate multiple samples. At a certain point, the sample preparation became a bottleneck to the development.

2.2.2.2 Development of an HTS –like method for the analysis of FA and DHA

When the research started requiring several samples per experiment, due to an increase in the amount of *A. limacinum* cultures, the original method caused a bottleneck. An individual culture required 4 or 5 samples. Because there were 3 replicates per sample, this meant that a single flask generated a minimum of 12 samples. At that moment, it was essential to develop a method that functioned in the same way as an HTS-like method, enabling to process different samples at the same time. Modifications were made to the number of samples, the equipment and consumables used. The previous method used 4 mL of the mixture reaction for 20 mg of lyophilized biomass. For the new method, 2 and 4 mg of biomass were evaluated in a reaction volume of 500 µL. This was sufficient volume to avoid surface tension interferences in a 1.5 mL vial while leaving a 1mL air space to allow the solvents to expand. It is important, because the reaction that was previously performed in balloons was instead performed in small vials. Sealed with aluminum stamp caps, these vials avoided solvent evaporation, which helped to maintain sample concentrations. Moreover, vials resistant to the high pressures generated by the reaction (data not shown). Small vials allow simultaneous sample processing and accurate temperature.

Once the innovations were applied, the optimal reaction conditions needed to be determined again. In order to investigate the different factors of the sample preparation method, as well as to investigate the interactions between them, a Taguchi matrix was applied. Time, temperature and load of sample were the factors explored in this experiment. Every factor level explored was the same as in the previous experiment: 70, 80, 90 and 100 °C and 30, 40, 50 and 60 minutes. The factors were investigated for a third factor; the amount of weighted biomass. As previously mentioned, the interaction between the factors are important for these investigations, which require several experiments with replicates. Taguchi's orthogonal matrices (see Appendix A) allow this to be done economically. Two factors consisting of four levels, combined with a factor

of two levels required a specially modified matrix. **L16 (2^{15})** was modified[37] to became **L16 (2^9, 4^2)** which can be allocated to those factors.

ANOVA was the statistical method used to interpret the experimental data. The resultant analysis of variance can be seen in Table 2.12. According to F-test (see Appendix A) only the temperature and the time of reaction are significant. It is clear that factor A, the temperature, is the most relevant factor contributing 68% of the transesterification of FA into FAME. It was clear that the time of reaction as well as the biomass load are less important, as the contribution is very low. The biomass load (C factor) and its interactions did not indicate important contributions. In this table, every column represents a factor in which the average response per level is listed. These average values are plotted in Figure 2.11.
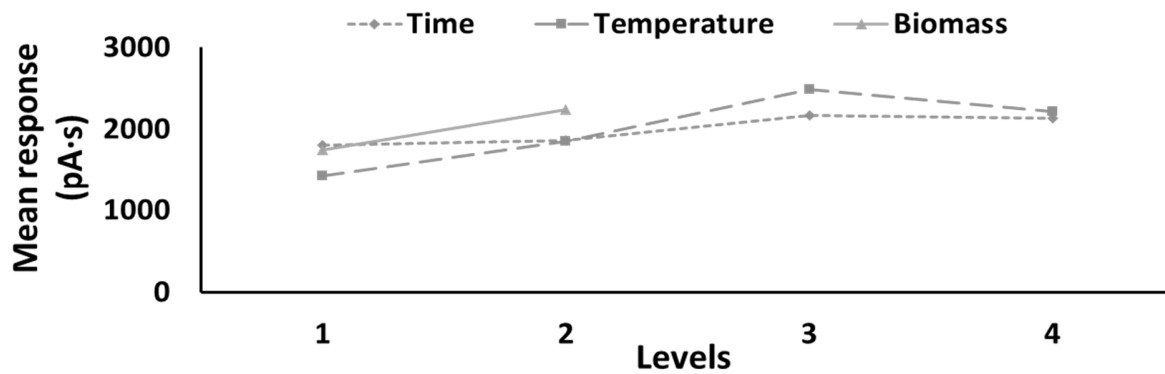
Figure 2.11 Average value of every factor level.

Table 2.12 ANOVA for the Taguchi matrix L16 (29, 42). Temperature (A), time (B) and biomass load (C) are the main factors, being AxC and BxC the interaction of both main factors with biomass load. The error is indicated as e. Sum of squares (SS); degrees of freedom (df); Mean square (MS); Computed value of F (Fo) which needed to be compared with F-table, $F_{0.05, 3, 2}=9.55$; $F_{0.05,1,2}=199.5$

	Factors	A	B	C	AxC	BxC	e
	1	1423	1819	1754	1999	1889	1954
	2	1846	1864	2236	1991	2101	2048
Levels	3	2481	2162				
	4	2231	2136				
	SS	2567255	382869	232742	57	45105	8811
	df	3	3	1	3	3	1
	MS	855752	127623	232742	19	15035	8811
	C (%)	69	10	19	0	1	1
	Fo	232.21	37.34	66.25	0.023	4.47	-

---

[37] Other, well-documented procedures exist to modify OA with statistical guarantees to maintain its properties.

The Biomass load factor was introduced to evaluate whether the reaction mixture could become saturated with FAME, within this range of biomass concentration. The mean responses from every factor's level are illustrated in Figure 2.12. After analysing the mean response for the two different levels of the biomass factor, it was clear that the response increase in the second level. This indicates that using a biomass load of 2 mg (first or lower level)[38] did not saturate the reaction. This plot reveals the best level for temperature and time, which appeared to be the third for both of them. It is significant that the fourth temperature level undergoes a response decrease. The maximum level is less clear in the case of reaction time. The evolution of the fourth levels of this factor, appear to show a plateau after the third level.

Table 2.13 ANOVA for the Taguchi's OA L16 (29, 42). Temperature (A), time (B) and biomass load (C) are the main factors, and AxB, BxC and AxC are their interactions. The error is indicated as e. Sum of squares (SS); degrees of freedom (df); Mean square (MS); Computed value of F (Fo) which are compared with F-table (AppendixA), $F_{0.05,\ 2,\ 8} = 19.37$.

	Factors	A	B	C	AxB	AxC	BxC	e
Levels	**1**	1219	1278	1097	954	1228	1322	1194
	2	1253	1199	1262	1199	1256	1140	1236
	3	1337	1579	1372	1579	1247	1270	1303
	SS	22260	240750	114627	593601	1213	52739	18057
	df	2	2	2	2	2	2	8
	MS	11130	120375	57313	559305	7490	38329	13251
	C (%)	1.4	14.9	7.1	69.3	0.9	4.7	1.6
	Fo	0.8	9.1	4.3	42.2	0.0	0.6	0.0

The Taguchi matrix used above has an important blind spot; the interaction between temperature and time. This was not considered in the transformed L_{16}. Most likely, the contribution of this interaction would have been more important and the combined levels may have shown a different maximum than that indicated. On the other hand, weighing small amounts of biomass could be a logistical constraint. For the developed method a scale that has an error of 0.1 mg was used. Thus, as long as the weighted sample was much higher than the error, the measure was reliable. In other words, starting with a higher amount of biomass would be better for the method repeatability. The analysis of the previous data provided some insight that helped develop a process for sample preparation to analyse fatty acids. However, the experimental design results added new interrogates which required new experiments.

---

[38] When discussing two levels per factor, these are commonly referred to as lower and higher level. When looking at more than two levels per factor, these are referred to by the number.

A second Taguchi matrix was proposed in order to investigate the factor levels within the most relevant ranges from the previous experimental design. The new array was the **L$_{27}$ (3^{13})**. This array
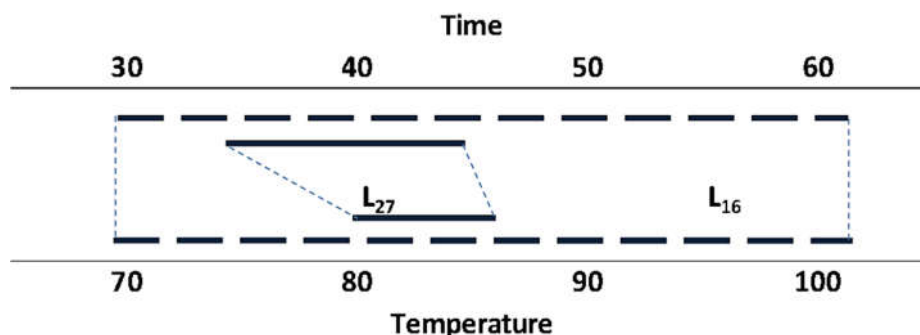
Figure 2.12 Differential window of temperature and time levels explored by both orthogonal arrays.

made it possible to investigate different factors with three levels and the interactions between them. Therefore, the experimentation can be allocated with three levels of temperature, time and biomass load. Again, the biomass factor is an extra to evaluate the method capacity to handle higher amounts of biomass, as well as a control to highlight significant factors in the experiment. The investigated levels are 35, 40 and 45 minutes of reaction time, 80, 82.5, 85 ºC for temperature and 4, 6 and 8 mg of biomass load. Figure 2.12 shows the range of time and temperature explored by both of Taguchi's experimental designs.

L$_{27}$ consisted of 27 runs and allowed researchers to study the interaction effects. In this case, only two replicates were performed due to the large number of samples required. Every sample was processed in the same conditions and in the heating bath simultaneously. The injection volumes in the HRGC were set at 1 µL instead of 2 µL, and for this reason the response values were lower from this point. The analysis of the results is detailed in the ANOVA, which is shown in Table 2.13. The percent contribution indicates the contribution of each factor and interaction to the total variation. In the L$_{27}$ ANOVA, the interaction between temperature and reaction time, with a contribution of almost 70% appears to be extremely important. By controlling both factors at the levels at which the interaction had a greater positive impact would lead to near optimal definitive improvement. The contribution of the error indicates the accuracy of the experiment, which is substantially good.

Observing ANOVA computed F values (Table 2.13) shows that the interaction between temperature and time is the most important factor. From this standpoint, only the combined levels of these factors had to be analyzed. As illustrated in Figure 2.13, the combined levels of temperature and time can be found. As seen in the figure, the maximum extraction values are given when the samples were run for 45 minutes at 80 °C as well as for 35 minutes at 85 °C. The difference was minimal, which indicates that the optimum values are within these ranges as shown in Figure 2.12. The selected sample preparation method was 85 °C for 35 minutes. This way, the new method reduces the time of the original method and also allows parallel samples to be processed.

Time (minutes)
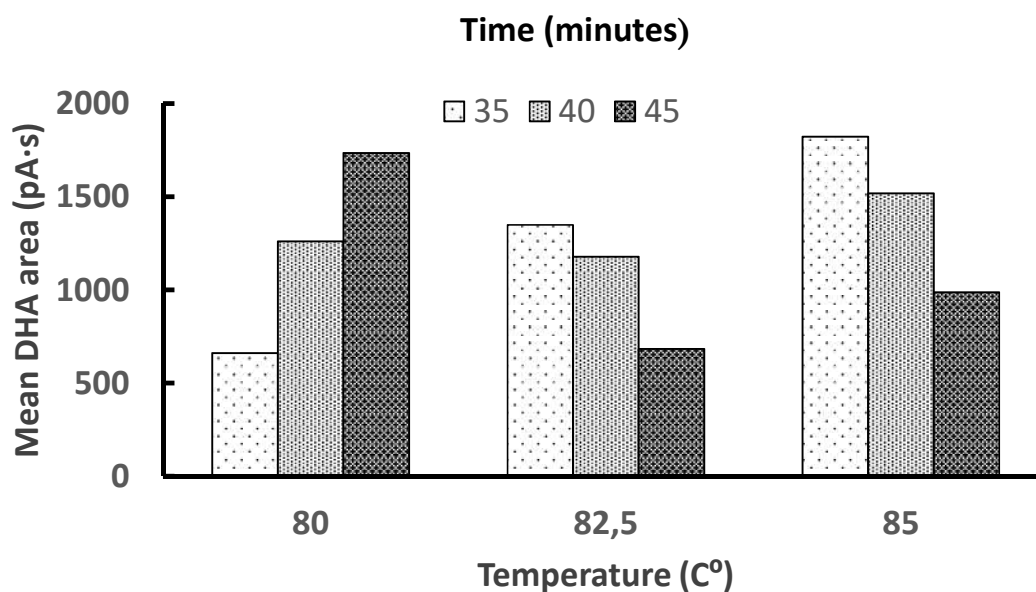
Figure 2.13. Response graph of every level from temperature and reaction time.

As the sample preparation is a fundamental tool enabling the DHA biotechnological production development, it was exhaustively validated. In addition to linearity and LOD and LOQ, method was validated in terms of repeatability and precision. The next section will explain the validation process of the DHA quantification method.

2.2.2.3 Validation of trans-esterification (sample preparation) method

The new method consists of different steps that occur during the reaction in the 1.5 mL vials. The sample preparation process must be validated. First, the release of FA from TG. The next stage is the transesterification of FA and finally the purification by phase separation. In order to ensure precise measurement, the DHA recovery percentage was also determined. In addition to proving that the method would scrupulously provide precise values of DHA during the project, discovering the percent of recovery of the method is important so the researchers can know the maximum DHA value possible. Of the steps mentioned above, the first presents the most difficulty.

An unambiguous validation could be performed for the following steps. **Glyceril tripalmitate (PPP)** is a triglyceride that contains three palmitic acids (P), which is one of the most abundant FA in *A. limacinum*. PPP is available as a standard and can be used to validate the remaining steps of the sample preparation method. Using the developed method, PPP would first release P moieties.

Then the released P would be esterified and finally the samples could be purified and analysed with HRGC-FID. Measuring the total amount of P extracted, and comparing it with the amount of

66

PPP added at the beginning, would provide the recovery percent of the entire process. This would show the method attributes to be validated as well as provide a recovery percent value of the transesterification process. Regarding DHA quantification, a standard of this free FA was used to perform a standard curve as well as to validate statistical attributes.

In order to achieve this, generating a calibration curve of P would be the first step. This would allow the quantification of P, which is the most abundant FA of *A. limacinum*, (together with DHA) and is the sole constituent of the TG standard, PPP. Therefore, knowing the response factor (Fr)[39] of P can be used to know the recovery percent of the procedure with PPP. For development purposes, the methyl ester of P (palmitic acid methyl ester, MP) was also analysed. MP was not processed through the sample preparation method. It was directly analysed by HRGC to ensure that the value of trans-esterified P is the maximum. This allowed to determine if there is any loss during the analyisis by HRGC-FID. The results of the three standards introduced above are shown in Table 2.14.

From Table 2.14, it is clear that the response factor (Fr) was equivalent for every standard, indicating that the previous method optimization allows a complete recovery of P from the reaction. The CV (%) values showed a high reliability because the higher CV (%) value as below 5%. In most cases, it was even below 1 %. The same happened with CV_f (%) values, whose highest value was 4% in P standards. Most importantly, the recovery percent listed as R in Table 2.14, indicates almost perfect values, which is further evidence that the method processed all of the P units. P transesterification showed a recovery of 99.7% relative to MP, and PPP exhibited a recovery of 100.3%. Finally, the R' shows the recovery percent of PPP relative to P, with a value of 100.7%, which indicates that the method is not losing standards during the sample preparation process.

Therefore, the current optimized method of extraction and transesterification of FA from *A. limacinum* guarantees the highest transesterification.

Considering the previous CV (%) and CV_f (%) values, the entire method (sample preparation and analysis) could be considered reliable due to excellent accuracy and precision, which thus indicates a good repeatability.

---

[39] Fr is the ratio between a signal produced by an analyte, and the quantity of analyte which produces the signal.

Table 2.14. Calibration curves of MP, P and PPP. The value of the area is the mean of three area measurements with the corresponding CV (%) showing the reliability of the measures. On the right, the response factor (Fr) is defined as the ratio between the concentration of the compound being analysed and the response of the detector to that compound. Fr statistics are listed below its column. The indicated mean value is the average of all the values with the corresponding standard deviation (SD). CV_f (%) is the Fr variation coefficient. P and PPP R (%) indicates the recovery of each, relative to the MP standard. On the other hand, R' (%) indicates the recovery of PPP relative to P.

[MP]	Area	CV (%)	Fr		[P]	Area	CV (%)	Fr		[PPP]	Area	CV (%)	Fr
2.84	2043	0.2	719.4		2.5	1752	4.5	701		2.5	1754	0.8	702
5.2	3599	0.7	692.1		5	3661	2.8	732		5	3695	0.9	739
7.28	5149	0.2	707.2		7.5	5260	3.2	701		7.5	5312	0.2	708
10.2	7541	0.5	739.3		10	7702	0.1	770		10	7322	1.3	732
12.6	8954	0.2	710.6		12.5	8995	0.9	720		12.5	8745	1.3	700
		Mean	713.7				Mean	711				Mean	716.1
Fr stats		SD	17.4		**Fr stats**		SD	28.6		**Fr stats**		SD	18.2
		CV_f (%)	2.4				CV_f (%)	4.0				CV_f (%)	2.5
							R (%)	99.7				R (%)	100.3
												R' (%)	100.7

Figure 2.14. Calibration line of palmitic acid (P).

LOD and LOQ were calculated (Appendix A) based on the residual standard deviation (RSD) of the response, and its regression versus the standard concentration. LOD and LOQ for palmitic acid were 0.41 g/L and 1.38 g/L, respectively. Thus, between 1.38-12.5 g/L accurate and precise P quantification could be achieved. The method was proven to be linear within this range. The evaluated range is broad enough, because biomass samples would only contain P concentrations between 2 and 4 g/L. The equation used to calculate a P concentration provided by a sample of *A. limacinum* in the following chapters was y = 766.29 x, as shown in Figure 2.14.
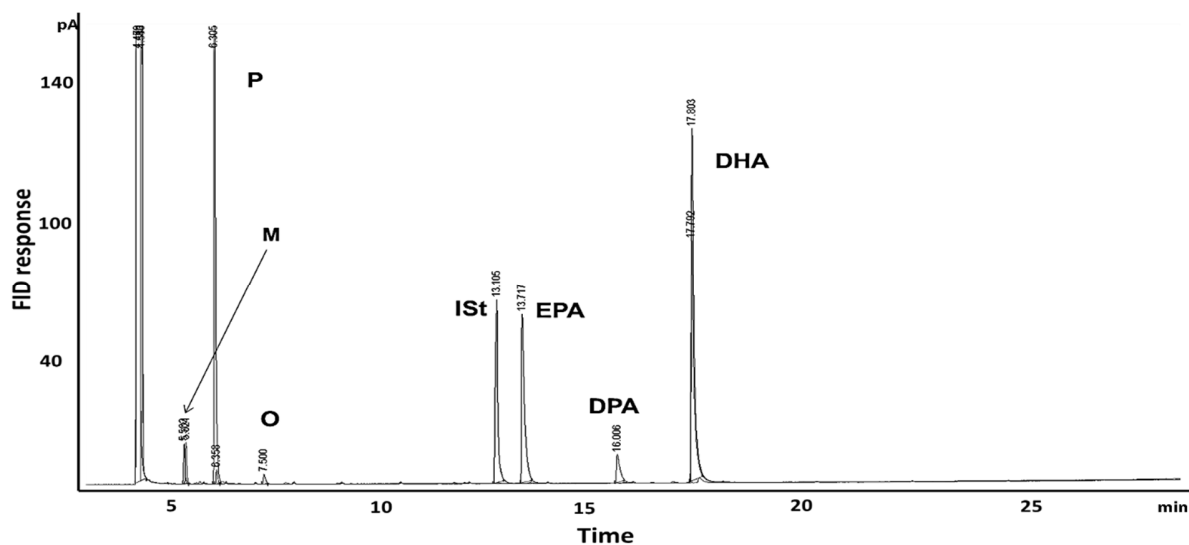
Figure 2.15. Fatty acid profile of A. limacinum processed with the current method. P is palmitic acid; M is myristic acid; O is oleic acid; ISt is the internal standard (tricosanoic acid; C23:0); EPA was added as a standard and corresponds to eicosapentaenoic acid; DPA is docosapentaenoic acid and DHA is docosahexaenoic acid. Every peak was identified by injecting Sigma 37 FAME standard.

The developed method has shown the capacity to measure the amount of FA such as P, and to perform a full release and trans-esterification, as evidenced by the standards. Observing the FA profile from *A. limacinum* (obtained using the current method), as illustrated in Figure 2.15, P was satisfactorily separated from other FA species that come from this microorganism. Thus, the method shows excellent specificity and selectivity. In Figure 2.15, two standards were included in the processed sample in order to evaluate their selectivity relative to DHA and DPA. Tricosanoic acid, which is the internal standard (ISt) and EPA. As previously explained, together with DHA, EPA is the most important n-3 PUFA for biology and human health. The validated method shows good selectivity for FA. This shows the suitability of the method to define the FA profile of other thraustochytrids. This way, any EPA produced would be detected by this method. This same method can also be applied to determine DHA sample abundance from *A. limacinum*. However, the method would need to be validated and calibrated specifically for DHA, in order to be able to quantify it. The following section details the assessment of statistical attributes for the quantification of DHA.

2.2.2.4 Validation of DHA quantification

The same method used to define the FA profile of thraustochytrids has enough selectivity to quantify DHA without any interference, as observed in Figure 2.15. The profile clearly indicates good selectivity of this method for DHA that comes from *A. limacinum* samples.

69

To execute the validation of the remaining statistical attributes, a DHA standard (a free FA form, not in a methylated form[40]) was used. Thraustochytrids can have between 20 to 50 % of lipids and almost 50 % of the total lipids are DHA. This means that, if the current method uses between 4 and 6 mg of biomass, every sample would have between 0.8 to 3 mg of lipids. And 0.4 to 1.5 mg of DHA. These values are very important when considering the range of curve calibration.

The DHA standard was necessary to evaluate the whole method process (sample preparation and HRGC analysis). As DHA contains 6 double bonds, it is susceptible to oxidation, boosted by the presence of oxygen and light. For this reason, DHA is more delicate than SFA, such as P, and needs special considerations. Therefore, processing DHA in 30 minutes of Fischer-Speier reaction may be too harsh for it. Accordingly, the same amount of sample was evaluated for different times of reaction. The results of this experiment are listed in Table 2.15[41].

Table 2.15 Results and statistics of the sample preparation process applied to a DHA standard with different times of reaction. Experiments were performed at 85 °C. SD stands for standard deviation; CV stands for Variation coefficient; Fr stands for response factor. R_{30} corresponds to the recovery % relative to 30 minutes' experiment. Mean response equals mean area.

Time (min)	[DHA] (g/L)	Mean	SD	CV (%)	Fr	R_{30}(%)
5	3	2952	43.8	1.49	984	96.3
10	3	3064	22.6	0.74	1021	98.3
15	3	3116	4.9	0.16	1039	99.0
20	3	3146	7.1	0.22	1049	99.4
25	3	3165	2.1	0.07	1055	99.9
30	3	3168	0.7	0.02	1056	100.0
35	3	3136	8.0	0.00	1045	99.0

Observation of the data in Table 2.14 surprisingly reveals that the DHA was more resistant than expected in the reaction environment. As can be seen in Table 2.15, it resisted the reaction for at least 30 minutes, even giving the maximum mean response. These results are in concordance with the optimization performed in section 2.2.2.3, in which the maximum was around 30 to 40 minutes. Nevertheless, 15 minutes is enough to convert 99 % of the DHA standard into a methyl ester. The stability of the recovery values while changing an important factor (time) is evidence of the process robustness. It is worthwhile to note that DHA coming from biomass requires 35 minutes, while a DHA standard only needs 15 minutes.

---

[40] This form is more stable and makes FA generally easier to handle. In the literature, DHA is generally used as a methyl ester to perform a calibration curve.
[41] Data in this table was generated using a Supelco SP™-2380 (60 m × 250 μm, df 0.20 μm) column over more than 10 years. In some experiments, a new one was used with the same characteristics but with better performance. This will be indicated as necessary.

A change in the HRGC column required a re-calibration. It is plotted in Figure 2.16, where figure ***a*** shows the calibration using the **new column** and ***b*** corresponds to the **old column**. As can be seen, despite the fact that the Fr experienced a slight change, the LOD and LOQ are basically the same. The calibration curve was reworked every 4 or 5 months during the research. GC columns tend to lose stationary phase material after every run and it was important to keep the method calibrated. The range of work was reduced from a maximum of 12 mg/mL of DHA to less than 7 mg/mL, because the real samples never reached such high concentrations.
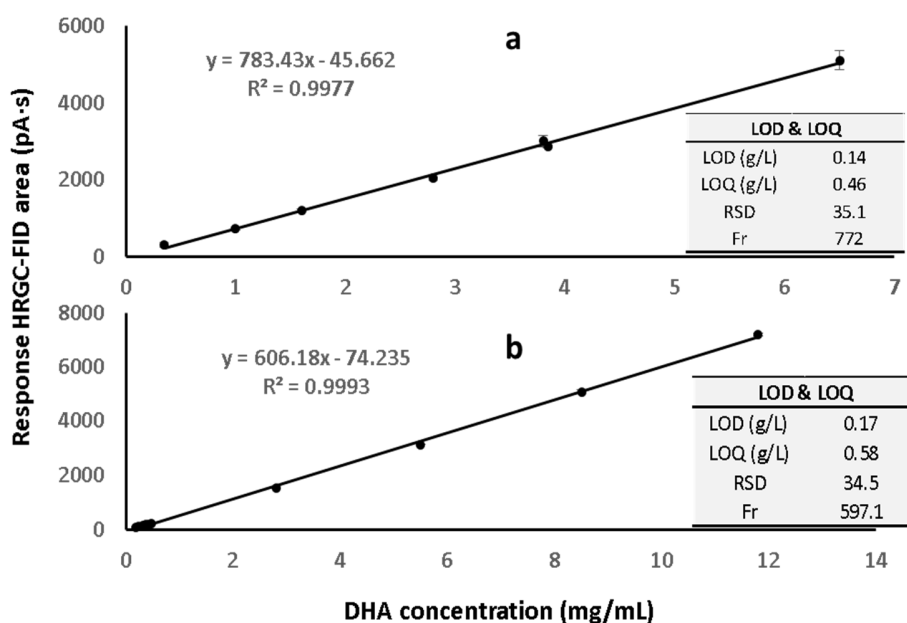
Figure 2.16 a) Calibration curve of DHA using a <u>new</u> column. b) Calibration curve of DHA using an <u>old</u> column. LOD and LOQ stand for the limit of detection and the limit of quantification, respectively. RSD stands for residual standard deviation and Fr for response factor. Final volume of samples, 500 µL.

As already mentioned, the method has shown perfect specificity to distinguish DHA from other fatty acids. The DHA quantification method was found to be linear from0.4 g/L to 6.5 g/l using the new column and 0.19 g/L to 11.5 g/L using the old column. Regression lines were plotted in Figure 2.16. LOD and LOQ for the new column are 0.15 g/L and 0.5 g/L, respectively. For the old column, LOD and LOQ are 0.17 g/L and 0.58 g/L respectively. The slope was 783.4 and the intercept was 45.7 in the mean DHA area vs. the DHA concentration (in the reaction mixture, g/l), for the new column. For the old column, the slope is 606.18 and the intercept was 74.2 in the mean DHA area vs. DHA concentration (in the reaction mixture, g/l). Table 2.16 summarizes the results, evaluating the repeatability and the accuracy between replicas and the calculated mean bias. The maximum variability among samples was 5 %. The mean bias (%) was 15 % for samples of 0.4 g DHA /L. Therefore, the method lost accuracy with the new column, when the concentrations were equal to or below 0.4 g DHA/L. Any degradation of the sample would be easily noticed in low concentrations, which is another influencing factor. The old calibration curve shows good repeatability as well as low variability.

Table 2.16 Precision calculations for the whole DHA quantification method (sample preparation and analysis) according to both columns. SD stands for standard deviation; CV stands for Variation coefficient; Fr stands for response factor. Mean stands for the average value of area measurements.

[DHA] (mg/mL)	Mean Area	SD	CV (%)	Mean bias (%)	[DHA] (mg/mL)	Mean Area	SD	CV (%)	Mean bias (%)
0.4	312	12	3.8	3.6	0.19	92.2	0.0	0.0	16.5
1.0	733	39	5.4	5.1	0.23	111.0	0.1	0.1	19.2
1.6	1198	37	3.1	3.0	0.33	147.3	0.0	0.0	24.1
2.8	2051	78	3.8	5.1	0.37	173.4	0.2	0.1	21.5
3.8	3007	151	5.0	2.5	0.42	187.8	0.1	0.1	24.2
3.8	2858	41	1.4	3.6	0.47	201.8	0.0	0.0	27.3
6.5	5106	252	4.9	1.7	2.80	1522.0	19.5	1.3	9.0
					5.50	3129.0	8.2	0.3	4.7
					8.50	5069.5	79.9	1.6	0.1
New Column	↑		Old Column ⟶		11.80	7166.7	58.7	0.8	1.7

The current DHA quantification methodology provides a statistical guarantee that the measurements are precise. Therefore, DHA values can govern the thraustochytrids bioprocess development. The DHA method together with the glycerol method composes the necessary analytical toolbox to proceed with the basic knowledge about A. limacinum behaviour and life cycle.

2.2.3 *A. limacinum* life cycle in batch and continuous bioreactor

Thraustochytrids have a complex life cycle that is not fully known and can change dramatically from strain to strain. In fact, the classification of thraustochytrids genera is based on morphological differences at various stages during their life cycle. For this reason, a microscopic coupled with an image processing algorithm was used to monitor cells morphology and sizes. The physiological composition of this microorganism also changes drastically during different morphological stages. Because this study used *A. limacinum* both as a thraustochytrid model and as a tool for a bioprocess development to produce DHA, further investigations were required. *A. limacinum* life stages have been investigated during regular batch culture in flasks and in a bioreactor. Observations of every stage have been made with confocal microscopy and processed with a Matlab® algorithm (see Appendix C). In order to calibrate the algorithm, different pictures of known distance objects, (e.g. the Neubabuer) chamber were processed. This allowed for unequivocal measurement of cell size to be done for different cell stages. Every microscope augmentation required calibration.

2.2.3.1 *A. limacinum* as a model of thraustochytrids complex life cycle
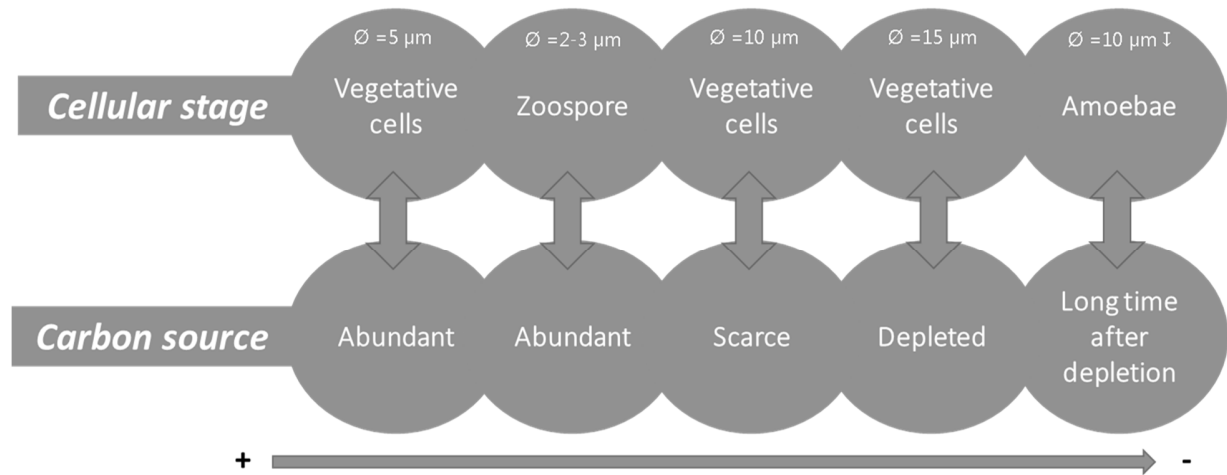
Figure 2.17 A. limacinum life stage in different carbon source availability scenarios, as observed in this thesis. Each cellular stage is described in section 2.3.3.2 and 2.3.3.3.

A. limacinum is a great example of thraustochytrids cell cycle complexity. Besides gaining knowledge about how *A. limacinum* and thraustochytrids behave in a batch reactor, observations can set "default" cycle characteristics. This default behavior provides an understanding of the microorganism adaptation to media changes. Interestingly, every cellular stage has a different FA profile. In some of these stages, the production of lipids and/or PUFA such as DHA are enhanced. Important scientists in thraustochytrids biology like Perkins, Porter, Moss, Gaertner A., and most recently S. Raghukumar, Daiske Honda and their colleagues have examined and recorded the general life cycle of different strains of thraustochytrids. This section offers the description of this life cycle in a lab scale bioreactor, the changes in the life cycle (as shown in Figure 2.17) and the changes of DHA during cultures (see Figure 2.25 from section 2.2.2.3). DHA values can indicate the best harvesting time to maximize productivity.

Figure 2.18 Conforocal microscopy picture (400x) from a culture of A. limacinum, showing different cell morphologies of the same strain.

A. limacinum stages in batch, changes depending on carbon source availability during a batch bioreactor as shown in Figure 2.17. The figure illustrates the sequence of the main and most abundant stages during a batch, however there are a few other stages that normally co-exist with the main ones. In some cases, there are cell types that only last for a few hours, representing a transient step. Interestingly, *A. limacinum* growing at steady state (in a continuous mode) only generates **vegetative cells**. Vegetative cells can present different characteristics in terms of size, shape and biochemical composition, depending on the environmental conditions as shown in Figure 2.17. The vegetative stage is the most abundant in many situations. An amoeba's final stage

is rarely formed because the cells are generally harvested shortly after carbon source depletion. **Amoebas** as well as **zoospores** are the consequence of strong morphological transformations. Both stages are related to low DHA accumulation. These transformations are detailed further in this section.

During a normal culture, different cell type populations co-exist. This, together with the significant morphological variability of every stage, shows the complexity of growing
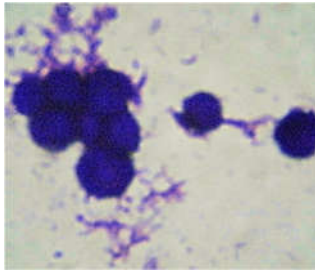
Figure 2.19 Conforocal microscopy picture (400x) from a culture of A. limacinum with crystal violet staining. The staining has revealed the ectoplasmic network which is barely visible without the dye.

thraustochytrids in a bioreactor. Figure 2.18 evidences the heterogeneity of this strain. In this picture, a zoospore, a cell that is metamorphosing after a zoospore stage, amoebe cells, vegetative cells and cell remnants (envelopes) of broken sporangium coexist. A supplementary video included in the thesis shows the movement of the cells. Contrary to what can be seen in Figure 2.19, vegetative cells are generally grouped in what is called settlement or large clusters. As introduced previously, the vegetative phase is the most common.

In their natural environment, thraustochytrids became vegetative cells in substrate rich environments, using zoospores and amoebas to move around, looking for new nutrient sources. For this reason, thraustochytrid cell clusters are called settlements, because they settle together until nutrient depletion. Then, they return to some of the stages with motility. Vegetative cells stay together to protect themselves from the environment as well as to "collaborate" in the nutrient obtention process. As introduced in Chapter 1, thraustochytrids have a very singular organelle called sagenogenetosome. This organelle is responsible for secreting an ectoplasmic network, which is a radiating matrix of cytoplasm bound by a plasma membrane [159]. The ectoplasmic network apparently help cells adhere to and penetrate substrates, and it secretes the digestive enzymes required to solubilize nutrients that can be absorbed by cells [128]. In the lab, when the reactor is poorly agitated, this ectoplasmic net can appear and impede the culture homogeneity (Figure 2.19). Despite that, the ectoplasmic net is a sign of a healthy cell and therefore of good adaptation to the media. On the other hand, this phenotype promotes enzyme synthesis which could be of interest due to their role in decomposing leaves and vegetable debris [160]. Therefore, if required, the production of potential hydrolytic enzymes could be promoted by growing thraustochytrids at a very low (or zero) agitation.

2.2.3.2 Main life stages

At the starting point of the culture, inoculum, the cells are in a **vegetative** stage. This inoculum has experienced the whole growing process until the final vegetative stage (Figure 2.17), which is far before the amoeboid stage. When these cells are introduced into a fresh medium, they start

to show ultrastructural[42] evidence of metabolism "acceleration". When a vegetative cell is rich in "black dots" (Box 2.5), it means that they have accumulated a large quantity of TG (with an

---

Box 2.5: Larsson's triple-layer structure model, evidence of "black spots"

Many studies have suggested different molecular distribution structures of TG containing DHA and DPA based on computational models and crystals of this individual FA. Most recently, Ashford et al. [162] suggested that TG accumulation in thraustochytrids might be following Larsson's triple chain-length model for mixed TG. They propose that TG with PUFA n-3 like DHA and possibly DPA n-6 may be segregated into an interlocking, dark-staining layer and that the saturated and less unsaturated FA chains may be segregated end-to-end to form light-staining layers. This type of arrangement may have been facilitated by the predominance of the long-chain, highly unsaturated fatty acids DHA and DPA n-6 in the sn-2 position of TG. Thus, following Larsson's triple chain-length model for mixed TG, the suggested secondary structure of the TG in Schizochytrium sp. may be illustrated by the model presented in the figure at the right.

This model was previously confirmed indirectly in milk samples, and now in thraustochytrids lipid bodies. The Triple-layer structure may be the native conformation of triacylglycerols in the cells prior to freezing. In order to show that this pattern is not an artefact of an electron microscopy sample preparation, Ashford et al. analysed oil-body structure in other algal and algae-like microorganisms with a variety of FA profiles. The results show that only thraustochytrids from the microorganisms evaluated show oil bodies with black spots. When observed closely, as in the picture in the lower right, it shows this light – dark phenotype. This interpretation is supported by two main statements: the thickness of the light and dark bands corresponds to known lengths of FA, and the fact that this pattern only appears when these lipid bodies contain either two fold PUFA relative to saturated FA, or viceversa.

---
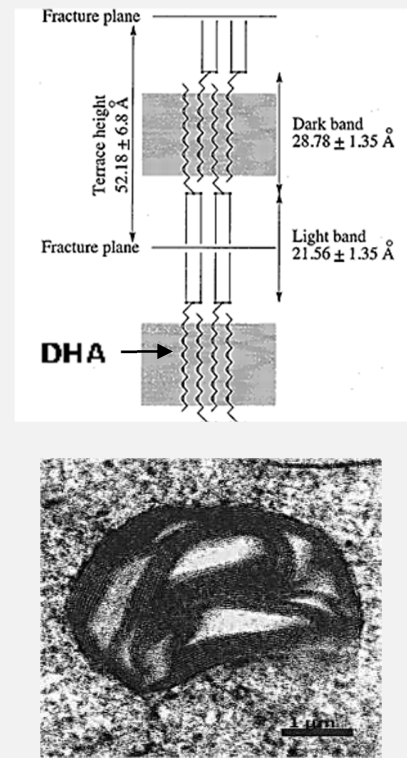
important number of PUFA), according to Larsson's triple chain-length model for mixed triglycerides. Thraustochytrids tend to accumulate triglycerides in oil bodies and in vesicles [127,161,162]. TG accumulation is more common at the end of the culture, because they tend to store energy if carbon source and nutrients are depleting [161]. Therefore, at the end of a culture, thraustochytrids should accumulate these small black dots.

Shortly after the introduction of these cells in a fresh medium, they tend to obtain energy from their stored TG to develop and express the metabolic machinery, as can be observed in Figure 2.25. Thus, obtaining energy enough to secrete the required enzymes to process nutrients. In their challenging natural environment, thraustochytrids have to compete with faster microorganisms. From an evolutionary standpoint, this extra stored energy, in the form of a non-processed carbon source in the cytoplasm, makes the difference, allowing the perpetuation of the strain. For this reason, the number of visible black dots tends to decrease after inoculation when compared with a finished culture, as shown in the Figure 2.21. Morita *et al.* (2006) [161] reported the same behaviour. This initial burst is concluded by the metamorphosis into a

---

[42] The ultrastructure of a microorganism can be defined as the close detail of a cell, with all visible organelles that can be seen by microscopy.

zoosporangium stage, which is illustrated in Figure 2.22 a. and b. The zoosporangium stage is relatively short compared with the vegetative stage and with the unique purpose of gestating zoospores. The size of this zoosporangiums can be approximately 10 – 30 µm and there can be between 8 to 32 zoospores with an initial size of 2-3 µm. This stage has a characteristic globular morphology that resembles a sphere containing many smaller spheres. In fact, after zoospores emerge from the zoosporangium, the remaining membrane will preserve the shape (Figure 2.18).
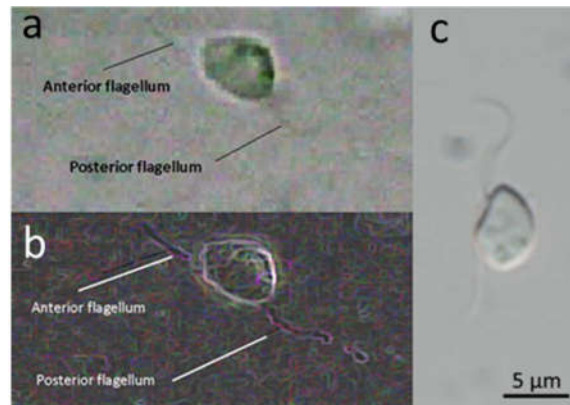
Figure 2.20 a. and b. Zoomed (1000x) confocal microscopy picture of an A. limacinum zoospore. b. Negative image of a, that allows a better view of flagellums. c. Zoospore image from Yokoyama et al.

Zoospores are very high energy consuming cells with an ovoid morphology and having extraordinary motility [126,163]. *A. limacinum* release 2 - 5 µm biflagellate zoospores. A smooth flagellum (posterior flagellum), which is the main source of motility. On the other hand, the one that bears tripartite tubular hairs (anterior flagellum) leads the zoospores and changes the direction (Figure 2.20). In their natural environment, the zoospore stage with a speed of 160 µm/s [126] allows them to find new settlement areas with resources and cover the maximum. Otherwise, as vegetative cells, they can only move when carried by the stream. This high motility stage has a poor lipid content and expends very large amounts of energy, in their formation and activity. Considering that after the zoosporangium phase, 32 offspring cells are released from the original vegetative cell, the growth rate is very high. From a bioprocess standpoint, a high growth rate could potentially help in reaching greater productivity. In Chapters 3 and 4, the growth rate will be explained and a description will be given to show how this could benefit an industrial process.
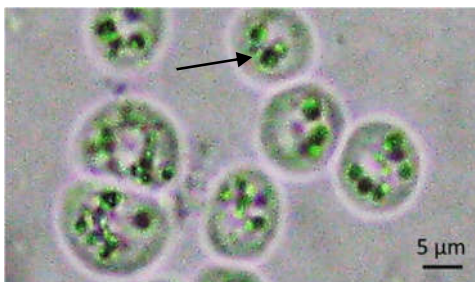
Figure 2.21 Oil immersion conforocal microscopy picture (1000x) from a culture of A. limacinum. The organelles like the one tagged with an arrow, are black dots.
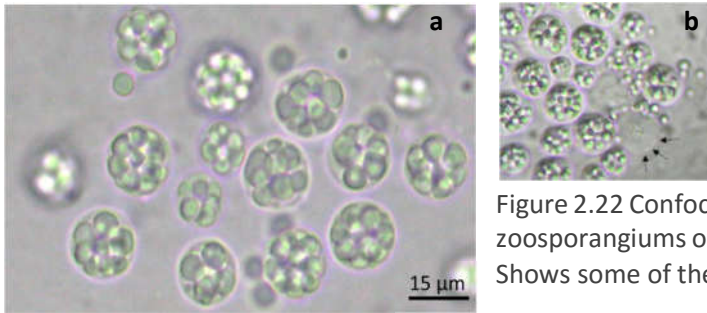
Figure 2.22 Confocal microscopy picture (400x) of A. limacinum zoosporangiums of a 12 h culture. a. Shows full sporangiums b. Shows some of the sporangiums realesing zoospores.
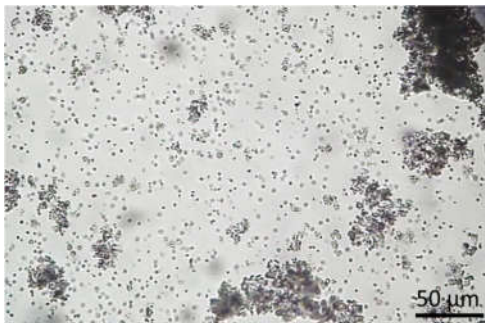
Figure 2.23 Frame of a video recorded by a confocal microscope (100x) of zoospores moving around the plane. The darkest sections of the image are grouped vegetative cells. The full video can be found in the supplementary CD.
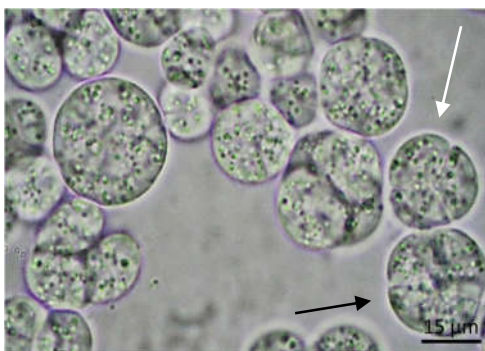
Figure 2.24 Confocal microscopy picture (400x) of A. limacinum vegetative cells with a high content of black dots. Cells present symmetrical bipartition with clusters of 2, 3 or 4 cells. The black arrow shows a tetrad configuration while the white arrow tags a triad.

In a batch reactor, *A. limacinum* grow without any competing population as they do in nature rich environment with homogeneous agitation. However, having no means to identify a well agitated environment (obviously) they spontaneously generate zoospores to cover the maximum area of nutrition. Interestingly, in a bioreactor there is only one stage of zoospore. Shortly after the first zoospores are released and start becoming small growing vegetative cells, biomass concentration increases dramatically. This high concentration of cells may be inhibiting a new zoospore stage. As a result, cells remain in a vegetative stage only proliferating with bipartition or in a proliferative stage (described below). During this period, the cells tend to accumulate FA grouped in TG that are stored in the black dots or dense bodies (see Box 2.5). This is interesting because bipartition processes are carried out symmetrically, resulting in the formation of the stages called the diad and the tetrad and in some cases triads [125], as shown in Figure 2.24.

The bipartition process does not prevent the accumulation of TG inside the black dots. The accumulation is supposed to be triggered by a low concentration of a carbon source, specific nutrients in the medium and/or other environmental parameters (fully investigated in Chapters 3 and 4). Accumulating TG is a common way to store energy in eukaryotic cells. For *A. limacinum,*

this guarantees a long term source of energy, but what makes this strain special is the high amount of DHA accumulated, as TG moieties. Therefore, monitoring the DHA yield gives an idea of TG accumulation. Figure 2.25 shows the evolution of DHA yield between culture time and the evidence and accumulation of TG from the middle to the end. On the other hand, comparing this with the specific growth rate provides more data about lipids accumulation in each stage.
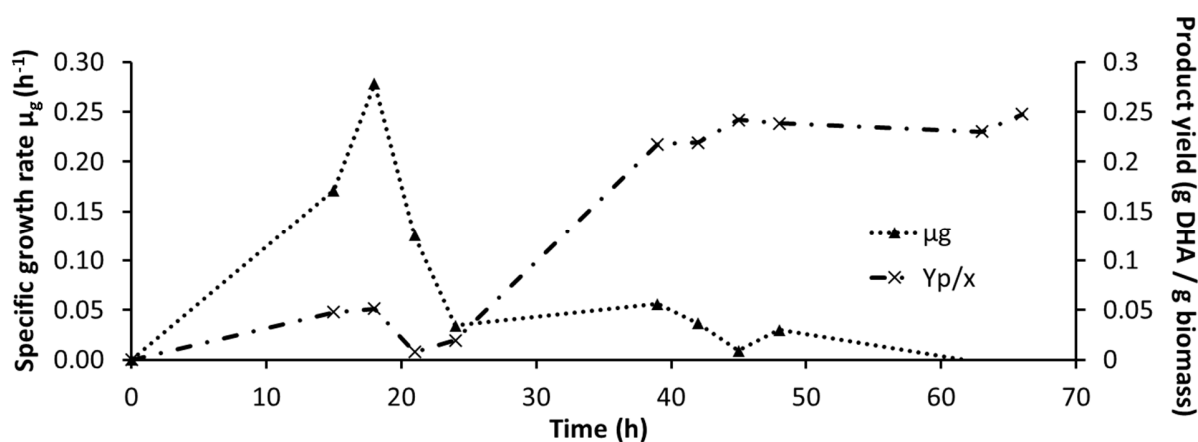
Figure 2.25 Plot of the evolution of the specific growth rate (μg) of *A. limacinum* and its DHA content, over time. DHA content is expressed as a yield of DHA g per every g of biomass (Y p/x).

During the initial hours of *A. limacinum* cultivation, the growth rate value dramatically increases after 15 hours. This peak corresponds to the zoospore release (see Figure 2.25). Comparing DHA values of the same time lapse shows the lack of lipids during zoospore release. The growth rate then drops drastically when the zoospores become vegetative cells. In this situation, the DHA values start to increase lineally as the growth rate remains constant between 0.04 and 0.05 h^{-1}. After 40 to 50 hours, the DHA yield stabilizes whereas the growth rate was reduced. During the last period there is slight growth rate fluctuation. This could be attributed to either minor carbon sources from complex ingredients of the media, or some of the minority *A. limacinum* life stages. These special life stages will be explained in the following section. Furthermore, the Figure 2.25 profile indicates that the best moment for cell harvesting is when the cells are at a vegetative stage with sizes of 10-20 μm. This will ensure that the maximum amount of DHA can be accumulated.

While in batch mode there is a zoospore stage in a continuous reactor *A. limacinum* only grows with successive bipartition or by releasing a small copy of the cell (as shown in Figure 2.27). In a continuous reactor, only vegetative cells appear, thus dramatically reducing the growth rate (extensively discussed in Chapter 4).

78

2.2.3.3 Minority cell stages

There are two life stages that may appear during the end of a batch culture. When the carbon source is completely and long since depleted, *A. limacinum* generates the amoeboid cells. It is not clear if the amoeboid cells appear as a low energy alternative to a zoospore due to its low motility, or as a way of degrading the remains of other cells in order to survive. In fact, it has been reported that some thraustochytrid species present bacterivory activity (phagocytic) [164,165]. Until now, only *Thraustochytrium aureum* and *Aurantiochytrium mangrovei*[43] have been unambiguously shown to phagocitate bacteria. This phagocytic activity might be an evidence of its capacity to degrade the cell remains of their own strain, or of a desperate search for nutrients.

Figure 2.26 Three zoomed A. limacinum pictures of three amoeboid cells without size calibration. The approximate longitudinal size is about 20 μm. The colour difference is caused by the difference in light and image processing parameters, when the pictures were taken.

Figure 2.26 shows three pictures of amoeboid cells with different shapes.

There are a few more stages of the *A. limacinum* life cycle that are worth mentioning. These have been detected during microscope observations and have also been reported for other thraustochytrids [110,127,163]. When the carbon source is scarcer, the cell generally behaves as a vegetative cell storing TG, but in some cases they can become semiproliferative cells. This occurs in a cell that remains in the vegetative cell stage while releasing either a small number of zoospores or just smaller cells Figure 2.27. These smaller cells may be converted into amoeboid cells as reported in the bibliography [163,164].
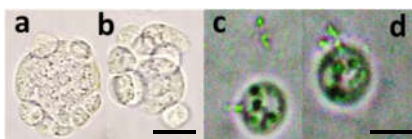
Figure 2.27 Pictures a. and b. show two vegetative cells that are releasing small cells. Pictures c. and d. show two vegetative cells that are releasing what looks like smaller zoospores. Bars a. and b. = 15 μm c. and d. 10 μm

2.2.4 *A. limacinum* as a source of other added-value metabolites

As outlined in section 2.1.5 of this dissertation, *A. limacinum* is capable of producing astaxanthin and/or squalene, while releasing oxalic acid and pyruvic acid. All of these are added–value biomolecules which could be produced in parallel with DHA production, making the process even more cost effective. In the following section, preliminary investigations about these metabolites are detailed.

Squalene

---

[43] Formerly (until 2007) *Schizochytrium mangrovei*

Squalene (2,6,10,15,19,23-hexamethyltetracosa-2,6,10,14,18,22-hexaene), is a dehydrotriterpenic hydrocarbon (C30H50) with six double bonds. It is typically marketed as shark liver oil. In addition to its uses in cosmetics and pharmaceuticals (additive in some vaccines), squalene is also used as a health supplement for cancer and heart health [119,142,166]. Though they look promising, the benefits of squalene have yet to stand the test of time and further scientific testing. Squalene is a large molecule that cannot be synthetized chemically and is generally extracted from shark liver. Figure 2.28 shows the production of DHA and squalene from *A. limacinum* in a batch culture. It clearly shows that *A. limacinum*
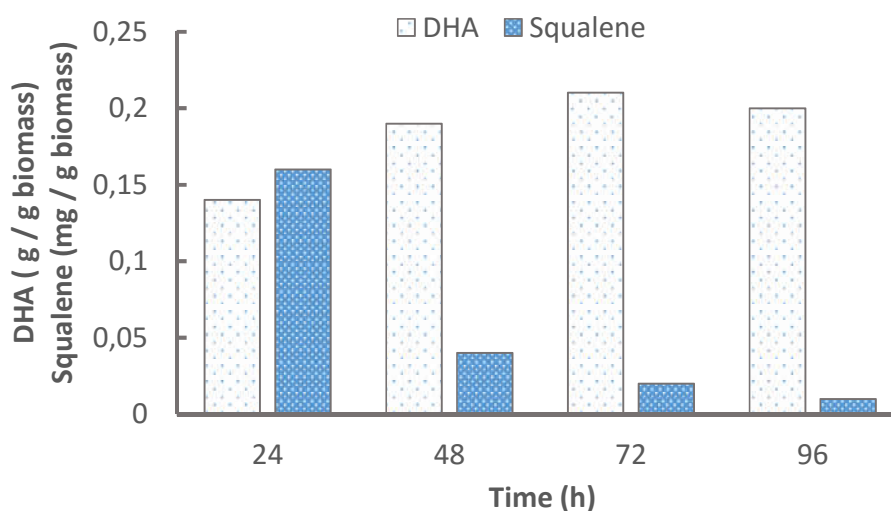
Figure 2.28 Evolution of DHA and squalene content in an A. limacinum during a bioreactor culture. Data obtained from a batch bioreactor with 10 g/L of glycerol. Data from C. Carnicé Master Thesis

has a great potential for producing squalene in a bioreactor. Interestingly, squalene is only produced during the initial stages of growth. Peak production appears after 24 hours of culture. After 48 hours of growth, the squalene content drops radically, maintaining a constant reduction during the following hours. The time recorded might indicate that after zoospore release (which generally occurs after 24 hours in a batch reactor), squalene is consumed to produce other molecules, because squalene is a known precursor of many other biomolecules. Therefore, during the vegetative stage squalene content is scarce. From the thraustochytrids collection of IQS, *A. mangrovei* stands out by producing 50% more squalene than any other according to literature [118,119,142,167–169]. Table 2.17 shows the production of *A.*

Table 2.17 Comparison of the squalene production of *A. limacinum* and *A. mangrovei* from this thesis and two other literary works.

Strain	Squalene (mg / g biomass)	Reference
A. limacinum	0.55	This study
A. mangrovei	1.09	This study
A. mangrovei	0.16	Jiang et al. [43]
A. mangrovei	0.38	Fen et al. [44]

limacinum and *A. mangrovei* using a medium with improved nitrogen sources (see Chapter 3 for more information). As can be seen, both cultures produce more squalene, especially *A. mangrovei.*

Organic acids

As can be seen in the chromatograms shown in Figure 2.29 (RID signal), thraustochytrids can release Oxalic and Pyruvic acid during growth. Therefore, a contaminant-free pyruvic acid production could be achieved with thraustochytrids. It is worth mentioning that thraustochytrids only secrete significant amounts of organic acids when they are grown in continuously operating cultures (as seen in this thesis). The production profile changes depending on the substrate concentration maintained in the reactor, as shown in Figure 2.29.
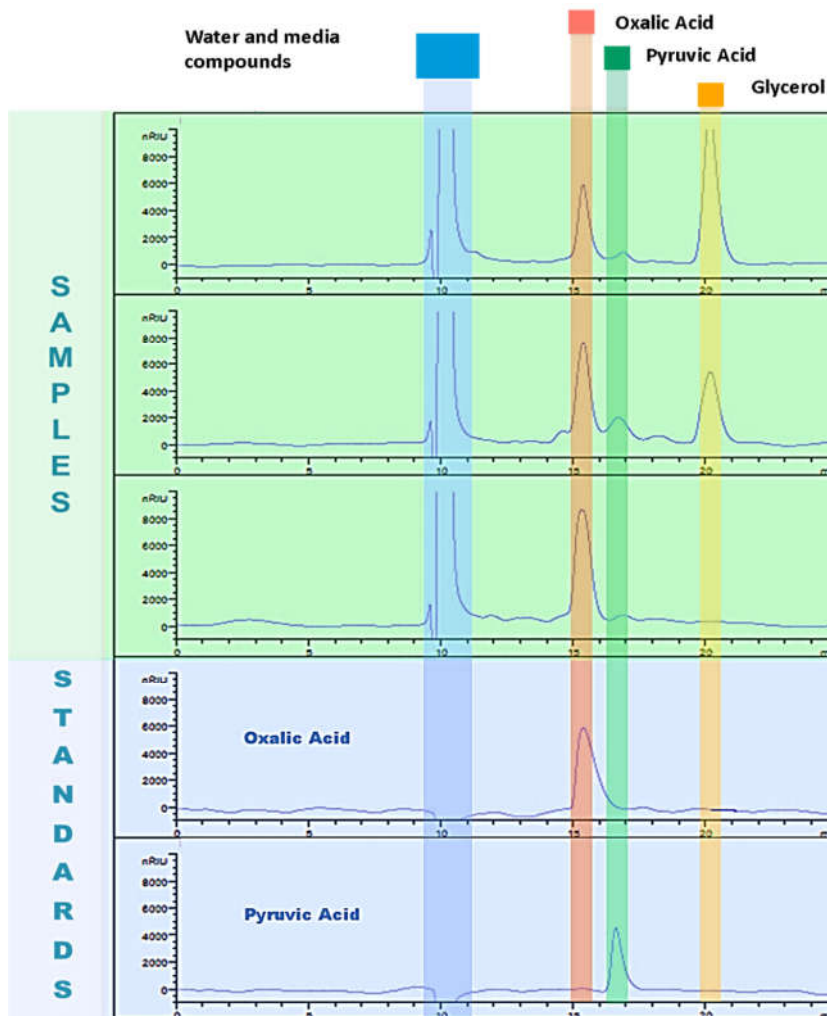
Figure 2.29 Chromatograms showing the production of two organic acids when growing in continuous mode. Each sample chromatogram shows the profile where glycerol concentrations drop due to A. limacinum growth. Below the samples, standard chromatograms are shown.

Astaxanthin

Astaxanthin is a carotenoid pigment (3,3'-dihydroxy-β, β'-carotene-4,4'-dione). It is added to food products and use as a colorant for cultured fish, poultry and shrimp. It also acts as a

scavenger of free oxygen radicals which damage DNA and oxidizes proteins [117,170]. Nowadays, *Haematococcus pluvialis* is the main source of this molecule. However, it has been reported that thraustochytrids can produce astaxhantin as well. Only Yokoyama *et al.* [171] mentioned that *A. limacinum* can produce this pigment. This has been shown in the present thesis.

Aurantiochytrium limacinum starts to produce astaxanthin after 20 hours of cultivation. As well as DHA, astaxanthin production can be enhanced under specific conditions (explained in chapter 3 and 4). For astaxanthin stimulation a high concentration of monosodium glutamate (5-10 g/L), a low N/C ratio (0.5) and the addition of $FeSO_4$ (0.8-1 g/L) into the media. Nuria Abajo Lima work (Master thesis, Bioengineering department, IQS) contains detailed information about the parameters investigation on specific stimulation of astaxanthin.

2.3   Chapter achievements

In summary, Chapter 2 has presented a great deal of information about *A. limacinum* and about the analytical techniques required to perform a DHA producing bioprocess development.

During this chapter, different analytical methodologies have been investigated in order to find the fastest method, while being able to process several samples at the same time. These methodologies have two main goals; to monitor glycerol consumption and to facilitate DHA quantification in thraustochytrids bioreactors.

The DotBlot assay was clearly the fastest method to quantify glycerol in fermentation samples. Moreover, it is the cheapest method that also ensures proper precision and accuracy. It enables the glycerol concentration determination in approximately a minute. The cost of the DotBlot assay is low compared to HPLC and enzymatic kits. In addition, a high number of replicas can be processed at the same time using the DotBlot, due to the low volume needed for this assay (only 2 µL per replica). The method can also be applied to other types of microbial cultures that use glycerol as carbon source. In screening as well as in process development, a relatively large number of cultures take place simultaneously. The DotBlot assay allows the simultaneous quantification of glycerol from the different cultures. HPLC-RID methodology is accurate and precise, but it is slower and requires a higher investment in equipment. The kits are faster than HPLC methods and presented the lowest LOD and LOQ of the three methods compared.

FA, PUFA and DHA determination and this quantification method has been developed, and validated. FA and PUFA analysis method includes the sample preparation and the HRGC-FID analysis. Sample preparation methodology can extract and process 100% of the FA content of the samples, as validated using three different palmitic standards. The DHA quantification method has been validated allowing an unmistakable quantification during thraustochytrid cultures or any similar microorganism. This can be applied to every sample of the bioprocess developed.

The basic tools for the thraustochytrids bioprocess development in order to produce DHA have been determined. Thraustochytrids needs a marine medium and grow slower than major bacteria. It has been shown, using *A. limacinum* as a model, that thraustochytrids have a complex life cycle during batch growth. Between different life stages, zoospores revealed the highest growth rate while the vegetative cell stage appears to contain the highest amount of DHA. The latter feature is especially important for the bioprocess development, because it defines the best harvesting time to maximize DHA production.

All the information presented in chapter 2 will act as a toolbox that can be used to introduce the medium optimization (Chapter 3), culture strategies investigation (Chapter 4) and the bioseparation of DHA and TGs containing DHA (Chapter 5).

This page intentionally left blank

Chapter 3: DHA prolific production & cost effective medium optimization
Formulation of a medium to assess large scale viability

3.1 Introduction

The next step after analytical methodologies development and *A. limacinum* characterization was the investigation of growth media. Some recent studies, already investigated media compositions for different thraustochytrids including *A. limacinum* SR21[44]. However, the formulation was still incomplete and showed some contradictions between different papers. Every reported media has not considered the implications of large scale production, where some medium components are not easy to apply. Apart from a few studies, no research work has used an experimental design procedure to investigate every factor. When working with black boxes like thraustochytrids (relatively new in bioprocess investigation), it is very important to use statistically focused experimental designs.

Every medium element from bibliography have been considered in this chapter. Moreover, the development has focused on the possibility to apply the medium in a large scale production. The medium was developed by monitoring the values of biomass production, cost of every medium version, the scalability of each one of the components tested, and most importantly **the production of DHA**. This chapter covers the materials required for the preparation of artificial sea water, the main recipes of stock solutions of trace elements and some complex ingredients. Methods and precautions that are required in its preparation were covered as well. The formulation of a medium for a marine microorganism is a very old science with many difficulties still present nowadays.

3.1.1 Artificial sea water history

The culture of marine microorganisms, especially autotrophic and heterotrophic eukaryote microorganism, has presented many challenges since their discovery. In 1850 Ferdinand Cohn, a Germanborn scientist working in Poland, was the first in keeping a unicellular marine microorganism (flagellate *Haematocoocus*) in his laboratory for some time. He called this procedure **cultivation**, and this work was the first published report of algal culture. However, Cohn did not isolate the marine microorganism from other organisms, he did not use a culture medium, and he did not establish an indefinitely maintained culture. It was just the beginning. The science and technology for algae and algae-like microorganism has been developed since the late 19th century facing different challenges. Culture media was the main source of difficulties.

The initial bottle-neck was the basic formulation of the media to enable algae growth. For many years, every artificial marine media had precipitation issues during sterilization. In order to avoid precipitations, media were sterilized for a few seconds to 120 ºC. This resulted in almost every culture until the mid-20th century being bacterized. Even during the culture itself it was easily contaminated due to the inability to avoid any prokaryote population invading the cultures. For this reason, for many years algal culture investigation were bacterized[45]. Moreover, the presence of precipitates was a way to provide a non-toxic reservoir of nutrients as well as providing very low reproducibility procedures.

---

[44] This is the exact same strain used in the present thesis.
[45] Meaning that undetermined bacteria were always present during algal cultures.

The first report of pure axenic[46] cultures of algae stems from the Dutch microbiologist Beijerinck (1890). He adopted the bacteriological technique introduced by Robert Koch, 10 years earlier, and mixed the sampled water, or the medium, with gelatin. Beijerinck was the first to isolate free-living *Chlorella sp*. and *Scenedesmus sp*. in allegedly bacteria-free cultures. He also successfully isolated symbiotic green algae, shortly after Pierre Miquel (1890) established the bases of artificial seawater [172]. He was the first to

Solution A			Solution B	
	MIQUEL (1890)			MIQUEL (1890)
$MgSO_4$	10	g.	$MgSO_4$	
NaCl	10	g.	$Na_2HPO_4 \cdot 12\ H_2O$	4 g.[2]
Na_2SO_4	5	g.	$CaCl_2 \cdot 6\ H_2O$	4 g.[3]
NH_4NO_3	1	g.	HCl conc.	2 ml.
KNO_3	2	g.	$FeCl_3$ (melted)	2 ml.
$NaNO_3$	2	g.	H_2O	80 ml.
KBr	0.2 g.		quantity of sol.	20 drops
KI	0.2 g.		B added to 1 l.	(1 ml.?)
H_2O	100	g.	of sea water	
quantity of sol. A added to 1 l. sea water	40 drops (2 ml.?)			

Figure 3.30 Solutions formulated by Pierre Miquel to enrich simple water culture to harbour algae life. The table comes from a 100 years old paper about marine microorganism cultivation.

isolate and perform axenic cultures of *Diatoms.* During his work, he observed that the waters of lakes, ponds and seas could not support laboratory continued growth of algae. Natural waters had to be enriched by the addition of some mineral salts that he compounded in the famous solutions A and B [173] Figure 3.30. Both solutions were used to create the first artificial seawater ever described while avoiding precipitation problems. Solution A could be sterilized by heat and the B by filtration, putting both together after the process to create the final medium. Twenty years later solution A was replaced by sea water and the new formula of Allen and Nelson (1910).

Allen and Nelson [174] found that using natural sea water with KNO_3 (20 g/L) was enough since sea water brings other minor salts. Solution B has been used for several years with minor changes getting other novel axenic cultures [173]. Allen and Nelson started the first mass cultures (somehow a scale up to the large scale of their epoch) attempts, encountering new problems. In the first place, the light limitations in larger vessels when growing with photo-autotrophic microorganisms and, that it was not possible to use sea water due to the amount of pollutants.

In 1912 Ernst G. Pringsheim [175] proposed the use of distilled water from condensers and he also started to use soil extracts, obtaining better growths. Shortly after Foyn (1934) [172] formulated the Erd-Schreiber medium which was a combination of Schreiber's (1927) [172] mineral sea water enrichment and the soil

---

[46] Axenic describes the state of a culture in which only a single species, variety, or strain of organism is present and entirely free of all other contaminating organisms.

extract from Pingersheim. It was a real step forward. Many algal strains were able to grow in this medium and even new strains (never reported) were detected. Moreover, by this time there appeared the concept of aged water (Box 3.6) providing a new source of sterile water, as it was believed. Probably, what happened is that bacterial activity replenished the water with products of their metabolism and lysis, some of which may be growth factors. This kind of water is no longer used nowadays.

> **Box 3.6. Aged sea water**
>
> The aged sea water that Barker and Sweeney (1935) porposed is ordinary sea water which has stood in large glass bottles in the dark for months or years. The authors believe that during this period a complete mineralization occurs as a result of bacterial activity.

Some years after, it was established that a few milliliters of natural sea water were needed to guarantee a proper algal growth. Any composition tested was not generating the same growth as when a minimum volume of natural sea water was added. Several simple experiments pointed to an **organic substance** as the cause of greater growth. When using a diluted water extract of a microalgae for the growth of another, it grew significantly more than when the culture was prepared by using the ashes of the same extract. This indicated that some organic molecules were contributing significantly to the growth. After this new current in the media definition, Allen and Nelson suggested that organic micronutrients similar to the vitamins where always needed, especially for eukaryotic microorganisms. Specifically Allen [174,176] noticed that the differences in productivity in coastal and oceanic waters may be due to the auxotrophy of algae and their need of organic molecules, micronutrients or oligonutrients. He was idiomatic and set the beginning of the complex nutrients incorporation, in many modern media. As will be seen in this chapter, nowadays yeast extract and peptone (or triptone) are essential **complex ingredients**, especially for thraustochytrids.

During 1950s many laboratories around the world joined in the investigation of algal and algal-like microorganisms, offering works on different salt and metal compositions. Helen Vishniac (1953) [177] developed the first medium formulation oriented to ***Labyrinthula***[47] (see chapter 1*)* growth. Interestingly, this resulted in a good all-purpose medium for several marine fungi. The next significant step was set by L. Provasoli and his colleagues (1957) [173] who were developing artificial culture media for about 40 years and performed the first algal culture using antibiotic. Prior to these experiments, they had performed many experiments on vitamin requirements and most importantly introduced the use of Ethylenediaminetetraacetic acid (EDTA) as a metabolically inert chelator, to replace organic chelators such as citrate. EDTA permitted the development of both enriched artificial media and enriched natural seawater media that were more reproducible than those depending on additions of soil extract.

Over the next 20 years Starr, a North American investigator, started to establish a major culture collection of algae at Indiana University, which was then transferred to Texas University at Austin. The collection was named as the *UTEX culture collection of algae*. Then Starr and Zeikus' (1993) [178] published the content of the collection which contained 2.300 strains of 200 different genera. Data published contained information about every strain and their requirements in terms of salts and metal traces. Starr and Zeikus work has been used as a starting point for every marine medium or enriched artificial seawater formulated in recent years, including the work presented here.

---

[47] Labyrinthula belongs to the brother linage of thraustochytrids, the Labyrinthulids. See chapter 1 for more information.

3.1.2   Marine culture media

Natural sea water is a complex medium containing more than 50 known elements and a large and variable number of organic compounds. For any culture of marine microorganisms the use of natural sea water is acceptable, but it contains many other contaminants which have to be avoided, and is not an option. Without the addition of further nutrients and trace metals, the yield would not be suitable for an industrial production process. Even by enriching the natural sea water, the variations of the water composition throughout the seasons and even the years would be hardly reproducible.

For these many reasons, this project worked with a completely **artificial sea water enriched medium**. In modern marine culture media investigation, the main concern is making a complete autoclavable medium without precipitation. This lead to the following extensive modifications in the formula:

- Addition of synthetic metal chelators such as EDTA or nitriliotriacetic acid (NTA) to decrease metal precipitation.
- Addition of a pH buffer such as Tris(hydroxymethyl)aminomethane (TRIS) or glycylglycine with a range of 7 to 8.5, because the amount of precipitate increases as the pH rises during autoclaving.
- Reduction in salinity, thereby reducing the amount of salts available for precipitation.
- Replacement of Mg^{2+} and Ca^{2+} with more soluble univalent salts.
- Replacement of inorganic phosphorous with an organic source to avoid the precipitation $Ca_3(PO_4)_2$.
- Introduction of weak solubilizers, which are acids having highly soluble salts with calcium, such as citric acid.

89

The general modifications detailed above are included in all the media reported in bibliography (for thraustochytrids or not). Nevertheless, as mentioned in the early introduction, some of these modifications are not viable for a large scale process (e.g. TRIS as buffer), or even not required for the medium explained in this chapter. In the following subsections the basic elements for a proper medium formulation are explained.

3.1.2.1 Macronutrients or major nutrient requirements

Besides carbon, macronutrients are generally considered to be **nitrogen**, **phosphorus** and for some autotrophic microalgae, silicon. Therefore, thraustochytrids only need to collect nitrogen and phosphorus from the medium. These macronutrients are generally required in a ratio of 16:1 of nitrogen:phosphorus (N/P), when the nitrogen source is inorganic (Redfield ratio). Working with organic nitrogen makes ratio identification impossible. On the other hand, carbon:nitrogen (**C/N**) ratios are rarely considered. This is a huge mistake when working with thraustochytrids (accumulate very large amounts of long carbon chains in fatty acid form). The present work has primarily focused on C/N ratio. The average C/N ratio of phytoplankton is 6.7:1 and this is expected to be greater for thraustochytrids.

Nitrate and phosphate are normally added as $NaNO_3$ and $NaHPO_4 \cdot H_2O$ which represent the most common source when formulating marine media. Ammonium added as NH_4Cl is a very popular alternative nitrogen source or even added together with nitrate. Ammonium at concentrations between 100 to 250 µM, may be inhibitory to some coastal species. Thraustochytrids are most abundant in coastal areas, therefore, this must be considered. In some special cases, urea is another form of nitrogen, but is less used because it gets decomposed when heated. Inorganic nitrogen sources need to be reduced to the level of NH_2 for

their incorporation into protein molecules. Thus, the less reductant form is available for energy generation.

When organic nitrogen sources like amino acids are included in the culture media, they may serve as a pre-fabricated carbon skeleton and give high apparent growth yield on glucose or glycerol. Then the remaining amino acids can be catabolized as a regular energy source. Even if the final yield is similar, using an organic nitrogen source would make a culture show a higher growth rate. This makes organic nitrogen sources very attractive for an industrial biotechnological process. Specially knowing that the bioproduct or the biopharmaceutical product depend on the enzymatic machinery of the microorganism. **Complex substrates** are often used in bioprocess. These are usually by-products of the food industry, such as: molasses from sugar refinery, malt extract from brewery, starchy waste from starch manufacturing, **yeast extract** from autolysis of baker's or brewery yeasts at 50-55 ºC, **peptones** as a product of acid or enzymatic hydrolysis of animal or plant residues and soy meal from soybean oil factory.

Table 3.18 Typical composition of tryptone. It can vary depending on the source and hydrolysis process. [240]

Table 3.19 Typical composition of yeast extract produced by autolysis. It can vary depending on the yeast and the extract preparation process [240].

	% w/v			% w/w total amino acid
Dry matter	70	Alanine		3.4
Total nitrogen	9	Amino butyric acid		0.1
Protein	55	Arginine		2.1
NaCl	<1	Asparagine		3.8
		Cystine		0.3
		Glutamic acid		7.2
		Glycine		1.6
	ppm	Histidine		0.9
Thiamine	20–30	Isoleucine		2.0
Riboflavin	50–70	Leucine		2.9
Pyridoxine	25–35	Lysine		3.2
Niacinamide	600	Methionine		0.5
Pantothenic acid	200	Ornithine		0.3
		Phenylalanine		1.6
		Proline		1.6
		Serine		1.9
		Threonine		1.9
		Tyrosine		0.8
		Valine		2.3

	Casein peptone % w/w
Total nitrogen	13
Amino nitrogen	7
Carbohydrate	—
NaCl	3
Ash	6
Water	5
Alanine	16.8
Arginine	30.2
Aspartic acid	8.7
Glutamic acid	38.6
Glycine	4.4
Histidine	13.3
Isoleucine	29.9
Leucine	71.9
Lysine	61.1
Methionine	22.7
Phenylanine	33.0
Proline	7.4
Serine	28.7
Threonine	21.5
Tryptophan	8.6
Tyrosine	14.0
Valine	36.4

Those highlighted in bold are the main organic nitrogen complex sources widely used in many processes. The others are commonly considered carbon sources and can be used to substitute crude and technical glycerol, for the process developed in this work. Many providers of medium ingredients offer standardized

products of yeast extract and peptone ensuring reproducibility, which is very important for a biotechnological industrial process. Yeast extract (Table 3.19) and especially peptone are present in many variations. The most used peptone in eukaryotes cultivation is called **tryptone** (Table 3.18), the assortment of peptides formed by the digestion of casein [48] by trypsin. It has specific distribution of peptides and amino acids that are more favourable for eukaryote microorganism. Another popular variation of peptone, called bacteriopeptone, offers a bacterial favorable distribution of amino acids.

In general, yeast extract and tryptone are the most used complex substrates in biotechnology. The challenge is always to find the proper and most prolific C/N ratio considering growth rate, growth yield and product yield. In the results and discussion section of this chapter the importance, ratio and optimization of this nutrients, for DHA production, is discussed.

The importance of the nitrogen sources is not different for thraustochytrids cultures [50,51]. It has been reported that between 14 to 20% of *Aurantiochytrium* cell weight is nitrogen [179]. Although nitrogen sources have been optimized individually [180], the C/N has hardly been investigated.

3.1.2.2 Seawater salts

Depending on where the seawater is collected, the salinity varies, especially within different seasons. For this reason, most marine microorganisms have evolved to be able to grow in a wide range of salinities. Knowing the isolation origin is important to establish a proper salinity medium. Most abundant ions in natural seawater are chloride and sodium which represent 55% and 31% of the total ion composition, respectively. Sulfate, calcium, potassium and magnesium are a step below in abundance totaling a 13.7%. This generally causes confusion between salinity and NaCl concentration.

91
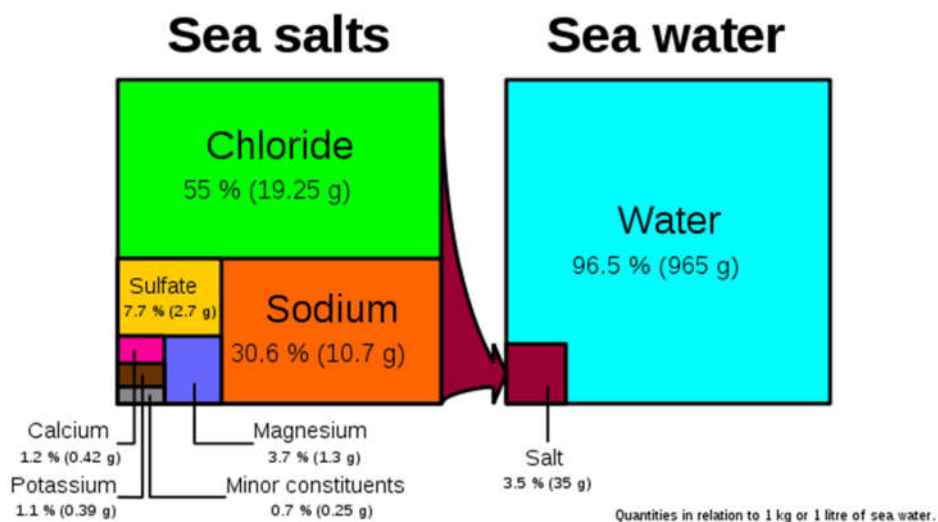
Figure 3.31 Proportion of salt to seawater (right) and chemical composition of sea salt (left). Diagram values are calculated as wt/wt. Originally created by Hannes Grobe (2007).

---

[48] Very common protein in milk.

Depending on the buffer used[49] it can generate solubility issues with minority ions. Nevertheless, a limiting amount of any of these ions would affect growth negatively. Accordingly, the amount of every salt species has to be accurately selected for any specific microorganism.

3.1.2.3 Trace metals

Trace metals are essential for any cell type growth. Only needed at very low concentration, they can become toxic at high concentrations. Trace metals are prepared separately and in a highly concentrated stock solution (weighing of reasonable amounts). Typical trace metal stock solution may consist of chloride or sulphate salts of Zn, Co, Cu, Mn, and Ni. These salts are generally kept in a solution containing a chelator such as EDTA. Fe is usually kept as a separate solution, and it should be chelated as well. Iron is either added as chloride or sulphate, as happens with the other metals. When working with artificial seawater, as is the case, boron should be added.

Of all the trace metals, **iron is the most important** limiting nutrient in the ocean. This is the micronutrient required in greatest quantity by marine microorganisms. Together with other trace metals it has a role in the cell respiration process. Many enzymes involved in the whole respiration process require metal atoms to reach a stable conformation with the proper activity. It also has the most complex speciation[50] chemistry, which often can be difficult to quantify and control in culture experiments. For this reason, iron is one of the most investigated trace metals in microorganism cultivations.

Iron forms insoluble hydrous ferric oxide precipitates that are unavailable to microorganisms. These ferric oxide precipitates absorb other essential metals and lower their availability. Due to these difficulties, providing an adequate and nontoxic supply of essential trace metals to marine microorganisms in a batch has presented a considerable challenge to scientists. Initially it was solved by adding soil extract, as explained before in section 3.1.1. Then many chelating or solubilizing agents have been added until the discovery of the EDTA potential.

3.1.2.4 Ethylenediaminetetraacetic acid - EDTA

Chelate: metal ratios 1.5:1 to 3:1 are commonly used. EDTA is the most common chelator and is usually purchased as the disodium salt Na2EDTA·2H2O which is very soluble in water. EDTA was first introduced as a replacement for soil extract in 1950 [181] and 7 years later was introduced as a metal buffering agent in seawater media. Nowadays it is essential for almost every medium whatever the cultured microorganism. Contrary to what is generally believed, EDTA + metal complexes are not directly available for the microorganism, but it creates an equilibrium between free metal ions and the complexes with it. This equilibrium phenomenon is represented by the Zn^{2+} shown below.

$$Zn2+ + EDTA \longleftrightarrow ZnEDTA$$
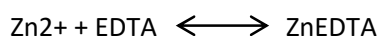
EDTA reacts creating complexes with the ions present in the medium while maintaining an equilibrium between free ions and its complexes. The non-chelated forms of the metal, including free ions and inorganic metal complexes such as $ZnCl^+$ are available to microorganisms. As these are removed by the activity of the microorganism, they are readily replaced by dissociation of an equivalent concentration of the metal chelate (complex with EDTA). Therefore, EDTA acts as a metal ion buffer and regulates the

---

[49] Buffers with
[50] Chemical speciation refers to the distribution of an element amongst chemical species in a system.

availability of metal ions in culture, such as pH buffer regulates the availability of hydrogen ions. This buffering system solves both the limitation (due to low solubility) and the potential toxicity of metals.

EDTA has been noted to inhibit the growth of some oceanic species, and could be substituted by Nitrilotriacetic acid (NTA) and citric acid. However, these are less effective than EDTA.

3.1.2.5 Vitamins
After many historical investigations about vitamin requirements for marine microorganisms three of them stand out as the most important: cyanocobalamine (also known as vitamine B12), thiamine and biotin. Very few algae need all three vitamins. The focus has never been put on these components when growing thraustochytrids as it has been in this chapter (more information see results section 3.2.5).

3.1.2.6 pH buffers
The proper functioning of biological systems requires control of pH, since most metabolic processes are inactivated outside a certain range of hydrogen ion concentration. A buffer is a system containing either a weak acid and its salt or a weak base and its salt, which resists changes in pH upon addition of acid or base. Therefore, a proper industrial bioprocess needs a buffer guarantee *A. limacinum* growth but at the lowest possible cost.

Two common pH buffers are used to prevent or reduce precipitiation as well as to maintain the pH range desired. TRIS buffer is the most common. Loeblich [182] compared the growth of marine dinoflagellate in several buffers. Dinoflagellates are in the chromoalveolates super-kingdom as thraustochytrids. In his work MOPS[51], HEPES[52], TRIS, glycylglycine and TAPS[53] were used as buffers and concluded that TRIS and TAPS provided maximal growth with minimal pH change. However, this buffer would not offer a suitable economic performance in a large scale process. For this reason, in this thesis a new buffer has been selected, as explained in section 3.3.4.

The buffer should not be able to permeate biological membranes, preventing concentration in the cell or organelles. Tris has a relatively high degree of fat solubility and may therefore permeate membranes. This also explains its toxicity for many mammalian cells in culture. On the other hand, the buffer should also not alter the ionic strength of the system as far as possible. The physiological ionic strength is between 100 – 200 mM KCl or NaCl. This can be very important, because the ionic strength of the solution is a measure of the ionic milieu, which may also affect the catalytic activity of an enzyme. At a pH of 7.5, for example, phosphate buffers add about 7x more ions to the medium than zwitterionic Tricine buffers at the same pH (Good & Izawa 1972).

3.1.3 Carbon sources and oxygen supply
In photosynthetic cultivations the carbon required for biomass production is generally pumped into the media as CO_2. Nevertheless, a heterotrophic microorganism needs a source of carbon dissolved in the media available to be catalyzed. The carbon substrate in the medium is the main energy source for an heterotrophic microorganism. The energy content of different substrates varies. A sample of different carbon sources energy content is shown in Table 3.20. Organic acids like oxalic acid have the lowest energy content with 2.4 Kcal/g carbon among the substrates listed in Table 3.20, and the maximum growth yield

---

[51] 3-(N-morpholino)propanesulfonic acid
[52] 4-(2-hydroxyethyl)-1-piperazineethanesulfonic acid
[53] N-Tris(hydroxymethyl)methyl-3-aminopropanesulfonic acid

Table 3.20 Energy content of different carbon sources [240]

C-substrate	Energy content (Kcal/g-carbon)
Oxalate	2.4
Formate	5.1
Citrate	6.5
Glucose	9.2
Glycerol	11.0
Methanol	14.6
Methane	17.4

reported is the lowest as well (0.14 g biomass / g carbon). As the energetic content increases, so does the growth yield. In addition to a higher energy content, the substitution of a traditional carbon source, such as glucose by crude or technical[54] **glycerol**, **a less costly source** has a positive impact on the economics of the bioprocess. Cost reduction on growth media with minimal undesired effects is crucial for a potential industrial implementation. In this scenario, crude glycerol as an industrial byproduct available in large amounts, seems an ideal match [183] (explained in chapter 1).

The **oxygen** content and other culture parameters determine the pathways of which a carbon/energy substrate is metabolized to yield different amounts of biochemically available energy in the form of ATP[55]. For example, 30 ATP moles are generated from a mole of glucose via oxidative phosphorylation, but only 1–3 moles of ATP are generated in anaerobic condition via the various pathways. This is not different for glycerol and other heterotrophic cultivations. Therefore, a well-developed medium for thraustochytrids cultivation would only work as intended in the proper oxygen conditions. Actually, oxygen supply has other singular effects on thraustochytrids that are discussed in the next chapter.

3.1.4 Medium formulation and optimization workflow

Once the basic requirements are defined the formulation of the medium can be started. Starting with the carbon source, the main energy source, glycerol and crude glycerol performance has to be compared with glucose cultivations. In this chapter a set of different bioreactors comparing these three carbon sources was reported and explained. These cultivations have been carried out with literature medium formulations as the starting point. The next step was the nitrogen source requirement characterization and the determination of the perfect C/N ratio. To define this ratio, both, DHA, biomass production and economic viability was considered. To do so, Artificial Neural Network (Appendix A) a family of statistical learning models allowing an exhaustive investigation over the desired factors have been used. Nitrogen source candidates were **NaNO₃** and **NH₃HCl** as inorganic sources, whereas **yeast extract and tryptone** were the organic candidates. Then the research focused on the **buffer** (TRIS) and **salts** (NaCl, MgSO₄, CaCl₂, KCl and CH₃COONa). **Vitamins** requirements have been investigated as well (Vitamin B12).

The work presented here investigated the full composition considering its viability to be applied in an industrial process. The objective has been the formulation of a cost effective medium allowing thraustochytrids to offer the maximum productivity of DHA.

94

---

[54] Partially purified.
[55] Adenosine triphosphate (ATP) is a nucleoside triphosphate used in cells as a coenzyme often called the "molecular unit of currency" of intracellular energy transfer.

3.2   Results and discussion

The starting thraustochytrids medium was generated based on the work of Starr and Zeikus (1993) [178]. As explained in the chapter introduction, Starr and Zeikus accumulated, over the years, several marine species (not only thraustochytrids) in their collection as well as the information related with it, such as medium composition and conservation / cultivation techniques. Other groups around the world started their own medium investigation following Starr and Zeikus work indications. The increasing interest in thraustochytrids as prolific producers of PUFA has generated many works referred to their medium. The standard medium elaborated based on bibliography is listed in Table 3.21.

Moreover, this medium can set the basics for other thraustochytrids medium, ensuring significant productivities, as will be discussed. The optimization presented here investigated different carbon sources, nitrogen sources and their concentration, the salts composition, the buffer, vitamin requirements and investigated some of the trace elements porposed by Starr & Zeikus.

This section first visits the capacity of *A. limacinum* to grow in a bioreactor using glycerol and crude glycerol as carbon source, with a standard medium, compared to glucose. The data obtained from these experiments have been used to define basic kinetic parameters of the microorganism, which will then be compared with the kinetics obtained with batch cultures using the optimized medium described in the following section, starting with the carbon source.

Table 3.21 Starting medium composition.

Component	Concentration
Tris	1 g/L
CH_3COONH_4	1 g/L
NaCl	18 g/L
$MgSO_4 \cdot 7H_2O$	2.5 g/L
$CaCl_2$	0.3 g/L
KCl	0.6 g/L
$NaNO_3$	1 g/L
NH_4Cl	0.03 g/L
KH_2PO_4	0.05 g/L
Yeast Extract	1 g/L
Tryptone	1 g/L
Vitamina B_{12}	0.15 µg/L
Carbon source	Between 10 g/L and 100 g/L
$Na_2EDTA \cdot 2H_2O$	0.20 mM
H_3BO_3	1 mM
$MnSO_4 \cdot H_2O$	0.097 mM
$ZnSO_4 \cdot 7H_2O$	7 µM
$CoCl_2 \cdot 6H_2O$	2 µm
$FeSO_4 \cdot 7H_2O$	0.83 mg/L
$FeCl_3 \cdot 6H2O*$	0.018 mM

3.2.1   Carbon sources and *A. limacinum* kinetic characterization in Batch cultures.

With the aim of exploring the industrial potential of thraustochytrids strains as heterotrophic microalgae for the enhanced production of PUFA (mainly DHA), the project was initiated by evaluating the performance of these microorganisms in bioreactors. A comparison using the three main carbon sources in parallel to report their growth kinetic parameters in fermenters has not been published. The first step was to determine the relationship between biomass dry cell weight (DCW) and OD (600 nm). Figure 3.32 illustrates this relationship, and allows the interpolation of absorbance values to dry weight using pure glycerol. The linear relationship was y = 1.55x   0.47, with a positive correlation of 0.92. Cultivations using glucose and crude glycerol showed identical values for the absorbance-dry weight curve. A full characterization in terms of typical growth kinetics and DHA production was then performed using each carbon source. With the aim of exploring the industrial potential of thraustochytrid strains as heterotrophic microalgae for the enhanced production of PUFA (mainly DHA), the project started evaluating the performance of the microorganism in bioreactors using simple literature medium and three carbon sources. To the best of the author knowledge a comparison using in parallel the three main carbon sources reporting their growth kinetic parameters in fermenters has not been published.

The first characterization step was the relationship biomass dry cell weight (DCW) and OD (600nm). Figure 3.32 illustrates such a relationship allowing the interpolation of absorbance values to dry weight using pure glycerol. The linear relationship is *y = 1.55x – 0.47*, having a positive nearly perfect correlation of 0.92. Cultivations using glucose and crude glycerol showed identical values for absorbance-dry weight curve (data not shown).
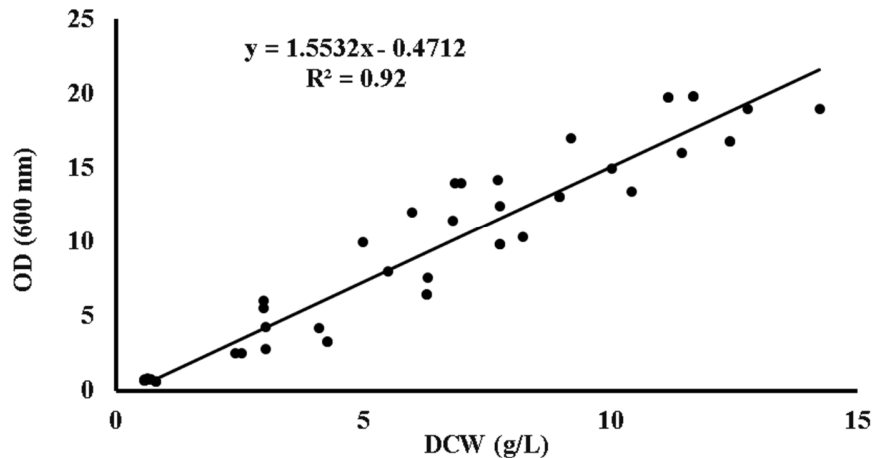
Figure 3.32 Dry cell weight vs. OD curve. The linear relationship was used to determine dry cell weight of the fermentations performed in the present work.

3.2.1.1 Growth rate

The complex life cycle of *A. limacinum* can be simplified classifying it into a zoospore phase and a vegetative phase. The strain used in the present work, can release up to 32 zoospores. Figure 3.33 shows a sporangium cell which is about to release zoospores. In *A. limacinum* the release of zoospores generates a peak in the growth rate, probably defining μ_{max} values in batch cultures. Cultures using glucose (0.21 ± 0.02 h^{-1}) as carbon source showed higher maximum growth rates than glycerol (0.18 ± 0.01 h^{-1}) and crude glycerol (0.19 ± 0.02 h^{-1}). On the other hand, when *A. limacinum* is growing in a vegetative phase only performing some bipartitions, the growth rate is much slower. Net growth rate were slightly higher in glycerol cultures (0.12 ± 0.01 h^{-1}) compared to glucose (0.10 ± 0.002 h^{-1}) and crude glycerol (0.10 ± 0.01 h^{-1}). Thus, indicating that growth in glycerol and crude glycerol have a more constant growth rate, as observable in Figure 3.34. The presence of impurities (at the concentration used in crude glycerol cultures) was not inhibiting the growth.
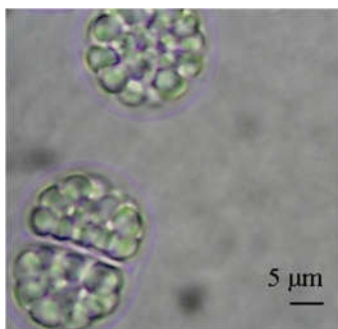
Figure 3.33 Image of A. limacinum sporangium full of zoospores ready to be released.
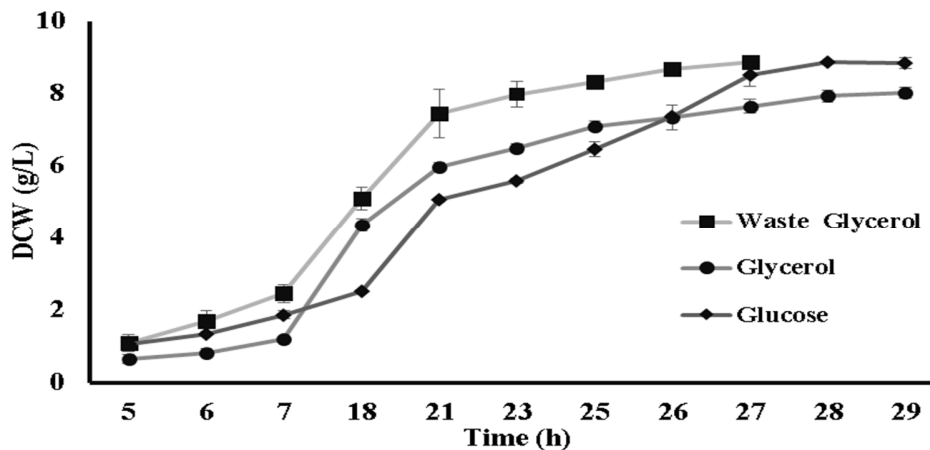
Figure 3.34 Cultivation of A. limacinum using 10 g/l of carbon source: glucose (♦), pure glycerol (•) and crude glycerol (▪).

3.2.1.2 Growth yield

In terms of growth yield ($Y_{x/s}$), pure glycerol has the lower values. Glucose and crude glycerol have rendered similar yields, the latter having the highest value of the carbon sources assayed. Interestingly, it has increased the final yield compared to the cultures with glucose and glycerol as carbon source. Figure 3.35 shows the growth yield graphical calculation of crude glycerol cultivations, showing a lower value (0.79 g/g) than those calculated with batch cultivations (Table 3.22, next page). The slope of the calibration curve (Figure 3.35) reveals the amount of biomass exclusively generated by the crude glycerol. The difference indicates that other carbon sources in the crude glycerol and the complex ingredients are contributing to biomass formation. In addition, some oligoelements coming from vegetal feedstock of biodiesel production could be contributing to the growth. In the bibliography, the disparity of values reported is quite high, ranging from low values as 0.2-0.3 g DCW/g carbon source [49,52,93,131], to higher values 0.6-0.8 g DCW/g carbon source [16,56,184]. Thus an equal performance comparison of different carbon sources should contribute to a global understanding of the process. Nitrogen source has an important role in growth and a lack of nitrogen can reduce the carbon source yield. Organic nitrogen
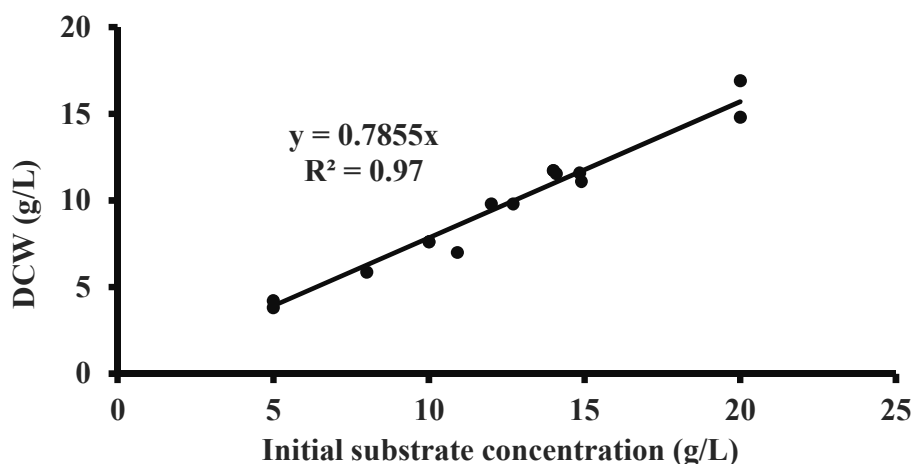
Figure 3.35 Linear relationship between final DCW and initial substrate concentration. The slope reveals the "real" biomass / glycerol yield without other energy sources from complex ingredients (Yeast extract and tryptone).

sources are preferred in thraustochytrids cultivations [93,185]. Yx/s obtained in the present study are comparable to the highest yields reported in bibliography.

3.2.1.3 Saturation constant (Ks)

The saturation constant is (typically) the hardest growth parameter to characterize in batch reactors, presenting more inaccuracies. Ks shows the affinity of the strain to a specific substrate and is expressed as g of substrate/L. In this study, the cultivation of a eukaryotic species with a complex life cycle added more difficulties. As seen in Table 3.22, *A. limacinum* has higher affinity, 2.48 ± 0.5 *gS/L* towards glucose compared to pure 5.03 ± 1.9 *gS/L* and crude glycerol 8.07 ± 1.1 g S/L. *A. limacinum* shows a lower affinity

Table 3.22 Summary of the growth kinetics parameters using different carbon sources.

	Glucose		Glycerol		Crude Glycerol	
X (g/L)	8.83	±0.15	8.21	±0.17	8.86	±0.11
$Y_{X/S}$ (g/g)	0.84	±0.04	0.74	±0.04	0.85	±0.1
μ_{max} (h^{-1})	0.21	±0.02	0.18	±0.01	0.19	±0.02
μ_{net} (h^{-1})	0.10	±0.002	0.12	±0.01	0.10	±0.01
K_s (g/L)	2.48	±0.5	5.03	±1.9	8.07	±1.1
m_s (g/g·h)	0.03	±0.001	0.06	±0.01	0.07	±0.01
$Y_{P/X}$ (g/g)	0.14	±0.02	0.15	±0.04	0.15	±0.02

for crude glycerol compared to pure glycerol and glucose. This might be a consequence of interference from other carbon sources, oligoelements and contaminants introduced with the crude glycerol. Growth rates and yields are not affected by different values of K_S. The K_S is an important parameter when designing continuous cultures, as it is in this study. However, the different cell cycles taking place in batch and continuous reactors have to be considered. Ks values could change drastically when calculated from a steady state of a chemostat, where only vegetative cells are present.

3.2.1.4 DHA yield ($Y_{P/X}$)

Finally, the DHA yield or $Y_{P/X}$ refers to the amount of DHA per each gram of biomass, expressed as g DHA/g. The values obtained show a slight advantage when glycerol-based fermentations are used. Crude and pure glycerol yielded 0.15 ± 0.02 g DHA / g. Glucose cultures yielded an average of 0.14 ± 0.02 g/g. DHA content was monitored during the cultivation (shown in Figure 3.36). In the conditions presented in this work, the DHA production was found to be linked to growth. The plot indicates that at the beginning, triglycerides are consumed to get extra energy for zoospore phase. When the microorganism changes back to the vegetative state, it accumulates lipids again accumulating DHA as well. As indicated in the bibliography, zoospores spend a high amount of energy [56,127]. The results reported here render a concentration of 1.24 g DHA/L using glucose, 1.23 g DHA/L pure glycerol, and 1.33 g DHA/L using crude glycerol. The results indicated that DHA production was not affected by the carbon source used.
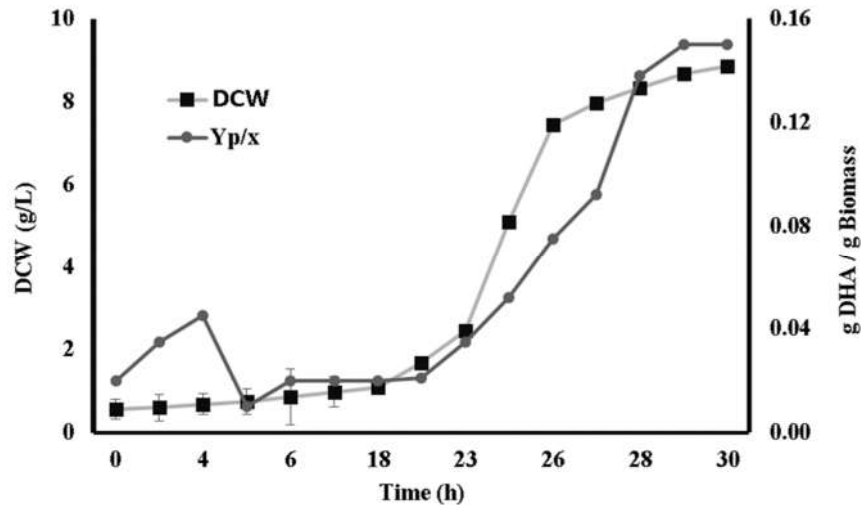
Figure 3.36 Evolution of DHA yield and biomass concentration over time during a batch reactor.

The current state of the art shows a remarkable variability in terms of DHA productivity, especially in glycerol cultures. Cultures using glucose reported yields of 0.23-0.26 g DHA/g glucose [9,186,187]. Cultivation using pure and crude glycerol reported variable yields of DHA. The strain used, but especially the glycerol source and process parameters cause notable variations in the obtained yield. Optimized growth media, and fatty acids stimulation via oxygen deprivation and carbon to nitrogen ratio (C/N) also increase the final DHA yield. Jakobsen *et al*. obtained a high productivity of 90 mg DHA/l-h using pure glycerol and stressing cells using nitrogen starvation [16]. Studies using glucose and batch reactor reported productivities ranging from 116 to 129 mg DHA l^{-1} h^{-1} [9,186,187]. Using pure glycerol productivities reported were from 38 to 90 mg DHA l^{-1} h^{-1} [16,49]. Crude glycerol references reported DHA productivities from 21 to 23 mg DHA l^{-1} h^{-1} [29,52,93]. Glucose-based fermentations reporting superior productivities rely on higher initial substrate concentration, and so final higher cell concentration reached. Crude glycerol fermentations typically use lower initial amounts of glycerol, in order to avoid accumulation of toxic compounds. This leads to lower final cell concentration and lower productivities. The productivities obtained in the present study (with equal initial substrate concentration) are lower using glucose and pure glycerol, 55 mg DHA l^{-1} h^{-1}, compared to crude glycerol, 60 mg DHA l^{-1} h^{-1} as reported in Abad and Turon 2015 [188].

Therefore, it was confirmed that DHA production is affected by other parameters different from the used carbon source. An optimization of the growth media and operational parameters are supposed to still increase the productivity of this system. These parameters will be discussed in Chapter 4.

3.2.2 Nitrogen source investigation – C/N ratio

To the best knowledge of this work's author, there are 92 (up to date) literature works talking about thraustochytrids cultivation and factors of the medium. Only 6 of these publications analyzed, in different ways, the medium composition for *A. limacinum* cultivation. Only a few have investigated nitrogen sources. Chi *et al.* (2007) [93] investigated three different nitrogen sources, CH_3COONH_4, $NaNO_3$ and NH_4Cl, based on Starr & Zeikus work. Huang *et al*. (2012) [189] reported the importance of the C/N ratio testing two yeast extract and tryptone combinations. Rosa *et al*. (2010) [9] tested three different C/N

ratios increasing lipid productivity. Zhou *et al*. (2007) [190] tested different yeast extract, tryptone and corn steep liquor concentrations.

Nitrogen sources demonstrated to have an important effect on microorganism growth as well as on lipid molecules accumulation. However, none of the literature works mentioned has ever performed a deep investigation. The effect of organic nitrogen and inorganic nitrogen sources over thraustochytrids growth has been compared in any of this publications. In this thesis it was decided to perform an exhaustive investigation of nitrogen requirements of *A. limacinum*. Four nitrogen sources were selected for different reasons. Ammonium acetate and sodium nitrate as inorganic nitrogen source, initially purposed in Starr & Zeikus [178] work whereas Chi *et al.* (2007) [93] suggested 1 g/L of ammonium acetate as optimum for *A. limacinum* growth. On the other hand, tryptone and yeast extract were selected as the sources of organic nitrogen. These organic complex mixtures also provide powerful oligo elements that might be very important for eukaryote growth. Especially yeast extract which contains growth factors, vitamins, etc.

The investigation of these four nitrogen sources was performed sequentially using different Taguchi matrices. After every group of experiments, data was validated performing a bioreactor cultivation. In order to be able to compare the large number (100 experiments approximately) of experiments generated in this section, the growth was measured between 4 and 34 hours of culture. Every culture was carried out in 250 mL Erlenmeyer flask with a culture volume of 70 mL. Starting OD was set to 0.5 points for every culture[56]. Measurements of DHA were performed on samples collected after 34 hours of culture. The starting medium composition was as detailed in Table 3.21, section 3.2, with 8 g/L glycerol as carbon source.

3.2.2.1 Nitrogen sources investigation through DoE

Several DoE have been carried out using flask cultures to obtain enough data to train and check the artificial neural networks (Appendix E). Also, the significant effects of each of the nitrogen sources have been evaluated using ANOVA. The following sections are divided by DoE indicated as Ni (where i corresponds to the number of the experiment) together with the response factor considered. Every DoE was analyzed by ANOVA.

Design of experiments N1- Response: growth

The project was initially seeking a reduction of organic nitrogen source concentration due to their higher cost. Therefore, only two levels of every factor (nitrogen substrate), yeast extract and tryptone were set at 0.6 and 1 g/L, whereas nitrate and ammonium were investigated between 1 to 3 g/L. The selected Taguchi matrix was a L_{16} (2^{15}) guiding every experiment variation. Results are shown in Figure 3.37. It is clear that nitrate has a null contribution to growth, whereas the other three factors have a significant influence. Level plots indicate the proper concentration from each factor.

A.limacinum growth was reduced in the presence of higher ammonium concentrations whereas, the response is increased in the presence of higher concentrations of both tryptone and yeast extract. The interaction between both organic sources was positive and increases at higher levels. Ammonium was contributing positively at the lower concentration. This factor gives the highest response value when it is combined with yeast extract higher level (as indicated in the lower table of the Figure 3.37). Results

---

[56] The inoculum OD was calculated to determine the volume needed to start every culture at 0.5 OD points.

indicate nitrate was not affecting the growth in any level studied. Ammonium concentrations of 3g/L appear to be negatively affecting growth, while showing the highest response in the design when its concentration was above 1 g/L. These data are in concordance with those reported by Chi *et al*. (2007) organic nitrogen investigation [93].

Ammonium and yeast extract revealed an important contribution on biomass growth. Tryptone showed a modest effect and nitrate did not enhance the growth in any studied situation. For this reason, the **next DoE was designed with the following modifications**:

➢ Tryptone – Two levels, 0 and 0.25 g/L. Justification: tryptone and yeast extract have a similar role, and the following DoE wanted to elucidate if this can be avoided in the medium.
➢ Nitrate – Four levels, 0, 2, 3 and 5 g/L. Justification: Increasing the concentration range might show if this nitrogen source could become important outside the ranges investigated before.
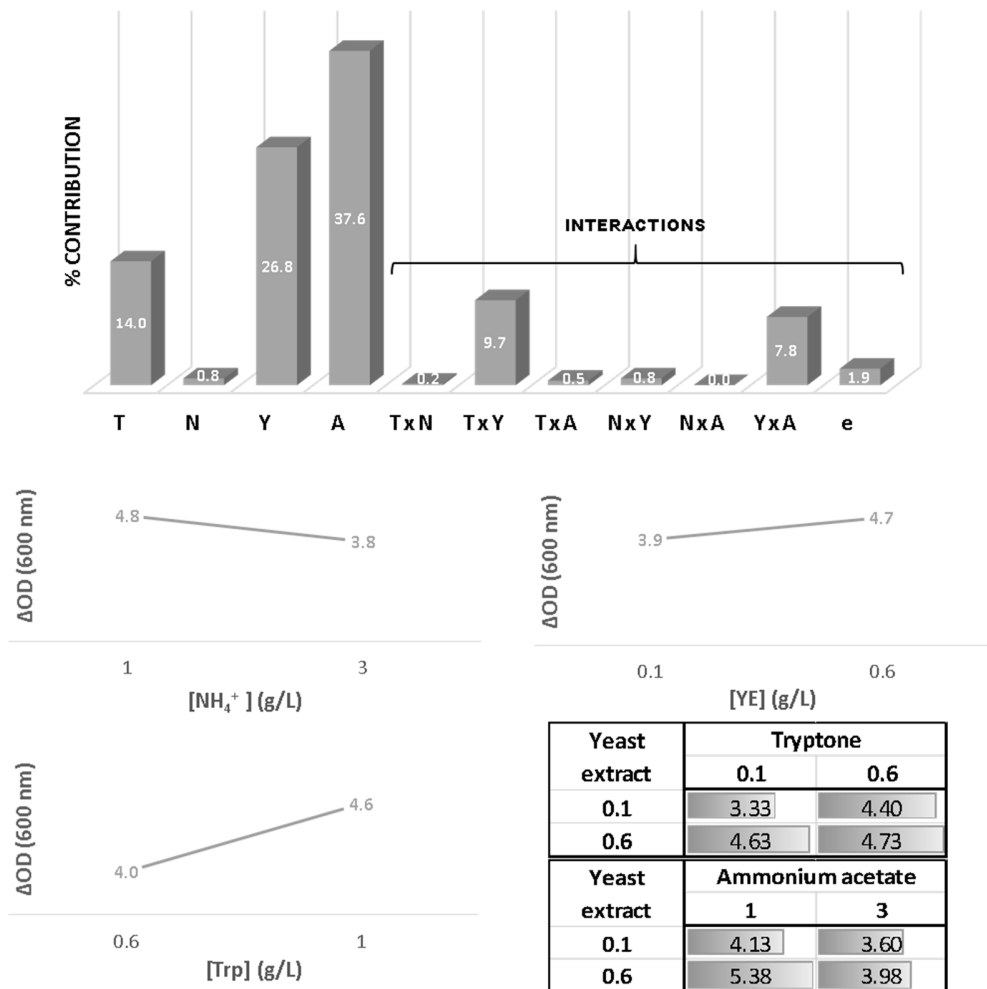
Figure 3.37. Histogram on the top of the figure indicates the contribution of every factor to the final values. The three plots show the response of every level from every factor. The small tables in the bottom right of the figure indicates the effect of every level from the significant interactions indicated in the histogram. T stand for tryptone, N for nitrate, Y for yeast extract and A for ammonium.

> ➢ Yeast extract – Four levels, 0.1, 0.2, 0.6 and 1 g/L. Justification: Broadening the concentrations will show if this is essential.
> ➢ Ammonium – Two levels, 1 and 3 g/L. Justification: This nitrogen source is fixed in order to investigate the others.

Design of experiments N2 - Response: growth

In order to allocate two levels with four factors and two more with two levels a $L_{16}(2^{15})$ matrix was modified into a $L_{16}(2^9 \times 4^2)$ using a multilevel formatting technique[57]. Results of the second DoE are shown in Figure 3.38.
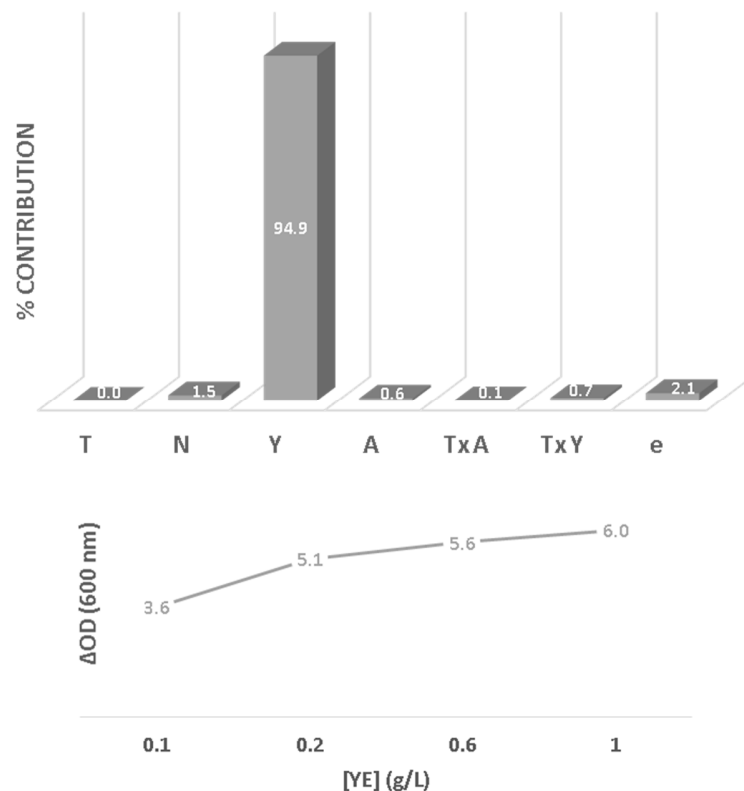
Figure 3.38 Results of the second nitrogen investigation (DoE) based on a $L_{16}(2^9 \times 4^2)$ OA. The plot above shows the contribution of every factor. The plot below shows level effects of yeast extract. T stand for tryptone, N for nitrate, Y for yeast extract and A for ammonium.

In the current frame of concentrations, yeast extract showed a massive contribution with a 95%. The effect increased compared to the previous experiment. According to the levels plot (Figure 3.38), there is room for improvement by increasing yeast extract concentration. Nitrate did not show any effect on *A. limacinum* growth despite the concentration increase. This time nor tryptone and ammonium generated any contribution. This indicates that the effect of yeast extract for the microorganism growth is very high and masks the other three factors. Thus, yeast extract might be the solution to simplify the medium

[57] One of many techniques which allows transforming the levels of any column while maintaining the orthogonality.

composition by only adding it in a higher concentration. According to these results and with the aim of determining the effect provided by any of the nitrogen source without yeast extract, **next DoE modifications are purposed as following:**

> ➢ Tryptone – Three levels, 1, 1.5 and 2 g/L. Justification: Investigate if tryptone might have powerful effects at higher concentrations. Just as happens with yeast extract.
> ➢ Nitrate – Three levels, 4, 6, 8 g/L. Justification: Increase even more the concentration of this salt to determine if there could exist any effect on *A. limacinum* growth.
> ➢ Yeast extract – 0 g/L. Justification: Avoid masking other factors in this experiment.
> ➢ Ammonium – Set at 1 g/L. Justification: This concentration of ammonium was near its optimal effect and will allowed to discover if any other of the factors (besides yeast extract) can surpass its importance.

Design of experiments N3 - Response: growth

NO3-	Tryptone		
	1	1.5	2
4	1.10	1.00	1.00
6	0.70	1.10	1.20
8	0.90	0.60	1.20
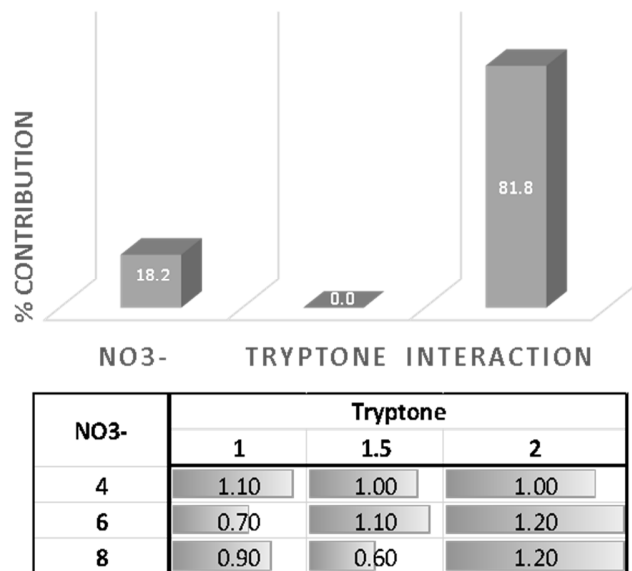
Figure 3.39 Results of the third experimental design. Top histogram indicates the % contribution of every factor. Table shows the response (OD at 600 nm) when different factor levels are combined.

This experiment was carried out following a L_9 (3^4) matrix which allows the investigation of two factors with three levels as well as their interaction. The results are shown in Figure 3.39. None of the factors are contributing individually. Only their interaction showed the main contribution to an increase of growth and observing the table (two factor level interaction) show that both factor's maximum level generated the best result. However, growth values are drastically lower than those showed in the previous experiments. This data was in concordance with previous results, indicating that nitrate influence was negligible within the range of concentrations studied so far. As a final experiment, a DoE including only inorganic nitrogen sources was purposed.

Next DoE modifications are as following:

➢ Tryptone – Set at 0 g/L. Justification: Investigate only inorganic sources.

➢ Nitrate – Three levels, 4, 6, 8 g/L. Justification: Increased even more, the concentration of this salt to determine if any effect on *A. limacinum* growth may exist as well as studying it in combination with ammonium.

➢ Yeast extract – 0 g/L. Justification: Investigate only inorganic sources.

➢ Ammonium – Three levels, 0, 0.75 and 1.5 g/L. Justification: The optimum of ammonium contribution was known to be around a concentration of 1 g/L, but in this work the range was wider to investigate the combination effect with nitrate.

Design of experiment N4 - Response: growth

Similar to the previous experiment, this DoE generated a noticeable lower response compared to experiments with organic nitrogen sources. Growth values (OD at 600 nm) were much lower than previous results (Figure 3.40). The contribution of ammonium and nitrate is 57% and 43% respectively. Their interaction is noncontributing as shown in the histogram from Figure 3.40. Level plots indicated that lower concentration of both factors is better for growth. These results add more evidence that yeast extract is essential for *A.limacinum* growth. In order to support this hypothesis, the following experiment focused on yeast extract.
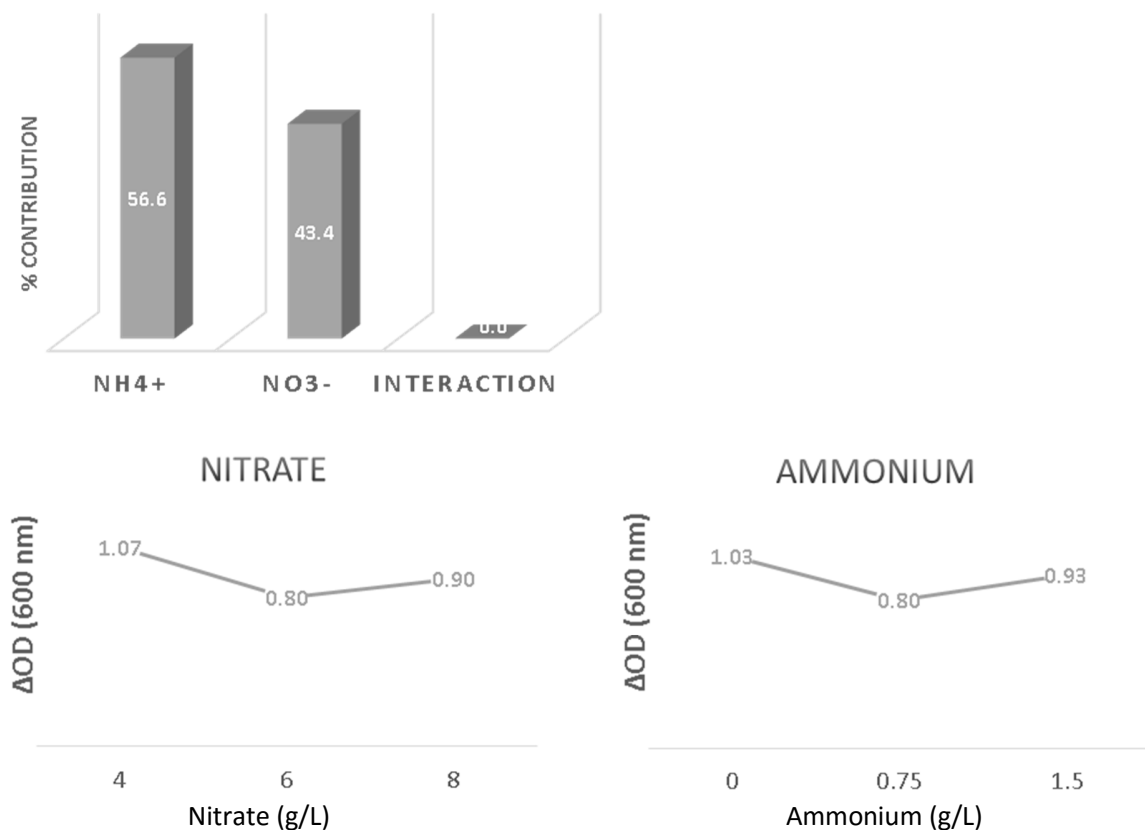
Figure 3.40 Results of the fourth nitrogen source design of experiments. Top histogram indicates the % contribution of every factor. Below level plots of every important factor from the set of experiments.

Yeast extract experiment – Response: growth & DHA yield

The following experiment set 0 g/L of tryptone, 1 g/L of nitrate and 0.75 g/L of ammonium while increased sequentially yeast extract concentration from 0.1 up to 0.9 in 9 different flasks. Since the DHA analytical methodology was implemented DHA yield was monitored. Results of yeast extract supplementation (Figure 3.41) clearly show a positive relationship between increasing yeast extract concentration and growth of *A. limacinum*. This data supports the importance of this organic nitrogen source as stated before.

DHA yield followed the same tendency as the growth. Maximum yield values of 0.105 g DHA / g biomass were obtained at the highest yeast extract concentration experimented here. Being maximum values at one side of the data, it might indicate that both the   OD and the DHA yield can increase even more. For this reason, the next experiment was again based in a $L_9(3^4)$ matrix with higher yeast extract concentrations and the following modifications:

- ➢ Tryptone – Set at 0 g/L. Justification: Investigate only yeast extract as organic source.
- ➢ Nitrate – Set at 0 g/L. Justification: Investigate only ammonium as inorganic source.
- ➢ Yeast extract – Three levels, 0, 1 and 2 g/L. Justification: Investigate this factor at higher concentrations than before.
- ➢ Ammonium – Three levels, 0, 0.75 and 1.5 g/L. Justification: The optimum of ammonium contribution is known to be around a concentration of 1 g/L. In this work the range was wider to investigate the combination effect with yeast extract.

105
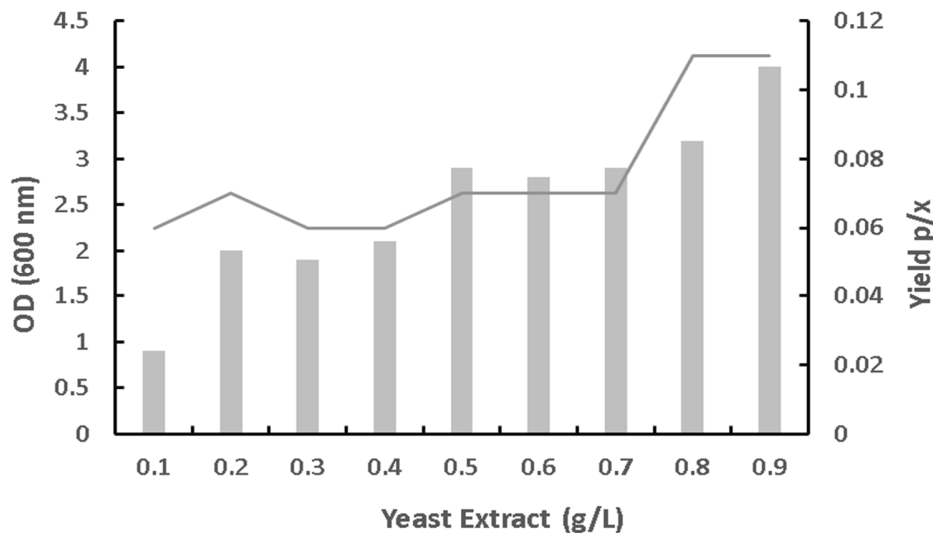
Figure 3.41 Results of A. limacinum growth and DHA yield among increasing yeast extract concentration. Bars - biomass growth; line – DHA yield.

Design of experiment N5 - Response: growth

Growth values in this experiment generated very interesting data as can be seen in Figure 3.42. OD values reached almost 7, which is higher than previous experiments in flask. Yeast extract showed a 90% contribution for the best growth of *A. limacinum*. Definitely this organic nitrogen source has a dominant impact on growth. The level plot also shown in Figure 3.42 indicates that the highest concentration of yeast extract generates the maximum growth in the conditions studied.

A last DoE was purposed to investigate different tryptone concentration in combination with ammonium concentrations. The next DoE consisted of the following modifications:

➢ Tryptone – Three levels, 0, 1 and 2 g/L. Justification: Investigate tryptone as organic source.
➢ Nitrate – Set at 0 g/L. Justification: Investigate only ammonium as inorganic source.
➢ Yeast extract – Set at 0 g/L. Justification: Investigate tryptone as organic source.
➢ Ammonium – Three levels, 0, 0.75 and 1.5 g/L. Justification: The optimum of ammonium contribution was known to be around a concentration of 1 g/L. In this work, the range was wider to investigate the combination effect with tryptone.
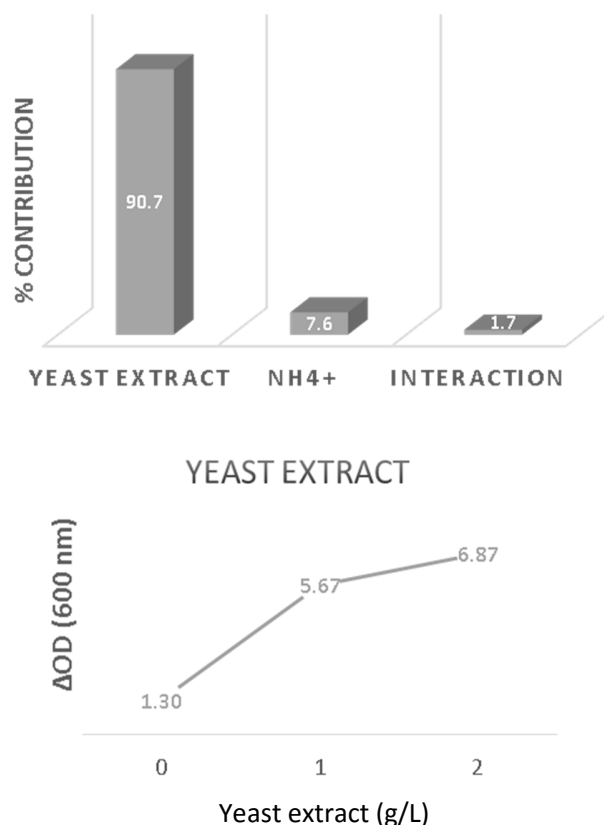
Figure 3.42 Results of the fifth nitrogen source DoE. Top histogram indicates the % contribution of every factor. Below level plots of every important factor from the set of experiments, which in this case is only yeast extract.

Design of experiment N6 - Response: growth & DHA yield

These experiments were carried out in $L_9(3^4)$ matrix. Data displayed in Figure 3.43 support the hypothesis of the exceptional effect of organic nitrogen sources on *A. limacinum* growth. Tryptone has shown a significant positive impact on the culture with a 79% contribution. Even though the growth is significantly poor compared with the experiments with yeast extract, it shows a maximum in the cultures with the middle level concentration. In other words, 1 g/L of tryptone would be enough to reach its maximum effect but this effect was lower than which yeast extract generated (Figure 3.41).

Results concerning DHA yield showed a different output. In this case, ammonium appears to be slightly more important than tryptone although the interaction of both factors has proved to be the most important one with a contribution of 68%. In concordance with previous experiments from this section,

ΔOD results

DHA yield results

Tryptone	Ammonium		
	0	0.75	1.5
0	0.06	0.08	0.12
1	0.12	0.08	0.06
2	0.08	0.06	0.06
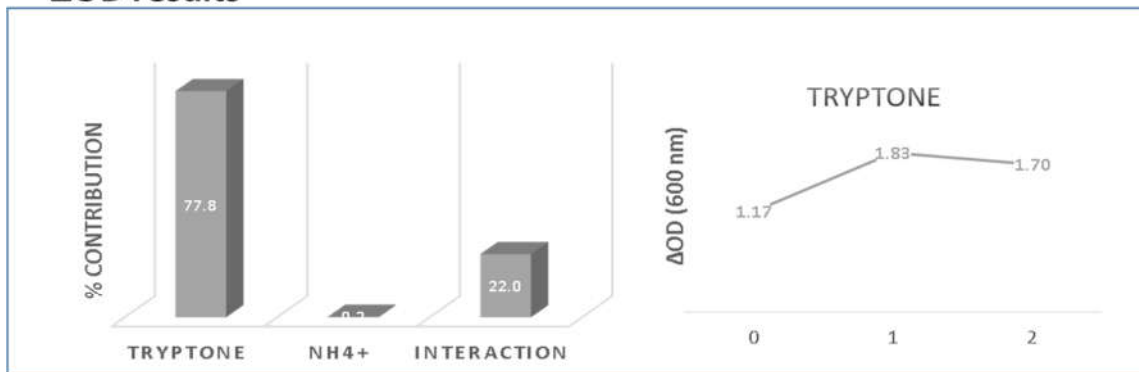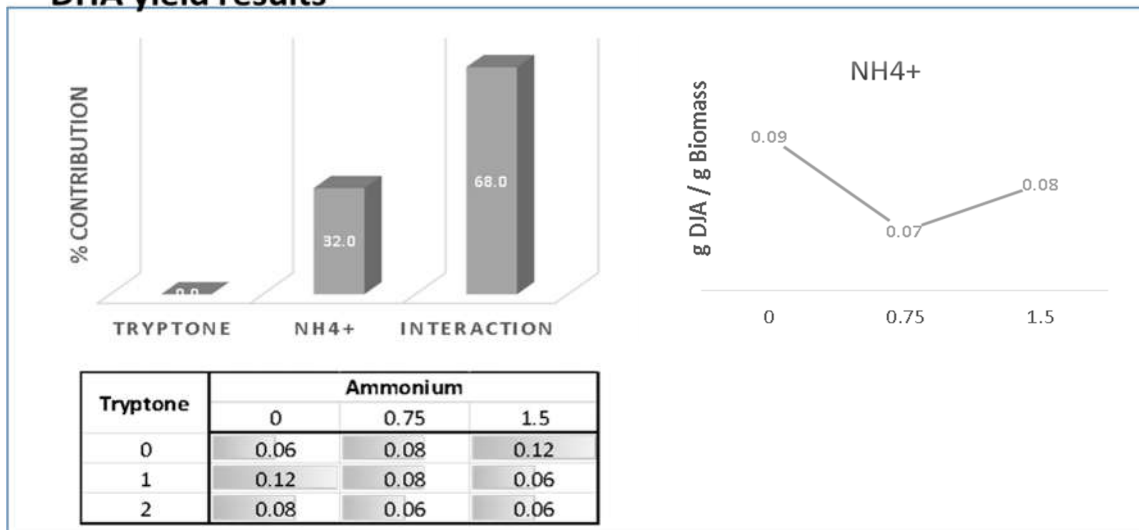
Figure 3.43 Results of the sixth DoE experiments regarding both responses, increase of OD and DHA yield, as indicated in the figure. Histograms show the % contribution of every factor on each one of the responses. Both set of results contain a level plot from the most important factor in each case. Bottom table show the tryptone ammonium interaction results regarding DHA yield.

ammonium showed the better result when the concentration was the lowest. Therefore, reported contribution is negative. The table of interaction levels contradict the data by placing one of the maximum yield values when the ammonium concentration is the highest and there is no tryptone. On the other hand, the yield is maximum when there is no ammonium in the medium and the concentration of tryptone is 1 g/L. Both yield values of 0.12 g DHA / g biomass.

In order to evaluate the effect of yeast extract and ammonium on DHA production, which showed the best results for biomass production, the very last nitrogen source DoE is purposed. According to DoE N4, yeast extract effect could be above 2 g/L. For this reason, this DoE includes higher concentrations of yeast extract. The experimental design included the following conditions:

- ➢ Tryptone – Set at 0 g/L. Justification: Investigate only yeast extract as organic source.
- ➢ Nitrate – Set at 0 g/L. Justification: Investigate only ammonium as inorganic source.
- ➢ Yeast extract – Three levels, 2, 3 and 4 g/L. Justification: Investigate this factor with higher concentrations in combination with ammonium.
- ➢ Ammonium – Three levels, 0, 0.75 and 1.5 g/L. Justification: The optimum of ammonium contribution is known to be around a concentration of 1 g/L. In this work the range is wider to investigate the combination effect with yeast extract.

Design of experiment N7 - Response: growth & DHA yield

In this last DoE, guided by a $L_9 (3^4)$, ammonium and yeast extract were investigated. Results are shown in Figure 3.44 Results of the last (seventh) nitrogen source DoE of the thesis. The results from every response are clustered with a gray line (OD results) and a black line (DHA yield results). Histograms show the contribution of every factor regarding each response. Factor level plots are shown for every important factor. Top level plots correspond to OD results while bottom level plots show the results from DHA yield results. Figure 3.44 and clustered in two groups according (DHA and growth). According to growth data, ammonium had an important effect compared to yeast extract. This is in concordance with previous results reported in DoE N1, unless the ammonium concentration exceeded 1.5 g/L as in the case of DoE N2. When the concentration of ammonium was too high, yeast extract showed a higher effect. In any case, the effect of ammonium was negative above 1 g/L. In this present case, the contribution represents a 74 %. Optimal growth was found at 0.75 g/L. This result is in concordance with the work of Chi *et al.* (2007) [93] as well. Chi have reported that the optimum ammonium concentration was 1 g/L.

On the other hand, yeast extract only showed a 26 % contribution. Yeast extract effect is always positive, as reported in previous experiment. In the present experiment, it showed a maximum growth at 4 g/L. Therefore, the best composition to maximize growth would be a combination of 0.75 g/L ammonium acetate and 4 g/L yeast extract.

Results concerning DHA yield did not show the same output. It is clear that the factor contribution is the same for both response types (DHA and growth). Checking the level plots (bottom Figure 3.44) show that both factors were affecting negatively the production of DHA, as both ingredients increase the concentration. In other words, the best production scenario appears to be at the lower levels. Interestingly, the lower level of ammonium was 0 g/L and 2 g/L for yeast extract. Therefore, there is a proper medium composition for growth and another for DHA enhancement.
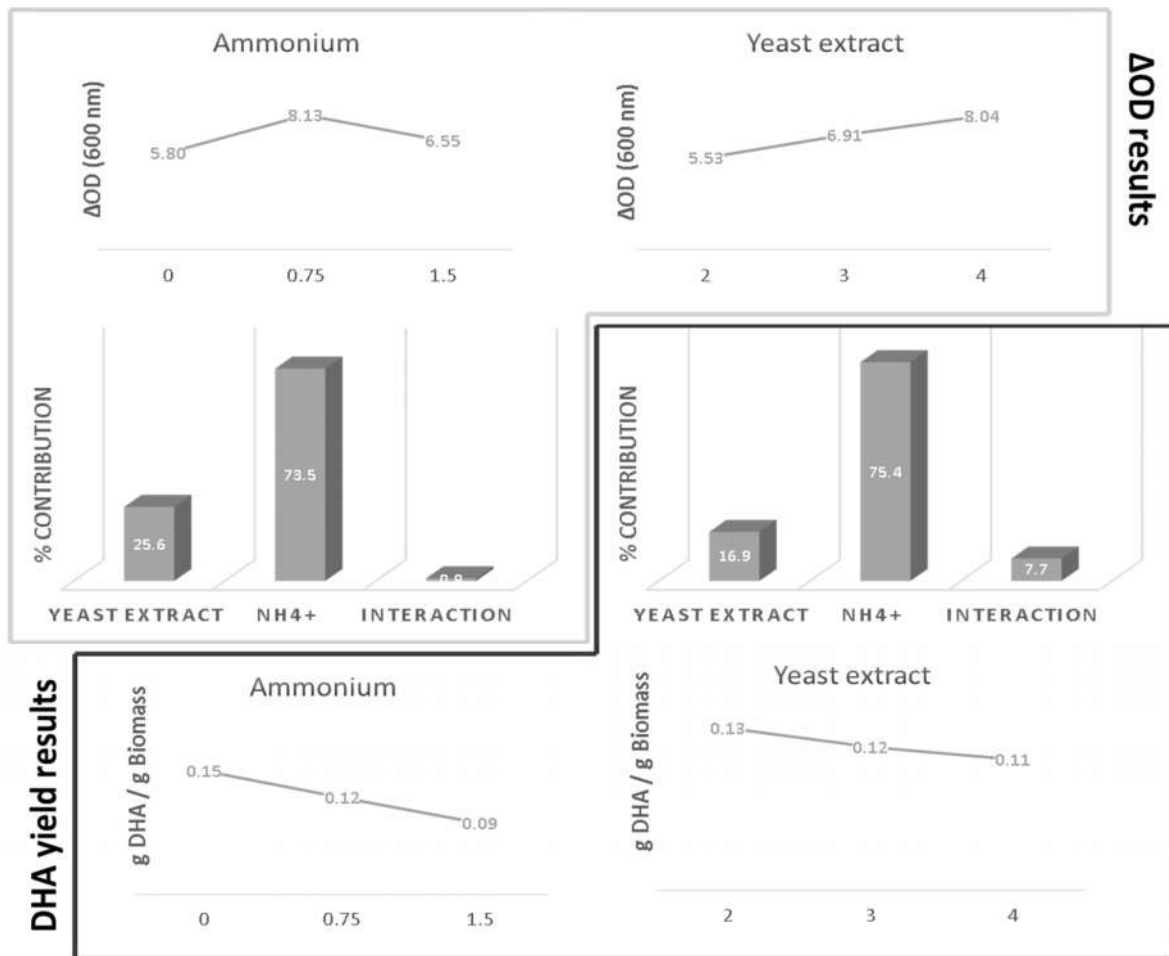
Figure 3.44 Results of the last (seventh) nitrogen source DoE of the thesis. The results from every response are clustered with a gray line (OD results) and a black line (DHA yield results). Histograms show the contribution of every factor regarding each response. Factor level plots are shown for every important factor. Top level plots correspond to OD results while bottom level plots show the results from DHA yield results.

The **presence of yeast extract is essential for the proper growth of *A. limacinum*.** A lack of this organic nitrogen source causes weak growth as repeatedly showed in the previous DoE. The combination of DoE N5 and DoE N7 indicates that the optimal concentration would be equal or greater than 4 g/L. However, as shown in the last DoE (N7) these concentrations of yeast extract cause a reduction in DHA accumulation. The opposite effect on growth and DHA production may be causing the divergences between literature works, reporting different suitable concentrations of nitrogen sources [9,93,187,189,190]. Tryptone just showed a slight increase of growth compared to those experiments only using inorganic nitrogen sources (DoE N4).

Also ammonium is important for growth in a concentration between 0.75 and 1 g/L. As mentioned before, Chi *et al*. [93] reported this feature as well. However, this nitrogen salt only showed its beneficial effect when combined with a minimum concentration of yeast extract. Moreover, it was detrimental for DHA production as elucidated in the last DoE (N7). In the absence of this salt, *A. limacinum* showed the best

yield. Nitrate did not show any effect either over the microorganism growth or the DHA production. Therefore, it can be eliminated from the medium composition

After several experiments about yeast extract, tryptone, nitrate and ammonium effects on *A. limacinum* performance to produce DHA, there is a clear winner. Yeast extract showed a positive and considerable effect on *A.limacnium* and DHA production, within the studied concentrations (0-4 g/L). Moreover, its omission resulted in a dramatic reduction of growth. Yeast extract is absolutely essential for *A.limacinum* growth and DHA production. Nevertheless, if the concentration of yeast extract is equal to 3g/L or superior, it could produce a reduction in DHA accumulation, as seen in the experiment N7. This was probably caused by a reduction of the C/N ratio that reduced general lipid accumulation. This result is in concordance with literature works investigating medium compositions for other thraustochytrids. Wu *et al.* (2005) [180] have seen the same effect on *Schizochytrium* sp. S31. Chen et al. (2010) [179] have reported that the best yeast extract concentration for *Aurantiochytrium* sp. growth was 3 g/L. However, a consensus concentration is required (considering growth and DHA), which is investigated in the following section.

Ammonium has been revealed to have a positive effect, being the optimal concertation 0.75 g/l. Unfortunately, ammonium undoubtedly exhibited a negative effect on DHA production. This is coherent with Chi et al. (2007) [93] and Yokochi *et al.* (1998) results. Both have shown that high concentrations of this salt caused a reduction in DHA accumulation even though this nitrogen source is positive for the microorganism growth. In this work as well as in literature, ammonium showed better results when it was the unique nitrogen source. This might be indicating that the composition of organic nitrogen sources is preferable for *A. limacinum* growth.

Nitrate and tryptone have shown lower effects. In the nitrate case the effect is negligible while tryptone exhibited a noticeable positive effect. Chu et al. (2010) and Wu et al. (2005) have shown that using tryptone as the sole nitrogen source, the microorganism grew satisfactorily although below yeast extract results.

In order to find an optimal concentration to maximize productivity of DHA, a model based on all the heterogeneous set of samples generated during the previous experiments was built. In addition, other experiments performed during the medium development were used to complement the existing set of samples. ANN is an excellent modeling technique in a heterogeneous scenario (Modeling process is explained in the section 3.3.3).

As discussed previously, yeast extract and tryptone are not only acting as nitrogen sources but also providing many other oligoelements. These complex ingredients contain amino acids which can be used as building blocks for the enzymatic machinery of the microorganism. Yeast extract also contain vitamins, growth factors and many other things helping to reach higher growth rates. For this reason, some bioreactor cultures are performed to validate DoE data before ANN. These bioreactor experiments were carried out to confirm the results obtained in flasks.

Bioreactor nitrogen source experiments

Bioreactor results are gathered in Table 3.23. A first set of control bioreactor were performed in order to evaluate medium modifications. The set N1 with a low amount of tryptone and yeast extract showed the lowest net growth rate. It took 45 hours to reach the stationary phase with an optical density of 15.

Interestingly, the lowest concentration of total organic nitrogen sources generated a slower growth. In the following set of bioreactors (N2 & N3) *A. limacinum* exhibited high growth rates. The N3 set, containing the highest amount of yeast extract, showed a net growth rate of 0.17 h^{-1}. This evidence supports the hypothesis that ***A. limacinum* growth is faster in the presence of organic/complex nitrogen sources** using bioreactors.

Final biomass values were approximately the same whereas DHA yield showed differences. Product yields are comparable to control bioreactor, except from the set of bioreactors containing 1.5 g/L yeast extract in the medium which yielded 0.11 g DHA / g biomass.

Bioreactor	Tryptone	Nitrate	Yeast extract	Ammonium	μ_{net} (h^{-1})	Time (h)	OD (600 nm)	g DHA / g Biomass
Control	1	1	1	1	0.11	30	13	0.09
N1	0.1	3	0.6	1	0.06	45	15	0.09
N2	1	5	0.1	1	0.11	30	13	0.08
N3	0.1	1	1.5	1	0.17	25	14	0.11

Table 3.23 Bioreactor experiments with different combinations of nitrogen sources. Net growth rate has been calculated including the lag and stationary phase. Time indicates when the culture reaches the stationary phase. Values are the average values of 2 reactors. Initial substrate concentration = 10 g/L of crude glycerol.

3.2.2.2 Nitrogen composition modeling - Optimization

Two models have been built using ANN to fit the data obtained by previous DoE. This was focused on finding the optimal nitrogen source concentration. The first model was fitted using each nitrogen source concentration as input and OD (4-34 h) [58] as target of the model. The designed ANN was composed by
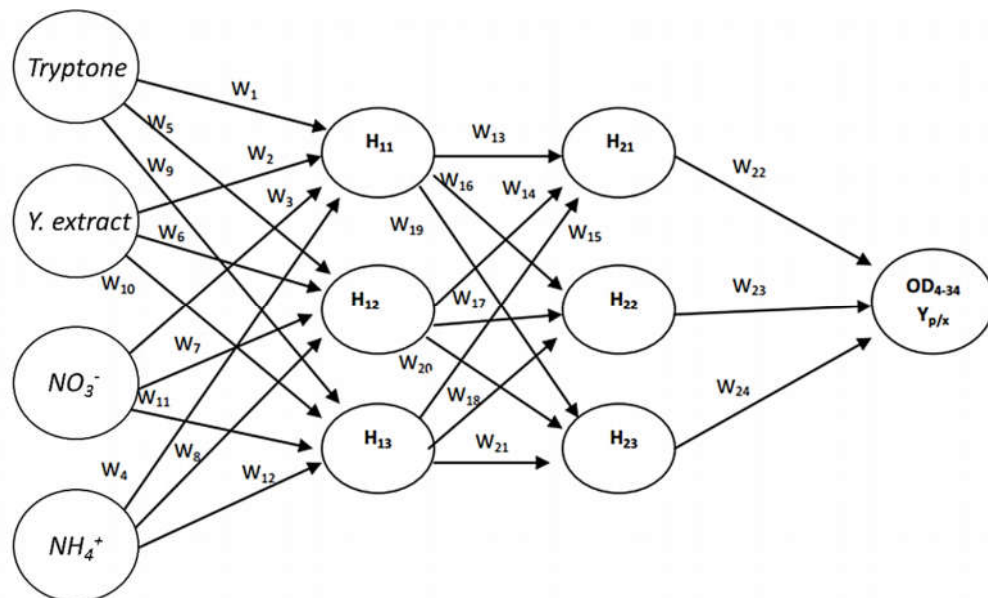
Figure 3.45 Artificial neural network structure used to investigate nitrogen source and A. limacinum performance in growth and DHA production.

---

[58] The same response used in previous DoE.

four inputs (four different nitrogen sources), **two hidden layers** with **three neurons** each one (H_{ik}), and finally the modeled response (different for each model). Moreover, neurons placed in the first layer are connected with the inputs (H1k), and those placed in the second layer (H2k), are connected with the previous ones as well as with the output node. Every connection has a parameter which defines it, called weight (W_j). Weights are the variables which, together with the intercepts[59], are modified while the system is learning. This configuration describes a fully connected structure which is represented in Figure 3.45. A Visual Basic application has been developed (Frances Padrès Master thesis) to compute this neural construction. Using this application, the 27 weights and 7 intercepts (31 total parameters) were adjusted.

3.2.2.2.1   OD (3-34 h) based model

Of the total experimental points, 65 have been used to train the ANN and 16 experimental points to validate the model. All used points are represented in the 4D plot-like (3D plot with a discrete variable) found in Figure 3.46. Once trained, an average relative error of 10.93% was obtained in the training set and an average relative error of 13.75% in the validation points. Note that, within cultivation repetitions, a variation coefficient average of 7.94% was obtained, which already conforms the error of the model.
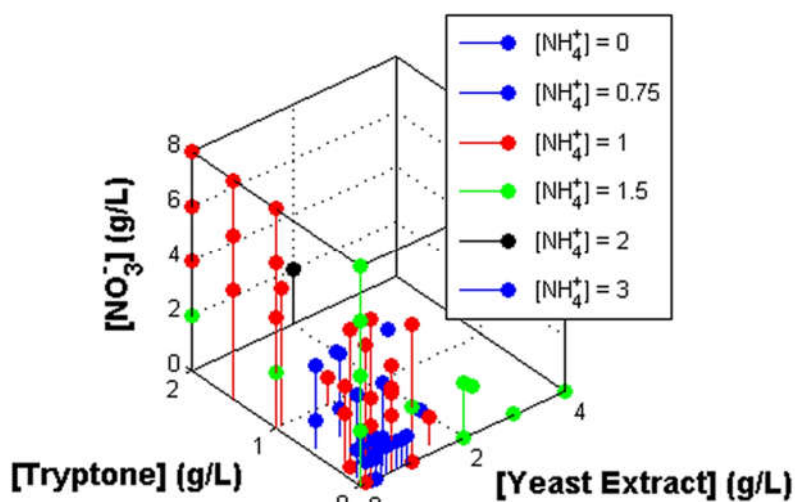
Figure 3.46 Data points used to train ANN. Three factors plot with a fourth factor represented as a discrete variable (4 Dimension-like plot).

---

[59] The intercepts are the interaction of the neurons connections.

To be able to interpret the results of the model, these have been represented as different response surfaces. One surface per each pair of variables. In other words, two variables/factors have to be fixed, while the two remaining are plotted with the corresponding response. Figure 3.48 shows the first response surface based on the model, which clearly prove the positive effect of yeast extract previously revealed by Taguchi's DoE. A dramatic decrease can be observed when yeast extract is scarcer. Moreover, Figure 3.48 show that tryptone has a positive extra effect when is combined with yeast extract, and only

$NO_3^- = 1$ g/L $NH_4^+ = 0.75$ g/L.
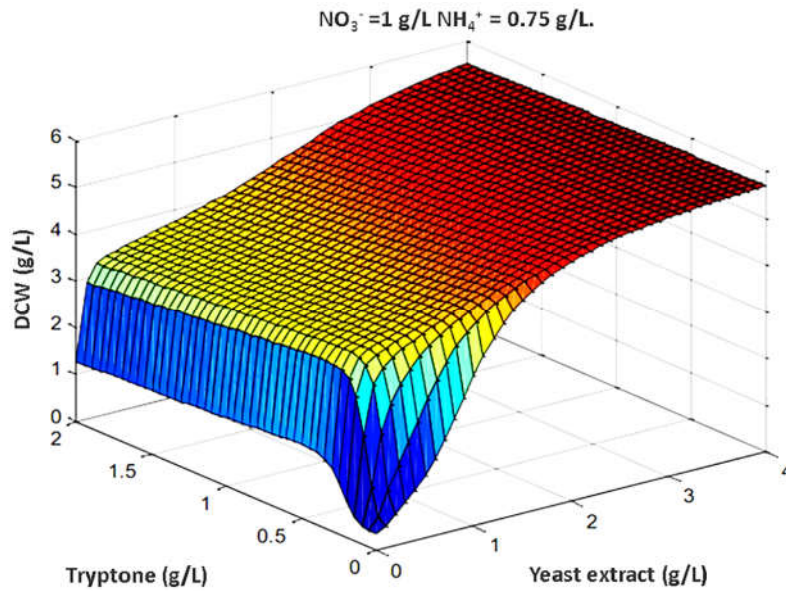
Figure 3.48 Response surface based on the OD (3-34) model built. Fixed variables are indicating on mesh top.

Yeast extract $= 2$ g/L Tryptone $= 0.25$ g/L
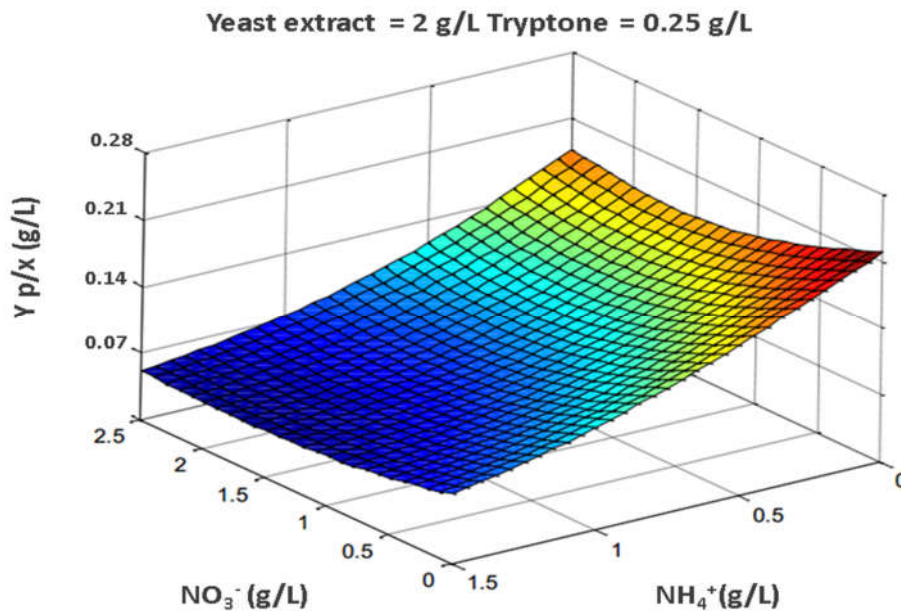
Figure 3.47 Response surface based on DHA yield response in the second model. Fixed variables are indicated on top of the figure.

when yeast extract concentration is high. Response surface also revealed that a minimum of tryptone (0.2-0.3 g/L) is essential.

On the other hand, as can be observed in Figure 3.49 nitrate has a different output in the built model. It has a positive effect on growth contrary to what was concluded from DoE. Especially when ammonium concentration was near 0 g/L, which was actually found by DoE experiments. Moreover, the mesh shows the negative effect of high concentrations of ammonium, revealing an optimum around 0.4 g/L. Despite the divergences, this plot considers the contribution of both yeast extract and tryptone. Therefore, as pointed out in the previous subsection discussion, inorganic nitrogen sources would not show this performance when yeast extract and tryptone are omitted.

3.2.2.2.2 DHA yield (g DHA / g dry biomass) based model

The second model was fitted to DHA production using each nitrogen source concentration as input and product yield $Y_{DHA / dry}$ **biomass (g/g)** as response. For this new model 34 experimental values have been used to train the ANN and 9 experimental points to validate the model. Once trained, an average relative error of 11.6% was obtained in the training set and an average relative error of 7.6% in validation points. Note that, in culture repetitions a variation coefficient average of 6.9% has been obtained, which already conforms model's error. The second model revealed that the optimum DHA production occurs when nitrate and ammonium are omitted as indicated in Figure 3.47. Thus, demonstrating that only organic nitrogen sources are contributing positively on DHA accumulation into cells. Second model results are in concordance with those obtained in previous flask experiments.

3.2.2.2.3 Final optimization

In order to find a consensus response between growth and DHA production, a third model was constructed using the final DHA concentration (g DHA/L). This was calculated using the output of both

114
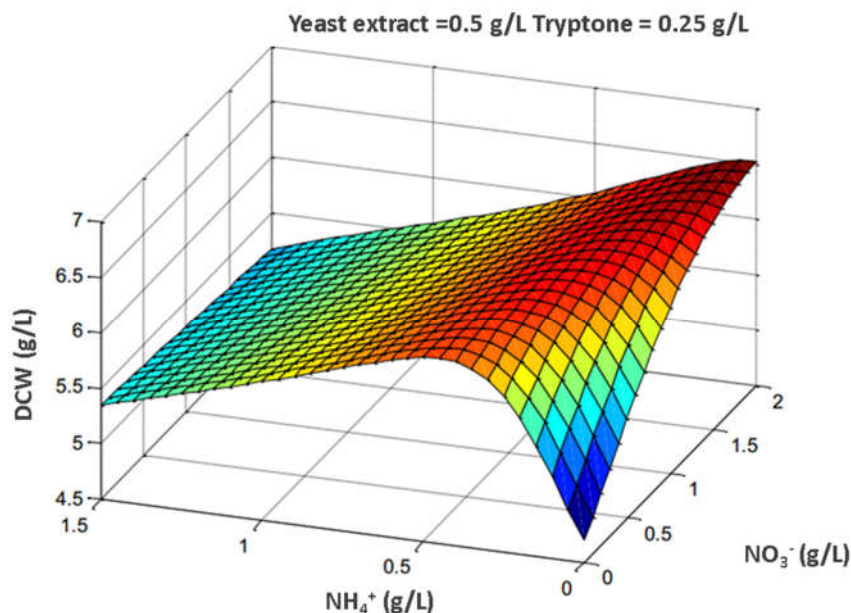
Figure 3.49 Response surface based on the OD (3-34) model built. Fixed variables are indicating on mesh top.

previous models. The new model exposed a maximum when the concentrations of nitrogen sources were the following: **0.4 g/l of tryptone, 2.3 g/l of yeast extract, 0 g/l of ammonium acetate and 0 g/l of sodium nitrate (**Figure 3.50**)**. These concentrations are in concordance with the ANOVA preliminary analysis. The results showed that growth and DHA production are strongly dependent of the nitrogen sources' composition. Yeast extract, besides being an important source of nitrogen, is also rich in many other biomolecules and oligo-elements, which might be contributing positively. Moreover, to consider a defined media for this kind of microorganism while obtaining good amounts of DHA seems difficult.

The purposed composition was optimized for media containing 10 g/L of carbon source. When the initial carbon source concertation is increased, nitrogen source needs to be increased correspondingly. Therefore, the optimization defines the following equation:

Nitrogen source = [(2.3 g yeast extract) · C/10] + [(0.4 g tryptone) · C/10]   Equation 3.1

C being the initial concentration of carbon source. This C/N will allow an effective compromise between growth and DHA accumulation, obtaining the optimum DHA production.
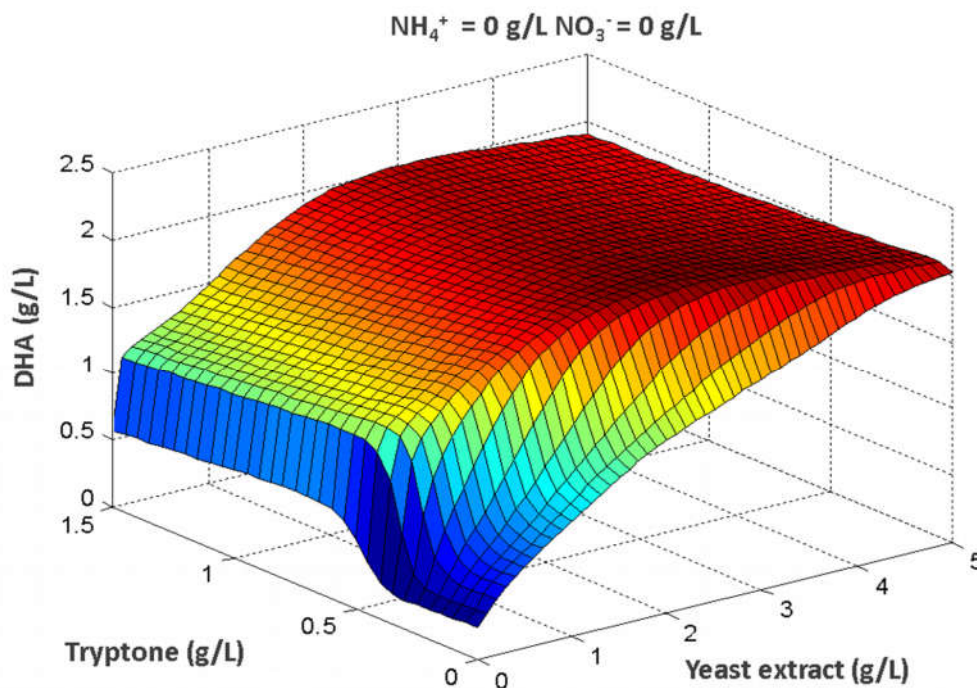
Figure 3.50 Response surface of both ANN models product, obtaining the concentration of DHA after 34 hours of culture.

3.2.2.2.4 Bioreactor validation

With the aim of validating the medium developed until this point, a set of bioreactors were performed with four different nitrogen source combinations and 10 g/L of carbon source. Every bioreactor had two replicates with the following nitrogen source composition:

> First (**Original**) - Standard medium: 1 g/L yeast extract, 1 g/L tryptone, 1 g/L NaNO$_3$ and 1 g/L CH$_3$COONH$_4$.
> Second (**1g/L Trp., 5 g/L NaNO$_3$**) - 0 g/L yeast extract, <u>1 g/L tryptone, 5 g/L NaNO$_3$</u> and 0 g/L CH$_3$COONH$_4$.
> Third (**Y. extract 1.5 g/L**) – <u>1.5 g/L yeast extract</u>, 0 g/L tryptone, 0 g/L NaNO$_3$ and 0 g/L CH$_3$COONH$_4$.
> Fourth (**Optimized**) – <u>2.3 g/L yeast extract, 0.4 g/L tryptone,</u> 0 g/L NaNO$_3$ and 0 g/L CH$_3$COONH$_4$.

The results of the set of bioreactors are listed in Table 3.24. Original medium evidently generated the worst results, lower yield, lower growth rate and consequently lower productivities. Bioreactors with only tryptone and nitrate showed even worst results. It can be assumed that the lack of yeast extract is the reason. When the concentration of yeast extract is slightly increased and inorganic source eliminated, the yield raises. Interestingly, even the growth rate has increased. Bioreactors with the optimized composition of organic nitrogen sources showed the best results. The yield is twofold higher. Even though growth rate dropped compared to the previous medium, productivities are greater. Again, the evidence suggeste that yeast extract plays a very important role in *A. limacinum* performance and its DHA productivity.

Table 3.24 Mean kinetic values of validation bioreactors. Bioreactors were maintained at 20º, with an airflow of 1.5 l/h and 500 rpm. Two replicates per bioreactor. Final volume of 1.5 L.

Medium	Y p/x (g/g)	μnet (h^{-1})	Volumetric productivity (m DHA / L ·h)	Productivity (mg/day)
Original	0.09 ± 0.001	0.11 ± 0.01	12.3 ± 1	442.8
1g/L Trp., 5 g/L NO$_3$	0.07 ± 0.001	0.11 ± 0.02	10.3 ± 2.1	370.8
Y. extract 1.5 g/L	0.11 ± 0.001	0.19 ± 0.008	18.6 ± 0.1	669.6
Optimized	0.21 ± 0.02	0.13 ± 0.005	33.6 ± 1	1209.6

3.2.3 Sodium chloride concentration

Yaguchi *et al.* (1997) [187] work was the first publication of *A. limacinum*. As already discussed in previous chapters its former name was *Schizochytrium limacinum*. According to Yaguchi *et al.* salinities 50% to 200% greater than natural seawater salinity (17.5 g/L to 70 g/L) can be used to grow the mentioned thraustochytrid. Ten years later, Zhu *et al.* (2007) [191] reported experiments with a different strain of *A.limacinum* were the highest biomass and DHA production using medium with NaCl between 18 - 27 g/L. Kim *et al.* (2012) [192] reported similar optimal salinity ranges (15 – 20 g/L) for thraustochytrids. Kim's work suggests that thraustochytrids could grow with near 0 g/L salinity values in determined media [192]. Shortly after, K. Chuang *et al.* (2012) [193] published a revision about some *A. mangrovei* growth media

components. In this work they have reported significantly good growth between 1 – 30 g/L but the cultures showed optimal DHA production when using 5 g/L NaCl.

Box 3.7. Difference in Thraustochytrium sp. growth in presence of mannitol.

The figures below are extracted from Shabala *et al.* (2009) showing the difference of *Thraustochytrium sp*. growth in presence of mannitol. The difference between both experiments clearly show the effect of this polyol.
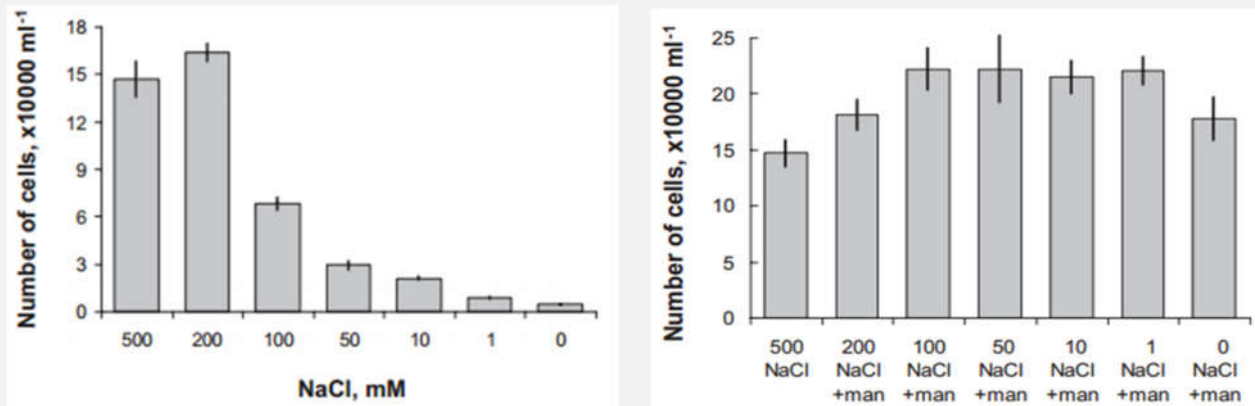
Earlier in 2009, Shabala *et al.* [194] suggested that thraustochytrids salinity requirements, specifically Na+ and Cl-, may be explained by their requirement for optimal osmotic adjustment. They have showed that *Thraustochytrium* sp. can grow with very low salinity mediums in presence of a polyol (i.e. mannitol) (Box 3.7). In this section of the thesis, sodium chloride concentration for *A.limacinum* culture was investigated as the main contributor to medium salinity[60]. Other important salts but less abundant, are investigated in section 3.2.6.

In this work, it was sought to study *A. limacinum* behavior **within a NaCl concentration range from 0 to 60 g/L**. Many microalgae cultivations are made in very high salinity conditions, preventing opportunist microorganisms from contaminating the culture. According to the literature [187], other thraustochytrids could grow at very high salinity concentrations as well. Twelve concentrations were investigated within this range focused on concentrations between 10 to 20 g/L of NaCl where *A. limacinum* should show its optimal growth.

A. limacinum has shown a remarkable growth with every NaCl concentration as displayed in Figure 3.51. Growth was not severely affected by low NaCl concentrations in concordance with similar results found in literature. For example, Shabala *et al.* (2009) [133] have already shown that thraustochytrids could grow without NaCl in the correct medium. On the other hand, Zhu *et al*. (2007) [54] have shown that despite the versatility of these microorganisms, optimum conditions are above 10 g/L.   The strain of *Aurantiochytrium* used for the thesis described here, showed a similar behavior to other genera of this superfamily. Figure 3.51 consistently shows that biomass production increases until reaching NaCl

---

[60] Sodium and chloride represent 85% of the total ion composition in seawater. In the starting artificial medium with 18 g/L sodium chloride, this salt was accounted for 90 % of the ion composition. Yeast extract and tryptone salts are not considered.

concentrations of 18 g/L. Cultures containing between 18 to 25 g/L of NaCl showed the highest values of growth. These concentrations of salt are above natural seawater concentrations (~ 35 g/L).

DHA production profile is slightly different, especially when working with extreme values of NaCl. Concentrations below 10 g/L of sodium chloride generated a significantly lower values of DHA. The values of this FA drop even more when NaCl concentration is above 30-40 g/L. Generally speaking, *A. limacinum*
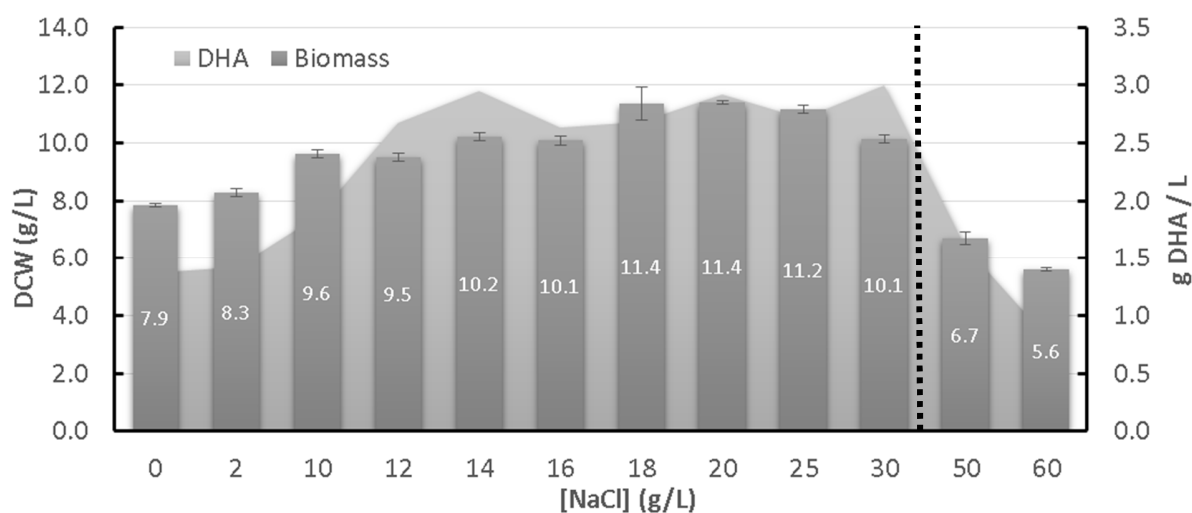
Figure 3.51 Biomass and DHA production after 72 hours of culture. Grey stacked area indicate the final DHA concentration after every experiment. The bars show the final biomass reached using each one of medium salinities. Biomass is indicated as dry cell weight (DCW). Dotted line indicates sweater salinity threshold. Error bars indicate standard deviation.

can grow adequately and satisfactorily produce DHA when the sodium chloride concentration is between 14 and 30 g/L. Therefore, this microorganism offers even more versatility. *A. limacinum* can grow either without NaCl or grow in open ponds[61] with high salinity. This ability could permit open pond cultivations and reduce costs by avoiding antibiotic utilization. Furthermore, if *A. limacinum* can grow with very low NaCl concentrations it would avoid corrosion problems with steel equipment.

Cell dimensions in different NaCl concentration.

Complementary experiments using laser scattering (Digisizer technology) elucidated cell size variations depending on NaCl concentration. Thraustochytrids are generally big microorganisms as explained in chapter 2. Greater dimensions offer more space to store DHA. Therefore, when the experiment was designed a relationship between DHA accumulation and cell diameter was expected. However, the cell contains less DHA in those situations in where diameters were higher (Figure 3.52). Considering data

---

[61] Open pond systems are suitable for very large scale production. This system uses high salinity mediums to avoid any opportunist microorganism shift algae population.

generated in this section *A. limacinum* DHA accumulation is not governed by salinity. Interestingly, when the medium salinity is higher, cell diameters are smaller due to osmotic pressure [133].
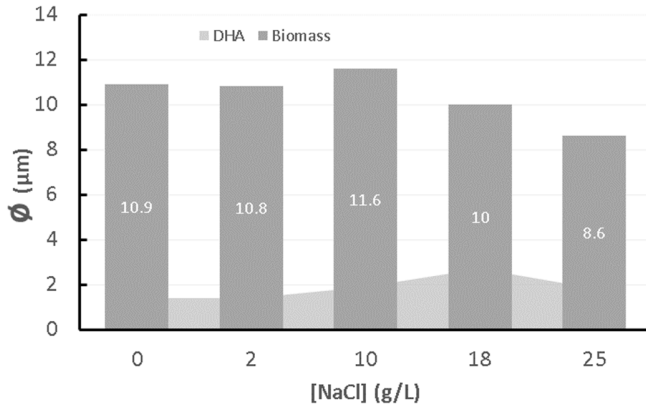
Figure 3.52 Effect of sodium chloride concentration on A. limacinum cell diameter (ø).

In this situation, the concentration of NaCl remains unchanged **being 18 g/L the apparent optimal value**. It should be said that complex ingredients such as yeast extract and tryptone contain salts, especially NaCl, but their concentration is less than 1 g. Therefore, this concentration can be used both for 10 g/L and 100 g/L of initial carbon source concentration. As indicated in the previous section, if initial carbon source is increased, nitrogen sources have to be increased ensuring proper growth. In any case, 18 g/L has to be NaCl concentration in the medium.

3.2.4 Buffer investigation

At present, only a few works have studied the best conditions for thraustochytrids cultivation and there is no data about buffer usage growing this microorganism. The last report about marine microorganisms and buffers dates from 1975 [182]. Loeblich (1975) compared the growth of marine dinoflagellate in several buffers. Dinoflagellates are in the chromoalveolates super-kingdom as thraustochytrids. In his work MOPS[62], HEPES[63], TRIS, glycylglycine and TAPS[64] were used as buffers and concluded that **TRIS and TAPS** provided maximal growth with minimal pH change. In fact, TRIS buffer is perfect for *A. limacinum* or any other thraustochytrid. This was demonstrated in all the works already mention in this chapter, because all of them used TRIS buffer to control the pH of their cultures. Nevertheless, growing *A. limacinum* at large scales would spend large buffer amounts and this ingredient needs to be cost effective. TRIS is an expensive buffer not suitable for large scale cultivations.

Table 3.25 Table of buffer suitable for thraustochytrids growth. Prices have been calculated using the cheapest pack of each one, from the same vendor.

pH Range	Buffer	Price		Total
5.8 - 8	$KH_2PO_4 + NaOH$	0.0008 € / g + 0.00043 € / g		0.00123
5.1 - 7.1	$H_2CO_3+NaHCO_3$	0.02 € / g + 0.021 € / g		0.041
7 - 9	*Tris buffer*	0.28 € / g		0.28

---

[62] 3-(N-morpholino)propanesulfonic acid
[63] 4-(2-hydroxyethyl)-1-piperazineethanesulfonic acid
[64] N-Tris(hydroxymethyl)methyl-3-aminopropanesulfonic acid

119

There are many salts which either individually or in combination with another can regulate the amount of protons dissolved in the medium. After an exhaustive search throughout different providers two stand out above other products. The search has followed two main parameters, cost and pH range. The selected buffers were KH_2PO_4 + NaOH and H_2CO_3 + $NaHCO_3$ as indicated in Table 3.25. However, H_2CO_3 + $NaHCO_3$ was finally rejected due to the limited pH range.
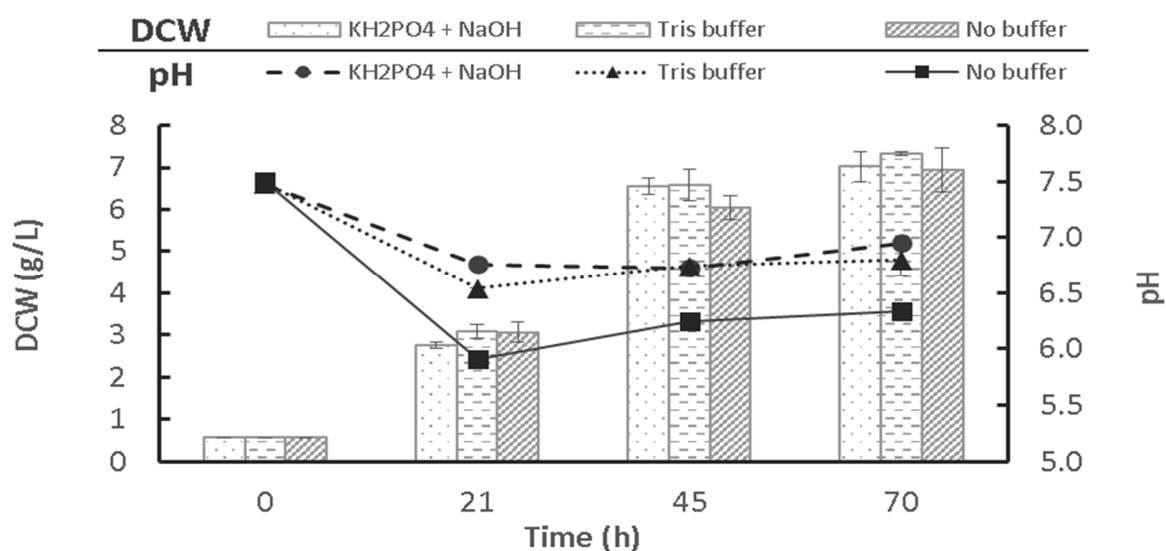
Figure 3.53 Buffer effects on pH values and biomass production in A. limacinum cultures. Biomass production is expressed as dry cell weight per liter.

KH_2PO_4 + NaOH has many advantages. First, KH_2PO_4 releases K^+ into the medium which makes it available for *A. limacinum* (more information in section 3.1.2.2 and 3.2.6.2). Therefore, the buffer is not only controlling the pH but also adding an important component of seawater making the buffer more cost effective. The other big advantage is the reduced cost compared with TRIS buffer. Interestingly, TRIS could be toxic for some microorganisms while KH_2PO_4 not. This would allow using this buffer with other thraustochytrids without risk. NaOH was added to adjust dissociation equilibrium[65] of $H_2PO_4^-$ fixing the medium pH value. Different buffering situations were evaluated at a pH of 7.5. KH_2PO_4 + NaOH buffer was evaluated in *A. limacinum* flask cultures compared to TRIS and unbuffered mediums (Figure 3.53).

Similar growth was observed, as can be seen in Figure 3.53. Regarding pH values, cultures with buffer remained near pH 7. Experiments using no buffer suffered a pH reduction down to 6.4. Despite medium acidification in the unbuffered cultures, *A. limacinum* has grown normally. The pH tolerance of these organisms is quite broad as certified by several studies. Ranging from 5 to 8 where optimal pH is 6.5–7.5 for high DHA yields [49,56,93,140,161,195]. DHA was monitored for each culture and the results are shown in Figure 3.54. While differences in buffer did not affect biomass production, DHA accumulation was reduced when *A.limacinum* was cultivated without buffer. It is important to remark that results in Figure 3.54 are indicated as yields. Yield might seem just slightly different, but if they are translated into final concentration, unbuffered cultures produced a lower amount. Therefore, a reduction in the pH

---

[65] $KH_2PO_4 \quad K^+ + \quad H_2PO_4^- \; ; \; H_2PO_4^- \quad H^+ + HPO_4^{2-}$
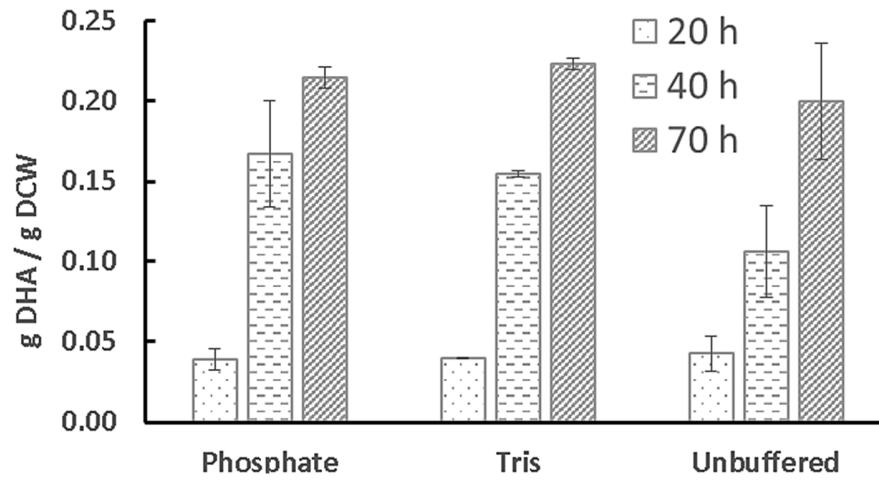
Figure 3.54. Medium buffer effects on DHA production, which is indicated as a yield, g DHA per every g of biomass dry cell weight.

during a culture could affect DHA accumulation. Anyway, the medium described in this chapter has been designed to sustain *A. limacinum* cultures with very high biomass concentration. A culture without any buffer in this scenario would generate a risk of variability. Considering the results just discussed, KH_2PO_4 + NaOH is an appropriate buffer for DHA production through a biotechnological process.

Buffer solubility in seawater mediums could be a problem, as already discussed in the introduction of this chapter (3.1.2.6). Autoclaving all the components together, is one of the important features of the medium developed. However, unlike most other compounds, the solubility level of $Ca(H_2PO_4)_2$ becomes lower as temperature increases. Thus heating causes precipitation. In this investigation it has been found that when KH_2PO_4 is added at a concentration greater than 1.25 g/L it generates a precipitate. Accordingly, only three concentrations of the selected buffer were investigated in order to elucidate if a variation of
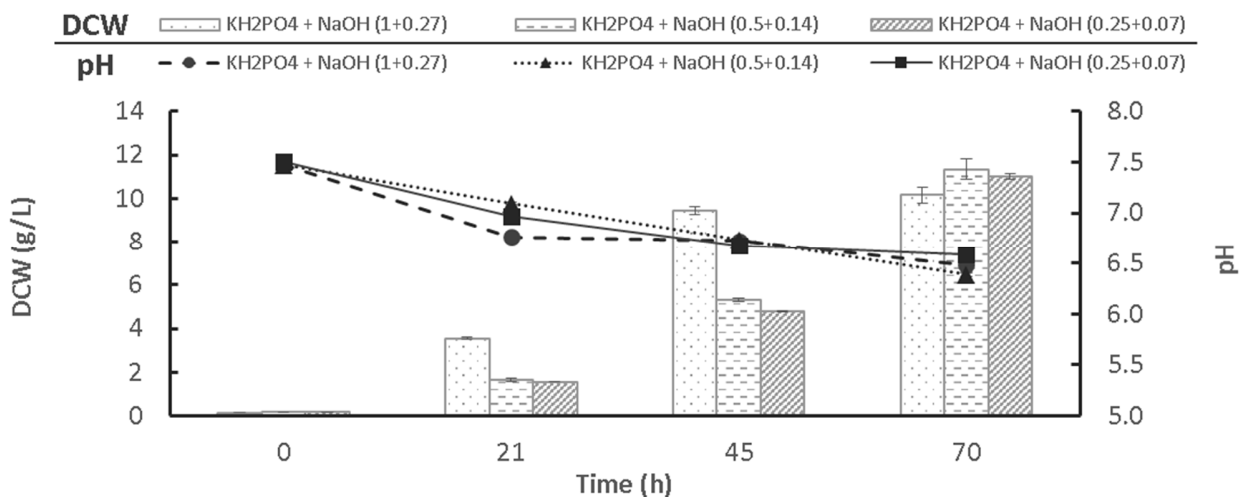
Figure 3.55 Effects of different concentrations on A. limacinum growth. Biomass is indicated as dry cell weight. First set of experiments had a concentration of 1 g/L KH_2PO_4 + 0.27 g/L NaOH, the second 0.5 g/L KH_2PO_4 + 0.14 g/L NaOH and the third 0.25 g/L KH_2PO_4 + 0.07 g/L NaOH.

buffer concentration could affect growth. Every experiment was carried out using KH_2PO_4 concentrations below 1.25 g/L limit concentration. Results can be observed in Figure 3.55.

For this experiment, not only different concentrations of KH_2PO_4 + NaOH were investigated. This experiment was also used to investigate what happens if the biomass concentration is higher[66]. In the first buffer experiment the final DCW values were 6-7 g/L, whereas in the second they are between 10 and 12 g/L. This biomass increase has a bigger impact on the pH. Actually, a higher biomass concentration lowered the pH value down to 6.5. Considering that a concentration of 12 g/L of biomass in a flask is quite high, the buffer alleviated the effect of the proton increase. Again, a set of samples showed similar behavior both in biomass production and pH values. Therefore, buffer concentration is not affecting *A. limacinum* growth.

As $CaCl_2$ concentration was not optimized yet, and $Ca_3(PO_4)_2$ tends to precipitate, **it was decided to use a concentration of 0.85 g/L KH_2PO_4 + 0.14 g/L**. This concentration would tolerate a CaCl2 concentration increase if required. Moreover, if this medium is used for high biomass concentration cultures, buffer must have enough ionic strength to alleviate protonation of the culture. For this reason, unbuffered media were discarded. It is worth mention that pH control of bioreactor units will help maintaining the pH value.

An H_2SO_4 solution and a NaOH solution were selected as control acid and control base, respectively. Sulphate does not affect *A. limacinum* growth because yeast extract contains high concentrations of this salt (SO_4^{2-}), and extra additions would not alter the concentration. In addition, NaOH will not affect the growth either. Sodium ion additions will not affect the current concentration of it already in the medium.

122

3.2.5 *Vitamins: Focus on c*yanocobalamin (Vitamin B$_{12}$) requirements

Vitamins have been extensively used in artificial seawater medium formulations. As mentioned in the introduction, vitamin load of marine media prepared in the lab is mainly composed of thiamine, biotin, cyanocobalamin also called Vitamin B$_{12}$, and in some cases riboflavin. Vitamin complementation for thraustochytrids cultures has only been investigated in a few works, especially cyanocobalamin. Almost every work applied to thraustochytrids used different concentrations of this vitamin, as can be observed in the Table 3.26.

Vitamin B$_{12}$ supplementation started with Bajpai and Ward's work of 1991 [51] in which they introduced Vitamin B$_{12}$ enhancing *T. aureum* growth (based on original artificial seawater media). They formulated a medium containing 10 µg/L thiamine and 1 µg/L Vitamin B$_{12}$ obtaining better results than previous works with the same strain [196]. Iida *et al.* (1996) investigated many different vitamins finding thiamine, vitamin B12 (0.01 µg/L), pantothenic acid sodium salt, nicotinic acid, riboflavin and biotin to be essential for better *T. aureum* growth. However, the final biomass values of their work were lower than the ones obtained by Bajpai and Ward. Later in 2002, Hur *et al.* (2002) included only 4 µg/L Vitamin B$_{12}$ to investigate *T. aureum* DHA productions. This work was focused on other parameters different from vitamins but is an example of vitamin concentration divergences among literature data.

---

[66] If the substrate initial concentration is increased, the culture can reach higher biomass concentrations unless a different ingredient becames limiting.

Unagul *et al.* (2007) investigated the same combination of vitamins as in Iida *et al.* but for *S. mangrovei* SK-02[67] cultures. However, concentrations of vitamins were very high (1 mg/L cyanocobalamin) compared to the previous works described above. Results indicated that vitamin solution has no effect either on *S. mangrovei* growth or n-3 PUFA production. Jakobsen *et al.* (2007) included 5 µg/L of cyanocobalamin in their medium growing a *Schizochytrium* strain. The same year, Chi *et al.* investigated two different Vitamin B_{12} concentrations in *S. limacinum*[68] cultures, 0.1 µM and 0.2 µM. This study was made based on a DoE investigation of other factors at the same time. They found that 0.1 µM cyanocobalamin was better for the strain used. In 2009 two new works not directly related with vitamin contribution on thraustochytrids growth, evidenced again the inconsistency of vitamin concentrations. Lippmeier *et al.* (2009) used 100 µg/mL calcium pantothenate, 50 mg/mL vitamin B_{12} and 100 µg/mL in a fatty acid characterization of *Schizochytrium* sp. On the other hand, Lian *et al.* (2009) used 10 mg/L cyanocobalamine, 1 mg/L biotin and 50 mg/L thiamin for a different research using *Schizochytrium* sp.

Table 3.26 Cyanocobalamin concentrations investigated for thraustochytrids growth.

Reference	[Vit. B_{12}]
This study	0 µM
Iida 1996	0.0074 nM
Quilodran 2010	0.37 nM
Bajpai 191	0.74 nM
Hur 2002	0.003 µM
Jackobsen 2007	0.0037 µM
This study	0.01 µM
Chi 2007	0.1 µM
This study	0.1 µM
Chi 2007	0.2 µM
Lian 2009	0.74 µM
Unagul 2007	0.74 µM
This study	1 µM
This study	10 µM
Lippmeier 2009	36.9 µM

Quilodran *et al.* (2010) is the only work that has focused investigation on the effect of vitamins. They worked with an unclassified thraustochytrids (strain name: AS4-A1) and saw that 1mg/L thiamine, 0.0005 mg/L biotin and 0.0005 mg/L cyanocobalamine, **stimulates ARA, EPA and DHA production**. According to this data, vitamins might affect eukaryote biosynthetic pathway. **Otherwise if PKS-like [69] was stimulated it would produce only more DHA** (PKS-like pathway is specific to DPA and DHA production as explained in chapter 1 section 1.3.3).

Flask experiments

The medium developed in this chapter contains yeast extract and tryptone (see section 3.2.2), which typically[70] contains thiamine, riboflavin, pyridoxine, niacinamide and pantothenic acid but not Vitamin B_{12}. Therefore, only vitamin B_{12} needed to be investigated. The effect of five different concentrations of Vitamin B_{12} on *A. limacinum* SR21 growth, DHA production and cell size were investigated. Vitamin B_{12} has shown no positive effect on the thraustochytrids investigated here. Experiments were initially carried out in Erlenmeyer flasks. Results are summarized in Figure 3.56 *a* and *b*.

Figure 3.56a clearly indicate a negative connection between cyanocobalamin concentration and final DCW. **Cultivating *A. limacinum* with 10 µM vitamin B12 resulted in 27% decrease in the final DCW**. This might be caused by a toxic effect from either the vitamin itself or the HEPES buffer provided by the vitamin stock solution, which could be causing a growth inhibition. The difference in final biomass between 0.01 µM and 0 µM was minimal indicating that low concentrations of Vitamin B_{12} had no effect on *A. limacinum* growth. Even a concentration of 0.1 µM, which was recommended as the ideal concentration by Chi et al.

123

---

[67] Nowadays classified as A. mangrovei SK-02
[68] Nowadays classified as A. limacinum, the main strain of this thesis.
[69] Polyketide synthase (PKS)-like synthesis of fatty acids
[70] Especially yeast extract.

(2007) [93], showed a decrease not higher than 10%. Analyzing DHA results, displayed in Figure 3.56b, was in concordance with the hypothesis that cyanocobalamin was not benefiting *A. limacinum* in any case. As can be seen, DHA yield was identical for each experiment. DHA yields and final biomass values indicate that a flask culture without Vitamin B_{12}, would render the best productivity of DHA.

The fact that cyanocobalamin does not affect DHA production was expected, because it had been reported that this vitamin only affects the regular FA biosynthetic pathway [47]. It is known that *A. limacinum* DHA specificity relies on the PKS-like pathway. In other words, the dominant PKS-like DHA synthesis pathway
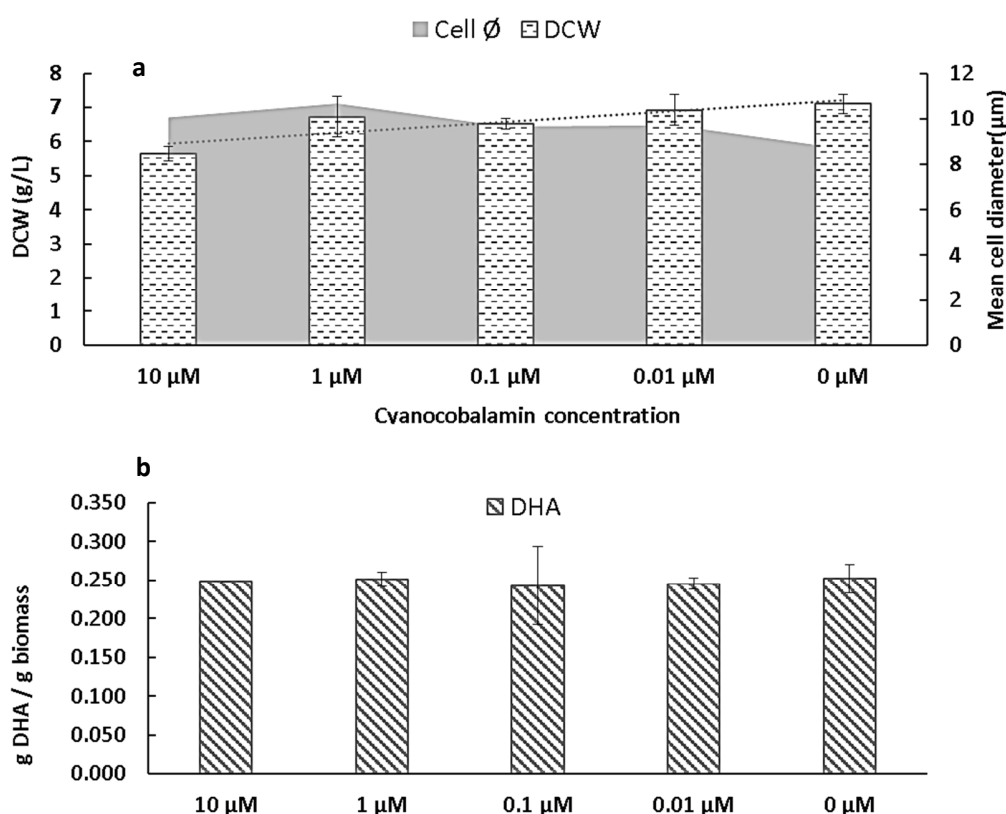
Figure 3.56 Effect of cyanocobalamin or Vitamin B12 on A.limacinum flask cultures. a. Growth indicated as dry cell weight (DCW) and mean cell diameter results regarding different vitamin concentrations. b. DHA production expressed in yield with different vitamin concentrations. Both sets of data were obtained after 80 h of culture at 20ºC. Medium composition based on previous section improvements. Initial substrate concentration was 10 g/L of crude glycerol. Four replicates per sample.

in *A. limacinum* is not affected by cyanocobalamin.

There is an interesting output not affecting DHA productivity, but worth mentions it, which is the reduction of cell size while the concentration of the cyanocobalamin is reduced (Figure 3.56a). Using the microscopy + Matlab® technique described in the previous chapter, a difference in zoospore production could be detected. **Those cultures with higher concentration of Vitamin B12 showed a lower amount of zoospores** (data not shown)**. Thus *A. limacinum* stayed in a vegetative stage for longer time, leading to larger cell size.** This should be the cause of the different cell diameter displayed in Figure 3.56a.

Bioreactor experiments

Using the same conditions from flask experiments, bioreactor cultures were carried out with the concentration range of cyanocobalamin from 0 to 10 μM. This experiments were willing to elucidate if vitamin B_{12} had the same effect in bioreactor cultures. Results of *A.limacinum* performance in bioreactor are given in Table 3.27. Similarly to what happened with flask cultures, the bioreactor without vitamin showed the best production of both biomass and final DHA (not DHA yield). If the cyanocobalamin concentration is increased the final biomass concentration is reduced. This data correlates with flask experiments results and supports the hypothesis that cyanocobalamin could inhibit *A.limacinum* growth. As mentioned above, this could be an indirect cause of zoospore formation inhibition.

Table 3.27 A.limacinum growth performance in 2L bioreactor using different Vitamin B_{12} concentrations. Data was obtained after 60 h of culture 20ºC; 1 L/min of compressed air and 500 rpm. Medium composition based on previous section improvements. Initial substrate concentration was 10 g/L of crude glycerol. No replicates. * Overestimated yields caused by the carbon charge of yeast extract, tryptone and crude glycerol others than glycerol. Yields are calculated only considering initial glycerol.

[Vit. B_{12}]	DCW (g/L)	Yx/s	DHA (g/L)	Yp/x
0 μM	11.01 ± 0.35	1.06*	1.66	0.151
0.01 μM	9.50 ± 0.01	0.84*	1.57	0.165
0.1 μM	6.34 ± 0.14	0.56	0.91	0.144
1 μM	7.36 ± 0.42	0.66	1.35	0.183
10 μM	6.11 ± 0.07	0.54	0.76	0.125

DHA yieds exhibited a greater variability as can be observed in Table 3.27. For example, the bioreactor using a concentration of 1 μM Vitamin B_{12}. Yield variability might be caused by other parameters during the bioreactor culture such as harvesting time, oxygen demand, inoculum variability[71], etc. Due to logistic limitations, every bioreactor was carried out during different weeks and different random situations could be the unexpected cause of variabilities. The most common variability source is the inoculum and the harvest time. In other words, if the culture spends more time in the lag phase, due to a weak inoculum, then the growth would be slower and the harvest time at a different cell stage. However, even with a lower DHA yield, the first bioreactor (0 μM) is produces more DHA.

Despite the variability of DHA yield among different bioreactors, data consistently points to an insignificant effect of cyanocobalamine on *A. limacinum* growth and DHA production performance. Thus, the **vitamin is eliminated from the formulation of the medium**. Flask and bioreactors data suggest that high concentrations of cyanocobalamin could be inhibiting zoospore formation. Consequently, the growth is limited.

3.2.6 Medium minority salts composition

Considering the established initial composition (detailed in Table 3.21 section 3.2), there are three salts which needed a revision. These salts are $MgSO_4$, $CaCl_2$ and KCl. There is not much information about this salt and its contribution for thraustrochytrids cultivation. What is known is that sulphate (7.7 %), magnesium (3.7%), calcium (1.2%) and potassium (1.1%) are important components of seawater. The effect of MgSO4, $CaCl_2$ and KCl was the aim of upcoming sections.

---

[71] Inoculums did not contain vitamin B_{12}.

3.2.6.1 Magnesium sulphate
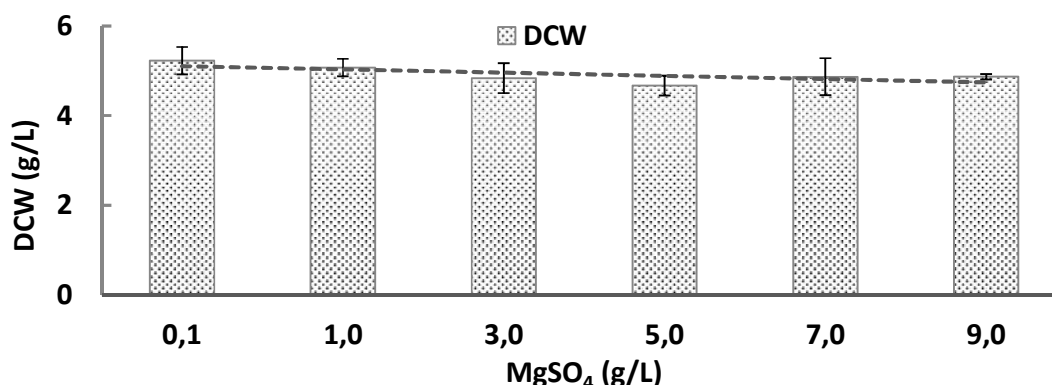
Figure 3.58 Effect of different MgSO4 concentrations on A. limacinum growth. Data was obtained after 72 h of culture at 20ºC. Medium composition based on previous section improvements. Initial substrate concentration was 8 g/L of crude glycerol. Four replicates per sample.

The usage of MgSO$_4$ for thraustochytrids cultivation was purposed by Bajpai and Ward (1991) [51]. Previous works only used this salt as a mere ingredient of seawater but Bajpai and Ward used mediums containing 5 g/L MgSO$_4$. Interestingly, Unagul et al. (2005) [92] performed an experiment where every salt was replaced by NaCl causing a significant reduction of T. aureum growth. Thus, indicating that other salts must have a role for this thraustochytrid strain. Nagano et al. (2009) [197] went further and investigated what happens when each one of the salts commonly composing seawater is omitted. They have found that for A. limacinum mh106 MgSO$_4$ is essential but MgCl$_2$ not. Chi et al. (2007) [93], contrary to Nagano et al. work, investigated two MgSO$_4$ concentration in A. limacinum SR21 finding no influence on its performance. Therefore, the influence might be caused by other factors in the medium. For this reason, a wide range of MgSO$_4$ concentration was investigated for A. limacinum cultures in the present

126
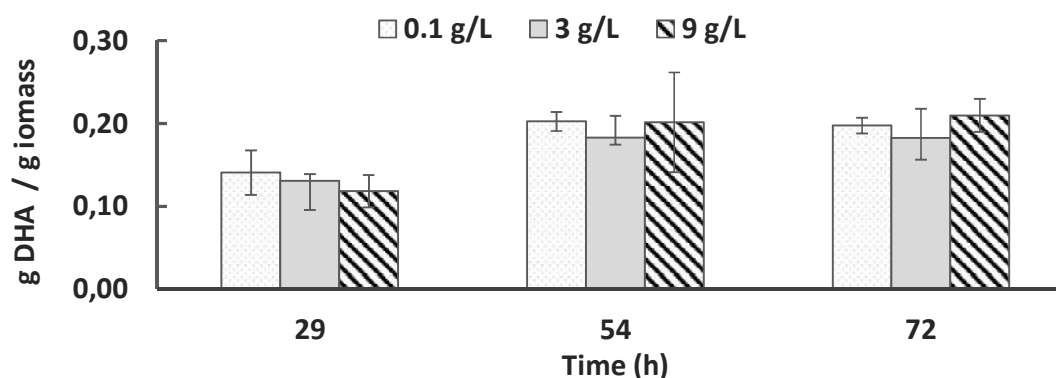
Figure 3.57 Effect of different MgSO4 concentrations on DHA production, which is indicated as DHA yield (g DHA / g DCW of A.limacinum). Data was obtained after 72 h of culture at 20ºC. Medium composition based on previous section improvements. Initial substrate concentration was 8 g/L of crude glycerol. Four replicates per sample.

section. MgCl was discarded because NaCl provides enough chloride, which in higher concentrations could generate corrosion in bioreactors [92].

MgSO4 effect on *A. limacinum* was investigated for 6 different concentrations, 0.1, 1, 3, 5, 7 and 9 g/L using the medium here developed. Biomass results are displayed in Figure 3.58. The effect of this salt on *A. limacinum* growth is not significant despite the slightly decreasing tendency described when the concentration increases. On the other hand, $MgSO_4$ addition neither have shown any impact on DHA production as shown in Figure 3.57. Yields are fairly the same, even compared with other experiment in this chapter.

Nagano *et al.* unequivocally showed a lack of MgCl2 does not impair thraustochytrids performance, whereas a lack of $MgSO_4$ generated dramatically low biomass concentrations. This could indicate that the important ion provided by $MgSO_4$ is SO^{42-}. Results in Figure 3.58 are evidence reinforcing this hypothesis. Moreover, yeast extract (and yeast extract in general) contains a small amount of magnesium (0.5 g/L aprox.) [92] and in some cases a huge amount of SO_4^{2-} (5 g/L aprox.). This might explain why an extra addition of **$MgSO_4$ is not affecting *A.limacinum* with the current medium**. Therefore, this is an important consideration for medium preparation. Actually, literature works are performing optimizations on salt composition without considering their complex components.

According to the results and discussion, **it was decided to keep 0.1 g/L of $MgSO_4$** in the medium recipe. In order to avoid any problem with magnesium limitation in highly concentrated cultures of *A. limacinum*. The amount of sulphate provided by yeast extract avoids any risk of limitation at high density cultures. Furthermore, **5 g/L of MgSO4 would be added in case of using a free sulphate yeast extract**.

3.2.6.2 Calcium chloride and potassium chloride

Calcium chloride and potassium chloride were investigated together looking for an optimum concentration of both salts. Thus, seeking a better culture performance and a reduction of chloride ions. Information about these salts either on *A.limacinum* or thraustochytrids is limited. In many works different concentrations are just used without criteria. In many cases the medium just follows the Starr and Zeikus [178] medium composition. Only two works cursorily investigated the effect in two salts. Chi *et al.* (2007) investigated two concentrations of both salts within a single DoE together with other many factors. They found that $CaCl_2$ and KCl have no important effects on *A. limacinum*. These results are
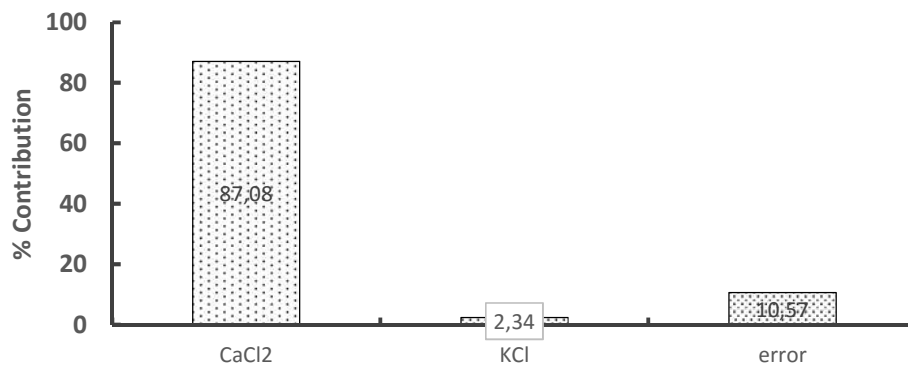
Figure 3.59 Contribution of $CaCl_2$, KCl and error on A. limacinum performance. Data was obtained after 72 h of culture at 20ºC. Medium composition based on previous section improvements. Initial substrate concentration was 10 g/L of crude glycerol. Four replicates per sample.

consistent with Nagano et al. (2009) [197], where they suggest that these salts are not essential for *A. limacinum*.

In this thesis a Taguchi matrix based DoE was performed in order to discover the best combination of $CaCl_2$ and KCl concentration. In this case, the selected matrix was an unmodified $L_9(3^4)$ which allowed the analysis of four factors with 3 levels. As there were only two factors, remaining columns of the matrix gathered the error contribution.

The investigated concentrations were 0, 0.3 and 0.6 g/L for $CaCl_2$, and 0, 0.5 and 1 g/L for KCl. Results were analyzed by ANOVA and the contribution of every factor is displayed in Figure 3.59. As can be observed, only $CaCl_2$ had an effect on *A. limacinum* growth, whereas KCl showed no impact. It was expected because Cl^- ions are already provided by NaCl, and the buffer (KH_2PO_4 – NaOH) is providing enough K^+ ions[72]. $CaCl_2$ is contributing positively to *A. limacinum* growth (data not shown). In order to find an optimum $CaCl_2$ concentration, both factors were collected to perform a quadratic multiple regression (using polynomial and interaction terms). The second order regression allowed fitting a response surface to find the optimum value of $CaCl_2$, which is displayed in Figure 3.60. The mesh clearly indicate that the optimum
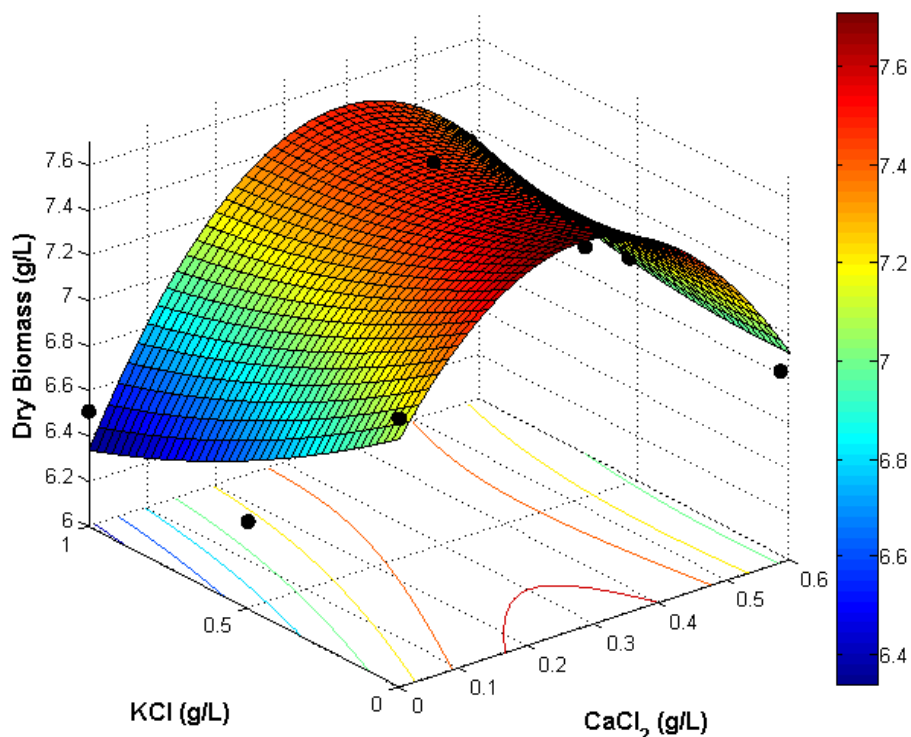
Figure 3.60 Response surface based on a second order regression performed using the points from the previous experiment. Black dots show the results from the raw data.

---

[72] K^+ ions don't have any role in pH buffering.

DCW values are obtained when the KCl concentration is 0 and $CaCl_2$ concentration is between 0.18 and 0.4 g/L. Due to a risk of solubility issues, final **chosen $CaCl_2$ concentration was 0.19 g/L**.

Table 3.28 Comparison of different medium performance in batch bioreactors A. limacinum cultivations. 10 g/L carbon source.

Component	Concentration	Component	Concentration
KH_2PO_4	0.85 g/L	$Na_2EDTA·2H_2O$	0.20 mM
NaOH	0.14 g/L	H_3BO_3	1 mM
NaCl	18 g/L	$MnSO_4·H_2O$	0.097 mM
$CaCl_2$	0.19 g/L	$ZnSO_4·7H_2O$	7 µM
$MgSO_4$	0.1 g/L	$FeSO_4·7H_2O$	0.83 mg/L
Yeast Extract	2.3·(C/10)	**Final medium composition**	
Tryptone	0.4·(C/10)		
Carbon source (C)	C value could be between 10 g/L y 100 g/L		

3.2.7 Final medium composition

The optimized seawater medium offers the best performance for *A. limacinum* growth and DHA production. The new medium can be autoclaved without any special requirement while avoids any precipitation. It uses a scalable (cost effective) buffer such as phosphate buffer. The medium avoids the use of cobalt without affecting growth performance. Moreover, the new medium has a lower cost. The original medium has a cost of 1.68 € / L whereas the new medium has a cost of 1.27 € / L, based on prices from the same. Bulk provision would lead to a more reduced cost. Finally, as evident by observing Table 3.29 organic nitrogen source supposed a significant increase in biomass production as well as in DHA accumulation (DHA yield). Thus, it resulted in a higher volumetric productivity of DHA. Furthermore, the remaining medium components supposed an extra increase in both parameters.

The final medium composition is indicated in Table 3.28. Left columns indicate the components that have been optimized. Trace metals composition (right column in Table 3.28) was formulated based on Starr and Zeikus [178] formulation. For this thesis only cobalt had been eliminated. Three batch reactors were carried out and show the differences between the original medium, the nitrogen source optimization and the final media composition. The results of these bioreactors are shown in Table 3.29. As can be observed, the main difference lies in the DHA yield. It shows an increase of 150% or more. Final biomass

Table 3.29 Comparison of different medium performance in batch bioreactors A. limacinum cultivations. 10 g/L carbon source.

Medium	$Y_{DHA/DCW}$	Final OD_{600}	Productivity (mg DHA/l-h)
Original	0.09	10.9 ± 1.2	27.2
Improved nitrogen source	0.21 ± 0.02	12.9 ± 0.83	56.3 ± 1.0
Optimized	0.24 ± 0.02	13.9 ± 0.4	60.17

concentration also showed an increase while using the improved media. Considering the yield and the biomass concentration, the productivity showed a notable difference.

3.3   Chapter achievements

Chapter 3 offered a complete bibliographic and experimental revision of *A. limacinum* cultivation medium. Carbon source, nitrogen sources, salts, buffer and vitamins have been investigated in Chapter 3 seeking an optimal *A. limacinum* growth.

It has been shown that glycerol is an excellent carbon font. Data obtained in this chapter showed a similar performance between glucose and glycerol cultivations. Moreover, *A. limacinum* has been characterized using different carbon sources (10 g/L) in batch reactors. This study generated the basic kinetic parameters which are important for the bioprocess development. Growth rate, growth yield and saturation give information about *A. limacinum* requirements in batch cultures. Furthermore, it has been shown that DHA yield increase is related with biomass growth in batch reactors at 20ºC.

Nitrogen source is also a key component in *A. limacinum* medium. Few DoE have been used to investigate the contribution from four different nitrogen sources. These nitrogen sources were selected after an exhaustive revision of bibliography. Yeast extract and tryptone were selected as organic nitrogen sources and ammonium and nitrate as inorganic nitrogen sources. When *A. limacinum* was grown using organic nitrogen sources it showed better DHA yields. On the other hand, both nitrogen source types generated similar growth yield. In order to determine the optimum nitrogen composition two models have been built using ANN. Several flask culture results were introduced into ANN to generate both models considering final biomass and DHA yield. Both models lead to a defined composition to maximize DHA production, with 2.3 g/L and 0.4 g/L (per every 10 g/L of carbon source) for yeast extract and tryptone, respectively. Nitrate and ammonium can be avoided from the formula.

131

The concentration of sodium chloride has been investigated as it has the main contribution to salts composition in the developed medium. *A. limacinum* can grow adequately and satisfactorily produce DHA when the sodium chloride concentration is between 14 and 30 g/L, showing a great versatility for different crude glycerol salinity.

In literature, different vitamins have been used to enhance thraustochytrids growth. From the vitamins described in the bibliography Cyanocobalamin is not present in yeast extract. For this reason, different vitamin B_{12} were investigated in this chapter. After investigating different cyanocobalamin concentrations results showed an insignificant effect of cyanocobalamin on *A. limacinum* growth and DHA production. Thus, this vitamin was eliminated from the medium.

Tris was used as buffer in the initial composition of the medium. However, it is an expensive buffer. In this chapter KH_2PO_4 + NaOH buffer was selected according to price and pH range. After this, $MgSO_4$, $CaCl_2$ and KCl concentration was investigated. The best final concentration was determined to be 0.1 g/L $MgSO_4$ and 0.19 g/L $CaCl_2$, whereas KCl was excluded from the medium.

This page intentionally left blank

Chapter 4: Growth characterization and production strategies investigation

Implications of A. limacinum in the cultures strategies

4.1   Introduction

Two main pillars constitute upstream bioprocess development. The first is the proper medium for a specific microorganism and the second is the cultivation parameters and operation mode. Culture medium for thraustochytrids has been already defined in Chapter 3. This medium has simply been tested in Erlenmeyer flasks and bioreactors with "standard" parameters. Initial pH and the ratio between air and volume are the only parameters that can be set, not even controlled, in a flask culture. In the literature, just some bioreactor runs were performed to validate flask data. The choice of reactor and operating strategy determines product concentration, number and types of impurities, degree of substrate conversion, yields, and whether sustainable, reliable performance can be achieved [198]. This thesis addresses operating considerations including key parameters for thraustochytrids.

Bioreactors are important tools for biotechnology. They can be used to investigate and characterize microorganisms as well as serve as precise equipment to produce constant quality products in the industry. By definition a bioreactor is a vessel in which a biochemical process is carried out, which involves organisms (mainly microorganisms) or biochemically active substances derived from such organisms. Cultivating a microorganism in a bioreactor allows a very narrow control of the culture environment. Generally equipped with an agitator[73], bioreactors ensure better substrate mixing easing mass transfer such as, gas / liquid, liquid / liquid, gas /solid and liquid / solid, and heat transfer. These major type of reactor are called stirred tank reactors (STR), and are by far the most common type of bioreactors used in industry. Most importantly, it provides a containment protecting the environment of the reaction, avoiding contamination from opportunist microorganism the culture. Nowadays, these bioreactor vessels are coupled with control devices which monitor many different parameters. Most common controlled parameters are pH, oxygen supply, oxygen concentration in the liquid phase, temperature and can monitor biomass concentration.

Three operation modes of STR have been investigated in chapter 4 for thraustochytrids growth and DHA production. Two unsteady state processes which are **batch** and **fed-batch**, and a steady state (with a transient interval) that is the **continuous stirred tank reactor (CSTR) or chemostat**.

4.1.1   Different operating strategies

Each operation mode has specific characteristics, with advantages and disadvantages which defines its suitability for a specific process.

4.1.1.1 Batch reactor

A batch operation refers to a culture with a specific initial substrate concentration that is not altered. Because nutrients are not added, nor waste products removed during incubation, batch cultures can only complete a limited number of life cycles before nutrients are consumed and growth stops. This form of cultivation is simple and widely used. It is versatile; the same equipment can be used for different reactions. This operating system can complete substrate consumption. Finalized the culture, batch is easy to shut down and clean for fouling service.

---

[73] Stirred tank reactors are the most common type of bioreactors which are evidently agitated. However, there are many other types of reactors which do not use a *de facto* agitator. As only stirred tank reactors were used for this thesis development, other reactor types are not addressed in this chapter, nor throughout the thesis.
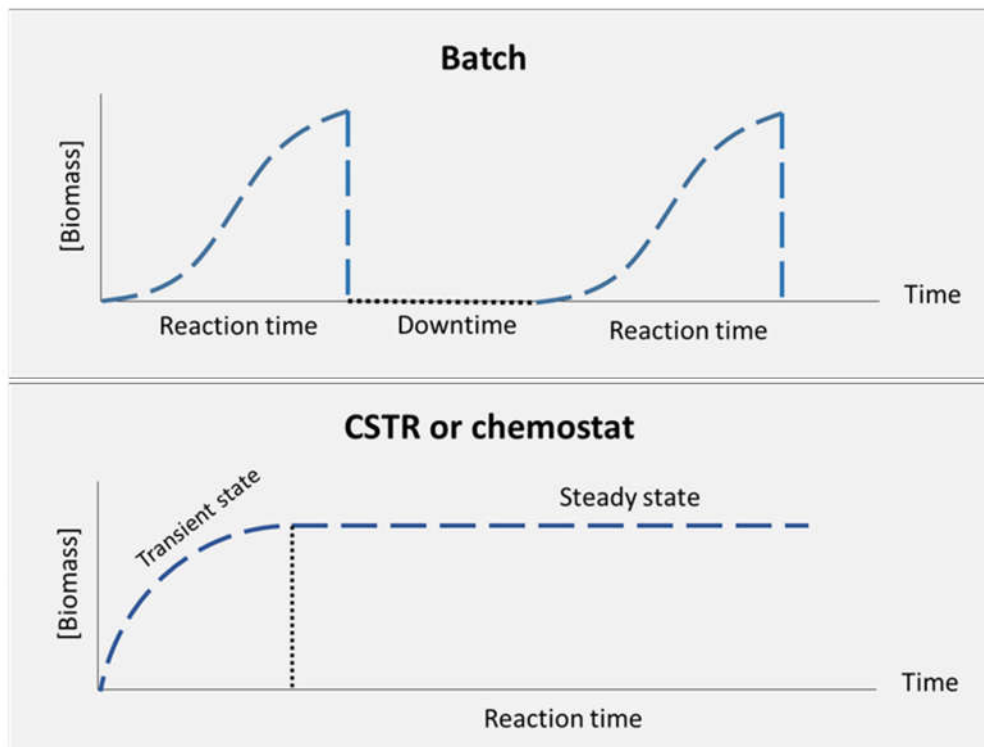
Figure 4.61 Comparison of batch and continuous operation.

In industry, batch reactors are larger and capital cost is usually high. It requires skilled labor, which is mainly required for **downtime** (Figure 4.61) between reactions. Downtime includes harvesting, cleaning, sterilization, inoculum growth and load between reactions. As batch is an unsteady state operation it entails exhaustive process control. It is more difficult to obtain product uniformity. Moreover, downstream equipment coupled to batch reactors works normally continuously and with reduced volume. Therefore, products need to be stored and buffered for a specific amount of time, and might not be suitable for labile products.

Any microorganism grown in batch describes the same behaviour in conditions of substrate limitation (with a single carbon source). Any culture includes lag phase, exponential growth phase, deceleration phase, stationary phase and death phase. The lag phase occurs immediately after inoculation. During lag phase the microorganism cultivated experiences an adaptation to the new environment. Adaptation time is variable and depends on the age[74] and size of the inoculum. Usually the lag phase is longer with old inoculums and faster with fresh inoculums. The exponential growth phase is also known as the maximum growth phase, where the cells have their metabolism adjusted and multiply themselves at maximum rate. Therefore, during this phase the growth rate is "constant" and a kinetic model can be established.

$$r_X = \mu_{net} \cdot X \qquad\qquad\qquad \text{Equation 4.2}$$

---

[74] How long the cells have been growing in a flask/reactor, and how long they have been maintained after carbon source depletion.

Equation 4.1 describes the exponential law of any population, in this case it is referred to cell concentration X. Specific (net) growth rate (μ_{net} (h^{-1})) is constant during growth phase. In a batch reaction the rate of change of X is the same as the rate of generation of biomass according to the typical batch mass balance. Integration of the mass balance with 4.1 gives:

$$ln\frac{X}{X_o} = \mu_{net} \cdot t \qquad\qquad \text{Equation 4.3}$$

Isolating X gives the following equation:

$$X = X_O \cdot e^{\mu_{net} \cdot t} \qquad\qquad \text{Equation 4.4}$$

Where X and Xo are biomass concentration at time t and initial time t=0, respectively. Using this equation biomass concentration or growth rate can be calculated. Moreover, using equation 4.2 a specific (defined time interval) growth rate can be calculated using a finite difference scheme (subdivision of the growth in short time intervals), maximum growth rate can be obtained.

Growth yield ($Y_{x/s}$) is the ratio of the amount of biomass produced to the amount of substrate consumed (g biomass/g substrate) [199]. This can be defined as

$$Y_{X/S} = \frac{X-X_o}{S_O-S} \qquad\qquad \text{Equation 4.5}$$

Where S and So are substrate concentration at time t and initial time t=0, respectively. This relates biomass and substrate for a specific microorganism. However, any of the equations offered cannot relate growth rate, biomass and substrate as Monod equation does. Monod expression serves as an approximate growth kinetics model.

Enzymatic reactions are in general explained by Michaelis-Menten kinetics. Cell metabolism involves numerous pathways and reaction steps. Each reaction step along the metabolic pathway of a microorganism corresponds to a single enzymatic reaction. Therefore, quantifying cell growth with all the governing parameters following all metabolic pathways would make the computation tedious. For this reason, a simplification of the kinetics is necessary and is what Monod did. Monod model derives from the premise that a single enzyme system with Michaelis-Menten kinetics is responsible for uptake of substrate and its activity is sufficiently low to be growth rate limiting. In other words, the microorganism is as fast as the slowest enzyme reaction involved in substrate uptake metabolism. Thus, Monod model is a transformation of Michaelis-Menten kinetics to approximate growth behavior in a controlled culture. Monod equation is the following:

$$\mu_g = \frac{\mu_m \cdot S}{K_s+S} \qquad\qquad \text{Equation 4.6}$$

where μm is the maximum specific growth rate, in general when $S \gg K_s$. The constant K_s is known as the saturation constant and it is equal to the concentration of the rate-limiting substrate when the specific rate of growth is equal to 1/2 of the maximum ($K_s = S$ when $\mu_g = \frac{1}{2}\mu_m$). With all described equations below, an investigator can monitor the parameters of any microorganism growing in batch mode. *Thraustochytrids* kinetic parameters calculation procedure is detailed in Material and Methods section.

4.1.1.2 CSTR or chemostat reactor

In a CSTR or chemostat[75] culture, fresh medium[76] is continually supplied to a well-stirred culture, where products and cells are simultaneously withdrawn. Growth and product formation can be maintained for prolonged periods in continuous cultureFigure 4.61. In CSTR systems, the required equipment volume is lower compared to batch and fed-batch making capital cost usually relatively lower.

Downtime is dramatically reduced, only expected for maintenance work. This reduces labor cost and increases utilization of the equipment, making it more cost effective. Generally, long term **productivities** are higher than any other operating mode. Recent advances in technology automation are very appealing for CSTR systems, which would reduce even more labor cost and variabilities (it might increase initial investment cost). Downstream process equipment must be adjusted to CSTR flow. Continuous downstream generally uses reduced volume equipment, which makes product purification even more cost effective.

Box 4.1. Mutations during continuous cultures

Natural mutations can take place in a chemsotat culture. Errors in DNA replication can take place with an average frequency of about 10^{-5} to 10^{-8} genes per generation. The vast majority of natural mutations in a chemostat are of little significance, unless it alters the function of a protein involved in growth. If the specific growth rate of the mutant is larger than that of the wild type, then the mutation outgrows the wild type in a chemostat [241].

Flow control is vital in CSTR operation, it defines the growth rate and the steady state. Even if the flow is controlled satisfactorily, long period cultures increase the risk of failing due to contamination as well as spontaneous mutation of microorganism (Box 4.1). In the particular situation of this thesis, thraustochytrids are cultured without any genetic manipulation. Wild type strains are genetically more stable. As thraustochytrids are generally slower than yeasts and bacteria, an opportunist microorganism population could shift thraustochytrids population rapidly. This may cause a shutdown causing a loss of production.

A chemostat material balance on biomass is shown:

$$FX_o \quad FX + V_R\mu_g X \quad V_R k_d X = V_R \frac{dX}{dt}$$

Equation 4.7

where F is the volumetric flow rate (L/h), V_R is the final volume (L) and K_d is the cell mass loss rate (h^{-1}). Mass balance 4.6 can be rearranged as

$$\frac{dX}{dt} = DX_0 + \left(\mu_g \quad k_d \quad D\right) X$$

Equation 4.8

where D is the dilution rate and is defined as D = F/V_R. However, **three factors simplify even more equation 4.7**.

➢ Feeding is always sterile **($X_0 = 0$).**
➢ Cell mass loss rate is tipically negligible compared to the growth rate **($k_d \ll \mu_g$).**

---

[75] The word chemostat implies that "the chemistry should be constant or stationary". Therefore, by definition a chemostat is a CSTR only during steady state period. Not including transients state.
[76] Nutrients or fresh medium with all required components.

➢ The system is in a steady state **(dX/dt = 0)**.

Therefore, in a chemostat the specific growth rate is equal to dilution rate **(μ_g = D)** if **($k_d \ll \mu_g$)**. This property allows the manipulation of the growth rate as an independent parameter. As D is governing the growth rate of the culture, Monod equation for continuous cultures can be expressed as following.

$$D = \frac{\mu_m \cdot S}{K_s + S}$$

Equation 4.9

where S is the substrate concentration inside/leaving the culture, not the feeding concentration S_o. Yield equation 4.4 can be applied identically to a chemostat. Thraustochytrids kinetic parameters calculation procedure is detailed in Material and Methods chapter.

4.1.1.3 Fed-batch operation
In fed-batch, feeding is continuously or semicontinuously supplied until reaching the final volume of the reactor. The advantage of the fed-batch culture is that one can control concentration of fed-substrate in the culture liquid at arbitrarily desired levels. In some cases, effluent is removed discontinuously and is called *repeated fed-batch* operation. In a repeated fed-batch the content is partially removed, and the rest is left in the bioreactor to serve as the inoculum for the next cycle. Fed-batch is mainly used to overcome substrate and/or product inhibition, or catabolite repression by intermittent addition of substrate. On the other hand, it can be used as a scenario for induction of product formation not related with the microorganism growth. Somehow, fed-batch is an extended batch reaction. Hence, it combines the advantages of batch and continuous operation. Fed-batch is excellent for control and optimization of a given production criterion and allows a superior control of environmental conditions (compared to batch). It is the most common operation system in industrial biotechnology.

As happen with CSTR, fed-batch requires feeding and most importantly, flow control. Downtime after a production require the same procedures as batch, whereas it has the same contamination risks from feeding. Fed-batch never reaches a steady state and product uniformity is harder to obtain. Coupling with continuous downstream processing requires storage and buffering tanks, as happens with batch reactions.

4.1.1.4 Multi-stage CSTR reactor
In some microorganism cultures, particularly for secondary metabolite production, the growth and product formation steps need to be separated, since optimal conditions for each step are different. Conditions such as temperature, pH, and limiting nutrients may be varied in each stage, resulting in different cell physiology and cellular products in multistage systems. Besides the advantages mentioned above, it obviously has the same features and drawbacks as a single tank CSTR (see section 4.1.1.2).

This type of operation could be a powerful tool enhancing DHA production through thraustochytrids cultivation. Thraustochytrids optimal growth conditions are very different from DHA yield optimal conditions. In Chapter 4, there is an in-depth investigation about these conditions and how to meet the perfect consensus production. Multistage continuous cultivation as a strategy to produce DHA is a novel solution described in the present thesis.

4.1.2 *A. limacinum* cultivation: state of the art
The vast majority of literature works about thraustochytrids cultivation have been carried out in flask. Differently from medium optimization, only bibliographic investigation performed with bioreactors has

138

been considered for Chapter 4. Flask cultivation conditions and parameters cannot be directly extrapolated to bioreactor. From 126 publications reporting thraustochytrids production of n-3 PUFA, only 14 reported investigations about operating strategies.

For batch bioreactors 4 publications have been found (2006-2013). Chi *et al.* (2009) [200] investigated the aeration influence on *A. limacinum* in a 5 L bioreactor, as well as having previously developed in Chi *et al.* (2007) [93]. They have clearly shown that oxygen is a limiting factor in Erlenmeyer flask cultures. Oxygen limitation causes an increase in DHA accumulation due to PKS-like synthase pathway (as explained in Chapter 1 and 2), whereas oxygen abundance enhances biomass growth. This might explain why in flask cultures DHA yields are generally higher than in bioreactor. Rosa *et al.* (2010) [9] investigates two media compositions for differential biomass and DHA enhancement. In other words, one medium is used to grow (300 mL) *A. limacinum* that are then centrifuged and cultivated in a bioreactor with a second medium. The second medium seeks DHA stimulation. Two years later, Prabu *et al.* (2012) [201] investigated the possibility of replacing NaCl by Na_2SO_3 to avoid high chlorine ion concentration and possible corrosion problems with stainless steel vessels. The last reported batch culture of thraustochytrids was from Qu *et al.* (2013) [202] where they investigated three different strategies for DHA production through *Schizochytrium* sp. These strategies are batch, fed-batch and repeated fed-batch. This work reveals that a fed-batch approach is more effective than batch. Reported batch productivities are very variable, because they depend on the interval time selected by the investigator (including inoculum, downtime, etc.). The values oscillate between 20 to 150 mg DHA /L ·h.

Jackobsen *et al.* (2009) work was the first purposing a fed-batch to increase DHA productivity. *Aurantiochytrium* sp. T66 was grown and reported a productivity of 93 mg/ L·h. In Qu et al. (2013) [202] a fed-batch and a repeated fed-batch showed higher productivities, with a maximum of 138 mg DHA/ L ·h in 136 hours cycle. The same group published two more works about fed-batch cultivation of *Schizochytrium* sp. [203]. They have investigated different aeration procedures during fed-batch cultivation obtaining a maximum productivity of 148 mg DHA/L · h [204,205]. Ganuza *et al.* (2008) [206] used a fed-batch distinguishing two main phases. First, the initial batch cultivation set an ammonium rich environment, to finally use a feeding stage to create nitrogen starvation. Results show that the second stage did not accumulate enough DHA to justify this approach. However, batch stage generated a notable amount of biomass. This data is in concordance with what has been reported in Chapter 3 (this study) about ammonium polar effect, and its negative impact on lipids accumulation but positive impact on cell growth.

A different group of investigators from South Korea have investigated different fed-batch strategies for a new strain, *Aurantiochytrium* sp. KRS101 [141,192,207]. What stands out about these works is the use of fed-batch to switch C/N ratio, seeking an increase of lipid accumulation. Their maximum DHA productivity was 125 mg DHA / L ·h. Chang et al. (2013) investigated another new strain, *Aurantiochytrium* sp. TC20. They have investigated different carbon sources in a fed-batch, to obtain a productivity of 102 mg/L·h (including inoculum time) [208]. Similarly, to batch, productivities depend on the cultivation time intervals considered.

Only two publications working with thraustochytrids in a continuous reactor have been found. Ganuza et al. (2007) investigated a continuous DHA production with *Schizochytrium* G13/2S. Using glucose, their work reported 39 mg DHA / L ·h produced continuously. Some years later, only one investigation on continuous production has been published. Ethier *et al.* (2011) studied *A. limacinum* SR21 in a continuous

reactor, obtaining a productivity of 21.6 mg DHA / L ·h. Reported *A. limacinum* continuous productivities are very low compared to batch and fed-batch, but there are many things to consider. First, thraustochytrids cell cycle is different in batch than in continuous (see section 4.1.3 of Chapter 4). Second, thraustochytrids growth and DHA enhancing conditions are different. A continuous culture cannot switch between conditions; otherwise steady state is lost. Accordingly, a single tank continuous reactor could not compete with batch or fed-batch. However, a multi-stage continuous culture could combine batch and fed-batch advantages conditions while producing DHA continuously.

4.1.3   *A. limacinum* implications and further investigations

In many ways, *A. limacinum* is a very special microorganism. As explained in Chapter 1 and 2, it has a complex cell cycle and metabolism that behaves differently depending on the conditions fixed during the culture. This happens with many strains of thraustochytrids, generating the huge divergence that can be found in literature. Thraustochytrids are still just black boxes and all the information is based on empirical statements (with some exceptions, e.g. Matsuda et al. (2012) [112]). Just the implication of oxygen and temperature are well known and explained in the present section. Other parameters like carbon source concentration or residence time in a continuous reactor are not considered.

Temperature is an important factor affecting cell performance. Temperature and thraustochytrids relationship is very well established. Growing this eukaryote microorganism at low temperatures[77] (e.g. 20 ºC) causes an increase in lipid accumulation. **Specially PUFA** because they confer fluidity to thraustochytrids membrane at lower temperatures [63,209]. Contrary, when temperatures are high[78] (e.g. 30 ºC) microorganisms accumulate less lipids but growth rates are significantly higher. Temperatures above 40 ºC could cause thermal death. Interestingly, Taoka *et al.* (2011) investigated both the growth of *A. limacinum* at very low temperatures (10 ºC) and a cold shock by storing biomass at 4ºC after carbon source depletion, but have not seen a DHA or lipids increase. Probably due to a reduced growth rate and metabolic activity at this temperature, likewise a lack of carbon source to build up new FA. There are several other works investigating different temperatures for different strains, where growth and DHA were monitored. In all cases the behaviour followed the same trend, cold is good for lipids and warm for biomass development.

During any culture, **pH** affects the activity of enzymes and therefore the microbial growth rate. The optimal pH for growth may be different from that for product formation. As explained in Chapter 3, thraustochytrids are especially versatile. This allows them to grow in a wide range of pH values. Unagul *et al*. (2007) [92] have shown that *A. mangrovei* can grow well with pH values between 5 and 7. Moreover, Arafiles et al. (2011) [210] have revealed that *Thraustochytrium sp.* can grow well in media with either pH 4 or pH 8. In the same work, they suggest that *Schizochytrium* sp. (phylogenetically closer to *A. limacinum*) can only grow in media with pH values between 5 and 8, never above 8. Different pH values with the current medium to cultivate *A. limacinum* are explored in this chapter.

Dissolved **Oxygen** (DO) is an important parameter in bioreactors and may be a limiting element, since oxygen gas is sparingly soluble in water. Oxygen effect on DHA accumulation in thraustochytrids has been widely studied. Literature works agree that oxygen has an important effect **specifically on DHA production**. As explained in Chapter 1 (section 1.3.3), many thraustochytrids have two FA biosynthetic

---

[77]Temperatures below room temperature (25 ºC).
[78] Temperatures above room temperature (25 ºC).

pathways. One of them, the standard pathway[79] is oxygen dependent, while the PKS-like synthase is not. Interestingly, the standard one produces different PUFA nonspecifically, but the PKS-like synthase has a great specificity for DPA and DHA production. Therefore, a reduction of available oxygen would cause the FA profile of thraustochytrids to shift towards DPA and DHA (Figure 2.7, Chapter 2).

It is worth mentioning three publications out of the great amount of oxygen investigations on thraustochytrids, because suggested good ideas about differential production between biomass and DHA. Chi *et al.* (2008) have explored a two stage cultivation of *A. limacinum*. The first stage consists of a simple fed-batch, while the second stage involves putting the biomass in a sealed flask to avoid any oxygen supply. They found 21% increase in DHA content. Qu *et al.* (2010) and Ren *et al.* (2010) have studied the effect of oxygen on *Aurantiochytrium* sp. They have investigated three different volumetric mass-transfer coefficient (K_La)[80] values, setting a high one during first part of fed-batch (batch) and a lower one for the second part of fed-batch. They report the same result, a low K_La enhances DHA production. k_La is influenced by many variables. Factors include everything from a bioreactor's size and design to the sparging of gas, mixing, cell line, media type, temperature, pH, salt content, and antifoaming agents [19].

Residence time is a key parameter for a repeated fed-batch and a CSTR. Thraustochytrids in a CSTR or repeated fed-batch, need a minimum residence time to accumulate the desired amount of DHA. Therefore, in a continuous production of DHA, residence time is a parameter to consider.

Carbon source starvation or **high C/N ratio** could be an important factor in the accumulation of lipid in thraustochytrids as well. Some experiments carried out in this thesis pointed to the fact that carbon source at lower concentrations could stimulate a nonspecific accumulation of lipids. This will be discussed in the following sections.

All the factors discussed above open a great opportunity to create a multi stage CSTR system to produce DHA continuously with high productivities.

4.1.4 *A. limacinum* kinetic characterization in CSTR

4.1.5 Multi-stage for DHA production

According to the factors highlighted and advantages of CSTR production, a multi-stage CSTR with shifting conditions seems a good idea. However, it has many logistic implications as well as some parameters which need to be modeled. In the first place, the best temperature for *A. limacinum* growth using the developed medium was examined. Furthermore, agitation and inlet airflow was modeled according to two responses: DHA production and DCW maximization. Thus, allowed setting the best conditions for each stage of the multi-stage CSTR. In order to explore different residence times, dilution rate (D) was varied in different experiments. Finally, some experiments have been addressed in order to elucidate if a low carbon concentration has any effect on *A. limacinum* DHA accumulation. These experiments would define the viability of a multi-stage CSTR with thraustochytrids.

---

[79] Common in eukaryotic microorganisms.
[80] k_La is the volumetric mass-transfer coefficient that describes the efficiency with which oxygen can be delivered to a bioreactor for a given set of operating conditions

4.2 Results and Discussion

With the aim of exploring the industrial potential of *A. limacinum* for the enhanced production of PUFA (mainly DHA), a personalized medium has been developed (Chapter 3). After the formulation of the medium, the project initiated the exploration of different cultivation strategies and key parameters, such as aeration, oxygen supply, temperature, pH and residence time. The first step was adjusting the best temperature and oxygen conditions. Temperature, which has been extensively studied, only required a few experiments to validate the values using the current medium. An optimization of agitation and oxygen is essential to control DHA stimulation. Optimization was achieved applying a special DoE (CCD, see Appendix A) using biomass and DHA production as responses.

The cultivation pH ranging from 5.8 to 8 was regulated by the phosphate buffer. Low pH values benefit the solubility and availability of some nutrients, for any microorganism cultivated. On the other hand, it has been reported in many literature works that some thraustochytrids are affected by pH values equal or above 8. Accordingly, *A. limacinum* has been cultivated within a pH range between 6.5 and 7.5. After the parametric adjustment and optimization different operating strategies have been investigated. The investigation started with **batch cultivations** using the new medium and a few runs of **fed-batch cultivation,** to investigate low carbon concentration effect. Then, a few **continuous reactors** and **multi-stage continuous reactors** with shifting conditions were investigated.

4.2.1 Optimum temperature for *A. limacinum* growth

In order to evaluate temperature influence on *A. limacinum,* a set of experiments using 250mL Erlenmeyer flask with 85 mL of medium was performed. Temperatures investigated ranged from 15 up to 33 °C, with six different values. Considering that low temperatures favour oxygen solubility, the cultures were agitated at 200 rpm, generating the same oxygen availability. Thus, culture differences would be only derivable from temperature differences.

142
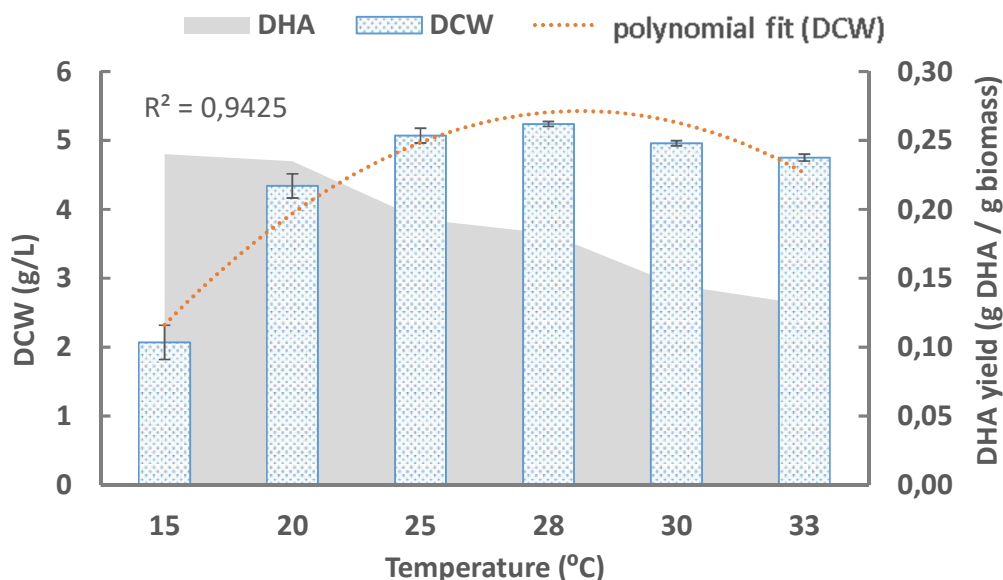
Figure 4.62 DHA and Biomass (DCW) profile of *A. limacinum* grown at different temperatures. Cultures performed in flask with 200 rpm stirring.

For the majority of microorganisms grown at suitable temperatures and without nutrient limitation, the maximal growth rate can be described solely as a function of temperature. Inspection of Figure 4.63¡**Error! No se encuentra el origen de la referencia.** indicates that temperatures between 20 and 28 °C represent thraustochytrids ideal growth range. Temperatures of 15°C caused an important decrease in the final biomass, whereas the cultures incubated at 30-33 °C showed better growth than 15ºC, but not the maximum. Therefore, 30 ° C would be the upper limit of *A. limacinum* using the current medium. Final biomass values from temperature experiments fit in a polynomial model, as indicated in Figure 4.62. The polynomial line suggests that maximum biomass values would be obtained in cultures incubated between 28 and 29 °C**.** This temperature boosts enzymatic activity of *A. limacinum* making them growth faster. Generally, an *A. limacinum* culture which has been incubated at 15 ºC it would reach the same final OD values as another cultivated at 20ºC. The difference is that at 15 ºC would need much more time, as understood from Figure 4.64. This data is in concordance with other temperature revisions in the
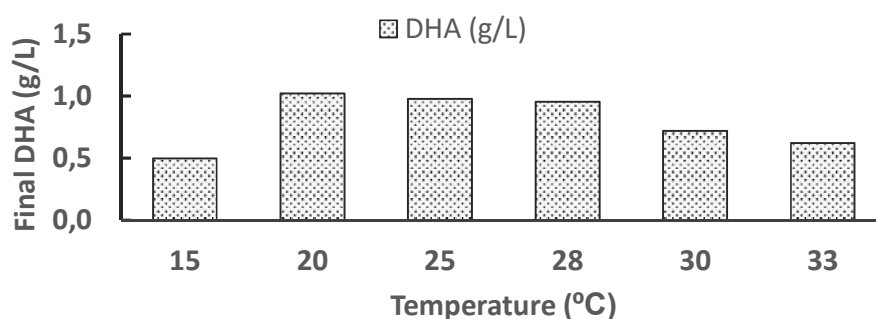
Figure 4.63 Final theoretical DHA concentration from *A. limacinum* cultures detailed in Figure 4.3.

literature [54,92,99,209].

Temperature has a different effect on PUFA accumulation, especially on DHA. As illustrated in Figure 4.62, DHA yield (g DHA / g biomass) showed a negative tendency when cultivation temperature was increased, suggesting that DHA production decreases more, above 33 °C. Thus, maximum DHA yield was obtained at 15 °C, and might be increased at even lower temperature. PUFA are generally liquid at room temperature due to their chemical characteristics (double bonds). When *A. limacinum* is in a low temperature environment, the extra DHA (and other PUFA) produced might be helping the membranes to fluidize as reported by Singh et al. (1996) [49]. Membranes are mainly composed of phospholids, which are diacylglycerols with a phosphate group (head) and two fatty acids (tails). At low temperature (low energy), a membrane with a lack of unsaturated FA would cause the membrane to enter into a crystallized state. Nevertheless, if the membrane is rich in unsaturated FA, double bonds would keep FA (from phospholipids) separated maintaining the fluidity even at low temperatures. Accordingly, producing PUFA could be an evolutionary and a natural response to colder environments, for thraustochytrids and many other organisms.

At this point it is clear that temperature affect very differently DHA and biomass production. As outlined in the introduction (section 4.1.3) a final cold shock does not increase DHA accumulation significantly [211], and a batch with a final switch to lower temperatures would not work. Therefore, a consensus value, an intermediate temperature assured both a good DHA and biomass production would be suitable for a batch operation. Figure 4.63 offers the computed value of the product between DHA yield and final

biomass concentration. These data indicate that the consensus temperature is between 20 and 25 ºC. Accordingly, 20 ºC was the selected temperature for every single tank culture strategy (batch, fed-batch and CSTR) performed in this thesis[81]. In the case of a multi-stage CSTR, different temperatures can be set. However, it needs further investigation because if part of DHA accumulation increase is due to membrane
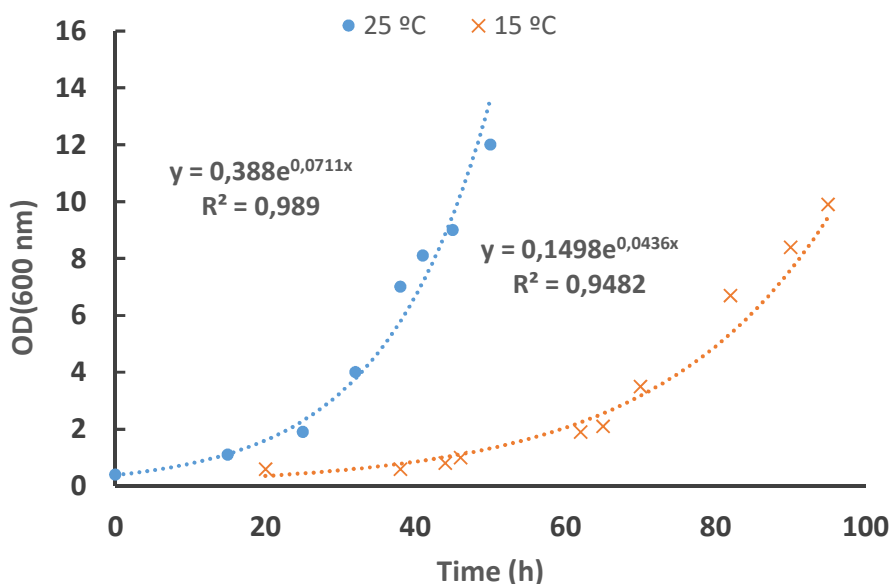
Figure 4.64 Difference in *A. limacinum* growth rate depending on incubation temperature. Data obtained from figure 4.3 experiments.

fluidization, those DHA moieties will not be extracted with the technique presented in Chapter 5.

Data presented in this section, only corresponds to the current medium developed in Chapter 3, any variations in the medium could vary the temperature output presented above.

4.2.2 Aeration and agitation modelling

Oxygen can become a limiting parameter in a badly agitated and/or aerated bioreactor. Oxygen is essential for many enzymatic reactions that power the cells, and a low availability could affect *A. limacinum* growth as well. Moreover, as discussed in section 4.1.3, dissolved oxygen could be the key in *thraustochytrids* to produce more DHA [112]. Because low oxygen concentrations enhance the specific accumulation of DHA, as reported in many works [16,184,189,200,212]. Therefore, *A. limacinum* cultivation brings another parametric contradiction which could be solved using a multi-stage CSTR (section 4.3.3). Factors which govern k_La, and consequently the amount of transferred oxygen in a CSTR were investigated. Such factors are agitation and aeration. Aeration provides sterile air rich in oxygen and agitation is responsible for breaking air bubbles down, increasing transfer area. Other factors can help dissolving the oxygen into the medium, but in a reactor are generally fixed, becoming just a constant.

Agitation and aeration parameters can be controlled in a bioreactor. Using a Central composite design (CCD) 5 levels per factor have been investigated. Agitation in a range between 298 and 1003 rpm, and aeration in a range between 0.1 and 3.5 L/min (0.06 and 2.05 in v/v·m [volume O_2 / volume of liquid ·

---

[81] With the exception of the section 4.3.2 experiment which has been carried out at 25 ºC.

min]). All these parameters were sequentially applied in a single tank CSTR (25°C and pH 7) with a feeding of optimized medium containing 20 g/L of purified crude glycerol (see glycerol purification procedure in Materials and Methods chapter). The reactor was stabilized 3 days after every applied change and measuring DHA yield and DCW. The whole CSTR system was maintained for six weeks without any contamination.

Applying a two factor CCD has permitted the construction of two (biomass and DHA yield) second-order models (containing 5 central points, 4 factorial points and 4 axial points, see Appendix A). The experimental matrix with codified levels is shown in Table 4.30. Every experimental point had two or three repetitions. Both models were then fitted according DHA and growth responses. DCW second-order model is shown in equation *4.9* and DHA second-order model is shown in equation *4.10*,

$$DCW \left(\frac{g\ biomass}{L}\right) = 17.16 \quad 0.24S + 1.01A \quad 1.47S2 \quad 0.48A2 + 0.62SA \qquad \text{Equation 4. 10}$$

$$DCW \left(\frac{g\ biomass}{L}\right) = 17.16 \quad 0.24S + 1.01A \quad 1.47S^2 \quad 0.48A^2 + 0.62SA \qquad \text{Equation 4. 10}$$

$$DHA \left(\frac{g\ DHA}{g\ biomass}\right) = 0.175 \quad 0.020S \quad 0.025A + 0.005S^2 + 0.002A^2 \quad 0.003SA \qquad \text{Equation 4. 11}$$

where **S** corresponds to agitation coded values and **A** to aeration coded values. Determination coefficient R^2 of both models was >0.9 suggesting that more than 90% of points can be explained with the models. The statistical significance of equations 4.9 and 4.10 were checked by F-test. ANOVA used to perform an analysis of both quadratic models is detailed in Table 4.31. It is evident from F-value[82] that both models are highly significant. Furthermore, a response surface has been plotted, illustrated in Figure 4.65. Three-dimensional plots help to understand how aeration and agitation affect growth and biomass production.

Table 4.30 Experimental matrix of second order CCD. Agitation codification (from − 1.42 to 1.42) = 298, 400, 650, 900 and 1003 rpm. Aeration codification (from − 1.42 to 1.42) = 0.1, 0.55, 1.8, 3 and 3.5.

Experiment	Agitation (RPM)	Aeration (L/min)
1	-1	-1
2	1	-1
3	-1	1
4	1	1
5	-1.4142	0
6	1.4142	0
7	0	-1.4142
8	0	1.4142
9	0	0
10	0	0
11	0	0
12	0	0
13	0	0

145

[82] F values above 2 are considered significant
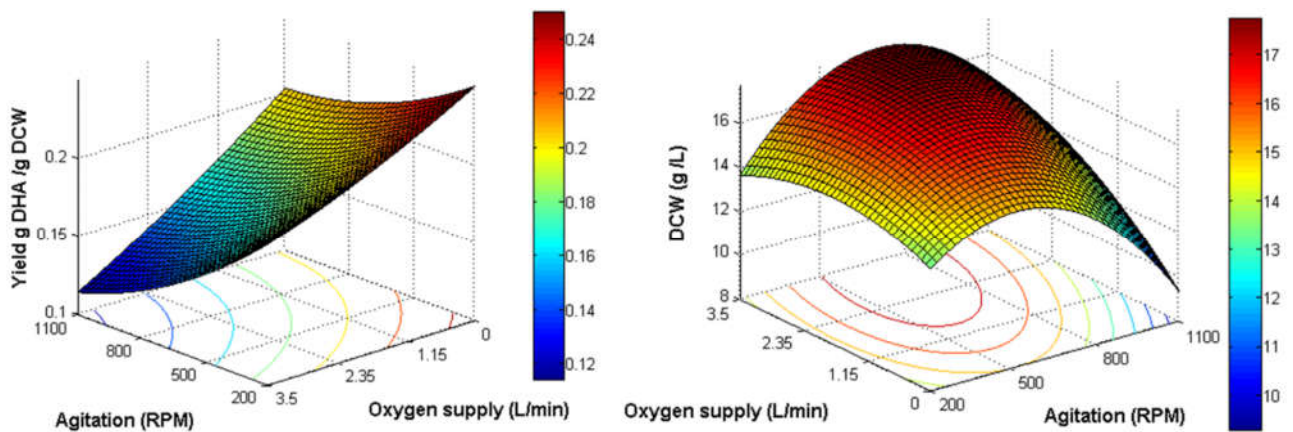
Figure 4.65 Response surface plot of DCW model (right) and DHA model (left).

The analysis of the plots allows the identification of the optimal values. Setting agitation at **680 rpm** and an airflow **of 3 L/m** (1.76 vvm[83]) would ensure a **maximum production of biomass**. These results are in concordance with Song *et al.* (2007) [191] where they have reported a similar behaviour of *A. limacinum* OUC88. However, the exact values are not comparable because Song *et al.* worked with very low agitation values. Optimal agitation and aeration found in this dissertation, would be slightly high for an industrial implementation, especially for batch cultures. Industrial scale batch reactors are generally bigger and require a lot of energy for the stirring system. Agitation energy requirements increase exponentially with the scale. Inspection of the DCW response surface in Figure 4.65 indicates that the agitation could be reduced 400 – 500 rpm without a great sacrifice in biomass productivity. On the other hand, an airflow of 3 L/min might be critical at large scale. As happens with agitation, the value can be reduced without a significant impact on biomass production, down to 1.5-2 L/min.

Table 4.31 ANOVA for the second-order models.

Source	Degrees of freedom	Sum of squares	Mean square	F	
Quadratic model	5	51.3	10.3	27.5	**DCW**
Lack of fit (residual)	20	7.5	0.4		
Total	25	58.7			
Source	Degrees of freedom	Sum of squares	Mean square	F	
Quadratic model	5	0.01688	0.00338	29.8	**DHA**
Lack of fit (residual)	20	0.00227	0.00011		
Total	25	0.01915			

Optimal parameters for DHA yield response are different. An agitation of **200 rpm** and an airflow of **0.1 L/min** would **maximize the yield of DHA**. These are the lowest levels considered in the response surface,

146

[83] The unit 'vvm' is used for bioreactor culture. The first 'v' stands for volume of air (e.g. liter) ; the second 'v' stands for per unit of medium (e.g. liter); 'm' stands for per unit of time (e.g. minute). For example, 2 vvm (l/l/m) means in 1 minute time there is 2 liter of air passing through 1 liter of medium.

suggesting that even lower values could enhance a greater DHA accumulation. According to the model the yield would be higher than 0.24 g DHA / g biomass, which is the maximum yield obtained in a reactor (in this study). Therefore, those values of DHA are in concordance with the data presented in this thesis, where a yield of more than 0.24 g DHA / g biomass is commonly found in flask cultures where the oxygen transfer is low. From an industrial standpoint, an agitation of 200 rpm and an aeration of 0.1 L/min conditions would be easy and cheap to reproduce.
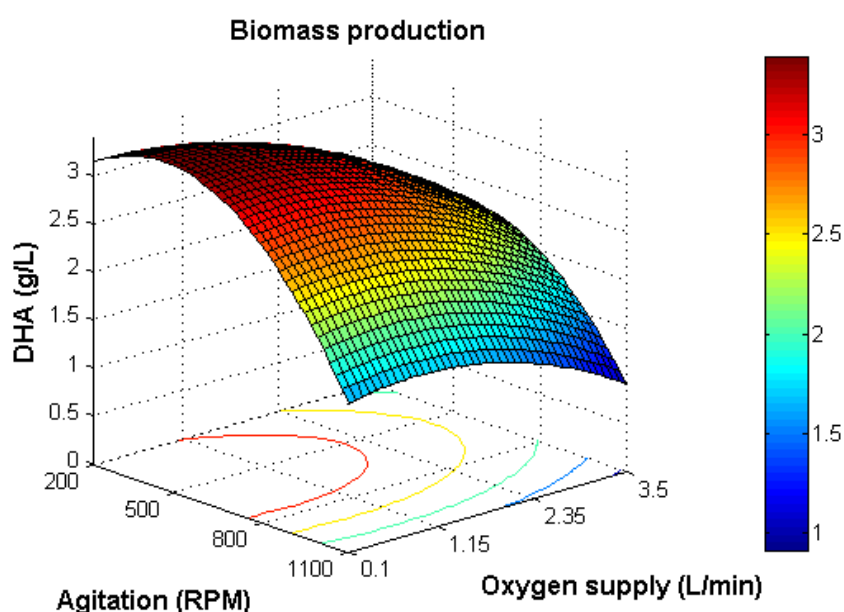
Figure 4.66 Response surface of the product of both models. F value of the model = 5.7.

Using a multi-stage CSTR optimized aeration and agitation conditions have been investigated in section 4.2.3.4, including different temperatures per tank. Furthermore, in order to find a consensus optimal values for future single tank experiments performed in upcoming sections, a response surface using the product of both models was calculated. The product plot is illustrated in Figure 4.66. Observing the mesh, it is clear that aeration has a key role on DHA final concentration, while the effect of the agitation is lower. Despite the fitting of this third model is less accurate than the previous, 500 rpm and 1L/min were selected as intermediate values for a better production of DHA.

4.2.3   Investigating culture strategies

4.2.3.1   Batch bioreactors (carbon source concentration)

Bioreactors operating in batch mode are commonly used, mainly because it is a flexible and simple way to produce many bioproducts. Thraustochytrids cultivation is not different, and is commonly carried out in batch reactors. Furthermore, in this thesis the main goal was to find the most productive way to produce DHA through *A. limacinum cultivation*. As detailed in the introduction, many literature works have already reported batch bioreactor cultivations [9,130,200–202,213]. Furthermore, Chapter 3 undoubtedly showed that *A. limacinum* grow well in batch reactors. In this section, batch reactors are used to explore the effects and viability of using higher carbon source concentration in *A. limacinum*

cultures growing in the optimized medium from Chapter 3. Accordingly, a set of bioreactors (six different initial carbon source concentrations) were performed with 4 replicates per experiment. Concentrations investigated were 80, 60, 40, 30, 20 and 10 g/L.
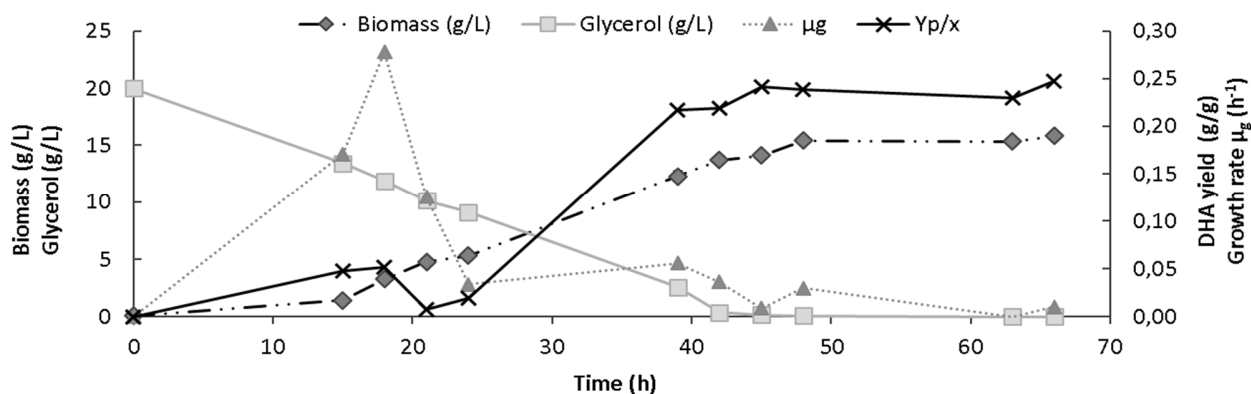
Figure 4.67 Monitoring profile from a 20 g/L (S$_0$) batch bioreactor of A. limacinum. 20 º C; pH 6.5-7. Agitation of 500 rpm and 1L/min of air supply.

Yield and productivity calculations were done at the end of exponential time. Figure 4.67 shows the output of a 20 g/L batch bioreactor which yielded a final biomass of more than 16 g/L and a DHA yield of 0.24 g/g, while all the substrate has been consumed. Calculated growth rate shows the typical two stage life cycle of a batch reactor with thraustochytrids. There was a first drastic increase in growth rate during zoospore release followed by a steady linear growth during vegetative stage. During a batch, other life stages are manifested (see more information in section 2.3.3) but zoospores and vegetative stage are the dominant ones (> 80 % of cell stage types). Every reactor was carried out with the same conditions except the carbon source initial concentration and the corresponding nitrogen source.

Table 4.32 gather the results of the set of batch bioreactors from S$_0$ 10 to 80 g/L. Mean biomass value follows a positive tendency while increasing glycerol concentration. By growing A. limacinum at 20 ºC or lower, enhanced DHA accumulation as observed in every reactor listed in Table 4.32. Obviously, a culture needs more time to reach higher biomass concentrations as well as to accumulate enough DHA. Cultivation time should be proportional to the amount of carbon source included at the beginning of the culture. There is a reduction in the substrate / biomass yield from 60 g/L (S$_0$).

This growth efficiency reduction might be caused by the increased viscosity. Increased viscosity reduces oxygen transference coefficient and hinders nutrient diffusion. Pyle et al. (2008) [131] already reported an inhibition behavior when the concentration of glycerol reached 100 g/L. Crude glycerol unknown contaminants might be another cause of growth inhibition. For example, residual soap and methanol re-concentrated as S$_0$ increases could be affecting A. limacinum negatively. On the other hand, it might be a matter of nutrient limitation rather than carbon source. For instance, a salt component of the medium or a trace metal. Contrarily, when the concentration of initial carbon source was low, substrate / biomass yields are very high (e.g. S$_0$= 10 g/L gives Y$_{x/s}$ =0.9). This might be caused by the abundance of some elements in the organic nitrogen sources that are acting as carbon source as well (e.g. amino acids which have not been used as building blocks for peptides). Plotting all the batch reactors with different S$_0$ versus final biomass gives the "real" carbon source yield. The slope generated is equivalent to the amount of

glycerol dedicated to produce biomass. The slope does not include other carbon sources which could be present in the medium. Therefore, it can be considered that per each gram of glycerol 0.73 g of biomass were generated.

Table 4.32 Results of A. limacinum batch cultures using different concentrations of carbon source. Every reactor was carried out at the following conditions: 20 ºC; pH 6.5-7; 500 rpm; 1 L air /min. * Mean biomass value. ** Volumetric productivity of DHA.

S0 (g/L)	80	60	40	30	20	10
Mean X (g/L) *	51.75	40.00	28.95	21.30	17.07	9.03
StD	1.26	2.12	4.95	0.92	0.85	0.28
r DHA (g/L·h) **	64.69	76.92	76.18	73.45	74.23	60.17
Time (h)	160	104	76	58	46	30
$Y_{x/s}$ (g/g)	0.65	0.67	0.72	0.71	0.85	0.90
$Y_{p/x}$ (g/g)	0.23	0.24	0.24	0.23	0.23	0.24

The cultures with a higher DHA productivity (r_{DHA}) are those with 40 and 60 g/L as S_0, with a maximum peak of 76.9 mg DHA /L·h. Chi *et al.* (2009) have reported a productivity of 23.3 mg DHA /L·h using glycerol as carbon source, whereas the maximum yield reported with glucose has been 124 mg DHA /L·h in the work of Yaguchi *et al.* (1997) [187]. There is another publication reporting batch bioreactor cultivating thraustochytrids [9] with similar productivities but it was a two stage batch[84]. Therefore, in a single and simple batch medium and parameters investigated in this study shows high productivities. Different
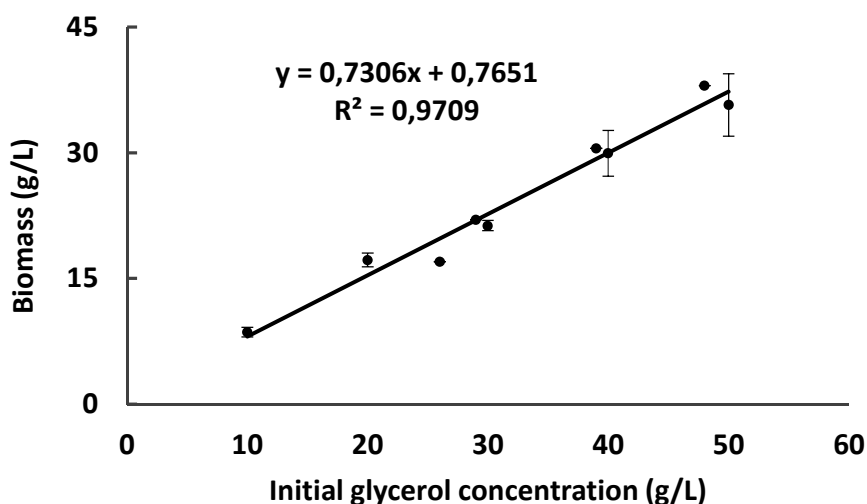
Figure 4.68 Linear regression between initial carbon source concentration and the final biomass obtained. Points collected from different bioreactor experiments, using the following conditions: 20 ºC; pH 6.5-7; 500 rpm; 1 L air /min.

---

[84] Two batch phases with switching conditions and medium.

culture strategies are investigated in the following sections, and will be compared at the end of this chapter to elucidate which one is the most prolific way to synthesise DHA.

Every factor discussed below has an effect on the final DHA productivity (r_{DHA}) as can be seen in Table 4.32.

4.2.3.2 Fed-batch bioreactors

Fed-batch bioreactors were planned in order to investigate if a sustained low amount of carbon source triggers unspecific triglycerides accumulation. When the carbon source is scarcer, thraustochytrids tend to accumulate a major amount of triglycerides, as happens at the end of every batch. Specific experiments were designed to investigate this phenomenon. These experiments indicated that adding a low amount of carbon source in a culture with depleted substrate increased the lipid and subsequently the DHA accumulation. An example of these experiments is shown in **Box 4.8**, where it can be observed that temperature and low carbon concentration have an effect on DHA accumulation. However, it is clear that a low amount of carbon source concentration causes a major increase in DHA final yield (**Box 4.8**).

Box 4.8. Carbon source experiment
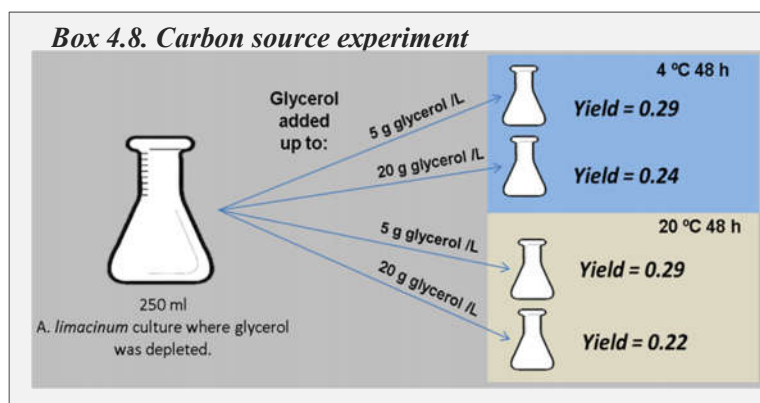
Two replicates of a fed-batch operation were performed in order to evaluate if this phenomenon could increase the final yield of DHA. Fed-batch was initiated after the complete depletion of carbon source in the initial batch[85], as can be seen in Figure 4.69. The feeding consisted of an optimized medium with 27 g/L of purified crude glycerol at an average flow of 0.032 L/h. The feeding was maintained until a final volume of 1.95 and the culture was carried out at 20 ºC. This flow guaranteed a carbon source concentration between 0 and 1 g/L (Figure 4.69). After fed-batch started, biomass remained constant (20-21 g/L) while the DHA yield increased progressively until reaching 0.23-0.24 g DHA / g biomass. The fed-batch final yield was not as high as expected from the experiments shown in **Box 4.8**. It seems that in flask cultures the accumulation of DHA was always higher, this may be caused by a low availability of oxygen. Considering only the fed-batch culture time, an r_{DHA} of 105 mg DHA / L·h was obtained.

---

[85] Considering that thraustochytrids keep glycerol in their cytoplasm until it is processed, when the concentration of substrate is 0, they still have substrate and the metabolism is not collapsed.

Fed-batch was seeking to reproduce an extra accumulation of DHA as high as in flask cultures. However, fed-batch showed similar results to batch bioreactors. Considering the conditions established in the fed-batch experiment, DHA stimulation might be only triggered by temperature and oxygen limitation. It is a common issue in literature, bioreactor cultures reported lower yields than flask cultures where oxygen is a limiting element [186,197,214]. Oxygen limitation implications were investigated in CSTR experiments. Furthermore, in a hypothetical situation of performing an 80 g/L carbon source feeding fed-batch r_{DHA} values would be between 81 mg/L· h and 72 mg/L· h. Such productivities are approximately the same as 80 g/L (S_0) batch bioreactors.
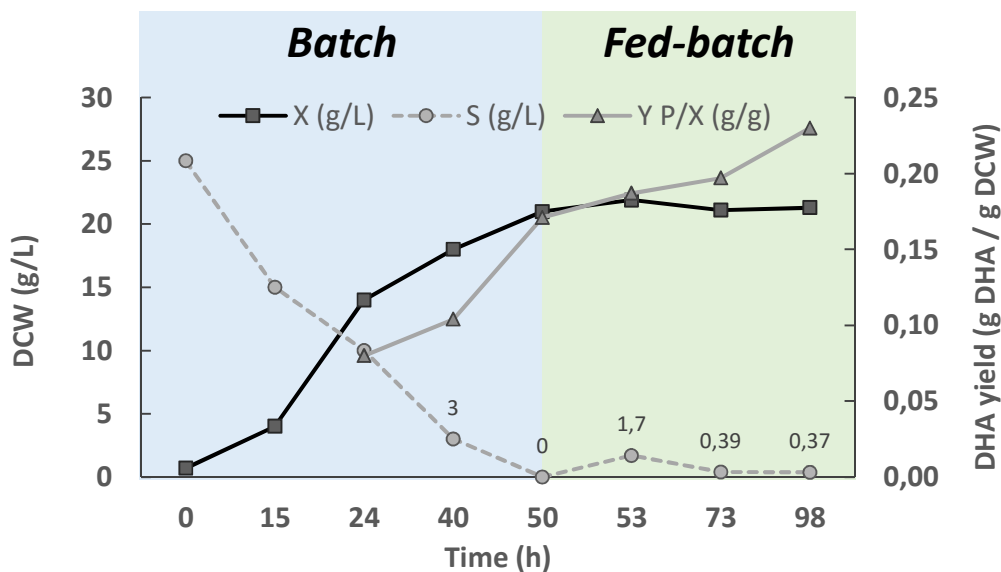
Figure 4.69 Fed-batch maintaining a very low substrate concentration to increase the yield. Final volume = 1.95 L; temperature at 20 ºC; 500 rpm and 1 L/min. Feeding concentration

4.2.3.3 CSTR reactors

The objective of this section is to show the investigation on cell growth kinetics and *A. limacinum SR21* DHA production through a CSTR culture. The present work seeks the kinetic characterization of *A. limacinum* growing with the medium developed. This way can be compared with those values obtained from batch reactors. A chemostat[86] is a powerful tool to study and calculate kinetic parameters of a microorganism by investigating the effects of environmental changes during the culture. It is generally more precise than batch reactors. It is worth mentioning that using a chemostat to investigate *A. limacinum* will only reveal vegetative cells kinetic parameters. As explained in Chapter 2, *A. limacinum* do not manifest zoospore life cycle during a continuous culture.

Chemostat as a tool to determine *A. limacinum* kinetics.

151

---

[86] It is a CSTR in a steady state situation.

Two chemostat reactors were purposed in order to investigate *A. limacinum* kinetics. The first started from a batch reactor of 20 g/L (S_0) and the second from a 25 g/L (S_0) one, with a feeding of 25 g/L and 27 g/L of carbon source (including the developed medium), respectively. Kinetic parameters were calculated as explained in materials and methods section, by applying different D[87] on the CSTR. The investigation started from the lowest D value. With a low dilution rate, the culture reached the highest biomass concentration of the experiment (as expected). Then, D was slightly increased and left for 3 days allowing the culture to stabilize. D was then increased until it reached a low biomass concentration. The results of one of those CSTR bioreactors are plotted in Figure 4.70.
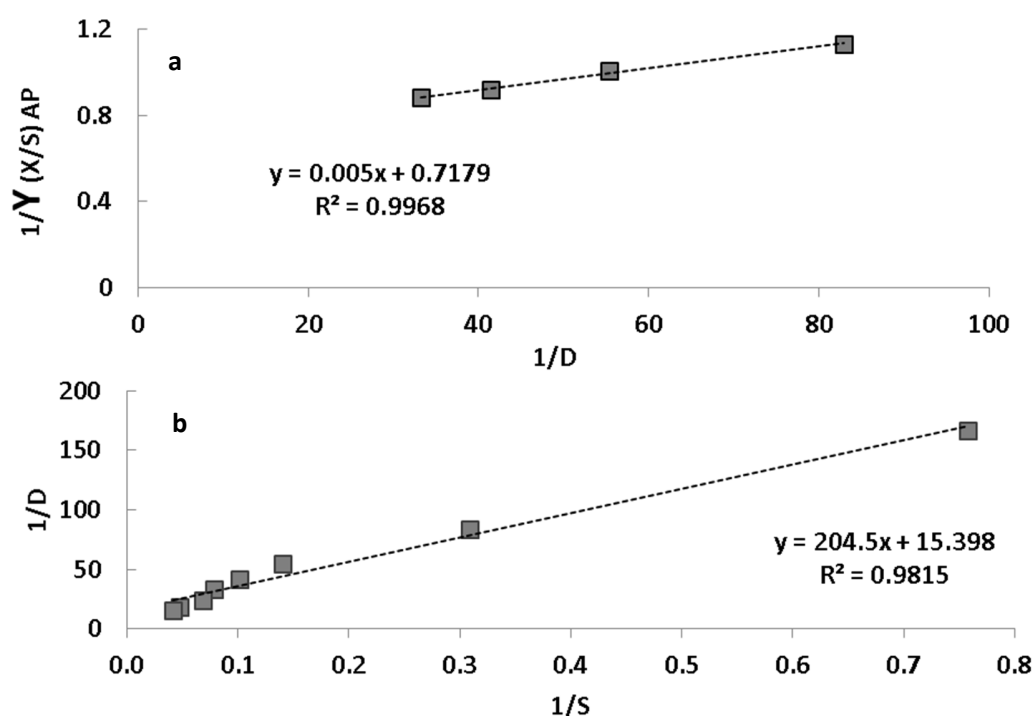
Figure 4.70 Graphical calculation from A. limacinum kinetic parameters growing in a continuous mode and glycerol as carbon source. CSTR with a feeding of optimized medium containing 27 g/L of purified glycerol. Plot a correlates specific growth rate and dilution rate divided by one. Plot b correlates dilution rate and

Saturation constant (k_s), maximum growth rate (μ_m), cell mass loss rate (k_d) and maintenance coefficient (m_s) were calculated analysing data obtained from both plots (the same procedure for both bioreactors). Using these type of plots, the kinetic parameters were calculated and the average result is shown in Table 4.33. Ks defines the affinity of the microorganism for a specific carbon source. Ks value found of *A. limacinum* for crude glycerol was 13.6 g/L. This value is

Table 4.33 Mean values from calculated parameters as indicated.

Ks (g S / L)	**13.6 ± 0.45**
μmax (h^{-1})	**0.07 ± 0.006**
ms (g S / g X ·h)	**0.0045 ± 0.001**
kd (h^{-1})	**0.0058 ± 0.002**

higher than those obtained in batch cultures (8.1 g/L). The difference is significant, but it can be attributed to the alteration of *A. limacinum* life cycle during a continuous reactor. Life cycle divergence impairs growth rates as well, thus giving lower μ_m for continuous reactors when compared with batch reactors. *A.*

[87] Reminder: D stand for dilution rate (h-1)

limacinum growing in a vegetative stage gave a μ_m of 0.07 h^{-1} whereas batch reactors showed μ_m values of 0.20 h^{-1}. Again, this is attributable to the lack of zoospores in a continuous reactor.

Finally, m_s and k_d could be calculated using the plot indicated in Figure 4.70a (see materials and methods) which represent the amount of substrate used for biomass maintenance per hour and the rate of cell mass loss. As m_s and k_d showed low values indicates that the microorganism was well adapted to parameters and medium conditions. Moreover, a prediction of biomass and substrate concentration as well as a biomass volumetric productivity could be predicted for every D applied, using the four determined parameters (plotted in Figure 4.71). D value ensuring the maximal productivity (while safely avoiding a wash ¡out phenomenon) is 0.04 h^{-1}. Above this value the cells would come out from the bioreactor too fast, whereas at much lower D would result in a productivity loss. Discovered kinetic parameters, the prediction shown and some logistical constraints defined the high time consuming investigation about CSTR cultivation as well as its variations (multi-stage CSTR).
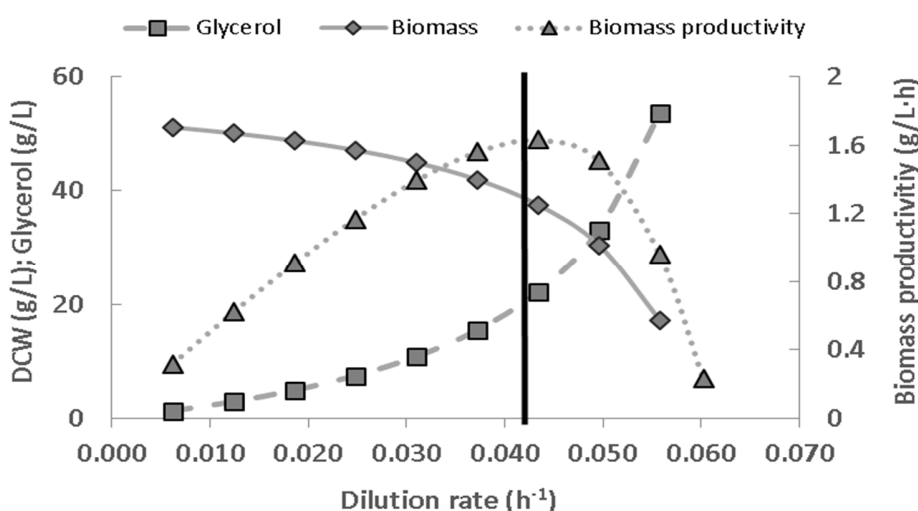
Figure 4.71 Prediction of biomass, substrate and volumetric productivity for different dilution rates (D) in a CSTR bioreactor with A. limacinum.

Single tank CSTR runs

Four single tank CSTR were performed using the developed medium. The substrate concentration in the feeding solution (S_f) was kept at 60 g/L and 80 g/L. The results are summarized in Table 4.34.

Ethier *et al.* (2010) [37] and Ganuza *et al.* (2007) [30] already investigated single tank CSTR with *S. limacinum SR21* and *Schizochytrium sp. G13/S2*, respectively. Ethier *et al.* used a standard medium reported by Chi *et al.* (2007) [93], and feeding glycerol concentrations between 60-90 g/L of crude glycerol to perform a CSTR bioreactor with *A. limacinum*. In their work a yield of 0.3-0.4 g biomass/g substrate was reported which is lower than the 0.6 g/g yield found in the present thesis for single tank CSTR (results shown in Table 4.34). A 10 mL centrifuged sample of the culture leaves an important pellet as can be seen in Figure 4.72. These results add evidences of the great growth yield obtained with the current medium and parameters.

In this study it has been demonstrated that the organic nitrogen source has to be increased parallel to carbon source concentration (extensively explained in Chapter 3). Therefore, the difference on medium composition and optimized oxygen supply (aeration and agitation) might be impairing glycerol uptake and its transformation to biomass and DHA, in Either *et al.* work. For the same reason, *A. limacinum* showed a lower affinity for crude glycerol as evident by K_s values reported in Ethier *et al.* [52]*.* They have reported a Ks of 45 g/L which is larger than the value of 13.6 ± 0.45 g/L reported in Table 4.33 of this study. Finally, μ_m value in Ethier *et al.* [52] was 0.029 h^{-1} whereas the experiments performed in this study gave a μ_m of 0.07 ± 0.006 h^{-1}. The divergence appearing in both cases is probably caused by a difference in growth parameters and especially medium composition.

Presumably, Either *et al.* [52]work was oriented to kinetic parameters investigation instead of seeking a maximum productivity. Contrary to Ganuza *et al.* (2007) [213], who investigated the possibility of producing lipids using *Schizochytrium* sp. in a continuous bioreactor. Ganuza *et al.* [213] have obtained an r_{DHA} value of 40 mg/L·h using a feeding of 40 g glucose /L. Therefore, they would be able to obtain a productivity of **80 mg/L·h** approximately, in hypothetical situation using 80 g/L of glucose. This value is similar to those obtained in this study, where a maximum r_{DHA} of 135 mg DHA /L·h has been obtained.

Carbon source feeding concentration is important to reach high biomass densities (Figure 4.72) resulting in a higher amount of DHA; obvious when observing r_{DHA} values from Table 4.34 These values are closer to Rosa *et al.* (2010) [9] "double" batch r_{DHA} of 154 mg DHA /L·h. Accordingly, multi-stage CSTR purposed in the following section would be able to reach these productivities.

OD = 25   OD = 60

Figure 4.72 Figure of 10 mL centrifuged samples of high OD A. limacinum cultures.

154

In the last single CSTR culture the residence time (τ) was varied by increasing the final volume. However, residence time has not altered the DHA accumulation as can be seen in Table 4.34. Higher DHA yield was expected from the CSTR bioreactor with higher residence time. Using optimized parameters from section 4.2.2 might be masking residence time effects. Because the optimized parameters for dissolved O_2 have already shown near maximum DHA yields. Nevertheless, residence time should be important in the following section were multi-stage CSTR is investigated. Initial tanks would enhance biomass production, and the cells would need time to accumulate DHA in the subsequent tanks.

τ (h^{-1})	**D** (h^{-1})	**S_f** (g/L)	**X** (g/L)	**$Y_{p/s}$** (g/g)	**$Y_{x/s}$** (g/g)	**r_{DHA}** (mg/L·h)
64	0.0151	60	34.7	0.23	0.58	120.4
64	0.0151	60	33.5	0.18	0.56	91.0
64	0.0151	80	47.7	0.19	0.6	136.7
197	0.0151	80	46.8	0.19	0.59	134.1

Table 4.34 Single tank CSTR results. Cultivation maintained at 20 ºC and pH between 6.5 and 7. 500 rpm and 1L/h. Feeding flow rate of 0.00264 L/h. Residence time τ was varied by increasing the final volume. S_f stands for substrate concentration in the feeding solution. $Y_{p/s}$ stands for DHA yield. In this case the first and the last tank. The cut line separate 60 g/L bioreactors from 80 g/L ones.

Thinking about a multi-stage CSTR, a first reactor being able to grow continuously *A. limacinum* zoospores would enhance the final productivity of the total process. Leaving the following steps to let vegetative cells develop and accumulate DHA. This possibility has been investigated during this study without any clear conclusion (data not shown). Therefore, it would require future investigations.

4.2.3.4 Multi-stage CSTR

Multi-stage CSTR system producing DHA through a thraustochytrids was purposed in this study considering the results described in previous sections. The first bioreactor/stage sets the best conditions for *A. limacinum* growth, as optimized in section 4.2.1 and 4.2.2. Therefore, the first tank was maintained at 28ºC, 681 rpm and 3 L/h of aeration. The outlet flow from the first bioreactor fed the second tank, where growth was low because it was maintained between 15-20 ºC. Cold conditions trigger a higher lipid accumulation, including DHA. Oxygen supply was limited by a low agitation (200 rpm) and aeration (0.1 L/h) in the second stage. The parameters in the second stage are the basic to keep the cells alive while producing DHA specifically, as explained in section 4.2.2. Therefore, the steps following (2 or 3) the first tank are considered as polishing steps.

In order to guarantee that *A. limacinum* had enough time to accumulate DHA, the residence time was increased. To do so, two or more tanks (coupled with the first tank; biomass producing one) comprised

Figure 4.73 Illustration of a triple tank system used in this study. Number 1 shows the first bioreactor with a volume of 1.7 L, and number 2 and 3 indicate the polishing bioreactors to produce DHA with a total volume of 9 L.

Table 4.35 Environmental parameters used during CSTR investigations.

CSTR systems	Tank	Temp. (C⁰)	Agitation (rpm)	Aeration (L/h)	pH
Single tank	1	20	500	1	7
Two-stage	1	28	681	3	6.5
	2	20	200	0.1	7
Three-stage	1	28	681	3	6.5
	2	20	375	0.4	7
	3	15	200	0.1	7

more than the **85% of the system total volume**. This way, the same flow for the whole system, assured a lower D in the biggest tanks which increased the residence time as well. Furthermore, the possibility of using more than two tanks allowed a progressive adaptation of the microorganism from the first tank conditions to the final polishing ones. Likewise, this system configuration allowed a higher final volume and resulted in a higher residence time. Figure 4.73 shows a picture of a three-stage system used in this thesis. Below the bioreactor tagged with a number 3, there was always a refrigerated collector to accumulate the DHA containing biomass. This collector was maintained between 15 and 20 ºC in sterile conditions. In a real industrial process, a downstream processing system could be connected to the system avoiding storage steps.

Due to time limitations, only five CSTR runs were connected to at least one more tank to enhance DHA production. The parameters of every reactor investigated in this section are listed in Table 4.35. Results of these five CSTR are listed in Table 4.36. The table includes flow rate values, because it became important for the final productivity. Interestingly, run 1 and 3 showed a lower r_{DHA} than the run 2 with 119.1 mg/L·h, which had the highest feeding flow rate. Therefore, this result indicates that the higher feeding resulted in an increased r_{DHA}. In any of the two-stage CSTR the polishing phase produced a good amount of DHA, giving a yield of 0.2 g/g. The yield is not as high as in batch bioreactors but the sustained production generates a greater final r_{DHA}. Accordingly, for three-stage CSTRs (run 4 and 5) the highest flowrate from previous experiments (run 1, 2 and 3) was selected, 0.0264 L/h. Moreover, the total system volume was increased by adding a third bioreactor to the system, thus increasing the residence time up to almost 400 hours. With an increased residence time a slight increase of r_{DHA} was expected. However, results listed in Table 4.36 show that DHA yields were mainly the same maintaining an average value of 0.2 g/g. On the other hand, r_{DHA} were much higher than expected. The maximum productivity from run 5 multi-stage CSTR was 152.6 mg DHA /L·h. This value is much larger than those previously reported by single CSTR reactors reported in literature.

Table 4.36 Results from two-stage (1, 2 and 3) and three-stage (4 and 5) CSTR bioreactors of A. limacinum. The cut line separate two-stage results from three-stage results. Residence time τ correspond to the total residence time of the system. S_f stands for substrate concentration in the feeding solution. $Y_{p/s}$ stands for DHA yield. In this case the first and the last tank.

Run	F (L/h)	$τ$ (h^{-1})	D (h^{-1})	S_f (g/L)	X (g/L)	$Y_{p/s}$ (g/g)	$Y_{x/s}$ (g/g)	r_{DHA} (mg/L·h)
1	0.0158	392	0.0090	60	37.5	0.2	0.63	71.2
2	0.0264	235	0.0151	60	38.3	0.2	0.64	119.1
3	0.0211	294	0.0121	80	50.8	0.2	0.64	82.2
4	0.0264	398	0.0151	80	45.0	0.19	0.56	123.3
5	0.0264	398	0.0151	80	53.0	0.2	0.66	152.6

Remarkably, single tank CSTR reported in this dissertation obtained high productivities by applying a flow rate of 0.0264 L/h as well. According to these results and the prediction made in section 4.2.3.3 indicates that, increasing the flowrate would increase final productivities Moreover, increased requirement of manipulation (caused by an often feeding bottle replacement) would increase the risk of contamination.

During three-stage CSTR experiments, the biomass in polishing steps (stage 2 and 3) turned orange-red colour when it normally has a brown-yellow colour as shown in Figure 4.74. Biomass investigation revealed two main discoveries. Firstly, the orange colour was produced by astaxanthin and secondly, *A. limacinum* produced two carboxylic acids, namely oxalic and pyruvic acid. Both productions are explained in Chapter 2 (section 2.3.4) where *A. limacinum* characterization is described. Astaxanthin production was investigated in the MSc Thesis of Nuria Abajo.

Figure 4.74 Image of lyophilized biomass coming from three different tanks, from a three-stage CSTR. From left to right, first, second and third bioreactor biomass, respectively. The last step show biomass with a strong orange colour.

As already outlined in the introduction, *A. limacinum* could not compete with *H. pluvialis.* Despite being a photosynthetic organism it is easily grown at very large scales [215–217] as well as yielding very high astaxanthin productivities. Nevertheless, it can be used to protect PUFA produced by *A. limacinum* because astaxanthin is a powerful antioxidant [218]. For example, it could help avoid DHA oxidation during downstream processing steps. Furthermore, microalgae product could be offered as a new nutraceutical product containing astaxanthin and omega-3 PUFA.

4.2.4   Comparing culture strategies for the highest DHA productivity

Volumetric productivity indicates the amount of product generated per hour allowing the comparison between different scale reactors. Table 4.37 displays every publication reporting different cultures strategies for thraustochytrids, aiming a high volumetric productivity of DHA. Thaustochytrids have been studied for more than 50 years. However, in 1996 [214]a prolific DHA producing strain was discovered, opening a new opportunity for industrial omega-3 synthesis. It is evident that *Aurantiochytrium* strains are the most prolific ones. This is evident by observing, in Table 4.36, the difference between bioreactor productivity reported by Bajpai and Ward in 1991 and other cultures. The maximum r_{DHA} obtained with *A. limacinum* SR21 operating in batch has been reported in this dissertation showing a value of 76.9 mg DHA / L · h. This is nearly twofold higher than those reported by Pyle *et al.* in 2008. The difference in productivity might be indicating that the medium developed in this thesis plays an important role in reaching high r_{DHA} with the strain SR21. Nevertheless, Burja *et al*. (2006) reported an r_{DHA} from a batch bioreactor growing *Thraustochytrium* sp. ONC-T18 (which is a mutant of an isolated thraustochytrid) of 88.5 mg DHA /L·h.

Table 4.37 List of productivities from every work reporting thraustochytrids cultivation to produce DHA. Culture strategy nomenclature: Batch (B), double batch (dB), fed-batch (F), repeated fed-batch,(RF), CSTR (C) and multi-stage CSTR (mC).

Culture strategy	Reference	Year	r_{DHA} (mg/L·h)	Strain
B	Bajpai and Ward [51]	1991	7.2	*T. aureum* ATCC 34304
B	Pooksawang et al. [130]	2009	25.8	*A. limacinum* SR21
C	Ethier et al. [52]	2010	27.8	*A. limacinum* SR21
F	Ryu et al. [95]	2013	32.3	*Aurantiochytrium* sp. KRS101
B	Yamasaki et al. [219]	2006	35.4	*Schizochytrium* sp. KH105
B	Pyle et al. [131]	2008	38.5	*A. limacinum* SR21
B	**This study**	2015	76.9	*A. limacinum* SR21
C	Ganuza et al. [213]	2007	79.7	*Schizochytrium* sp. G13/2S
B	Nagano et al. [197]	2009	83.9	*A. limacinum* mh0186
B	Burja et al. [14]	2006	88.5	*Thraustochytrium* sp. ONC-T18
F	Jakobsen et al. [16]	2008	92.9	Aurantiochytrium sp. T66
F	**This study**	2015	105	*A. limacinum* SR21
F	Qu et al. [184]	2010	111.0	*Schizochytrium* sp. HX-308
RF	Huang et al. [189]	2012	122.6	*A. limacinum* SR21
dB	Rosa et al. [9]	2010	136.1	*A. limacinum* SR21
C	**This study**	2015	136.7	*A. limacinum* SR21
RF	Qu et al. [202]	2013	138.8	*Schizochytrium sp.*
F	Kim et al. [192]	2013	140.3	*Aurantiochytrium* sp. KRS102
F	Ren et al. [203]	2010	145.8	*Schizochytrium* sp.
B	Hong et al. [220]	2013	150	*Aurantiochytrium* sp. KRS101
mC	**This study**	2015	152.6	*A. limacinum* SR21
RF	Chang et al. [208]	2013	204.3	*Aurantiochytrium* sp. TC20

Fed-batch bioreactors to produce DHA through thraustochytrids increased its popularity in the last 5 years. Many different groups in the world started investigating these culture strategies to increase batch r_{DHA} with positive results. As can be seen in Table 4.37 fed-batch strategies offered higher r_{DHA}, even in the one reported in this study which showed 105 mg DHA /L·h. Interestingly, there are no other works reporting fed-batch cultures with *A. limacinum* SR21 but literature is full of different trhaustochytrid fed-batch works. Ren *et al.* (2010) revealed the highest r_{DHA} (145.8 mg DHA / L· h) growing a *Schizochytrium* sp. strain operating in fed-batch. Generally, repeated fed-batch (explained in 4.1.1.3) showed greater r_{DHA} than regular fed-batch in literature. Remarkably, this type of operation generated the highest r_{DHA} reported in Chang *et al.* (2013) as displayed in Table 4.37. They have obtained an r_{DHA} of 204.3 mg DHA / L ·h cultivating a new strain, *Aurantiochytrium* sp. TC20. In their work a surprisingly fast growth was reported. This might be because in repeated fed-batch reactors, the productivity is calculated based on every cycle. In every cycle, the final biomass is considered to calculate the productivity together with the short time (that a cycle takes). However, not all the biomass is harvested because it is used as the inoculum

of the next cycle. In other words, productivity is calculated considering the biomass left in the reactor to serve as inoculum for the next cycle.

Finally, publications regarding continuous reactors are very rare. Only two investigations about DHA production through thraustochytrids have been published. As already introduced in section 4.2.3.3 these publications are Ganuza *et al*. (2008) [213] and Ethier *et al*. (2010) [52] works. Ethier *et al*. reported an r_{DHA} of 27.8 mg DHA / L· h cultivating *A. limacinum* SR21**.** This value is significantly lower than the one reported in this dissertation, which is an r_{DHA} of 136.7 mg DHA /L·h. The value obtained in this thesis is even higher than batch and fed-batch investigated as explained in section 4.2.3.3 and 4.2.3.4. Ganuza *et al.* work showed a r_{DHA} of 79.7 mg DHA /L ·h growing *Schizochytrium* sp. G13/2S. Probably due to the developed medium formulation and parameters optimization the r_{DHA} is twofold higher than those reported in Ethier *et al.* and Ganuza *et al.* (operating in continuous). Additionally, using the developed medium allows reaching very high cell densities that is directly boosting the final r_{DHA}. These three main factors might be causing the difference in productivity, as happens with batch and fed-batch reactors presented in this dissertation.

Multi-stage CSTR reactors was the final step of continuous culture strategy investigation. Such strategy is not common but in this case it has an important role. Multi-stage CSTR strategy allows a first step enhancing biomass production coupled with a second polishing or DHA triggering stage. During the second stage the growth is negligible. This strategy allows fast and continuous production while maintaining a good DHA yield, as explained in section 4.2.3.4. There are no similar strategies reported in the bibliography. **The multi-stage CSTR generated a maximum r_{DHA} of 152.6 mg DHA / L · h**, only below Chang *et al*. work which used a different strain. Lastly it is worth mentioning that there is a work reporting a productivity of 337 mg DHA / L ·s [221]. However, in this work they are reporting a DHA yield of 0.39 g DHA / g biomass as well as an 80% cell weight being lipids, which is impossible.

Undoubtedly, new thraustochytrid strains might be discovered during the following years. Some of these new strains could possibly grow faster and produce more DHA. However, the bioprocess purposed in this dissertation could be applied on new strains, reaching higher r_{DHA}. Moreover, it could be applied to enhance the production of other FA and/or added value metabolites. It is hoped that this work will stimulate the scale up work to industry scale as well as to stimulate further research about thraustochytrids and PUFA.

159

4.3   Chapter achievements

Culture temperature, aeration, agitation and three operation modes of STR have been investigated in chapter 4 for *A. limacinum* growth and DHA production. Two unsteady state processes which are batch and fed-batch, and a steady state (with a transient interval) that is the continuous stirred tank reactor (CSTR) or chemostat were investigated.

A set of experiments have been performed to evaluate temperature influence on *A. limacinum*. The data indicates that the consensus temperature is between 20 and 25 ºC. The best temperature for DHA production was 15 ºC while the best for biomass production was 28 ºC.

Low oxygen concentration enhances the specific accumulation of DHA whereas impairs biomass production. For this reason, the two main factor governing oxygen transference, aeration and agitation, were investigated. Using a CCD design 5 levels from each factor were investigated operating in a continuous mode. An agitation of 200 rpm and an airflow of 0.1 L/min would maximize the yield of DHA. Setting agitation at 680 rpm and an airflow of 3 L/m would ensure a maximum production of biomass. Furthermore, in order to find a consensus optimal values for single tank productions, a response surface was calculated by using both previous models. 500 rpm and 1L/min have been selected as intermediate values.

The main goal of chapter 4 was to determine the best strategy to produce DHA. Different initial carbon source concentrations were investigated operating in batch. The cultures with 40 and 60 g/L S_o that generated a higher r_{DHA}, with a maximum peak of 76.9 mg DHA/L·h. Fed-batch cultures were evaluated to investigate if a sustained low amount of carbon source triggers unspecific triglycerides accumulation. Data obtained indicate that DHA yield was the same than in batch reactors. However, r_{DHA} was higher reaching a value of 105 mg DHA/L·h.

Two different continuous reactors strategies to enhance r_{DHA} were investigated. Single tank continuous reactor gave a maximum r_{DHA} of 135 mg DHA/L·h. The maximum r_{DHA} obtained with *A. limacinum* SR21 operating in Multi-stage CSTR was 152.6 mg DHA/L·h. Using multi-stage strategy produces large quantities of biomass at the beginning while stimulating DHA production in later tanks. Moreover, *A. limacinum* produces a natural antioxidant called Astaxanthin, which protects DHA during downstream.

This page intentionally left blank

Chapter 5: A scalable process for recovery and purification of DHA

Scale up work and industrial viability evaluation

5.1   Introduction

The increasing market demand for contaminant-free and concentrated n-3 PUFA products has led to the search for new sources and development of new processes for its production. Currently, *A. limacinum* is the most promising source of n-3 PUFA [4–7]. *A. limacinum* produce DHA rich TG in an unmodified form. The n-3 PUFA present in fish are almost exclusively TG, which have been in the human food chain for approximately for million years. Therefore, the human body has evolved to process TG. In fact, fats are stored and transported in the body as TG [9].

Despite the wide range of marketed omega-3 supplements, no one offers a product with unmodified TG containing n- PUFA like DHA and EPA. Unmodified TG rich in n-3 PUFA offer a number of advantages over other forms of omega-3 products. Recent studies provide strong evidence that TG have superior bioavailability and significantly raise n-3 PUFA cellular levels [10–13]. In other words, they are more efficiently absorbed than other product types such as ethyl esters. Currently, the n-3 PUFA in TG form being used in nutraceutical products are derived from a process of re-esterification. In this process desired fatty acids are purified in ethyl ester form and then re-esterified to produce a TG. However, the enzymatic process of converting ethyl ester back to re-esterified TG (re-TG) is expensive and adds more steps, during which the n-3 PUFA can be oxidized.

To produce unmodified TGs from microalgae, a scalable process to recover and purify TG is needed. Recovery involves separating the TG from the microalgae and purification involves separating individual TG and cellular components from each other.

163

Because TG production in microalgae is intracellular, recovery begins with lysis of cells followed by extraction. Cell lysis can be carried out by a number of different methods, including bead beating, sonication, high-pressure homogenization, high temperature treatment (microwave, autoclave), and even laser disruption [14–18]. In studies comparing several disruption methods for release of TG from microalgae, sonication has been reported to be effective [15,17,18]. The resulting lysate must be clarified (i.e., cellular debris removed) as part of the recovery process. Bacterial bioprocesses commonly use any number of operations for clarification, including centrifugation, depth filtration, and tangential flow microfiltration. These operations should be suitable for microalgae as well.

Purification (i.e., separation of n-3 PUFA from cell components and other TG) has been demonstrated using a number of methods, including crystallization [19], urea complexation [20,21], enzymatic concentration [22–24], winterization [26-27,32–34], molecular distillation [28–32], and supercritical fluid extraction (SFE) [33–41]. However, there are no methods currently used at large scale to purify TG containing n-3 PUFA individually from a complex mixture.

Chromatography has been shown to be effective for separating mixtures of TG. The most widely reported chromatographic methods are immobilized-metal affinity chromatography (IMAC) and reversed-phase chromatography (RPC) [42–45]. Both methods are capable of producing excellent separation of FA-based compounds; however, most work has involved the use of chromatography for analysis, not production.

This work focuses on the development of a scalable process for recovery and purification of TG containing n3-PUFA produced by *A. limacinum SR21,* with a focus on cell lysis and chromatography steps. We recover TG by sonicating the biomass. Sonication is the method of choice because it is scalable, is compatible with

organic solvents, and does not require addition of any chemical agents. Lysate clarification is accomplished by filtration or centrifugation, both scalable operations. Given the hydrophobic nature of TG, we chose to focus on use of reversed-phase chromatography as the primary purification step to separate TG from cellular components and other TG.

5.1.1 Sample models

Development of a methodology to separate different TG has been carried out using two different sample models. One model was based on pure TG standards from Sigma-Aldrich. The second was based in two commercial products such as omega-3 pills and Palm cooking oil. These two models were selected considering the basic attributes which define TG. The total carbon number (CN) is the sum of the alkyl chain lengths of each of the 3 FA in a TG. The degree of unsaturation in each FA.

These attributes can be converted into the Equivalent Carbon Number (ECN) system [32,222]. **ECN is equivalent to the CN of the TG minus two times the total amount of double bonds of the same TG.** Moreover, there is a linear relationship between ECN and k' factor (retention factor), which can be used to predict the retention time of a specific TG.

Both models were selected considering the ECN values of *A. limacinum* TG. According to profiles described of similar species [108] and the fatty acid profile (defined by HRGC in chapter 2) the TG profile of *A. limacinum* might have an 80% of TGs with at least one moiety unsaturated. The TG distribution of both samples are detailed in Material and Methods section. The combination of omega-3 pills content with palm oil was equivalent to a sample with a complex mix of saturated, monounsaturated and polyunsaturated TG. Palm oil TG profile is well known [223] and is represented in Materials and Methods. On the other hand, the commercial omega-3 TG are in fact re-esterified TG.

Both sample models were key tools in order to develop TG separation and purification from *A. limacinum* clarified lysate.

164

5.2 Results and Discussion

5.2.1 Selection of the solvent for TG separation

The strong hydrophobic nature of TGs suggests the use of organic solvents in the process. There are a number of factors to be considered when selecting organic solvents for use, including solubility of the TG, performance in reversed-phase chromatography, and the ability to remove the solvent at the end of the process to produce a solvent-free TG. In addition, environmental impact is a concern, and because the TGs produced by *A. limacinum* are targeted for nutraceutical use, health and safety are primary considerations to ensure that the TGs produced are safe for human consumption.

There are numerous organic solvents to choose from. Among the "best" from an environmental, health, and safety perspective are ethanol, methanol, hexane, isopropanol and 1,3-propanediol [224–227]. These are the solvents we initially considered in this work.

To provide an initial determination of the feasibility of using these organic solvents and/or water in the process, the solubility of a saturated TG – glyceryl tripalmitate (PPP) – was assessed. PPP, which is a solid at room temperature, was chosen due to its strong hydrophobic nature. This qualitative study was

Table 5.38 Solubility of PPP in different solvents at different temperatures. – indicates that PPP is not soluble; + indicates that PPP is partially soluble, showing some white particles in the solvent; ++ indicates that PPP is fully soluble.

Solvent	Temperature (C)							
	25		**30**		**40**		**50**	
Water	–	–	–	–	–	–	–	–
1,3-Propanediol	–	–	–	–	–	++	++	++
Methanol	+	+	+	++	+	++	++	++
Ethanol	+	+	+	+	+	++	++	++
Hexane	NA	++	NA	++	NA	++	NA	++
2-Propanol	+	+	+	++	++	++	++	++
Hexane/ Ethanol (50%)	+	++	++	++	++	++	++	++
Hexane/ Methanol (50%)	+	++	++	++	++	++	++	++
	50% water	No water	50% water	No water	50% water	No water	50% water	No water

executed by adding PPP to a level of 3 mg/mL at the various conditions and visually observing the degree of dissolution. The results are shown in Table 3. As expected, PPP is not soluble in water at any temperature. As can be seen, at room temperature PPP is completely soluble only in hexane and the hexane/ethanol and hexane/methanol mixtures. There is only limited solubility with the other solvents and solvent/water mixtures. As temperature increases, improvements in solubility are observed, as shown in Table 3. Because we want the process to operate at room temperature, we removed both water and 1,3-propanediol from consideration. The limited solubility of PPP in each, especially at the lower temperatures studied, would likely result in processing challenges.

Both non-polar solvents, hexane and 2-propanol, showed good solubility of PPP. Therefore, due to an environmental, health and safety index (EHS) score[227], 2-propanol was discarded. Hexane, methanol and ethanol where the best in this index as well as showed good solubility.

5.2.2   Cell disruption: Sonication of *A. limacinum*

To quantify the extent of lysis during sonication of *A. limacinum*, the concentration of a reference TG was monitored by HPLC-UV. The TG PDHADHA[88] is one of the most abundant TG from *A. limacinum* according

---

[88] Composed of palmitic acid and two DHA chains.

to this study (showed later in this chapter) and Nakahara *et al.* [108]. It is one of the most valuable TG as well, because it contains two DHA moieties. For this reason, this specific TG was selected as a reference.

A. limacinum clarified lysate was sonicated at 0, 100, 250, 500, 750, 1000, 1500, 2000, 3000 and 3500 J/mL to determine the energy input that led to maximum TG recovery. The amount of reference TG extracted was monitored. A plot showing the peak height (measured as UV absorbance at 200 nm) of the reference TG against sonicator input energy is shown in Figure 5.*75*.Figure 5.75 PDHADHA extracted from A. limacinum as a function of sonicator energy input. The amount of PDHADHA extracted is represented
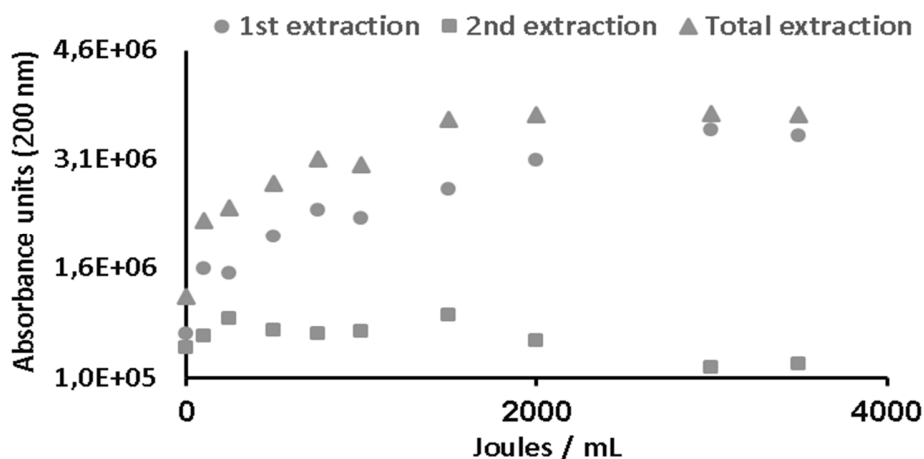
Figure 5.75 PDHADHA extracted from A. limacinum as a function of sonicator energy input. The amount of PDHADHA extracted is represented by the absorbance units of the peak height from HPLC by the absorbance units of the peak height from HPLC analysis of the lysate.

Every extraction consisted of a sonication process on biomass suspended in methanol at a concentration of 7.5%. As can be seen in Figure 5.*75*, the first extraction recovers the majority of TG. Recovery increases as more energy is applied. During the first extraction, astaxanthin was recovered as well, giving the extract an orange color. The second extraction shows a considerably lower amount of PDHADHA obtained. The first extraction obtains 90% of the important TG. Comparing the first extraction with the total amount of TG extracted (Figure 5.*75*) makes it clear. Above 1500 J/mL, HPLC peak height values plateau at approximately 3.7x106 AU, which suggests that all TG have been extracted from *A. limacinum*. Data from the second extraction supports this hypothesis as UV absorbance values for those samples processed at higher energy input actually decrease, due to the absence of TG available to be extracted.

To further confirm that all TG have been extracted, gravimetric quantification of extracted compounds was performed, and values reached a plateau at energy levels of 2000 J/mL as well (data not shown), similar to results obtained with HPLC measurements. Additionally, third extractions on lysed cells were performed with chloroform to test whether the relatively polar nature of methanol inhibits extraction of hydrophobic TG from *A. limacinum*. The results showed only negligible amounts of additional TG being extracted (data not shown).

Based on these experiments, a sonicator operated at approximately 2000 J/mL is appropriate for extracting nearly 100% of intracellular TG from *A. limacinum*, in less than 20 minutes. It is worth noting that the second extraction showed no additional recovery of TG. Therefore, this should not be

implemented in a production process. And while these results demonstrate the feasibility of sonication as a lysis method for TG recovery from *A. limacinum*, scaling up would likely require use of a continuous flow sonicator, which are currently available from a number of vendors.

5.2.3   Composition of *A. limacinum* lysate

Gas chromatography was used to analyze *A. limacinum* lysate for fatty acids using HRGC-RID method. As indicate in the chromatogram (Figure 5.76 Gas chromatography analysis of fatty acids from A. limacinum SR21.), the following fatty acids are present: myristic acid (M), P, DHA, docosapentanoic acid (DPA), and stearidonic acid (S) are present. In separate experiments, a sample of *A. limacinum* clarified lysate was also analyzed using HPLC- tandem mass spectrometry (HPLC-MS/MS). FA identified using this method are in agreement with the fatty acid profile measured by HRGC-RID.
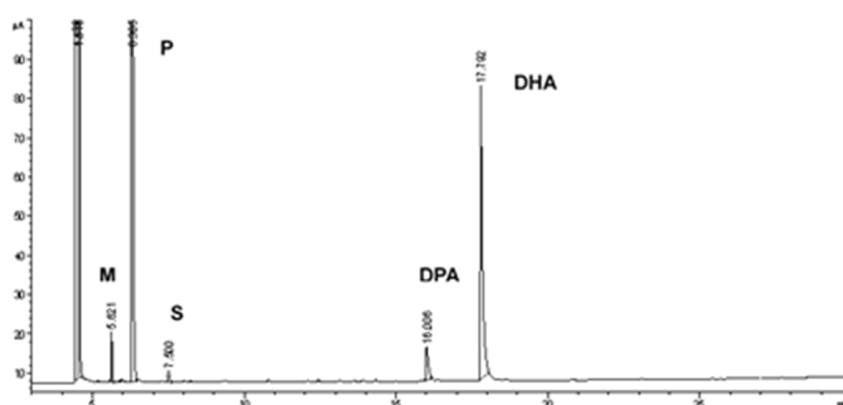
Figure 5.76 Gas chromatography analysis of fatty acids from A. limacinum SR21.

Using an HPLC method developed for downstream investigation (detailed in Materials and Methods), the TG profile present in *A. limacinum* clarified lysate was determined. The results are shown in Table 4. In addition, based on gravimetric analysis (described in the Materials and Methods section), it was determined that the amount of extracted matter is 4.6 g/L.   Based on HPLC chromatograms, approximately 30% of total peak area is TG. Therefore, a TG concentration of 1.38 g TG/L in clarified lysate was obtained.

Table 5.39 TGs from A.limacinum based on HPLC analysis of clarified lysate.

Triglyceride	ECN
PDHADHA	36
PDPADHA	38
MPDHA	40
PPDHA	42
PPDPA	44
MPP	46
PPP	48

5.2.4 Chromatography method (process) development

Chromatography method development was initiated by attempting to separate a mixture of the Sigma-Aldrich TG standards (see Material and Methods). Different condition combinations of hexane, ethanol, and methanol were evaluated as mobile phases. On the other hand, 4 columns consisting of both C4 and C18 reversed-phase chromatography resins were used as stationary phase. All columns used all had bead diameters of 5 μm.

This initial portion of the study posed challenges as none of the column gave good resolution between TG, likely due to the choice of mobile phase conditions. Specifically, it became evident that the use of relatively nonpolar hexane inhibited binding to the reversed-phase resin particles. Therefore, a solvent with greater polarity was required.

In order to give greater attention to mobile phase conditions, the work was limited only to the use of one of the columns with the highest carbon load (hydrophobicity) in the market, the Kromasil® C18 packed with 5μm beads. This resin is also available in a larger bead size of 16 μm, which is more appropriate for the preparative applications which is the aim of this work. The profile from every sample model is presented in Figure 5.77.
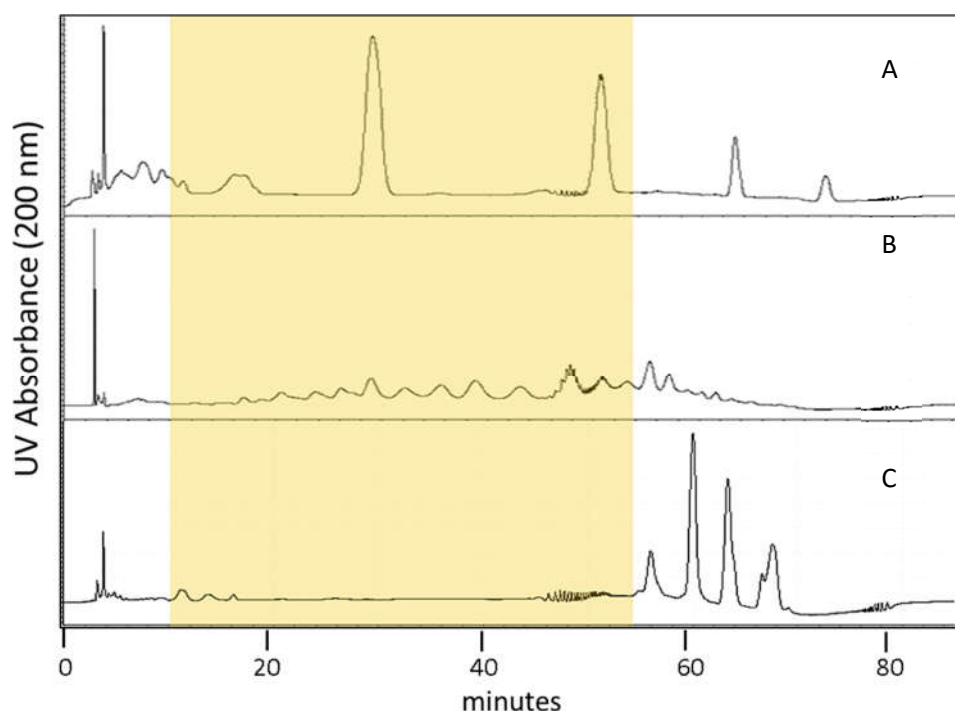
Figure 5.77 Elution profile of different model samples processed by the optimized HPLC method describe below. A = Sigma-Aldrich standard mixture; B = omega-3 pills; C = Palm Oil.

Further optimization of the chromatographic method was performed using a mixture of the Sigma-Aldrich TG standards together with omega-3 pills content and palm oil mixture. This was investigated using the 5μm Kromasil® column. To perform the optimization, Taguchi's L8 matrix was used [228]. Selected factors

were: methanol concentration in the mobile phase, flow rate, and introduction of hexane as a gradient. Factor levels are as follows:

- Methanol concentration: 2:3 v/v methanol/ethanol, 4:1 v/v methanol/ethanol, and pure methanol

- Flow rates: 0.75 mL/min, 1.25 mL/min, and 1.5 mL/min

- Gradient: no gradient was used as the lower level and hexane gradient as the higher level.

The factors were placed in the matrix following orthogonality of the vectors.

The response parameter for a DoE was the relative resolution between two specific peaks. One represents a TG with an ECN of 36 and the second represent a TG with an ECN of 48. Resolution, R, was calculated using equation 5.1.

$$R = (rt1 \quad rt2)/[\tfrac{1}{2}(w1 + w2)]$$ \hfill Equation 5.1

where tr is the retention time of the peak, w is the width of the chromatographic peak, and 1 and 2 refer to two different TG.

The TG with an ECN 36 correspond to the TG containing DHA (from *A.limacinum* clarified lysate, PDHADHA), while the TG with an ECN 48 correspond to the first eluting TG not containing any n-3 PUFA. By comparing Sigma-Aldrich standards elution time with an ECN between 36 and 48, the corresponding

169

Table 5.40 Results from DoE runs separating TGs from a Sigma-Aldrich/omega-3 pill/palm oil mixture on a Kromasil® C18 column packed with 5 µm beads. Experimental design is based on Taguchi's L8 matrix.

Methanol conentration (%)	Flow rate (mL/min)	Hexane gradient	Relative resolution	Signal / Noise
40	0,75	N	7.7 ± 0.3	17,7
40	0,75	Y	11 ± 0.1	20,9
40	1,25	N	6.5 ± 0.6	16,1
40	1,25	Y	7.9 ± 0	18,0
80	0,75	N	14.8 ± 0.7	23,4
80	0,75	Y	16 ± 0.2	24,1
80	1,25	N	14.2 ± 2	22,9
80	1,25	Y	25 ± 1.3	28,0
100	0,75	N	21.35 ± 0.2	23,6
100	0,75	Y	22.9 ± 0.9	24,2
100	0,75	N	18.8 ± 1.5	22,5
100	1,25	N	25.2 ± 0.4	25,0
100	1,25	Y	**32 ± 0.6**	27,1
100	1,25	N	24.3 ± 0.9	24,7
100	1,5	N	23 ± 0.3	24,2
100	1,5	Y	**31.3 ± 0.7**	26,9
100	1,5	N	25 ± 0.2	24,9

peaks in the Sigma-Aldrich + omega-3 pills + palm oil mixture were identified. Results from these runs are summarized in Table 5.40 Results from DoE runs separating TGs from a Sigma-Aldrich/omega-3 pill/palm oil mixture on a Kromasil® C18 column packed with 5 µm beads. Experimental design is based on Taguchi's L8 matrix..

Observing the results in Table 5.40 Results from DoE runs separating TGs from a Sigma-Aldrich/omega-3 pill/palm oil mixture on a Kromasil® C18 column packed with 5 µm beads. Experimental design is based on Taguchi's L8 matrix. show that the resolution increases as methanol concentration increase in the mobile phase. An ANOVA was performed to determine the factors contributing most significantly to resolution. As expected, ANOVA indicates that methanol is the main contributor to resolution (67% positive contribution towards a higher resolution). A maximum resolution of 32 between peaks with ECN of 36 and 48 was reached. Results are indicating that the optimum mobile phase composition is 100% Methanol. Beyond methanol concentration, the flowrate (contribution of 80% from the rest of factors) appears to be the most important factor the interaction between flowrate and gradient showed a positive contribution (18.8 %).

Based on the optimization described above, the chromatography method for TG from clarified lysate using the Kromasil® C18 column (5µm beads) is as follows: pure methanol for 130 minutes followed by an increase in hexane concentration from 0% to 35% (in methanol) from 130 minutes to 170 minutes followed by 100% methanol from 170 minutes to 180 minutes. Column temperature was maintained at 30ºC due to repeatability requirements, but the process can be carried out at room temperature. The flow rate during the entire procedure is 1.25 mL/min. The load volume of 10 µL of clarified lysate corresponds to 13.8 mg of TG.

There are several modifications that can be made when implementing this method to production scale. The TG of interest (those containing n-3 PUFA) elute within 50 minutes of sample injection (load); therefore, 130 minutes of isocratic elution can be reduced to 50 minutes. Hexane can be viewed as a cleaning/regeneration step for the column; therefore, after the TG of interest have eluted, the mobile phase composition can be switched to 100% hexane. The full chromatographic procedure as it would be implemented in a production environment is shown in Table 5.41.

Table 5.41 Chromatography procedure for separating TGs in a production environment. The flow rate for steps is 1.25 mL/min when using the Kromasil® C18 column with 5µm beads and diameter of 4.6 mm.

Step #	Step Description	Mobile Phase	Time (min)	Column Volumes*
1	Equilibration	100% methanol	2.4	3
2	Load	*A. limacinum* clarified lysate (in methanol)		
3	Elution	100% methanol	50	15.1
4	Regeneration (cleaning)	100% hexane	40	12
5	Storage	100% hexane	2.4	3
6	Additional periodic cleaning**	100% water	2.4	3

*ratio of mobile phase volume to chromatography bed volume

Figure 5.*78* shows the elution profile for *A. limacinum* clarified lysate using the final method. It is worth mention that although optimization focused on separation of TG containing n-3 PUFA from monounsaturated/saturated TG, the method appears to give good separation between individual TG containing n-3 PUFA as well.
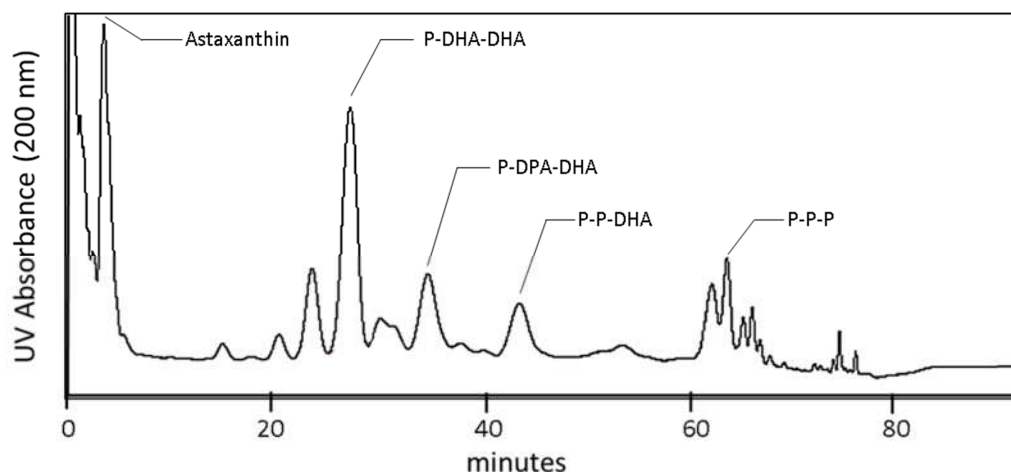
Figure 5.78 A chromatogram showing the elution of A. limacinum clarified lysate using the optimized procedure for TG purification from. The Kromasil® C18 column with 5µm beads was used for this run.

Classical HPLC requires high pressure equipment that process scale chromatography cannot reach [64]. Therefore, the reversed-phase step for an industrial TG purification will use a Kromasil® C18 column with a bigger bead size. For the scale up process, a 16 µm bead size rather the 5 µm bead size was selected. Pressure drop in a bed packed with rigid beads like silica varies inversely with the square of the particle diameter per the Blake-Kozeny equation. Thus, a column packed with 16 µm beads (the largest bead available for a Kromasil® C18 column) will have a pressure drop of approximately 1/10th that of a column packed with 5 µm beads. At the flow rates used in this study (1.25 mL/min), column pressures of slightly less than 10.7 bars were measured. Assuming an approximately equal pressure drop from a production-scale system (not including the column) would result in a medium pressure chromatography system [64]. Larger bead size would be required for truly low-pressure operation.

The larger bead size is expected to decrease the number of theoretical plates, which would lead to a decrease in resolution between the various TG species. Figure 5.*77*A shows a chromatogram resulting from the optimized method described in Table 5.41 applied to a Kromasil® C18 column with a 16 µm bead size. The resolution between the PDHADHA peak and subsequent peak was 1.70. When the 5 µm bead size is used, the resolution was 1.71. Therefore, the difference in resolution between the two columns was not significant. For scale up of the chromatography step, an acceptable load volume per unit column volume was needed. To determine this value, the Kromasil® C18 column packed with 16 µm beads was used to execute the chromatography method described in Table 5.41 at four different load amounts: 0.112, 0.85, 4.2 and 11.2 g of clarified lysate/mL of resin. The resolution between key components of the TG profile (peaks R-1 and R, and R and R+1 in Figure 5.79) was calculated for each load condition using Equation 5.1. In Figure 5.*79* the reference TG is tagged as R while the TG eluting before and after are R-1 and R+1, respectively. Can be seen in the same figure that when the sample load increases, the resolution

171

between peaks is reduced. Thus, increasing the sample load reduces the purity of each TG. Results of the resolution calculations for every sample are shown in Figure 5.78.
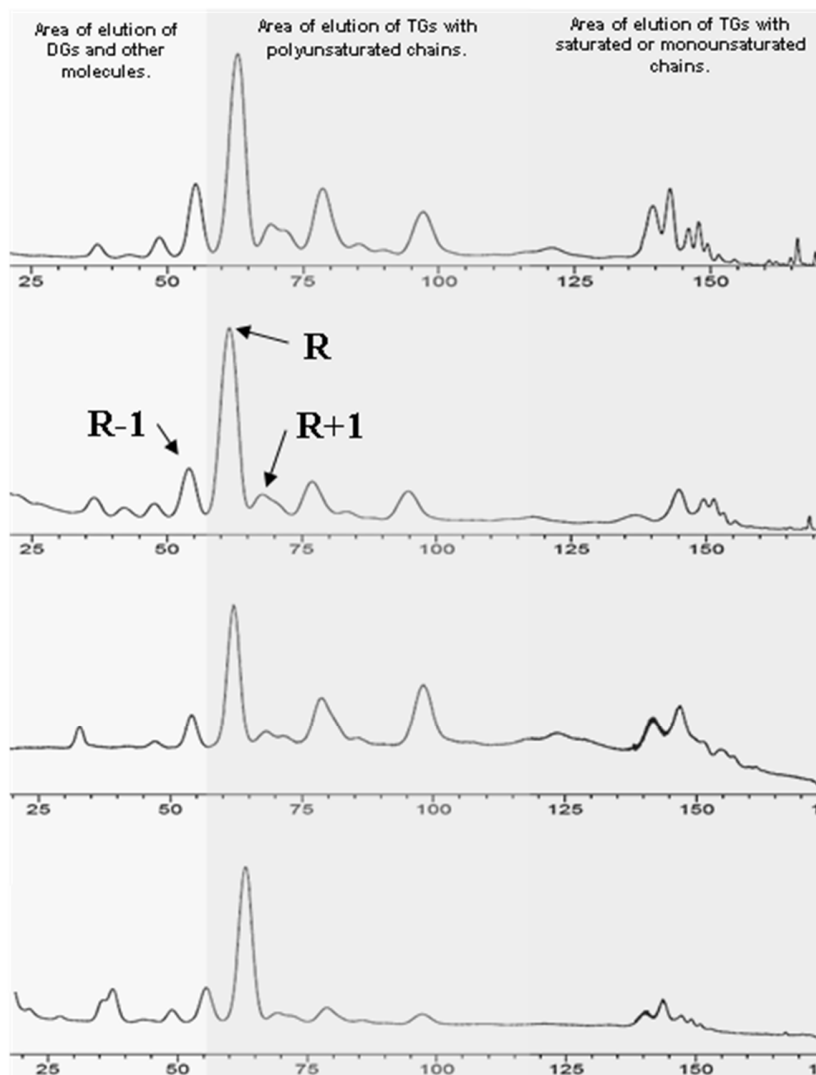
Figure 5.79. Chromatograms from runs in which amount of load (clarified lysate) was varied as follows: (a) 0.112, (b) 0.85, (c) 4.2 and (d) 11.2 mg of TGs from clarified lysate/mL resin. (a) is the bottom chromatogram, (d) is the top. All runs used the Kromasil® C18 column with 16 µm beads operated as shown in Table 5 at a flow rate of 1.25 mL/min. Peak R-1 is a diglyceride; peak R is PDHADHA; and peak

As can be seen, the resolution between R and R-1 is always higher than R and R+1. A resolution of 1.5 provides nearly complete separation of components; and a resolution of 1 is acceptable for most separations [64]. Therefore, separation of PDHADHA from the diglyceride is nearly complete for all TG loadings. For separation of PDHADHA from PDPADHA, the resolution falls below 1.0 at approximately 4 mg TGs/mL resin. It is important to note that if the objective is the separation of TG containing n-3 PUFA from monounsaturated or saturated TGs, maximum loading of clarified lysate would be significantly higher than 4 mg TGs/mL resin.
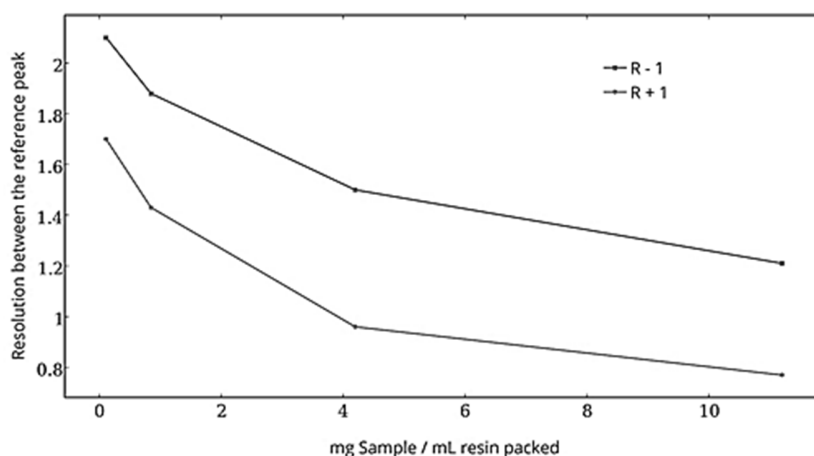
Figure 5.81 Resolution between peaks R vs R-1 and R vs R+1 as a function of the mass of TGs loaded to the 16 um Kromasil® C18 column.

During the same experiment, when the maximum load of 11.2 g TG/L clarified lysate was processed, the fraction corresponding to PDHADHA was collected (as shown in Figure 5.80). This sample was then analyzed by analytical version of the HPLC method. This allowed to determine the reference TG purity and recovery. At these load conditions, the purity of PDHADHA was measured as 92.78 % and the recovery was 84 %. Purity was measured as the ratio of the area of the PDHADHA peak to the area of all peaks. On the other hand, the recovery was calculated by collecting the material eluting at the reference TG time. Then this TG was re-injected, a third time, in the HPLC system and areas (second injection and third injection) were used to calculate the recovery %. Purity could be increased by reducing recovery.
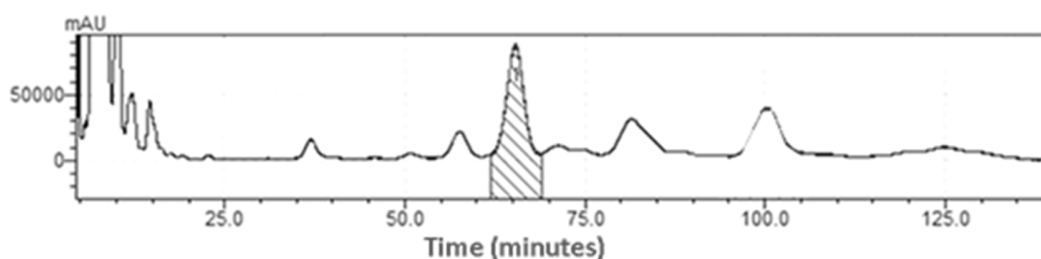
Figure 5.80 Chromatogram showing the collection of the PDHADHA peak for purity and recovery analysis.

The impurities are probably other molecules containing PUFA. Regardless, at this high purity, PDHADHA would have a very high value as a nutraceutical product. There is even the potential that this method could be used for the production of standard TGs with long chain n-3 PUFA, which are not currently commercially available.

5.2.5 Process scale chromatography example

As an example of chromatography scale up, consider a scenario in which a 200-L *A. limacinum* fermentation is processed. *A. limacinum* can reach a concentration of 60 g/L, where almost 40% are lipids and a 20% are PUFA. Therefore, 12 g/L of TG containing n-3 PUFA would be obtained. Using a scale up methodology in which liquid residence time is kept constant by maintaining column height and linear velocity at both small and large-scale, the following relationships apply:

$$bed1 = bed2 \qquad\qquad \text{Equation 5.2}$$

$$\frac{Q1}{Abed1} = \frac{Q2}{Abed2} \qquad\qquad \text{Equation 5.3}$$

hbed is the bed height; Q is the volumetric flow rate to the column; Abed is the cross sectional area of the bed; and subscripts 1 and 2 refer to parameter values at small and large scale, respectively. Using these relationships, and assuming a column capacity of 40 g TGs/L column volume, the parameters presented in Table 5.42 result for the 200-L fermentation scenario. The objective of the chromatography step is separation of TG made up of n-3 PUFA from monounsaturated/saturated TG. In this case, resolution is not a constrain.

Table 5.42 Scale up of the reversed-phase chromatography step for processing a 200-L A. limacinum fermentation.

Parameter	Value
Clarified lysate (load) volume	200 L
Column height	25 cm
Column volume (assume capacity 40 mg TG/mL resin)	= (12 g/L x 200 L)/40 g/L = 60 L
Column diameter	= 60000 cm^3=π x d^2/4 x 25 cm, d = approx. 55cm
Volumetric flow rate	= v x A = 451.518910 cm/h x 2760 cm^2 =1246 L/h
Grams triglycerides produced	= 12 g/L x 200 L = 2400 g

Based on this analysis, a 60-cm column packed with Kromasil® C18 reversed-phase column with a 16 μm particle size would be suitable for processing a 200-L *A. limacinum* fermentation.

Considering the cost of methanol, resin, fermentation broth, operations and power (industrial suppliers) the cost of the product would be 800 €/Kg. Unmodified TG rich in n-3 PUFA is not currently available in the market. Purified DHA price ranges between 100 to 8000 €/Kg depending on purity and format. Therefore, if the market demands this new product it may have a high value, similar to purified DHA.

The downstream process would use disk-stack centrifugation as harvesting technique. Cells of similar size and concentration (in fermentation/cell culture broth) are commonly recovered using disc-stack centrifugation.

Collected cells are suspended in methanol at a concentration of 7.5% by volume and lysed using sonication. This concentration may be increased significantly but a deeper investigation is needed. A flow through sonicator would be preferable for scale up. Lysate must be clarified to make it suitable to load to a chromatography column. This could be accomplished using centrifugation, depth filtration, or some combination of both. These are commonly use operations for lysate clarification for other applications.

Then the clarified lysate can be loaded onto a reversed-phase column. As designed in this study, that step is capable of separating n-3 PUFA from each other or from monounsaturated/saturated TG. The final purified methanol/TG solution could go through an evaporation step to remove methanol, leaving behind purified TG. For example, using a sanidry vacuum dryer. Evaporating methanol off after the purification would allow the reformulation of the final product if desired. Unsaturated TGs is the main component of

the product which makes it liquid at room temperature. To increase its volume and facilitate its manipulation, the product can be dissolved either in ethanol or glycerol.

5.2.6 Identification of the reference peak R by Mass spectrometry

Mass spectrometry was performed to confirm the identification of the PDHADHA chromatography peak (corresponding to ECN 36 from the final chromatography method). This analysis will also allow to confirmation that the remaining peaks have been correctly identified according to their ECN / retention time.

The same fraction used to measure purity and recovery (described previously) was used to perform MALDI-TOF mass spectrometry. The resulting MALDI-TOF mass spectrum is shown in Figure 5.82.
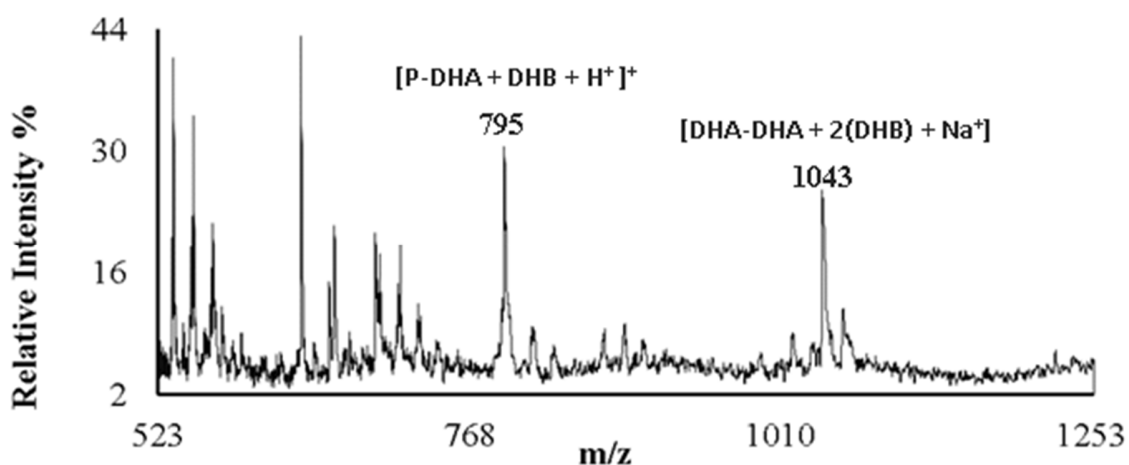
Figure 5.82 MALDI-TOF mass spectrum of the PDHADHA fraction shown in

Despite the spectrum is showing low resolution two main peaks give a significant high relative intensity. As reported by Petković *et al.* [63] large hydrophobic molecules tend to create clusters (complex adducts) with the matrix and salts. This phenomenon was considered to identify peaks from MALDI-TOF. Those peaks appear to be [PDHA + DHB + Na$^+$]$^+$ and [DHADHA + 2(DHB) + Na$^+$]$^+$ corresponding to 795 m/z and 1043 m/z, respectively. These results are a strong evidence that the purified fraction is PDHADHA.

To further confirm the identification, a sample of *A. limacinum* clarified lysate (without purification) was processed by HPLC-MS/MS. Results of HPLC-MS/MS analysis are displayed in figure 11. As can be observed, the most abundant FA are P, DPA and DHA. This results are in concordance with HRGC analysis and the A. limacinum clarified lysate elution profile.

Moreover, the resolution is substantially higher compared to MALDI-TOF mass spectrum. Basically all adducts are based on sodium. Sodium comes from the artificial seawater in where the microorganism was grown. [PDHA + 2(Na) − H$^+$]$^+$ is the most abundant species in the samples. This is in concordance with previous results, indicating that PDHADHA and PPDHA are the most abundant TGs in *A. limacinum*.

Although it is extremely difficult to demonstrate these are the exact clusters formed during the ionization, the obtained mass spectrum is a strong evidence that the purified fraction is constituted by the TG PDHADHA. The results are in concordance with HPLC chromatograms and the ECN number of the mention TG. Moreover, HPLC-MS/MS chromatogram reinforce the evidence by showing that probably PPDHA and PDHADHA are the most abundant TGs in *A. limacinum*.

m/z	Species	m/z	Species
351.3	[DHA + Na]$^+$	685.7	[PDHA + 2(Na) - H]$^+$
353.4	[DPA + Na]$^+$	735.7	[DHADHA + Na]$^+$
568.5	[PP + H]$^+$	829.9	[PPP + Na]$^+$
590.5	[PP + Na]$^+$	900.8	[PPDHA + Na]$^+$
663.7	[PDHA + Na]$^+$		
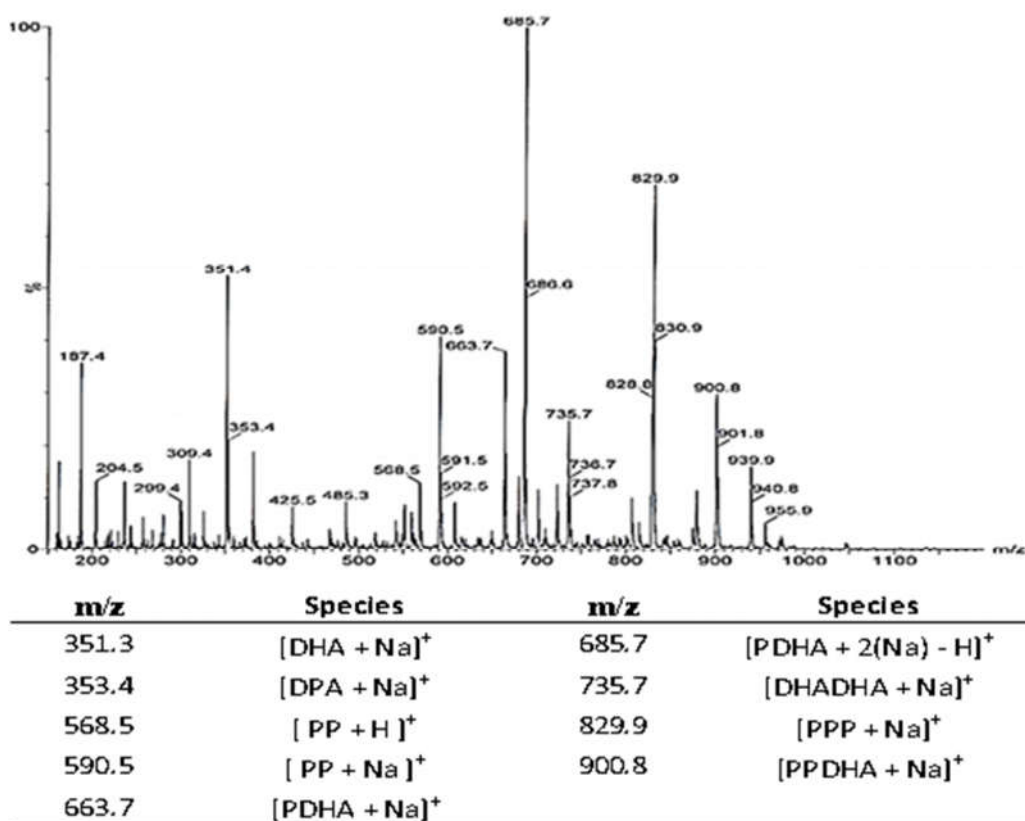
Figure 5.15 HPLC-MS/MS mass spectrum of the PDHADHA fraction shown in

5.3   Chapter achievements

During this chapter, an alternative approach to purify unmodified TG containing n-3 PUFA have been investigated. Unmodified TG are not marketed nowadays while some works suggest that it would be the best supplementary form [229,230].

PPP was used in order to evaluate different solvents solubility with TG. All the solvents were initially selected based on its EHS score, being the "greenest" possible. Methanol, ethanol and hexane appeared to be the best in solubility and EHS score. After HPLC studies methanol and hexane turned to be the best mobile phase combination of polar and non-polar solvents. Considering that unsaturated FA have a higher solubility in methanol, cell disruption and simultaneous extractions was carried out using this solvent. It has been shown that one run of 2000 J/mL was enough to extract 90%-95% of the objective material.

In order to investigate TG purification without standards of TG containing DHA, 2 sample models were formulated. The first was a combination of Sigma-Aldrich standards with known ECN. Some of this standards have the same ECN number than those TG containing DHA. This allowed to predict the elution time of any TG based on ECN. The second sample was the content of commercial omega-3 pills combined with commercial palm oil. This model served to investigate chromatographic conditions to separate TG containing unsaturated moieties versus those not containing any.

177

Various methodologies were explored in order to purify TG containing unsaturated moieties. This investigation resulted in two main methodologies based on reverse-phase chromatography using a very hydrophobic resin. The first was an analytical methodology to investigate *A. limacinum* clarified lysate elution profile. This served as the starting procedure for the scale up work on a preparative methodology (the second method) with a 16 μm bead size column. The preparative methodology showed that this resin can be used in process scale chromatography. On the other hand, the preparative procedure itself could be used to produce novel standards of TG containing DHA.

In the last part of this thesis, the reference peak was identified by mass spectrometry using MALDI-TOF and HPLC-MS/MS. This confirmed that the reference peak was a TG composed of PDHADHA.

This chapter represents a great approach to purify valuable nutraceutical TG that needs further investigation to perform a final implementation in an industrial process.

This page intentionally left blank

Conclusions

Conclusions

Using *A. limacinum* SR21 as a model it has been shown that thraustochytrids have a complex life cycle during batch growth.

In a batch culture, *A. limacinum* SR21 showed five different stages; vegetative cells, zoosporangium cells, zoospores, amoeboid cells and semi-proliferative cells. Between different life stages, zoospores revealed the highest growth rate while the vegetative cell stage appears to contain the highest amount of DHA. During continuous cultures *A. limacinum* SR21 only shown the vegetative cell stage.

A Matlab® algorithm has been satisfactorily adapted to measure cell dimensions using current microscopy equipment and a smartphone.

A method has been developed and validated for successfully determine and quantify DHA from *A. limacinum SR21* samples. The method includes both the sample preparation procedure as well as the HRGC-FID analysis. Sample preparation procedure has been simplified and permits simultaneous sample processing. Besides *A. limacinum* samples this method would allow the quantification of DHA from other thraustochytrids species.

It has been shown that HPLC-RID, Enzymatic kit and DotBlot-Matlab® methods can measure precisely the glycerol concentration from culture broth. DotBlot - Matlab® analysis was the cheapest and fastest analytical method for glycerol quantification which allows a high number of samples to be processed simultaneously. This is the most convenient method for glycerol consumption bioprocess monitoring.

DotBlot methodology was coupled with a Maltab algorithm exclusively developed for this purpose. The Matlab® algorithm was successfully applied to calculate glycerol concentration from the DotBlot based on a standard curve.

Cultivating *A. limacinum SR21* with crude glycerol as carbon source showed an equivalent performance between glucose and glycerol.

It has been shown that *A. limacinum SR21* grow comparably well either with organic or inorganic nitrogen sources. Nevertheless, organic nitrogen sources enhance DHA and lipid production in *A. limacinum SR21*. After several DoE and three ANN models a constant relationship was established between carbon and nitrogen concentration. In order to avoid a limiting nitrogen situation, 2.3 g/L of yeast extract and 0.4 g/L of tryptone are needed per every 10 g/L of carbon source.

A. limacinum SR21 showed a great versatility for a wide salinity range. *A. limacinum* can grow and produce DHA satisfactorily when sodium chloride concentration is between 14 and 30 g/L.

Phosphate buffer (KH_2PO_4 + NaOH) was selected according to price and pH range, and Tris buffer was successfully substituted.

The best concentration for $MgSO_4$, $CaCl_2$ and KCl was determined to be 0.1 g/L, 0.19 g/L and 0 g/L, respectively. Therefore, KCl did not show any effect either on *A. limacinum* SR21 growth or DHA production.

Cyanocobalamin or Vitamin B_{12} showed no effect on *A. limacinum* growth. After investigating different concentrations, it has not shown any effect either on biomass or DHA production. Thus, Vitamin B_{12} was excluded from the medium.

It has been seen that low oxygen concentration enhances the specific accumulation of DHA whereas impairs biomass production. For this reason, the two main factor governing oxygen transference, aeration and agitation, were satisfactorily modelled using a CCD design and RSM concluding that:

> ➤ An agitation of 200 rpm and an airflow of 0.1 L/min maximize DHA yield.

> ➢ An agitation of 680 rpm and an airflow of 3 L/m (1.76 vvm) ensure a maximum production of biomass.
> ➢ An agitation of 500 rpm and 1L/min would work as consensus parameters for single tank reactors.

Batch cultures between 40 and 60 g/L S_o generated a highest r_{DHA}, with a maximum peak of 76.9 mg DHA/L·h. Batch cultures with S_o higher than 60 g/L showed a reduced growth yield. The highest growth yield was obtained in batch reactors with S_o 10 g/L were reached 0.9 g X/gS.

Batch reactors showed an average DHA yield of 0.23 g DHA/g biomass which is the highest reported in bibliography and in this the present thesis in bioreactor cultures.

Fed-batch cultures showed no evidence of unspecific triglycerides production stimulation by a sustained low carbon source concentration. Data obtained indicate that DHA yield was the same than in batch reactors. However, r_{DHA} was higher reaching a value of 105 mg DHA/L·h.

Two different continuous reactors strategies were successfully performed and investigated to enhance r_{DHA}. Singe tank continuous reactor gave a maximum r_{DHA} of 135 mg DHA/L·h. The maximum r_{DHA} obtained with *A. limacinum* SR21 operating in Multi-stage CSTR was 152.6 mg DHA/L·h.
In all continuous reactors DHA yield was always lower showing an average value of 0.19-0.2 g DHA/g biomass.
Using multi-stage strategy *A. limacinum* SR21 produces a natural antioxidant called Astaxanthin, which may protect DHA during downstream.

181

For the downstream processing an alternative approach to purify unmodified TG containing n-3 PUFA have been developed. After HPLC studies, methanol and hexane turned to be the best mobile phase combination of polar and non-polar solvents.

Considering that unsaturated FA have a higher solubility in methanol, cell disruption and simultaneous extractions were carried out using this solvent. It has been shown that one run of 2000 J/mL was enough to extract 90%-95% of the objective material.

In order to investigate TG purification without standards of TG containing DHA, 2 sample models were formulated. The first was a combination of Sigma-Aldrich standards with known ECN. Some of this standards have the same ECN number than those TG containing DHA. This allowed to predict the elution time of any TG based on ECN. The second sample was the content of commercial omega-3 pills combined with commercial palm oil. This model served to investigate chromatographic conditions to separate TG containing unsaturated moieties versus those not containing any.

Two main methodologies based on reverse-phase chromatography using a very hydrophobic resin were successfully developed. The first was an analytical methodology to investigate *A. limacinum* clarified lysate elution profile. This served as the starting procedure for the scale up work on a preparative methodology (the second method) with a 16 μm bead size column. The preparative methodology showed that this resin can be used in process scale chromatography. On the other hand, the preparative procedure itself could be used to produce novel standards of TG containing DHA.

PDHADHA was identified by mass spectrometry using MALDI-TOF and HPLC-MS/MS. This confirmed that the reference peak was a TG composed of PDHADHA.

This page intentionally left blank

Chapter 6: Materials and Methods

This section gathers all the information of materials & methods.

6.2   Cultivation of Thraustochytrids

6.2.1   Thraustochytrid strains and conservataion

Aurantiochytrium limacinum (ATCC MYA-1381) and *Thraustochytrium aureum* (ATCC 34304) were purchased from the American Type Culture Collection (ATCC), USA. *Aurantiochytrium mangrovei* (NBRC 103269), *Sicyoidochytrium minutum* (NBRC 102975), *Ulkenia amoeboidea* (NBRC 104106) and *Botryochytrium radiatum* (NBRC 10407) were purchased from NITE Biological Research Center (NBRC), Japan. To establish a culture from the frozen state place an ampule in a water bath set at 35°C (2-3 min). Immerse the vial just sufficient to cover the frozen material. Do not agitate the vial. Immediately after thawing, aseptically remove the contents of the ampule and inoculate into 5 mL of in a sterile culture flask or 16 x 125 mm screw-capped test tube. Incubate at 25°C overnight. Inoculate the culture content into a 250 mL flask with 80 ml growth media (see below). Then, an aliquot of the culture with 30% glycerol was used for long term conservation of the microorganism at -80°C.

6.2.2   General growth media

The starting growth media of the current study was made of artificial sea water, 1 g/L yeast extract, 1 g/L tryptone, and streptomycin sulphate 25 µg/mL [147]. The seawater composition was (per L): 18 g NaCl, 2.44 g $MgSO_4$, 0.6 g KCl, 1.0 g $NaNO_3$, 0.3 g $CaCl_2 \cdot 2H_2O$, 0.05 g KH_2PO_4, 1 g Tris buffer, 0.027 gNH_4Cl, $15x10^{-8}$ g vitaminB_{12} combined with 10 mL/L metal solution, and 3 mL/L chelated iron solution as reported in Starr & Zeikus (1993) [178]. Crude glycerol, pure glycerol or glucose was added as carbon source. Any modification is indicated in the corresponding section of this thesis.

Pharma-grade glycerol, also referred to as pure glycerol, was purchased from Fisher Scientific Spain. For crude glycerol samples, raw glycerol used was graciously provided by Transportes Ceferino Martínez S.A. It was obtained as the residual fraction from the transesterification of used cooking oil (UCO) to biodiesel through an alkali catalysed process. The crude glycerol generated has a dark brown colour and a glycerol content of 80%. Glucose was purchased from Sigma-Aldrich Spain.

6.2.3   Erlenmeyer flask cultivation

Inoculums were prepared using 40 mL of an artificial seawater medium plus a carbon source (generally crude glycerol) and incubated at 20°C, while being shaken (200 rpm). After 48 hours, the cells were used to inoculate the new flasks at a 2 - 2.5% volume ratio, the final dilution is equivalent to 0.5 OD600[89]. Cultures were grown in 250 mL Erlenmeyer flasks using an artificial sea water medium volume of 80 mL. The culture media used artificial sea water, as reported in the previous section using 10 g/L of carbon source. The flasks were incubated at 20 ºC in an Infors incubator (Switzerland). Samples consisting of 2 mL were collected to monitor cell growth by measuring OD600 using a Jenway 6310 spectrophotometer, dry weight of biomass, residual glycerol and glucose concentrations as well as DHA quantification. All

---

[89] The OD is measured in a spectrophotometer at 600 nm. The underlying principle is that most of the light scattered by the cells no longer reaches the photoelectric cell, so that the electric signal is weaker than with a cell-free cuvette. The OD of a bacterial culture is thus primarily not an absorbance as in the case of a dissolved dye. Cells of many bacteria are almost colorless and real light absorption is marginal. It is therefore not correct (even though unfortunately common) to designate the OD of a culture an absorption; the most appropriate term would indeed be turbidity.

assays were conducted in triplicate. Any modification of these general conditions are indicated in the corresponding section of this thesis.

6.2.4 Bioreactor cultivation

Inoculums were prepared using 40 ml of an artificial seawater medium plus a carbon source (generally crude glycerol) and incubated at 20°C, while being shaken (200 rpm). After 48 hours, cells were used to inoculate the bioreactor at a 2 - 2.5% volume ratio, equivalent to 0.5 of initial OD600. The culture media used artificial sea water, as reported in section 6.2.2 using different concentrations of carbon source. Cultures were grown in a bench scale batch 2.5-liter bioreactor, Minifors, Infors (Switzerland), using 1.5 liters of working volume. The fermenter was stirred using a turbine that was equipped with Rushton impellers at a speed of 500 rpm. An aeration rate of 1.5 l/min was used in all experiments. Any modification will be noted in the corresponding section. Samples consisting of 10 mL of the fermentation broth were taken as desired. The samples were used to monitor cell growth by evaluating OD600, dry weight of biomass, residual glycerol and glucose concentrations as well as DHA quantification. All assays were conducted in triplicate.

Standard parameters for different Bioreactor types

Reactor type	Temperature (°C)	Agitation (rpm)	Airflow (L/min)	pH
Batch	20	500	1,5	7
Fed-Batch	20	500	1,5	7
Single tank Continuous	20	500	1	7
Two stage Continuous	FT: 28 ST:20	FT: 680 ST: 200	FT: 3 ST: 0.1	FT: 6.5 ST: 7
Three stage Continuous	FT: 28 ST:20 TT:15	FT: 680 ST: 375 TT: 200	FT: 3 ST: 0.4 TT: 0.1	FT: 6.5 ST: 7 TT:7

6.2.5 Bioreactor cultivation with feeding

Bioreactors that include a feeding stream were initiated as batch cultures following the instructions in section 6.2.4. To avoid any contamination, the feeding container as well as the tubing equipment was autoclaved together and connected immediately after sterilization process. Thus, the medium has a temperature of 90ºC avoiding contamination during this procedure. Always use thermoresistant gloves to manipulate the feeding system after sterilization and during the connection procedure. In fed-batch reactor the feeding container was a 2 L Pyrex bottle. In continuous reactors the feeding container was a 5L Pyrex bottle. Moreover, during the connection procedure every important part was gently sprayed with 70% ethanol. In order to avoid any opportunistic microorganism was contaminating into the feeding media even after the mentioned precautions, streptomycin sulphate was added reaching a final concentration of 25 µg/mL.

6.2.6 Kinetic parameters calculation

Specific growth rate (μ, h^{-1}) was evaluated on the basis of values of biomass at the exponential phase of growth as expressed in

$$\frac{dX}{dt} = \mu_g \cdot X$$

Equation 6..

$$\frac{dX}{dt} = \mu_g \cdot X \qquad \qquad \text{Equation 6.2}$$

The growth yield ($Y_{X/S}$) was calculated as the amount of biomass obtained compared to the substrate consumed, as in equation 6.3.

$$Y_{X/S} = \frac{dX}{dS} \qquad \qquad \text{Equation 6.3}$$

where X stands for biomass concentration (g/l) and S for substrate concentration (carbon source, g/l).

Sometimes, calculated yields based on produced biomass can show higher values due to other carbon sources included in the complex ingredients of the media (i.e. triptone, yeast extract adn crude glycerol). This might be particularly important when using crude glycerol as carbon source, which is a complex mixture itself. Accordingly, a set of cultures with different initial carbon source concentration were performed. The resultant final biomass concentration was plotted versus different initial carbon source concentrations (Figure 6.83), showing a linear relationship. The resultant slope is equivalent to the yield of g biomass per g of glycerol added.

y = 0,7037x + 0,2017
R² = 0,9916
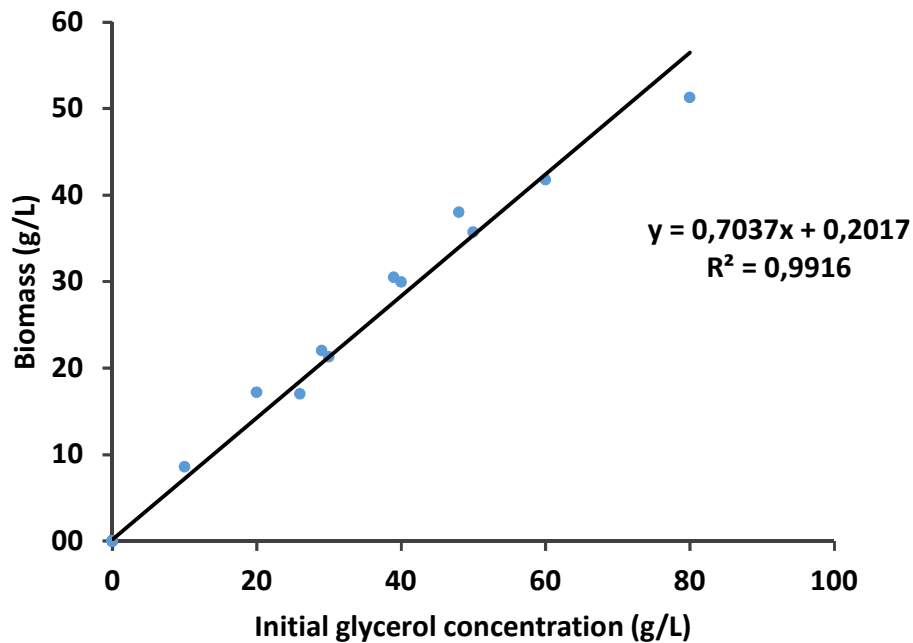
Figure 6.83. Biomass concentration vs Initial glycerol concentration. The slope corresponds to YX/S.

The specific DHA yield, which is the amount of DHA obtained (GC-FID analysis) per gram of biomass, was calculated as in equation 6.4

$$Y_{P/X} = \frac{dP}{dX} \qquad \qquad \text{Equation 6.4}$$

where P stands for product mass (g) and X for biomass (g).

The maximum specific growth rate μ_{max}(h^{-1}) was the maximum of the specific growth rates calculated during the exponential growth phase, as expressed in

$$\frac{dX}{dt} = \mu_g \cdot X \qquad\qquad \text{Equation 6.}$$

The net specific growth rate μ_{net}(h^{-1}) was calculated between the inoculation and the end of the exponential growth phase, using

$$\frac{dX}{dt} = \mu_g \cdot X \qquad\qquad \text{Equation 6.}$$

Therefore, μ_{net} includes the lag phase.

The affinity or semi-saturation constant or K_S, is the concentration of substrate that causes a $\mu_g = 1/2\,\mu_{max}$. The value reported is an average of the repetitions, where K_S was determined using a graphical approach by the linearization of Monod equation in a batch scenario. According to the Equation 6.7,

$$\frac{1}{\mu_g} = \frac{K_S}{\mu_m} \cdot \frac{1}{S} + \frac{1}{\mu_m} \qquad\qquad \text{Equation 6.7}$$

where μ_g is the specific growth rate, Ks the saturation constant, S the substrate concentration and μ_{max} is the maximum growth rate. Using the Lineweaver-Burk double reciprocal plot ($1/\mu_g$ vs $1/S$), as used in the Michaelis-Menten enzymatic kinetic determinations, the resultant slope equals to $\frac{K_S}{\mu_m}$.

Using a similar approach, the maintenance coefficient was calculated (g carbon source / g biomass · hour). According to the equation 6.8

$$\frac{1}{Y_E} = \frac{1}{Y_G} \cdot + \frac{m_s}{\mu_g} \qquad\qquad \text{Equation 6.8}$$

where Y_E is the overall yield, Y_G is the specific growth yield, m_s the maintenance coefficient and μ_g the specific growth rate. In this case, the slope is equal to the maintenance coefficient value.

6.2.7 Monod kinetic parameters calculation using a Chemostat

From data collected using a chemostat, Monod Equation kinetic parameters can be obtained. Data include S at several dilution rates D. Any continuous reactor in this thesis was started after a batch culture. After the batch stage is finished, the feeding is initiated and set up to ensure the lowest D possible. Thus, the biomass reached the highest concentration possible in a continuous operation mode. After the biomass concentration is stabilized, D is increased and the feeding was maintained during 3 days. The flow was increased every 3 days to determine *A. limacinum* performance in different D value conditions.

Rearranging equation 4.9, equation 6.9 is obtained:

$$\frac{1}{D} = \frac{1}{\mu_{max}} + \frac{K_S}{\mu_{max}} \cdot \frac{1}{S} \qquad\qquad \text{Equation 6.9}$$

Using S points obtained at different D rates, 1/D vs 1/S was plotted according the Linwaeber-Burk linearization of Monod equation 6.6, at steady state situations. Using every plotted points, a regression line was calculated. The slope m corresponds to Ks/μ_{max} and the intercept corresponds to $1/\mu_{max}$.

In order to determine maintenance coefficient m_s the following equation was used

$$\frac{1}{Y_{X/S}^{AP}} = \frac{1}{Y_{X/S}^{M}} + \frac{m_s}{D}$$

Equation 6.10

According to equation 6.7 m_s was calculated by plotting $\frac{1}{Y_{X/S}^{AP}}$ versus $\frac{1}{D}$. The slope is equal to the maintenance coefficient and the intercept is equal to $\frac{1}{Y_{X/S}^{M}}$. Thus, kd can be calculated using equation 6.8.

$$m_s = \frac{k_d}{Y_{X/S}^{M}}$$

Equation 6.11

6.2.8 Dry cell weight

Dry weight of biomass was determined after centrifugation of 10 ml of the sample (Sigma 1-14 Microfuge) at 4000 rpm for 15 min. The pellet was rinsed with a saline solution (5 g/L) and centrifuged again. Then it was lyophilized (LyoAlfa 6 freeze drier, Telstar Spain) and finally weighted. The result off different sample measurements are plotted in Figure 6.84.
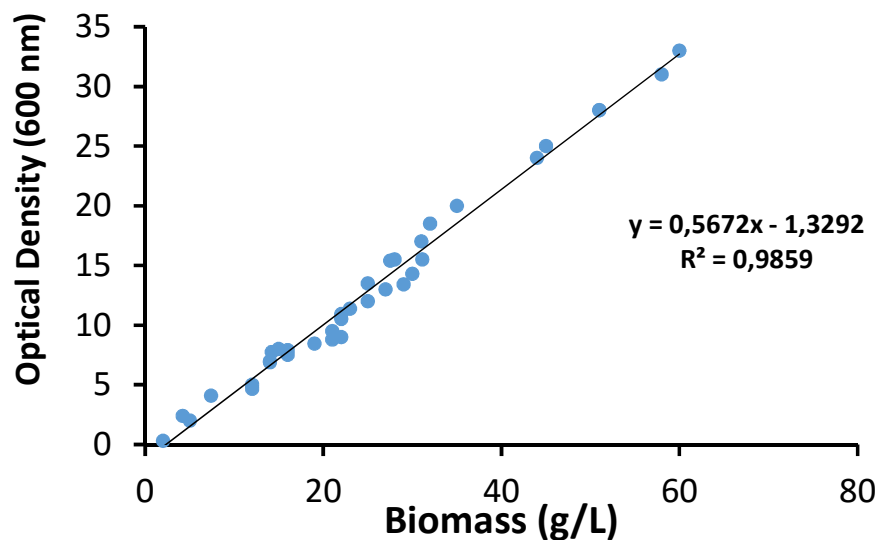
Figure 6.84 Different samples OD vs resultant biomass concentration (based on dry cell weight after lyophilized).

6.3   Glycerol quantification

6.3.1   Sample preparation

For residual glycerol determination, fermentation samples were centrifuged at 4000 rpm (Sigma 3-16K, Germany), for 5 min at 5ºC. The supernatant was collected for direct analysis or stored at -80ºC to avoid possible zoospore proliferation, until the sample was analysed.

6.3.2   HPLC analysis

For crude glycerol determination using HPLC, a calibration curve was prepared by a series of dilutions in the range of 0 to 10 g/L. Dilutions were prepared with artificial seawater media instead of water because to reproduce the conditions of fermentation, it was necessary to mimic salinities found in the ocean where the microorganism naturally grows. In this case, 18 g/l of sodium chloride and other salts in minor amounts were used. Citric acid (Sigma-Aldrich, Spain) was added as an internal standard.

An HPLC 1100 series from Agilent Technologies® equipped with a Transgenomic™ ICSep COREGEL 87H3 column and a refraction index detector (RID), was used for glycerol analysis. A column temperature of 80ºC was used. The mobile phase was 0.04N sulphuric acid in MilliQ water at 0.4 ml/min. The concentration of sulphuric acid was higher than usual, to avoid column damage from the cationic load of the seawater. The injection volume was 10 µl of sample. Chromatograms were analysed with ChemStation Software from Agilent Technologies®.

6.3.3   Analysis with an enzymatic kit

K-GCROL kit (Megazyme International) uses tablets that contain nicotinamide-adenine dinucleotide (NADH), adenosine-5'-triphosphate (ATP) and phosphoenolpyruvate. Glycerol is phosphorylated by ATP to L-glycerol-3-phosphate in the reaction catalysed by glycerokinase. The adenosine-5'-diphosphate (ADP) formed in the reaction reconverted by phosphoenolpyruvate (PEP) with the aid of pyruvate kinase into ATP with the formation of pyruvate. In the presence of L-lactate dehydrogenase, pyruvate is reduced to L-lactate by oxidizing NADH which is stoichiometric with the content of glycerol and can be measured by the decrease in absorbance at 340 nm.

6.3.4   Analysis with a Dot Blot assay

Plates of silica gel 60 F_{254} (Merck, Germany with a height of 10 cm and variable lengths were used. Two microliters of supernatant samples were spotted. Spots must be separated by at least 7 mm, because concentrated samples tend to suffer from considerable diffusion on DB. After spotting, the samples must be immediately dried by heated air. To visualize the spots, a solution of potassium permanganate (Sigma Aldrich, Spain) 37 mM, potassium carbonate 0.29 M (Panreac, Spain) and 0.05% NaOH (Panreac, Spain) in MilliQ water was added. Then, spots were scanned with HP ScanerJet 5100 (resolution of 1200 ppi). The scanned Dot Blot layer was processed and the resulting image was analysed using Matlab®® (Mathworks Inc., MA).

6.3.5   Comparison of Glycerol quantification methods during the cultivation

A cultivation of *A. limacinum* was monitored in order to evaluate DotBlot capabilities to measure crude glycerol compared to the other methods. Immediately after pumping the samples out of the reactor, they

were kept in a cold room (ca. 5ºC). All of the samples were analysed at the same time. Three replicas were analysed for each method.

6.4 Fatty acids determination and quantification by HRGC

6.4.1 Biomass lyophilisation

A. limacinum cells were harvested and centrifuged at 4000 rpm during 15 min at 5ºC. Supernatant was collected and stored at -20 ºC to perform glycerol analysis. The pellet was collected and stored at -80 ºC during 24 h. After this period samples were lyophilized individually using a LyoAlfa (Telstar, Spain).

6.4.2 Original glassware sample preparation

To prepare the sample, FA methyl esters (FAME) were synthesized using a one-step extraction-transesterification method as described originally by Majid et al. (1999) and Indarty et al. (2005). They were then adapted for the microorganism's lipid extraction. The biomass was weighed (20 mg) using clean, 10mL screw-top glass balloons, to which 4mL fresh solution of a mixture of methanol, concentrated sulphuric acid, and chloroform (1.7:0.3:2.0 v/v/v) was added. The balloons were closed with a Graham refrigerator which were tightly sealed with a Teflon cap to avoid leakage. Every balloon was weighed to evaluate leakages. Transesterification (without prior extraction) was studied at different combinations of temperature and reaction time. On completion of the reaction, the balloons were cooled down to room temperature and weighed again to dismiss leaking samples. Then, 1mL of distilled water was added to the mixture and thoroughly vortexed for 1 min. After the formation of two phases, the lower phase containing FAME was transferred to a clean, 10mL balloon and dried with anhydrous Na_2SO_4. Then, every sample was analyzed using gas chromatography.

6.4.3 New sample preparation method

FA analysis was performed in triplicates, and consisted of two consecutive steps; the preparation of FAME and the chromatographic analysis. FAME were synthesized by a four-in-one step procedure. The method is a modification of Indarti et al. adapted to extract and transform triglycerides to methylated fatty acids (FAMEs) from microorganisms. In a 2 mL glass vial, lyophilized biomass was weighed (5 mg) and dissolved in 500 µL fresh methanol, sulfuric acid and chloroform (1.7:0.3:2 v/v/v) mixture. The vials were sealed with aluminum crimp caps to avoid volume los during the Fischer reaction. To do so, samples were maintained in a water bath at 80 °C during 30 min. After that samples were cooled during 2 min at room temperature. Then 100 µL of water were added to separate two phases, having FAMEs dissolved in chloroform.

Chloroform phase was collected and analyzed by HRGC 7890GC (Agilent technologies, Waldbronn, Germany) equipped with a flame ionization detector and Supelco SP™-2380

6.4.4 High resolution gas chromatography (HRGC) with a flame ionization detector (FID)

The chloroform phase was then collected and analysed with an HRGC 7890GC (Agilent technologies, Germany) that was equipped with a flame ionization detector and a Supelco SP™-2380 (60 m x 0.25 mm x 0.20 µm) capillary column. The oven temperature was programmed to run at 210 ºC for 4 minutes, then 2 ºC / min. to 230 ºC for 5 minutes and then 15 ºC to 255 ºC for 0.5 min. The injection module was heated above oven temperature, 250 ºC, with a split ratio and flow of 33:1 and 33 mL/min. respectively. Helium

was used as carrier gas at a linear velocity of 24.28 cm/sec. The detector was heated to 250ºC. Different fatty acids were identified by comparing the retention times with those of standard fatty acids (Sigma-Aldrich, Spain), such as DHA (ref. D2534-100MG) and P (ref. P0500-10G).

6.5   *A. limacinum* life characterization

6.5.1   Microoscopy and Matlab® algorithm

A random, 2 µL sample of *A. limacinum* was taken from the culture and deposited on a glass microscope slide. After covering the culture drop with a cover slip, the sample was then analysed at magnification of 40x 100x 400x and 1000x. For crystal violet staining, cells were dried after deposition on a cover slip and then left with a small volume of the dye. Thereafter, the sample was rinsed with miliQ water and analyzed by microscopy. Stored pictures were processed using a Matlab® algorithm (Appendix C) that was specially adapted for this purpose. This method was validated with laser scattering equipment (Saturn Digisizer 5200), to measure the diameter of *A.limacinum* cells.

6.6   Determination and quantification of squalene

6.6.1   Extraction of squalene

In order to extract squalene, a sample of 100 mg of lyophilized biomass was put in a glass tub with 6 mL of methanol:chloroform (v/v) mixture. The tube was vortexed for 30 seconds. Then, the samples were incubated overnight using mild agitation (100 rpm – orbital shaker). Thereafter, 2 mL of the same mixture were added to an additional 2mL water. The tube with the sample was agitated and centrifuged at 3000 rpm during 5 minutes. Three clear phases were expected to appear. The upper and middle phases were discarded, while the lower phase was collected in a glass balloon to be rotavaporated. Once evaporated, the sample was suspended in a known volume of chloroform. At that point, the sample was ready to be analysed.

6.6.2   Analysis of squalene using HRGC-FID

The sample was analysed using an HRGC 7890GC device (Agilent technologies, Germany) equipped with a flame ionization detector and an HP-5MS-UI (30 m x 0.25 mm x 0.25 µm) capillary column. The oven temperature was programmed at 170 ºC. A ramp of 10 ºC/min. was immediately applied, until reaching a final temperature of 280 ºC. The final temperature was maintained for an additional 10 minutes. The injection module was heated to 250 ºC, with a split ratio and flow of 20:1 and 1 mL/min. The detector module was heated to 275 ºC. Helium was used as a carrier gas.

6.7   Determination and quantification of astaxanthin

6.8   Determination of organic acids

Bioreactor samples were centrifuged at 4000 rpm (Sigma 3-16K, Germany), for 5 minutes at 5ºC. The supernatant was collected for organic acids determination using HPLC. A set of different organic acid standards were injected. An HPLC 1100 series from Agilent Technologies® equipped with a Transgenomic™ ICSep COREGEL 87H3 column and a refraction index detector (RID) was used for glycerol analysis. A column temperature of 80ºC was used. The mobile phase was 0.04N sulphuric acid in MilliQ water at 0.4 ml/min. The concentration of sulphuric acid was higher than usual conditions to avoid column damage from the cationic load of seawater. The injection volume was 10 µl of sample. Chromatograms were analysed with ChemStation Software from Agilent Technologies®.

6.9 Downstream processing

6.9.1 Microalgae biomass preparation (for cell disruption)

A. limacinum was grown in a 2 L bioreactor (Sartorius Stedim Biotech BIOSTAT® BPlus culture system equipped with a 2L UniVessel BB-8846906) using enriched artificial seawater. An enriched artificial seawater culture solution with the following components (per L) was used: 18 g NaCl, 2.44 g $MgSO_4$, 0.6 g KCl, 1.0 g $NaNO_3$, 0.3 g $CaCl_2 \bullet 2H_2O$, 0.05 g KH_2PO_4, 1 g Tris, 0.027 g NH_4Cl, $15x10^{-8}$ g vitami45n B12 combined with 10 mL/L metal solution, and 3 mL/L chelated iron solution as reported in Chi *et al.* [47] and Starr & Zeikus [48]. The culture was maintained at 20 ºC for one week with more than 50 % dissolved oxygen. The cells were collected by centrifugation (Eppendorf 5810 R centrifuge, USA) at 4000 rpm for 15 min at 5ºC. 750 mg of cells were collected and suspended in 10 mL of a solution containing 30 g/L glycerol and 10 g/L NaCl to prevent any cell disruption. The cell concentration in each 10 mL aliquot was 7.5% solids. The mixture was stored at -20 ºC for the experiments.

6.9.2 Disruption of *A. limacinum* by sonication

A 10 mL aliquot (see section above) of cells was thawed and centrifuged using a benchtop Sigma 2-16HKL centrifuge at 4000 rpm for 15 min at 5ºC. The resulting pellet was recovered and suspended in 10 mL of methanol (Sigma-Aldrich, USA; 32213-2.5L-D) or chloroform (Sigma-Aldrich, USA; 288306-1L), maintaining 7.5 % solids (v/v) concentration for the process. Cells were disrupted using a bench scale sonicator (Misonix s-4000, USA) with an output voltage of 1kV and a frequency of 20 kHz. The sonication system was equipped with a 13-mm tip connected to a standard ½-inch diameter tapped horn. The amplitude was set at 70% of the system's capacity with pulses of 3 seconds followed by 5 seconds of cooling until reaching the desired total energy.

Sonication at each condition was performed on 3 replicates. The sonication was carried out in a 50 mL Falcon® tube in an ice bath to minimize temperature increase due to sonication. After this, samples were agitated for 10 minutes using a vortex or a plate shaker. To ensure repeatability all the samples were shaken with a titer plate shaker (Thermo Scientific, USA) for 5 minutes. Samples were then centrifuged and the supernatant collected to complete what is referred to as the first extraction. Supernatant was stored while the pellet was collected for a second extraction. This extraction was carried out using fresh methanol. The extraction capacity was gravimetrically quantified to determine the total mass extracted. Extraction of TGs was also quantified by HPLC using a UV detector.

6.9.3 Gravimetric quantification of *A. limacinum* extract

A 1.5 mL volume of *A. limacinum* clarified lysate (with methanol as solvent) was transferred to a previously weighed Eppendorf tube. Lysates were then dried using a Vacufuge™ Concentrator (Eppendorf, Westbury, NY, USA). The concentrator was operated at 1400 rpm and 30 ºC with a vacuum pressure of 20 mbar. The samples were processed until the mass stabilized. The extracted content in each vial was then gravimetrically quantified by subtracting the weight of the Eppendorf tube from the gross weight of the tube/residue.

6.9.4 Fatty acid profile quantification by gas chromatography

Total fatty acid content and fatty acid composition were also determined in *A. limacinum* lysate. Fatty acid analysis was performed in triplicate and consisted of two consecutive steps: preparation of fatty acid methyl esters (FAME) and analysis by gas chromatography. The method used is detailed in section New sample preparation method and High resolution gas chromatography (HRGC) with a flame ionization detector (FID).

6.9.5   HPLC for TG analysis

To analyze TG as part of process development, a basic HPLC procedure was established and used. It was performed using a Shimadzu Prominence HPLC system (Shimadzu Corporation, Kyoto, Japan) consisting of a double LC-20AS pump, SIL-20AC auto-sampler, a system controller CBM-20A, a column chamber CTO-20A, and a SPD-M20A photodiode array (PDA) detector operating with both the deuterium (D2) lamp and tungsten (W) lamp. A Kromasil® C18 reversed-phase column with a 5μ particle size, 100Å pore diameter, and dimensions of 250 mm x 4.6 mm was installed. TGs were resolved with 40 minutes of isocratic operation using a 2:3 v/v mixture of methanol (Sigma-Aldrich, USA; 32213-2.5L-D) to hexane (Sigma-Aldrich, USA; 34484-2.5L), followed by a linear gradient from 60% methanol in hexane to 100 % methanol over 60 minutes. Wavelength acquisition was set up at 190 nm - 230 nm. The cell measuring temperature was set to 40 ºC and the column chamber was set to 30 ºC.

Individual peaks for TGs produced by *A limacinum* were identified as follows: retention time as a function of ECN was determined using known TGs from a standard mixture purchased from Sigma-Aldrich (described below). That standard mixture did not contain many of the TG expected in *A limacinum* lysate. But the peaks resulting from injections of *A limacinum* lysate could be easily identified based on retention time since ECN (and therefore retention times) are known for the TG previously reported to be produced by *A limacinum* [43].

6.9.6   Chromatography method (process) development

Development of a reversed-phase chromatography method for purification of TGs from *A. limacinum* was performed using the same Shimadzu Prominence HPLC system (Shimadzu corporation, Kyoto, Japan) described previously for analysis of TGs. Data and chromatograms were collected using LabSolution software (Shimadzu Corporation, Kyoto, Japan). The autosampler was programed to clean the needle with hexane. Wavelength acquisition was set at 190 nm 500 nm. The cell measuring temperature was set to 40 ºC and the column chamber was set to 27 or 30 ºC. Different mixtures of hexane (Sigma-Aldrich, USA; 34484-2.5L), methanol (Sigma-Aldrich, USA; 32213-2.5L-D) and ethanol (Sigma-Aldrich, USA; 34870-2.5L) were used as mobile phase during the work. Reversed-phase resins used in this study are listed in Table 6.43.

Table 6.43 Reversed-phase columns used for method development and scale up.

Brand	Resin Type	Bead Size (µm)	Pore Size (Å)	Length (mm)	Column Diameter (mm)
Alltech® RP18	C18	5	100	250	4.6
Jupiter®	C4	5	300	250	4.6
Kromasil®	C18	5	100	250	4.6
Kromasil®	C18	16	300	250	4.6

Initial chromatography method development relied on purchased triglycerides. TG standards containing DHA are not commercially available; therefore, TGs were purchased with equivalent carbon numbers (ECNs) similar to those for TGs previously reported by Nakaharah et al. [43] from *A. limacinum*. The ECN for a TG is defined as follows: ECN = number of carbon atoms – 2x the total amount of double bonds.

There is a linear relationship between ECN and k´, the chromatographic retention factor. Because of this relationship, retention times for two different TGs with the same ECN will be the same, using the same

chromatographic method. By matching ECN values of standards to ECN for TGs obtained from *A. limacinum* lysate, chromatographic performance between purchased TGs and *A. limacinum* TGs should be similar. Detailed information regarding TGs in the standard sources is found in Table 6.44.

Table 6.44 TGs in purchased mixtures used in this study. Fatty acid abbreviations are as follows: P=palmitic acid; M=myristic acid; Ln=α-linolenic acid; L=linoleic acid; O=oleic acid; G=gadoleic acid; E=erucic acid; S=stearidonic acid. All TGs making up the Sigma-Aldrich standards are unsaturated. The omega-3/palm oil mixture contains both unsaturated and saturated TG (. Trierucin 0.9 mg/mL, Tri-11-eicosenin 0.7 mg/mL, trilinolenin 0.91 mg/mL, trinolein 0.96 mg/mL, trioelin 0.99 mg/mL, tripalmitin 1.15 mg/mL and trimysristin 1.04 mg/mL).

Sigma-Aldrich standards		Omega-3 pill/palm oil mixture	
TG	**ECN**	**TG**	**ECN**
LnLnLn	36	LLO	44
MMM	42	LLP	44
LLL	42	LOO	46
PPP	48	LOP	46
OOO	48	LPP	46
GGG	58	OOO	48
EEE	64	POO	48
		PPO	48
		PPP	48
		SOO	50
		SOP	50
		PPS	50

6.9.7 Mass spectrometry for TG identification (MALDI-TOF)

MALDA-TOF mass spectrometry was used to identify peaks eluting from the process chromatography method using Shimadzu Prominence HPLC system (Shimadzu Corporation, Kyoto, Japan). Collected samples were concentrated by evaporation using an Eppendorf Vacufuge plus (Eppendorf, USA) and dissolved in a 50% by volume solution of acetonitrile and water for a total volume of 4 mL. Analysis by mass spectrometry were carried out using 2 µL volume of the purified TG. Measurements were performed using a MALDI-TOF Axima system. The laser frequency was 50 Hz, the acceleration voltage was 20 kV, and the extraction delay time was 200 ns. The spectra were recorded in linear positive mode within a mass range of 500 to 1300 m/z.

This page intentionally left blank

Appendix A: Experimental design tools

7.1 Experimental Design (Part I)

Experimentation is one of the most common activities performed by researchers; including scientists and engineers. The results of the experiments offer insight for a wide range of applications from social science to biotechnology. Experimentation is used to understand and/or improve a system. The system may be simple or complex, and it can result in either a product or a process. This work has applied different DoE in order to develop and optimize a bioprocess. In any experimentation, the investigator attempts to determine the effect that input variables have on the output/performance of the product process. This enables the investigator to determine the optimum settings for the input variables.

Experimental design is a body of knowledge and techniques that help the researcher conduct experiments economically, analyse the data, and make connections between the conclusions from the analysis and the original objectives of the investigation. The application of DoE in this thesis is for; the development of the analytical methods found in chapter 2 and the investigation and optimization of the biotechnological process that is explained in chapters 3, 4 and 5. The traditional approach to industrial and scientific investigation is to employ trial and error methods to verify and validate the theories that may be advanced to explain a certain observed phenomenon. This may lead to prolonged experimentation without useful results. The approaches include experimentation that looks at one factor at a time (box 2.1), several factors individually[90], several factors all at the same time[91] and full factorial designs[92]. Full factorial designs are orthogonal, which means that there are an equal number of test data points under each level of each factor. By taking advantage of this property, both the factors and the interactions can be estimated. These approaches have many variations and statistical modifications.

A full factorial design is very powerful but is only acceptable when working with a few factors. When several factors need to be investigated, the number of experiments to be run with a full factorial design is very large. For this reason, statisticians have developed more efficient test plans, which are referred to as fractional factorial experiments. These designs use only a portion of the total possible combinations to estimate the main factor effects and only some of the interactions. The main reason for designing the experiment statistically is to obtain unambiguous results at a minimum cost. The statistically designed experiment permits simultaneous consideration of all possible variables that are expected to have a bearing on the problem under consideration and as such, even if interaction effects exist, a valid evaluation of the main factors can be made. From a limited number of experiments, it would be possible to uncover the vital factors that would lead to further trials in which the researcher could determine the most desirable combination of factors to potentially yield the expected results.

The statistical principals employed in the design and analysis of experimental results assure impartial evaluation of the effects on an objective basis. The statistical concepts used in the design, form the basis for a statistical validation of the results from the experiments. The statistical foundations for the design of experiments and the **Analysis of Variance** (ANOVA) was first introduced by Sir Ronald A, Fisher, who was curiously, a biologist. ANOVA is a method for partitioning total variation into accountable sources of variation in an experiment. It is a statistical method used to interpret experimented data and make

197

---

[90] Evaluate different factors modifying only one per experiment.
[91] Evaluate different factors modifying all per experiment.
[92] An orthogonal experimental design in which every experiment includes one or multiple modifications of the factors, ensuring the investigation of every possible combination.

decisions about the parameters that are under investigation. More information about ANOVA can be found in section 7.3.1.1.

> ### Box 2.9. Experimental design terminology
>
> **Factor**: A variable or attribute that influences or is suspected of influencing the characteristic being investigated. All input variables which affect the output of a system are factors. Factors are varied in the experiment, can be controlled at fixed levels or set at levels of interest. They can be qualitative (*e.g.* shape of the Erlenmeyer) or quantitative (*e.g.* temperature).
>
> *Levels of factors*: The values of factors being investigated in an experiment. If the factor is an attribute, each of its states is a level, *e.g.* an Erlenmeyer with deflectors or not. If the factor is a variable, the range is divided into the required number of levels.
>
> *Response*: The output obtained from a trial of an experiment, e.g. the production of DHA.
>
> *Degrees of freedom*: A degree of freedom in a statistical sense is associated with each piece of information that is estimated from the data. In other words, it equals the total number of samples/responses minus 1.
>
> *Orthogonality*: The combination of factors with different levels in a factorial design conforms a matrix of values grouped in vectors. Two vectors are orthogonal if the sum of the products of their corresponding elements is 0. For example, consider the following vectors *a* and *b*:
>
> $$a = \begin{pmatrix} 2 \\ 3 \\ 5 \\ 0 \end{pmatrix} \qquad b = \begin{pmatrix} -4 \\ 1 \\ 1 \\ 4 \end{pmatrix} \qquad \begin{aligned} a \cdot b &= 2(-4) + 3(1) + 5(1) + 0(4); \\ &-8 + 3 + 5 + 0; \\ a \cdot b &= 0 \end{aligned}$$
>
> This shows that the two vectors are orthogonal.

7.2   Taguchi Methods

The construction of fractional replicate designs generally requires good statistical knowledge on the part of the investigator and is subject to some constrains that limit the practical applicability and ease of conducting experiments. For this reason, Dr. Genichi Taguchi suggested the use of **Orthogonal Arrays** (OAs)[93] for designing the experiments. He has also developed the concept of the linear graph[94], which simplifies the design of OA experiments. These designs can be applied by engineers and scientists without acquiring advanced statistical knowledge. The main advantage of these designs lies in their simplicity; they are easily adaptable to more complex experiments that involve a number of factors with a different number of levels. They provide the desired information with the least possible number of trials and yet yield reproducible results with adequate precision.

The basis of Taguchi's methods is the *additive cause-effect* model. To explain this model; suppose there are two factors, e.g. temperature and time of culture, which influence a process. Let α and ß be the effect that the temperature and time of culture factors respectively, had on the response variable *Y*. Taguchi

---

[93] OAs where mathematical invention is dated in early 1987 by Jacques Hadamard, a French mathematician.
[94] Taguchi's linear graphs are graphical representations of the columns and their interaction in an orthogonal matrix. This allows for better planning of an experiment, predicting which factors and interactionds could be analysed before starting the experiments.

showed that in many practical situations, these effects can be represented by an *additive cause-effect* model. This model has the following form:

$$Y = \mu + \pmb{\alpha_i} + \ss_j + \pmb{e_{ij}}$$
<div align="right">Equation 7.1</div>

where μ is the mean value of *Y* in the region of experiment, α_i and $\ss_j$ are the individual or main effects of the influencing factors (temperature and time of culture) and e_{ij} is the error term.

The term main effect designates the effect on the response *Y* that can be attributed to a single process or design parameter, such as temperature. In the additive model, it is assumed that interaction effects are absent. The additivity assumption also implies that the individual effects are separable. Under this assumption, the effect of each factor can be linear, quadratic or higher order. When interactions are included, the model becomes multiplicative or non-additive. In other words, the model becomes more complex. The Taguchi methods will facilitate the experimentation when there are complex scenarios.

The Taguchi method offers the perfect opportunity to apply DoE due to its simplicity and capacity to identify the proper factors. In Chapter 2, the Taguchi methods will be applied to the analytical chemistry that will be discussed.

7.3   Analytical Methods statistics

3 main analytical methods (two for glycerol quantification and one for DHA quantification) have been developed and documented. This includes the quantification and monitoring of glycerol consumption, fatty acids profile determination and DHA quantification, and the microscopy based measurements of cell dimensions and its qualitative analysis. DHA quantification is done with the challenging sample preparation method and the *High Resolution Gas Chormatography* (HRGC) method. This research has also used other general analytical procedures, which haven't been developed during the research and that are explained in the Materials and Methods section (chapter 2.2).

> *Box 2.17. Nomenclature of arrays*
> Every matrix used in this thesis will be indicated in the corresponding experiment section. For more information about how to apply Taguchi methods see Appendix B.
>
> L = Latin square
>
> $L_a\ (b^c)$ a =number of rows
>
>   b = number of levels
>
>   c = number of columns (factors)
>
> Degrees of freedom associated with the OA = a -1

7.3.1.1 Sum of squares

In many applications, the **sum of squares is an important tool**. It allows the determination of factors effects on any experiment to which it is applied. This tool is used when it is necessary to look at distance, because the sum of squares (SS) is a mathematical calculation of distance. In order to know how far one sequence of numbers is from another, it is possible to simply take the differences between the corresponding terms in the two sequences, and add them. However, if that method is used, the cancellation of positive and negative terms would be achieved and the sequences would seem closer together than they actually are. Objects of interest for mathematicians are actually quadratic forms. It is important to note that the sum of squares is a special type of quadratic form.

A metric or distance function is a function *d(x,y)* that defines the distance between the elements of a set as a non-negative real number. If the distance is zero, both elements are equivalent under that specific metric. Distance functions thus provide a way to measure how close two elements are. These elements do not have to be numbers but can also be vectors, matrices or arbitrary objects. Distance functions are often used as error or cost functions that can be minimized in an optimization problem.

In this context, SS represents a measure of variation or deviation from the mean. It is calculated as a summation of the squares of the differences from the mean. The calculation of the total sum of squares (SS_T) considers both the sum of squares from the factors (SS_E) and from residuals[95] (SS_R). In this work, the SS has been used for both **ANOVA** and linear regression secondary calculations. In ANOVA from Pareto that was used in this thesis, the total sum of squares helps express the total variation that can be attributed to various factors and it also helps to determine its contribution. Converting the sum of squares into mean squares by dividing by the degrees of freedom allows researchers to compare these ratios and determine whether there is a significant difference due to factor. The larger this ratio is, the more the treatments affect the outcome.

In ANOVA, mean squares are used to determine whether factors are significant.

> ➤ The factors of the mean square are obtained by dividing the treatment sum of squares by the degrees of freedom. The factors mean square represent the variation between the sample means.
> ➤ The mean square of the error (MSE) is obtained by dividing the sum of squares of the residual error by the degrees of freedom. The MSE represents the variation within the samples.

In linear **regression**, the total sum of squares helps express the total variation of the y's.

The total sum of squares or proportional variance is defined in Equation 7.2.

$$SS_T = \sum_i (y_i \quad \bar{y})^2$$
Equation 7.2

In addition, $SS_T = SS_R + SS_r$, defined in Equation 7.3 and Equation 7.4, respectively.

$$SS_R = \sum_i (f_i \quad \bar{y})^2$$
Equation 7.3

$$SS_r = \sum_i (y_i \quad f_i)^2$$
Equation 7.4

By comparing the regression sum of squares to the total sum of squares, it is possible to determine the proportion of the total variation that is explained by the regression model. R2, the coefficient of determination will be explained in the following section.

---

[95] Residual of an observed value is the difference between the observed value and the estimated value.

7.3.1.2 Assay attributes

The development of an efficient and reliable biotechnological process is dependent on having suitable analytical methods. This means that it is important that work on analytical methodology for the bioproduct of interest, is initiated at the very beginning of process development. Analytical studies are important throughout the development and a scale up of the process is also necessary, because changes can occur either to the product or to its associated impurities. This chapter will explain the basic attributes that are required for any analytical procedure in order to show its usefulness.

Precision is a measure of the reproducibility of an assay. Precision is expressed as a relative standard deviation, defined as the standard deviation divided by the mean response, also known as the coefficient of variation (CV). Typically, this is converted to a percentage. The precision indicates the likelihood that a repeat test will have the same result. Assays that result in a precision that is greater than 5% are generally unacceptable. Precision is evaluated based on standard deviation (SD), which can be seen in equation 7.5.

$$SD = \sqrt{\frac{\sum_{i=1}^{n}(x_i - \bar{x})^2}{n-1}}$$

Equation 7.5

where $\bar{x}$ the mean of n measurements, and x_i is an individual measurement. At least three replicates must be made before a meaningful standard deviation can be determined. The standard deviation is an estimate of the true variability of the assay, based on a limited sample. The true variability requires infinite replicates to measure. Almost all measurements in this thesis have done three replicates unless the specific situation made it difficult to achieve. For example, in cases where the research implied several cultures with several samples per culture, the replicates had to be reduced for logistic constraints.

Accuracy is a measure of closeness of the assay result to the "true value". Accuracy is often measured on the basis of the recovery of pure product added into the sample. Therefore, this can be easily measured by adding an internal standard during the sample preparation and by analysing the recovery of this product. The analytical method needs to be calibrated on a curve in order to quantify it. When working with FA, internal standards are normally odd FAs which are either rare or non-existent in nature.

Specificity is the ability of the method to distinguish between the analyte and similar components. This means that no other molecules in the sample matrix interfere with the quantification of the target molecules. Therefore, the purity can be demonstrated with the resolution between the species that were analysed.

The **linearity** of a method is its ability to produce a response that is proportional to the concentration of the analyte. Linearity is assessed by creating a standard curve for the analyte by a linear least-square fit of the response against the concentration. The correlation coefficient (r^2) is the measure of the linearity and is defined as indicated in *Equation 7.6* which is based on *Equation 7.2* and *Equation 7.3*.

$$r^2 = 1 - \frac{SS_r}{SS_T}$$

Equation 7.6

Where SS_E is the sum of squares that was introduced in section 7.3.1.1 and SS_T is the total sum of squares as explained in 7.3.1.1. The square of the correlation coefficient varies over the range $0 \leq r^2 \geq 1$ and is a measure of the amount of variability in the data explained or accounted for by the linear model. Linearity is important because responses from assays for any given analyte amount assayed may not always be identical. Assays become nonlinear at both high and low concentrations, where detectors become

saturated or when noise becomes a significant proportion of the response. The slope is the response factor or signal, whose intercept should be zero. If the intercept is not zero, there may be some noise present, especially at lower limits of the calibration curve.

For this reason, it is important to determine the limit of detection (LOD) and the limit of quantification (LOQ), which are precise measurements made at the lower extreme of the linearity curve. LOD and LOQ can be determined in three different ways: based on visual evaluation, based on signal to noise ratio and based on the residual standard deviation (RSD) of the response and the slope of the linear regression. For this work, RSD is used to calculate the LOD and LOQ for the current method. The calculation is done as expressed in Equation 7.7.

$$RSD = \frac{\sqrt{\Sigma(Y-Yest)^2}}{n-2}$$
Equation 7.7

where Y is the obtained response, Y_{est} is the calibration curve estimated response and n is the number of samples per replicate. Once RSD is obtained, all data is available to calculate LOD and LOQ. LOD is considered to be 3 times RSD divided by the slope while LOQ is considered 10 times RSD divided by the slope.

Range refers to the upper and lower limits within which the assay can produce accurate and precise results. Normally, these limits are delimited by the particular slope linearity and by the LOD and LOQ at lower limits. For example, in the quantification of DHA, the upper limit of the range would be delimited by the last data point maintaining the linearity of the method whereas the lower limit would be set by the LOQ, which equals the minimum concentration that can be quantified precisely.

Robustness refers to the assay conditions. This can be defined as the capacity to be reliable despite unpredicted minor changes of the method conditions. Robustness is not generally evaluated, because if a method is not robust, it will result in low accuracy and imprecise statistics.

7.4   Experimental design (Part II)

As already explained in the introduction of chapter 2, the thesis presented here not only looking for documentation of a bioprocess development. It also aims to serve as a guide providing information about different optimization techniques. In this chapter two new techniques were used which need to be introduced. Those techniques are artificial neural network and response surface methodologies.

7.4.1   Artificial Neural network

Artificial neural networks (ANN) are mathematical models emulating an animal brain acting [231]. They are considered a black box approximation because ANN cannot return information about the system, just to uncover an empirical model between inputs and targets (responses), giving an output. This is a powerful feature, because internal mechanism of any investigated relationship are not needed. ANN can adapt to any set of data with nonlinear relationship making it so powerful for fitting very heterogeneous. It can handle with big amounts of data. Therefore, is a potential tool for bioprocess modeling, where the microorganism mechanisms are unknown.

ANN can have different very different structure but generally are composed of a layer of input neurons, a hidden layer of neurons (or more) and an output data. Every element in ANN is interconnected with the others. Every connection has a parameter which defines it, called weight (W_j). Weights are the variables which, together with the intercept, are modified while the system is learning. In other words, the weights

vary their effect until the target result fits with the validating points. Validation points are the response of experiments which haven't been included for the machine training. This test if the model is adjusted or not.

Adjusting the model in ANN require several iterations of W_j adjustment. This process consists of performing a lineal combination of the W_j which converge in each neuron. Every neuron in the system is a processing unit performing the combination as indicated in Equation 7.8:

$$y = \sum_{i=1}^{n} x_i + w_j + \theta \qquad \text{Equation 7.8}$$

Where xi is the input I, Wj is the weight j associate with every connection and θ is the intercept from every neuron. Then the activation function is applied on the result y from every lineal combination. Activation function is expressed in Equation 7.9:

$$f(y) = \frac{1}{1+e^{-y}} \qquad \text{Equation 7.9}$$

The activation function gives a nonlinear nature to the model and secondly, is normalizing the value calculate in every neuron between 0 and 1. There are other sigmoidal function which could be used for this objective as well. However, this was chosen due to having an easier derivatization. Output neuron is not applying the activation function, because is releasing the results. During every iteration, the system seeks the reduction of the error by using the backpropagation algorithm which decides the new W_j value after every iteration. This process is repeated until error requirements are achieved.

This optimization technique has been used for the medium development in the section 3.3.2 of this chapter.

7.4.2   Response surface methodology

In experimental investigation we study the relationship between the input factors and the response (output) of any process or systems. The purpose may be either to optimize the response or to understand the system. If the input factors are quantitative and are a few, RSM can be used to study the relationship. For example, the influence of NaCl and yeast extract on *A. limacinum* growth. The growth is a function of the levels of NaCl and yeast extract which can be represented as in Equation 7.10.

$$Y = f(X_1, X_2) + e \qquad \text{Equation 7.10}$$

Where e is the observed error of the growth (response) Y.

However, the secret theoretical relationship between two factors and its response is unapproachable. Making some reasonable assumptions about the underlying relationship between the factors and the response an empirical model can be developed. For example, if it is believed that factors X_1 and X_2 are independent and that each has only a first-order effect on the response, then Equation 7.11 is a suitable model.

$$R = \beta_0 + \beta_a X_1 + \beta_b X_2 + e \qquad \text{Equation 7.11}$$

Where R is the response, X1 and X2 are the factors (levels), and β_0, β_a and β_b are adjustable parameters whose values are determined by linear regression and would define the "shape" of the model. Although an empirical model may provide an excellent description of the response surface, it has no basis in theory and could not predict correctly unexplored parts of the explored data.

In a situation where the factors are not independent, an interaction parameter is included, leaving the following first-order Equation 7.12:

$$R = \beta_0 + \beta_a X_1 + \beta_b X_2 + \beta_{ab} X_1 X_2 + e$$
Equation 7.12

Finally, if a first-order empirical model cannot be fitted into the data, it may fit in a second-order models. A second-order model need quadratic terms, which confers curvature to the model. Equation 7.13 corresponds to two factor expression.

$$R = \beta_0 + \beta_a X_1 + \beta_b X_2 + \beta_{ab} X_1 X_2 + \beta_a X_1^2 + \beta_b X_2^2 + e$$
Equation 7.13

Every empirical model can be adjusted by linear and multiple linear regression, but the correct data needs to be collected. Generally, to obtain valuable data for fitting a first-order model, only two levels per factors are needed (2^k DoE)[96]. However, for second-order models 3 levels per factor (3^K DoE) are needed but the experiments demand increases. The most popular 3k factorial design is called Central composite design (CCD). It is used in the next chapter and therefore, introduced.

7.5 Experimental design (Part III)

This is the last part of experimental design techniques introduced. In Chapter 3 ANN and RSM have been introduced, where RSM was built with data from polynomial regressions. In Chapter 4 it is being introduced a new experimental design called Central Composite Design (CCD) that is commonly used to build RSM. CCD has been used for agitation and aeration modeling to be then applied to the multi-stage CSTR approach. Agitation and aeration influence the oxygen transfer rate, therefore, these two parameters will define the best oxygen conditions for biomass growth and DHA production.

7.5.1 Central composite design (CCD) and RSM

The Bow-Wilson CCD is an experimental design commonly used to build response surfaces due to its special characteristics. CCD is composed by a fractional factorial design[97] with a central point (generally 0,0) and "star" or axial (Figure 7.83) points. Hence, it is a hybrid type of DoE. Star points allow describing the plane curvature that defines a response surface. CCD can be applied for 2, 3 and 4 factors k with the levels defined by the architecture of the experimental design as following:

➢ **nF** factorial points (corner cube points) indicated by *+1* and *-1*.
➢ **nC** central points of the design indicated as *0*.
➢ **α** axial or star points. The number of axial points is defined by the number of factors = 2k.

---

[96] Two levels per factor k, which gives the amount of experiments needed.
[97] *A factorial experiment in which only an adequately chosen fraction of the treatment combinations required for the complete factorial experiment is selected to be run. Used to economy high loads of experiments.*
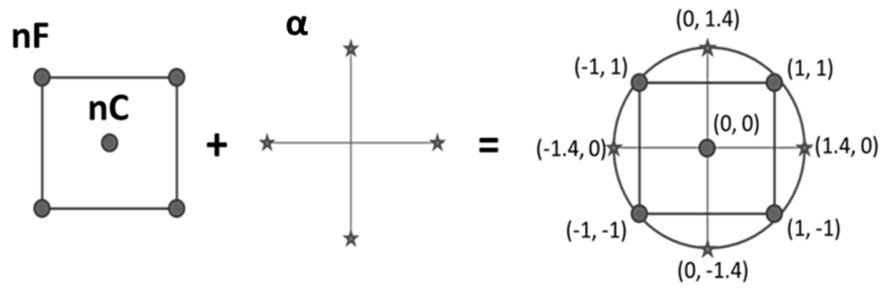
Figure 7.85. Architecture of the spherical CCD used in Chapter 4.

In general, the α selected value ranges between 1 and √k. This value will define the geometric nature of the design. When α is equal to √k the design is called spherical CCD, and is the one used in chapter 4. CDD allows a deeper study of the plane described by factor levels. Moreover, it explores 5 different levels geometrically selected. Then, RS generated through CCD data offers a more precise model as well as an optimization of the factors analyzed. The experimental matrix is detailed in the results section of chapter 4.

205

This page intentionally left blank

Appendix B: Algorithm I

This algorithm was developed exclusively in this thesis for glycerol monitoring in a bioprocess development. Paste of the text below in a Matlab® terminal with Image processing toolbox installed will compute the tool.

```
% Nostromo Algorithm by Sergi Abad Sánchez

tic; % Inici del contador.
clc; % Borrar la pantalla.
clear all; % Borra les variables y matrius emmagatzemades
disp('In the space no one can hear you scream!'); % Missatge d'inici.
workspace; % Fa apareixer el panell de variables de Matlab®.

% Canvia la ruta de l'archiu
if(~isdeployed)
    cd(fileparts(which(mfilename)));
end

% Read in  MATLAB®
[fn,pn]=uigetfile('*.*', 'Select an image');
spots = imread(fullfile(pn,fn));
spots = rgb2gray(spots);
spots = imadjust(spots);
spots = imcrop(spots);
subplot(2, 3, 1);
imshow(spots);
% Maximitza la pantalla que mostra les figures.
set(gcf, 'Position', get(0, 'ScreenSize'));
% Força a mostrar la figura, si no es mostra es que tenim un punt de rotura
caption = sprintf('Imatge original en escala de grisos');
title(caption);
axis square;

% Histograma.
[pixelCount grayLevels] = imhist(spots);
%a = pixelcount-100;
%axis(a);
subplot(2, 3, 2);
bar(pixelCount);
title('Histogram of original image');
%xlim([0 grayLevels(end)]); % Ajusta la escala del 0 al valor máxim dels
pixels.


% Converteix la imatge a binary, mitjançant un llindar donat
% Utilitzant una operació lógica
message = sprintf('Cal analitzar de forma diferents els spots més concentrats
i els més diluits');
reply = questdlg(message, '%s\n\nYes = Spots concentrats No = spots
diluits?','70', '30', '100');

if strcmpi(reply, '70')
    thresholdValue = 70 ;
elseif strcmpi(reply, '30')
    thresholdValue = 30;
elseif strcmpi(reply, '25') %modificat aquí, abans era 15
```

```
    thresholdValue = 25;
else
    thresholdValue = 70;
end

    binaryImage = spots > thresholdValue; % "Bright objects will be the chosen
if you use >."
% binaryImage = spots < thresholdValue; % "Dark objects will be the chosen if
you use <."

% Omplir el gaps per desferse de valors similars al background dins dels
% "spots"
binaryImage = imfill(binaryImage, 'holes');

% Mostra el llindar sobre l'histograma en forma d'una barra vermella.
hold on;
maxYValue = ylim;
hStemLines = stem(thresholdValue, maxYValue(2), 'r');
children = get(hStemLines, 'children');
set(children(2),'visible', 'off');

% Col·loca una etiqueta sobre la barra vermella.
annotationText = sprintf('El llindar equival %d nivells de gris',
thresholdValue);

% Per text(), x i y han de ser del tipus "double", per tant cal convertir-los
text(double(thresholdValue + 5), double(0.5 * maxYValue(2)), annotationText,
'FontSize', 10, 'Color', [0 .5 0]);
text(double(thresholdValue - 70), double(0.94 * maxYValue(2)),
'"Background"', 'FontSize', 10, 'Color', [0 0 .5]);
text(double(thresholdValue + 50), double(0.94 * maxYValue(2)),
'"Foreground"', 'FontSize', 10, 'Color', [0 0 .5]);

% treu objectes de conjunts de pixels menors de mil, per eliminar soroll
binaryImage = bwareaopen(binaryImage, 1000);

% Aquest codi, només cal activarse per evitar soroll de fons.
%SE = strel('disk', 60, 0);
%binaryImage = imdilate(binaryImage, SE);
%SE = strel('disk', 60, 0);
%binaryImage = imerode(binaryImage, SE);

% Mostra la imatge en binari (blanc i negre; 1 i 0).
subplot(2, 3, 3); imagesc(binaryImage); colormap(gray(256)); title('Imatge
binaria obtinguda seguint el llindar mostrat'); axis square;

labeledImage = bwlabel(binaryImage, 8);      % Marca cada spot per mesurar els
valors associats
coloredLabels = label2rgb (labeledImage, 'hsv', 'k', 'shuffle'); % marcatge
pseudo aleatori

subplot(2, 3, 4);
imshow(labeledImage, []);
title('Imatge marcada amb diferents escales de gris bwlabel()');
axis square;
```

209

```matlab
subplot(2, 3, 5);
imagesc(coloredLabels);
axis square;
caption = sprintf('Marques de label2rgb().\n Els spots s ordenen de dalt a
baix i d esquerra a dreta.');
title(caption);

% Calcula totes les propietats dels spots, mitjançant una funció predisenyada
"regiondrops".
mesures = regionprops(labeledImage, spots, 'all');
numcalculs = size(mesures, 1);

% bwboundaries() retorna una taula on s especifiquen les coordenades dels
diferents spots. S'aplica sobre l'imatge original per encerclar els spots.
subplot(2, 3, 6); imagesc(spots);
title('Marges de bwboundaries()'); axis square;
hold on;
boundaries = bwboundaries(binaryImage);

%el nombre de "cercles" s'utilitzen com a contador per a la seguent iteració.
numberOfBoundaries = size(boundaries);
for k = 1 : numberOfBoundaries
    thisBoundary = boundaries{k};
    plot(thisBoundary(:,2), thisBoundary(:,1), 'g', 'LineWidth', 2);
end
hold off;

fontSize = 14;  % Determina les dimensions dels números de marcatge
labelShiftX = -7;   % S'utilitza per a centrar la marca just al centre del
spot.
sECD = zeros(1, numcalculs);

% Escriu l'encapsalament en el terminal de comandes.
fprintf(1,'Spot #  Intensitat  Area   Perimetre\n');

% Entra en una iteració amb for per mostrar les mesures indicades
anteriorment. El contador equival al número de vegades calculades les
propietats anteriors
for k = 1 : numcalculs          % Entra en loop per a tots els spots.

    sMitjana = mesures(k).MeanIntensity; % La intensitat mitjana
    sIntens = mesures(k).MaxIntensity;
    sArea = mesures(k).Area;          % Area.
    sPerimeter = mesures(k).Perimeter;      % Perimetre.
    sCentre = mesures(k).Centroid;      % Centre.
    sECD(k) = sqrt(4 * sArea / pi);             % Diametre - Equivalent
Circular Diameter.
    fprintf(1,'#%2d %8.0f %12.0f %8.0f\n', k, sMitjana, sArea, sIntens);
    % Posa el número sobre els spots en els spots amb límits i en l'escala de
grisos.
    text(sCentre(1) + labelShiftX, sCentre(2), num2str(k), 'FontSize',
fontSize, 'FontWeight', 'Bold');
  end

% Posa les marques en les imatges en color (codi rgb).
```

```matlab
subplot(2, 3, 5);

for k = 1 : numcalculs          % Loop de nou als spots
    sCentre = mesures(k).Centroid;      % Calcula el centre
    text(sCentre(1) + labelShiftX, sCentre(2), num2str(k), 'FontSize',
fontSize, 'FontWeight', 'Bold');
end



elapsedTime = toc;
% Avisa que l'anàlisi ha finalitzat i et demana si vols guardar la imatge i
els spots.
message = sprintf('Finalitzat CapaFina.m \n \n Temps de calcul = %.2f
segons.', elapsedTime);
message = sprintf('%s\n\nRevisa la figura per veure les imatges del
proces.\nRevisa el terminal per consultar els resultats numérics.', message);
message = sprintf('%s\n\nVoldries guardar els spots per separat?', message);
reply = questdlg(message, 'Guardar la figura?', 'Yes', 'No', 'No');
% Resposta = 'espai' per apretar X (o X amb el ratolí), 'Yes' per sí, i 'No'
per No.

if strcmpi(reply, 'Yes')

    % Demana el nom que li volem posar a l'arxiu.
    FilterSpec = {'*.tif', 'TIFF images (*.tif)'; '*.*', 'All Files (*.*)'};
    DialogTitle = 'Guarda el nom de l archiu';
    % Funció estándar per a guardar l'archiu i evitar errors
    thisFile = mfilename('fullpath');
    [thisFolder, baseFileName, ~, version] = fileparts(thisFile);
    DefaultName = sprintf('%s/%s.tif', thisFolder, baseFileName);
    [fileName, specifiedFolder] = uiputfile(FilterSpec, DialogTitle,
DefaultName);
    [folder, baseFileName, ext, version] = fileparts(fileName);
    fullImageFileName = fullfile(specifiedFolder, [baseFileName '.tif']);
    imwrite(uint8(coloredLabels), fullImageFileName);

end

message = sprintf('T agradaria guardar els spots per separat per a fer l
informe?');
reply = questdlg(message, 'Extreure les imatges?', 'Yes', 'No', 'Yes');
% Les mateixes opcions de resposta que abans.

if strcmpi(reply, 'Yes')
    figure;
    % Optimitza les dimensions de la figura.
    set(gcf, 'Position', get(0, 'ScreenSize'));
    for k = 1 : numcalculs          % Entra en loop sobre els spots.
        % Busca les dimensions més adients per a la figura.
        Box = mesures(k).BoundingBox;
        % Extreu cada spot a la seva box
        subImage = imcrop(spots, Box);
        % Mostra la imatge amb les dades desitjades
        subplot(3, 4, k);
```

```
        imshow(subImage);
        caption = sprintf('Spot #%d\nDiameter = %.1f pixels\nArea = %d
pixels', k, sECD(k), mesures(k).Area, sPerimeter(k));
        title(caption, 'FontSize', 14);
    end

end
```

This page intentionally left blank

Appendix C: Algorithm II

This second algorithm was adapted from _Jan Neggers_ algorithm, "measure tool". Paste the text below in a Matlab® terminal with Image processing toolbox installed would compute the tool. (The font of the algorithm has been reduced to avoid a major waste of paper).

```matlab
function varargout = measuretool(varargin)
% This tool (measure tool) is intended to aid measuring on images.
% In order to do this the image needs to have some visual scale to
% calibrate the pixel to length ratio on, e.g. scale bar, ruler.
%
% This is a two file GUI (Graphical User Interface)
%     measuretool.m   - the code, run this file to start the GUI
%     measuretool.fig - the figure, keep this file toghether with
%                       measuretool.m
%
% Quick Help:
% =============================%
% - Select a folder containing images using <Browse>
% - Press <Load>, and select one image from the list'
% - Press <Calibrate> and select two points of which the distance is known'
% - Use the zoom function of the toolbar and correct your initial selection'
% - Double Click the line to confirm'
% - Enter the length of the selected distance in the calibration panel'
% - Calibration is ready:'
% - Use the <Distance>, <Caliper>, <Circle> or <Angle> tools to measure'
% - Each measurement can be deleted using <Delete> or modified using <Edit>'
%
%
% For a more elaborate help, hit the <Help> button in the GUI

% Initializing the GUI:
gui_Singleton = 1;
gui_State = struct('gui_Name',       mfilename, ...
    'gui_Singleton',  gui_Singleton, ...
    'gui_OpeningFcn', @measuretool_OpeningFcn, ...
    'gui_OutputFcn',  @measuretool_OutputFcn, ...
    'gui_LayoutFcn',  [] , ...
    'gui_Callback',   []);
if nargin && ischar(varargin{1})
    gui_State.gui_Callback = str2func(varargin{1});
end

if nargout
    [varargout{1:nargout}] = gui_mainfcn(gui_State, varargin{:});
else
    gui_mainfcn(gui_State, varargin{:});
end

% --- Executes just before measuretool is made visible.
function measuretool_OpeningFcn(hObject, eventdata, handles, varargin)
handles.output = hObject;

if isfield(handles,'Data')
    Data = handles.Data;
end

% setting default plot options
options.marker1 = 'o';
options.marker2 = '.';
options.markersize = '10';
options.linestyle1 = '-';
options.linestyle2 = '--';
options.linewidth = '1' ;
options.color1 = 'r';
options.color2 = 'k';
options.textcolorfg = 'k';
options.textcolorbg = 'none';
options.fontsize = '14';
options.zoomfactor = 2;
options.splinemethod = 'spline';

% storing the ascii degree symbol
Data.degree = char(186);% i.e. ??

% put the tool on the right side of the screen
movegui('southeast')
```

```matlab
% detect old Matlab® version
if verLessThan('Matlab®', '7.9.0')
    set(handles.Quickmeasure,'Value',1,'foregroundcolor',[0.5 0.5 0.5]);
end

% detect image processing toolbox
if ~exist('imline','file')
    set(handles.Quickmeasure,'Value',1,'foregroundcolor',[0.5 0.5 0.5]);
end

% storing in the Data structure
Data.options = options;
handles.Data = Data;
% Update handles structure
guidata(hObject, handles);

% optional, use the tool on a figure already open
if ~isempty(varargin)
    argin = varargin{1};
else
    argin = [];
end
if ishandle(argin)
    Data.gcf = argin;
    handles.Data = Data;

    % Update handles structure
    guidata(hObject, handles);

    % configure the gui for use without file selection
    currentfigure_fun(hObject, eventdata, handles)
end

function varargout = measuretool_OutputFcn(hObject, eventdata, handles)
varargout{1} = handles.output;

function currentfigure_fun(hObject, eventdata, handles)
% read the Data structure
Data = handles.Data;

tmpname = 'measuretool_gcf.fig';
tmpfile = fullfile(tempdir,tmpname);

saveas(Data.gcf,tmpfile,'fig');

% Fill the Data structure
Data.unit     = 'pixels';
Data.cfile    = tmpname;
Data.ctype    = '*.fig';
Data.cfilenum = 1;
Data.files    = {tmpname};
Data.ftypes   = {'*.fig'};
Data.path     = tempdir ;
Data.Im(1,1,3) = 0;

% Disable the file selection options
set(handles.FileBrowse,'Enable','off')
set(handles.FileBox,'Enable','off')
set(handles.FileBox,'String',{'Current Figure'})

% Disable the calibration options
set(handles.Calibrate,'Enable','off')
set(handles.CalibLength,'Enable','off')
% set(handles.CalibUnit,'Enable','off')

handles.Data = Data;
% Update handles structure
guidata(hObject, handles);

plotfun(hObject, eventdata, handles)

function FileBrowse_Callback(hObject, eventdata, handles)
% load the Data structure
Data = handles.Data;

% start browsing from the current folder
if isfield(Data,'path')
```

```matlab
    oldpath = Data.path;
else
    oldpath = pwd;
end

% possible image types to list
imagetypes = {'*.png';'*.jpg';'*.jpeg';'*.gif';'*.tif';'*.tiff'};
imagetypes = [imagetypes ; upper(imagetypes)];

% popup, ask for a fiel
[filename, filepath] = uigetfile({'*.jpg;*.jpeg;*.tif;*.png;*.tif;*.tiff;*.PNG;*.JPG;*.TIF','All Image
Files';'*.*','All Files' },'Select an Image',oldpath);

% if cancel
if filename == 0
    set(handles.Status,'string','Browse: no file selected')
    return
end

% get a list of fiels
files = {}; filetypes = {};
% for each file type
for i = 1:length(imagetypes)
    % read the files from the dir for this type
    filestmp = dir([filepath filesep '*' imagetypes{i}]);
    filestmp = {filestmp(:).name};
    filetypestmp = repmat(imagetypes(i),1,length(filestmp));

    % store them with the other types
    files = {files{:} filestmp{:}}.';
    filetypes = {filetypes{:} filetypestmp{:}}.';
end

% get the current file from the list
n = length(files);
for k = 1:n
    if strcmp(files{k},filename);
        cfile = files{k};
        ctype = filetypes{k};
        cfilenum = k;
    end
end

% select the current file from in the list
set(handles.FileBox,'String',files);
set(handles.FileBox,'Value',cfilenum);

% update status
set(handles.Status,'string','Browse: file loaded')

% storing in the Data structure
Data.cfile    = cfile ;
Data.ctype    = ctype ;
Data.cfilenum = cfilenum ;
Data.files    = files ;
Data.ftypes = filetypes ;
Data.path    = filepath ;

% Update handles structure
handles.Data = Data;
guidata(hObject, handles);

% plot the figure
plotfun(hObject, eventdata, handles)

function [u v] = zoomselect(h,zoomfactor)
% store current axes
xlim = get(h,'xlim');
ylim = get(h,'ylim');

% get the position of the zoomed box
[u v] = ginput(1);

% calculate size of the zoombox
fovx = diff(xlim)./zoomfactor;
fovy = diff(ylim)./zoomfactor;
```

217

```matlab
% position zoombox centered around selected position
xzoom = [u-fovx/2 , u+fovx/2] ;
yzoom = [v-fovy/2 , v+fovy/2] ;

% shift the zoom xlimit to be within the initial view
if xzoom(1) < xlim(1)
    % zoom select is on the left edge of the axes
    xzoom(1) = xlim(1);
    xzoom(2) = xlim(1) + fovx;
elseif xzoom(2) > xlim(2)
    % zoom select is on the right edge of the axes
    xzoom(2) = xlim(2);
    xzoom(1) = xlim(2) - fovx;
end

% shift the zoom ylimit to be within the initial view
if yzoom(1) < ylim(1)
    % zoom select is on the bottom edge of the axes
    yzoom(1) = ylim(1);
    yzoom(2) = ylim(1) + fovy;
elseif yzoom(2) > ylim(2)
    % zoom select is on the top edge of the axes
    yzoom(2) = ylim(2);
    yzoom(1) = ylim(2) - fovy;
end


% zoom
set(h,'xlim',xzoom,'ylim',yzoom)

% select a point
[u v] = ginput(1);

% restore old axes
set(h,'xlim',xlim,'ylim',ylim)
```

```matlab
function plotfun(hObject, eventdata, handles)
% read the Data structure
Data = handles.Data;
O = Data.options;

if ~isfield(Data,'cfile')
    return
end

% Evaluate options
% ==============================
marker = {O.marker1 ; O.marker2};
markersize = eval(O.markersize);
if length(O.color1) == 1 || strcmpi(O.color1,'none')
    color{1,1} = O.color1;
else
    color{1,1} = eval(O.color1);
end
if length(O.color2) == 1 || strcmpi(O.color2,'none')
    color{2,1} = O.color2;
else
    color{2,1} = eval(O.color2);
end
linestyle = {O.linestyle1 ; O.linestyle2};
linewidth = eval(O.linewidth);
if length(O.textcolorfg) == 1 || strcmpi(O.textcolorfg,'none')
    textcolorfg = O.textcolorfg;
else
    textcolorfg = eval(O.textcolorfg);
end
if length(O.textcolorbg) == 1  || strcmpi(O.textcolorbg,'none')
    textcolorbg = O.textcolorbg;
else
    textcolorbg = eval(O.textcolorbg);
end
fontsize = eval(O.fontsize);
```

```matlab
% Plot the image
% ==============================
% some shorthands
filename = Data.cfile;
filetype = Data.ctype;
filepath = Data.path;
fileext  = regexprep(filetype,{'\*','\.'},'');

% start a new window
if ~isfield(Data,'gcf')
    Data.gcf = figure(1234);
    clf(Data.gcf);

    % get the screensize
    fullscreen = get(0,'ScreenSize');
    P = fullscreen .* [50 50 0.8 0.8];
    % fix the new figure
    set(Data.gcf,'Name','measure window','HandleVisibility','callback','NumberTitle','off')
    set(Data.gcf,'Position',P)
else
    figure(Data.gcf);
    clf(Data.gcf);
end

% Read the image
if strcmp(fileext,'fig')
    position = get(Data.gcf,'Position');
    close(Data.gcf);
    Data.gcf = openfig(fullfile(filepath,filename));
    Data.gca = get(Data.gcf,'Children');
    set(Data.gcf,'Position',position);
    set(Data.gcf,'Name','measure window','HandleVisibility','callback','NumberTitle','off')
    Im = Data.Im;
else
    Im = imread(fullfile(filepath,filename),fileext);
    Data.Im = Im;
end

% set the default unit
if ~isfield(Data,'unit')
    Data.unit = 'pixels';
end

% check the size (ndims = 3 for RGB images)
if ndims(Im) == 3
    [n m k] = size(Im);
else
    [n m] = size(Im);
    % fix for showing grayscale images as colored
    colormap(gray);
end
% create default x and y vectors
x = 1:m;
y = 1:n;

% if calibrated update x and y vectors
if ~strcmpi('...',get(handles.CalibRatio,'String'))
    if isfield(Data,'Lppx')
        % length per pixel
        Lppx = Data.Lppx;
        % update x and y vectors
        x = x*Lppx;
        y = y*Lppx;
    end
else
    Lppx = 1;
end

% store x and y vectors
Data.x = x;
Data.y = y;

% plot the image
if ~strcmp(fileext,'fig')
    Data.imagehandle = imagesc(x,y,Im);drawnow
    % get the axes handles of the image
    Data.gca = get(Data.imagehandle,'Parent');
else
    Data.gca = get(Data.gcf,'Children');
```

```matlab
end
% tune the axes settings
set(Data.gca,'Box','On','NextPlot','add','DataAspectRatio',[1 1 1]);


% add labels
if strcmp(Data.unit,'um')
    Data.xlabh = xlabel(Data.gca,'\mum');
    Data.ylabh = ylabel(Data.gca,'\mum');
else
    Data.xlabh = xlabel(Data.gca,Data.unit);
    Data.ylabh = ylabel(Data.gca,Data.unit);
end

% set fontsize
set(Data.gca,'FontSize',fontsize);
set(Data.xlabh,'FontSize',fontsize);
set(Data.ylabh,'FontSize',fontsize);


% Plot the calibration scale bar
% ==============================
if isfield(Data,'Calib')
    X = Data.Calib.X*Lppx;
    Y = Data.Calib.Y*Lppx;
    h = plot(Data.gca,X,Y,'-xw',X,Y,':+k');drawnow
    set(h,{'Marker'},marker)
    set(h,'MarkerSize',markersize)
    set(h,{'MarkerEdgeColor'},color)
    set(h,{'LineStyle'},linestyle)
    set(h,{'Color'},color)
    set(h,'LineWidth',linewidth)
end

% store and update the handles structure
handles.Data = Data;
guidata(hObject, handles);

% Plot the measurements
% =====================================
if ~isfield(Data,'Mdata')
    return
end
Mdata = Data.Mdata ;

% put the tool again back on top
figure(Data.gcf)

% forloop over each measurement
n = length(Mdata);
for k = 1:n

    % read the Mdata structure
    type  = Mdata(k).type;
    value = Mdata(k).value;
    unit  = Mdata(k).unit;
    X     = Mdata(k).X;
    Y     = Mdata(k).Y;
    circ  = Mdata(k).circ;
    spl   = Mdata(k).spline;

    % set the fancy units
    if strcmp(unit,'um')
        unit = '\mum';
    elseif strcmp(unit,Data.degree)
        unit = '\circ';
    end

    % use intensity instead of value
    if get(handles.Intensity,'Value')
        value = Mdata(k).intensity;
        unit  = '';
    end

    % convert the value to string
    value = sprintf('%.2f',value);
```

```matlab
% skip measurements from other images
if ~get(handles.ShowAll,'Value')
    if Data.Mdata(k).filenum ~= Data.cfilenum
        continue
    end
end

% plot the measurement, and set the plot options
switch type
    case 'Distance'
        ht = text(X(2),Y(2),[' ' value ' ' unit]);
        h1 = plot(X,Y,'-xw',X,Y,':+k');
        h  = h1;
    case 'Caliper'
        ht = text(X(3),Y(3),[' ' value ' ' unit]);
        h1 = plot(X(1:2),Y(1:2),'-xw',X(1:2),Y(1:2),':+k');
        h2 = plot(X(3:4),Y(3:4),'-xw',X(3:4),Y(3:4),':+k');
        h  = [h1 ; h2];

        set(h2,{'Marker'},marker)
        set(h2,'MarkerSize',markersize)
        set(h2,{'MarkerEdgeColor'},color)
        set(h2,{'LineStyle'},linestyle)
        set(h2,{'Color'},color)
        set(h2,'LineWidth',linewidth)
    case 'Circle (R)'
        ht = text(circ.xc,circ.yc,[' ' value ' ' unit]);
        h1 = plot(circ.xc,circ.yc,'xw',circ.xc,circ.yc,'+k');
        h2 = plot(X,Y,'-w',X,Y,':k');
        h  = [h1 ; h2];

        set(h2,'Marker','none')
        set(h2,{'LineStyle'},linestyle)
        set(h2,{'Color'},color)
        set(h2,'LineWidth',linewidth)
    case 'Angle'
        ht = text(X(3),Y(3),[' ' value unit]);
        h1 = plot(X,Y,'-xw',X,Y,':+k');
        h  = h1;
    case 'Spline'
        ht = text(spl.x(end),spl.y(end),[' ' value ' ' unit]);
        h1 = plot(spl.x,spl.y,'xw',spl.x,spl.y,'+k');
        h2 = plot(X,Y,'-w',X,Y,':k');
        h  = [h1 ; h2];

        set(h2,'Marker','none')
        set(h2,{'LineStyle'},linestyle)
        set(h2,{'Color'},color)
        set(h2,'LineWidth',linewidth)
end

set(h1,{'Marker'},marker)
set(h1,'MarkerSize',markersize)
set(h1,{'MarkerEdgeColor'},color)
set(h1,{'LineStyle'},linestyle)
set(h1,{'Color'},color)
set(h1,'LineWidth',linewidth)

if strcmp(type,'Spline')
    set(h1,'LineStyle','none')
end


set(ht,'verticalalignment','bottom');
set(ht,'Color',textcolorfg)
set(ht,'BackgroundColor',textcolorbg)
set(ht,'FontSize',fontsize)


% process the checkboxes in the gui, switch for [Show Points]
if ~get(handles.PlotPoints,'Value')
    set(h,'marker','none')
end
% process the checkboxes in the gui, switch for [Show Lines]
if ~get(handles.PlotLines,'Value')
    set(h,'LineStyle','none')
end
% process the checkboxes in the gui, switch for [Show Text]
```

```matlab
    if ~get(handles.PlotText,'Value')
        set(ht,'Visible','off')
    else
        set(ht,'Visible','on')
    end
end

% put the tool again back on top
figure(handles.figure1)


function PlotOptions_Callback(hObject, eventdata, handles)
% This function provides a popup menu to change the plotting preferences,
% e.g. color, linestyle, etc.
Data = handles.Data;
O    = Data.options;

% build the popup window
prompt={'Marker Style 1',...
    'Marker Style 2',...
    'Marker Size',...
    'Line Style 1',...
    'Line Style 2',...
    'Line Width',...
    'Color 1',...
    'Color 2',...
    'Text Foreground Color',...
    'Text Background Color',...
    'Text Fontsize',...
    'Zoom Factor',...
    'Spline interp. meth.'};
name='Plot Options';
numlines=1;

fields = fieldnames(O);
n = length(fields);

% builde the default answer from the options structure
for k = 1:n
    defaultanswer{k} = O.(fields{k});
    if ~ischar(defaultanswer{k});
        defaultanswer{k} = num2str(defaultanswer{k});
    end
end

% pop the menu
A = inputdlg(prompt,name,numlines,defaultanswer);

% if cancel
if isempty(A)
    set(handles.Status,'string','Options: Canceled')
    return
end

% store the answer back to the options structure
for k = 1:n
    O.(fields{k}) = A{k};
end

% evaluate the field of view
O.zoomfactor = eval(O.zoomfactor);

% error detection switch
optionerror = false;

% check if a proper interpolation method is entered
if ~any(strcmp(O.splinemethod,{'spline','linear','nearest','cubic'}))
    set(handles.Status,'string','Options: invalid method, use "linear", "cubic", or "spline", value reset to
default')
    O.splinemethod = 'spline';
    optionerror = true;
end

% check if a proper marker entered
if ~any(strcmp(O.marker1,{'o','s','^','d','v','*','<','>','.','p','h','+','x','none'}))
    set(handles.Status,'string','Options: invalid marker, value reset to default')
    O.marker1 = 'o';
    optionerror = true;
```

222

```matlab
    end
    if ~any(strcmp(O.marker2,{'o','s','^','d','v','*','<','>','.','p','h','+','x','none'}))
        set(handles.Status,'string','Options: invalid marker, value reset to default')
        O.marker1 = '.';
        optionerror = true;
    end

    % check if a proper linestyle is entered
    if ~any(strcmp(O.linestyle1,{'-','--','-.',':','none'}))
        set(handles.Status,'string','Options: invalid linestyle, value reset to default')
        O.linestyle1 = '-';
        optionerror = true;
    end
    if ~any(strcmp(O.linestyle2,{'-','--','-.',':','none'}))
        set(handles.Status,'string','Options: invalid linestyle, value reset to default')
        O.linestyle1 = '--';
        optionerror = true;
    end

    % check if a proper color is entered
    if ~any(strcmp(O.color1,{'y','m','c','r','g','b','w','k','none'})) ...
        && isempty(regexp(O.color1,'\[[(\d*)(\s*)(\.*)]*\]', 'once'))
        set(handles.Status,'string','Options: invalid color, value reset to default')
        O.color1 = 'r';
        optionerror = true;
    end
    if ~any(strcmp(O.color2,{'y','m','c','r','g','b','w','k','none'})) ...
        && isempty(regexp(O.color2,'\[[(\d*)(\s*)(\.*)]*\]', 'once'))
        set(handles.Status,'string','Options: invalid color, value reset to default')
        O.color2 = 'k';
        optionerror = true;
    end
    if ~any(strcmp(O.textcolorfg,{'y','m','c','r','g','b','w','k','none'})) ...
        && isempty(regexp(O.textcolorfg,'\[[(\d*)(\s*)(\.*)]*\]', 'once'))
        set(handles.Status,'string','Options: invalid color, value reset to default')
        O.textcolorfg = 'k';
        optionerror = true;
    end
    if ~any(strcmp(O.textcolorbg,{'y','m','c','r','g','b','w','k','none'})) ...
        && isempty(regexp(O.textcolorbg,'\[[(\d*)(\s*)(\.*)]*\]', 'once'))
        set(handles.Status,'string','Options: invalid color, value reset to default')
        O.textcolorbg = 'none';
        optionerror = true;
    end


    % storing in the big Data structure
    Data.options = O;

    if ~optionerror
        set(handles.Status,'string','Options adjusted')
    end


    % update the gui
    handles.Data = Data;
    guidata(hObject, handles);
    plotfun(hObject, eventdata, handles)


function CalibLength_Callback(hObject, eventdata, handles)
    % called when changing the calibration Length
    Data = handles.Data;

    % update the current unit
    unit = get(handles.CalibUnit,'String');
    unit = unit{get(handles.CalibUnit,'Value')};
    Data.unit = unit;

    if ~isfield(Data,'Calib')
        % update the measurements
        if isfield(Data,'Mdata')
            Mdata = Data.Mdata;
            n = length(Mdata);
            for k = 1:n
                Mdata(k).unit = Data.unit ;
            end
            Data.Mdata = Mdata ;
```

```matlab
        end
        % update the gui
        handles.Data = Data;
        guidata(hObject, handles);
        plotfun(hObject, eventdata, handles)
        return
    end

% store previous Length per Pixel (if any)
if isfield(Data,'Lppx')
    oldLppx = Data.Lppx;
else
    oldLppx = 1;
end

% get the current length
L = eval(get(handles.CalibLength,'String'));

% update the length per pixel ratio
Lppx = L/Data.Calib.Pixels;
Data.Lppx = Lppx;


%update the gui
set(handles.CalibRatio,'String',sprintf('%.2f %s',Lppx,unit));

% correction, for recalibration
Lppx = Lppx / oldLppx;


% update the measurements
if isfield(Data,'Mdata')
    Mdata = Data.Mdata;
    n = length(Mdata);
    for k = 1:n
        Mdata(k).X = Mdata(k).X * Lppx;
        Mdata(k).Y = Mdata(k).Y * Lppx;
        Mdata(k).value = Mdata(k).value * Lppx;
        Mdata(k).unit = Data.unit ;
        if isstruct(Mdata(k).circ)
            Mdata(k).circ.xc = Mdata(k).circ.xc * Lppx;
            Mdata(k).circ.yc = Mdata(k).circ.yc * Lppx;
            Mdata(k).circ.R  = Mdata(k).circ.R  * Lppx;
        end
        if isstruct(Mdata(k).spline)
            Mdata(k).spline.x = Mdata(k).spline.x * Lppx;
            Mdata(k).spline.y = Mdata(k).spline.y * Lppx;
        end
    end
    Data.Mdata = Mdata ;
end

set(handles.Status,'string','Calibration done')

% update the gui
handles.Data = Data;
guidata(hObject, handles);
plotfun(hObject, eventdata, handles)


function CalibLength_CreateFcn(hObject, eventdata, handles)
if ispc && isequal(get(hObject,'BackgroundColor'), get(0,'defaultUicontrolBackgroundColor'))
    set(hObject,'BackgroundColor','white');
end

function CalibUnit_Callback(hObject, eventdata, handles)
CalibLength_Callback(hObject, eventdata, handles)

function CalibUnit_CreateFcn(hObject, eventdata, handles)
if ispc && isequal(get(hObject,'BackgroundColor'), get(0,'defaultUicontrolBackgroundColor'))
    set(hObject,'BackgroundColor','white');
end

function Calibrate_Callback(hObject, eventdata, handles)
% this function allows the user to calibrate on the scalebar, ruler, etc.
if ~isfield(handles.Data,'gcf')
    return
```

```
end
Data = handles.Data;
buttons = findobj(handles.figure1,'Enable','on');
buttons = setdiff(buttons,[handles.Status handles.Clear]);
set(buttons,'Enable','off')

figure(Data.gcf)

% select two preliminary points
set(handles.Status,'string','Calibrate: Select two points to form a Line')
if get(handles.ZoomSelect,'Value')
    [u v] = zoomselect(Data.gca,Data.options.zoomfactor);
else
    [u v] = ginput(1);
end
h = plot(u,v,'r+',u,v,'bo','markersize',10);
if get(handles.ZoomSelect,'Value')
    [u(2) v(2)] = zoomselect(Data.gca,Data.options.zoomfactor);
else
    [u(2) v(2)] = ginput(1);
end
h(3:4) = plot(u,v,'r+',u,v,'bo','markersize',10);
% remove the points
delete(h);

if get(handles.Quickmeasure,'value')
    position = [u(1) v(1) ; u(2) v(2)];
else
    set(handles.Status,'string','Calibrate: Adjust the Line, double click the line when ready')
    h = imline(Data.gca,[u(1) v(1) ; u(2) v(2)]);
    % update status info
    % get the position, and wait for double click
    position = wait(h);
    % remove the line
    delete(h);
end

% calculate distance (hypot = robust sqrt(x^2+y^2))
A = diff(position(:,1));
B = diff(position(:,2));
pixels = hypot(A,B);

% store the position
X = position(:,1);
Y = position(:,2);

% put the tool again back on top
figure(handles.figure1)

if isfield(Data,'Lppx')
    Lppx = Data.Lppx;
else
    Lppx = 1;
end

X = X / Lppx;
Y = Y / Lppx;
pixels = pixels / Lppx;

% store calibration data in the Data structure
Data.Calib.Pixels = pixels;
Data.Calib.X = X;
Data.Calib.Y = Y;

% update the status
set(handles.CalibPixel,'String',sprintf('%.2f',pixels));drawnow
set(handles.Status,'string','Calibration done')

handles.Data = Data;
guidata(hObject, handles);
% redraw the image (first check the unit and length)
set(handles.Status,'String',sprintf('Calibration: %g pixels selected',pixels));drawnow
set(buttons,'Enable','on')

CalibLength_Callback(hObject, eventdata, handles)

function Distance_Callback(hObject, eventdata, handles)
```

225

```matlab
% this function preselects the distance measurement
if ~isfield(handles.Data,'gcf')
    return
end
Data = handles.Data;

buttons = findobj(handles.figure1,'Enable','on');
buttons = setdiff(buttons,[handles.Status handles.Clear]);
set(buttons,'Enable','off')


% first ask for 2 points, plot each point and remove the points when done.
set(handles.Status,'string','Distance: Select two points')
figure(Data.gcf)
% select two preliminary points
if get(handles.ZoomSelect,'Value')
    [u v] = zoomselect(Data.gca,Data.options.zoomfactor);
else
    [u v] = ginput(1);
end
h = plot(u,v,'r+',u,v,'bo','markersize',10);
if get(handles.ZoomSelect,'Value')
    [u(2) v(2)] = zoomselect(Data.gca,Data.options.zoomfactor);
else
    [u(2) v(2)] = ginput(1);
end
h(3:4) = plot(u,v,'r+',u,v,'bo','markersize',10);
delete(h);

% call the real distance measurement function
Distancefun(hObject, eventdata, handles,u,v)
set(buttons,'Enable','on')


function Distancefun(hObject, eventdata, handles,u,v)
% this function allows the measuring of a two point distance
Data = handles.Data;

if get(handles.Quickmeasure,'value')
    position = [u(1) v(1) ; u(2) v(2)];
else
    % place an imline using the two points
    set(handles.Status,'string','Distance: Adjust the Line, double click the line when ready')
    h = imline(Data.gca,[u(1) v(1) ; u(2) v(2)]);
    % wait for double click, and get position
    position = wait(h);
    % remove the line
    delete(h);
end

% calculate the distance (hypot = pythagoras)
A = diff(position(:,1));
B = diff(position(:,2));
Distance = hypot(A,B);

% store position for later plotting
X = position(:,1);
Y = position(:,2);

% create image space (for intensity)
[x y] = meshgrid(Data.x,Data.y);

% calculate a length vector
t = [ 0 ; hypot(diff(X),diff(Y)) ];
t = cumsum(t);

% discretize the measurement line
Ni = 200;
ti = linspace(0,max(t),Ni);
xi = interp1(t,X,ti);
yi = interp1(t,Y,ti);

% grayscale the image
im = grayscale(Data.Im);

% interpolate the intensity profile along the measurement line
profile = interp2(x,y,im,xi,yi);
```

226

```matlab
% calculate the average intensity
intensity = mean(profile);

% get the unit, or set it to pixels
if ~isfield(Data,'unit')
    Data.unit = 'pixels';
end

%Save the measurement in the structure
if ~isfield(Data,'Mdata')
    % if first measurement
    n = 1;
else
    % or open a new slot in the measurement data structure
    n = length(Data.Mdata) + 1;
end

% store the measurement
Data.Mdata(n).n         = n;
Data.Mdata(n).type      = 'Distance';
Data.Mdata(n).value     = Distance;
Data.Mdata(n).unit      = Data.unit;
Data.Mdata(n).X         = X;
Data.Mdata(n).Y         = Y;
Data.Mdata(n).spline    = [];
Data.Mdata(n).circ      = [];
Data.Mdata(n).filenum   = Data.cfilenum;
Data.Mdata(n).file      = Data.cfile;
Data.Mdata(n).intensity = intensity;
Data.Mdata(n).profile   = [ti ; profile];


% update the status
set(handles.Status,'String',sprintf('Distance: %.2f %s stored to measurements',Distance,Data.unit));drawnow

% put the tool again back on top
figure(handles.figure1)

% update the gui
handles.Data = Data;
guidata(hObject, handles);
plotfun(hObject, eventdata, handles)

function Caliper_Callback(hObject, eventdata, handles)
% start the caliper measurement (preselecting)
if ~isfield(handles.Data,'gcf')
    return
end
Data = handles.Data;
buttons = findobj(handles.figure1,'Enable','on');
buttons = setdiff(buttons,[handles.Status handles.Clear]);
set(buttons,'Enable','off')

% first select 2 points to position a line
set(handles.Status,'string','Caliper: Select two points, to position the Line')
figure(Data.gcf)
% select two preliminary points
if get(handles.ZoomSelect,'Value')
    [u v] = zoomselect(Data.gca,Data.options.zoomfactor);
else
    [u v] = ginput(1);
end
h = plot(u,v,'r+',u,v,'bo','markersize',10);
if get(handles.ZoomSelect,'Value')
    [u(2) v(2)] = zoomselect(Data.gca,Data.options.zoomfactor);
else
    [u(2) v(2)] = ginput(1);
end
h(3:4) = plot(u,v,'r+',u,v,'bo','markersize',10);
delete(h);

if get(handles.Quickmeasure,'value')
    L = [u(1) v(1) ; u(2) v(2)];
else
    % position the line
    h = imline(Data.gca,[u(1) v(1) ; u(2) v(2)]);
    set(handles.Status,'string','Caliper: Adjust the Line, double click the line when ready')
```

```matlab
        L = wait(h);
        delete(h);
    end

    % when done plot the temporary line
    X = L(:,1);
    Y = L(:,2);
    h = plot(X,Y,'-+r',X,Y,'--ob','markersize',10);

    if get(handles.Quickmeasure,'value')
        set(handles.Status,'string','Caliper: Select the perpendicular Point')
        if get(handles.ZoomSelect,'Value')
            [u v] = zoomselect(Data.gca,Data.options.zoomfactor);
        else
            [u v] = ginput(1);
        end
        P = [u(1) v(1)];
    else
        % now position a point
        set(handles.Status,'string','Caliper: Adjust the Point, double click the line when ready')
        hp = impoint(Data.gca);
        P = wait(hp);
        delete(hp);
        delete(h);
    end

    u = [X ; P(1)];
    v = [Y ; P(2)];

    % the real caliper measurement part
    Caliperfun(hObject, eventdata, handles,u,v)
    set(buttons,'Enable','on')


function Caliperfun(hObject, eventdata, handles,u,v)
    % this function allows a distance measurement of a line-point type
    Data = handles.Data;

    % calculate the perpendicular distance
    % ==================================
    x1 = u(1);
    x2 = u(2);
    y1 = v(1);
    y2 = v(2);

    x3 = u(3);
    y3 = v(3);

    % The perpendicular distance (http://mathworld.wolfram.com/Point-LineDistance2-Dimensional.html)
    D = ( (x2-x1)*(y1-y3) - (x1-x3)*(y2-y1) ) / hypot(x2-x1,y2-y1);
    Caliper = abs(D);

    % now determine the location of the fourth point for plotting
    dx = x1-x2;
    dy = y1-y2;
    dist = sqrt(dx*dx + dy*dy);
    dx = dx / dist;
    dy = dy / dist;
    x4 = x3 + D*dy;
    y4 = y3 - D*dx;

    % Storing the four points
    X = [x1 ; x2 ; x3 ; x4];
    Y = [y1 ; y2 ; y3 ; y4];

    % create image space (for intensity)
    [x y] = meshgrid(Data.x,Data.y);

    % calculate a length vector
    t = [ 0 ; hypot(diff(X(3:4)),diff(Y(3:4))) ];
    t = cumsum(t);

    % discretize the measurement line
    Ni = 200;
    ti = linspace(0,max(t),Ni);
    xi = interp1(t,X(3:4),ti);
    yi = interp1(t,Y(3:4),ti);
```

228

```matlab
% grayscale the image
im = grayscale(Data.Im);

% interpolate the intensity profile along the measurement line
profile = interp2(x,y,im,xi,yi);

% calculate the average intensity
intensity = mean(profile);

if ~isfield(Data,'unit')
    Data.unit = 'pixels';
end

%Save the measurement in the structure
if ~isfield(Data,'Mdata')
    n = 1;
else
    n = length(Data.Mdata) + 1;
end
Data.Mdata(n).n         = n;
Data.Mdata(n).type      = 'Caliper';
Data.Mdata(n).value     = Caliper;
Data.Mdata(n).unit      = Data.unit;
Data.Mdata(n).X         = X;
Data.Mdata(n).Y         = Y;
Data.Mdata(n).spline    = [];
Data.Mdata(n).circ      = [];
Data.Mdata(n).filenum   = Data.cfilenum;
Data.Mdata(n).file      = Data.cfile;
Data.Mdata(n).intensity = intensity;
Data.Mdata(n).profile   = [ti ; profile];

% update the status
set(handles.Status,'String',sprintf('Caliper: %.2f %s stored to measurements',Caliper,Data.unit));drawnow

% put the tool again back on top
figure(handles.figure1)

handles.Data = Data;
guidata(hObject, handles);
plotfun(hObject, eventdata, handles)

function circ = circlefit(x,y)
% least squares circle fitting (see Matlab® help/demo (pendulum))
n = length(x);
M   = [x(:), y(:) ones(n,1)];
abc = M \ -( x(:).^2 + y(:).^2);
xc  = -abc(1)/2;
yc  = -abc(2)/2;
R   = sqrt((xc^2 + yc^2) - abc(3));

circ.xc = xc;
circ.yc = yc;
circ.R  = R;

function Circle_Callback(hObject, eventdata, handles)
% initiate the circle measurement
if ~isfield(handles.Data,'gcf')
    return
end
Data = handles.Data;
buttons = findobj(handles.figure1,'Enable','on');
buttons = setdiff(buttons,[handles.Status handles.Clear]);
set(buttons,'Enable','off')

% ask for two points (center and radius)
if get(handles.Quickmeasure,'value')
    set(handles.Status,'string','Circle: Select Point 1 / 5 on the Edge of the circle')
else
    set(handles.Status,'string','Circle: Select the Center of the circle')
end
figure(Data.gcf)
if get(handles.ZoomSelect,'Value')
    [u v] = zoomselect(Data.gca,Data.options.zoomfactor);
else
    [u v] = ginput(1);
end
```

229

```matlab
h = plot(u,v,'r+',u,v,'bo','markersize',10);
if get(handles.Quickmeasure,'value')
    set(handles.Status,'string','Circle: Select Point 2 / 5 on the Edge of the circle')
else
    set(handles.Status,'string','Circle: Select a Point on the Edge of the circle')
end
if get(handles.ZoomSelect,'Value')
    [u(2) v(2)] = zoomselect(Data.gca,Data.options.zoomfactor);
else
    [u(2) v(2)] = ginput(1);
end
h(3:4) = plot(u,v,'r+',u,v,'bo','markersize',10);
delete(h);

Circlefun(hObject, eventdata, handles,u,v)
set(buttons,'Enable','on')


function Circlefun(hObject, eventdata, handles,u,v)
% This function allows the measurement of a radius, using a cirlce
Data = handles.Data;
% calculate the box around the circle
A = diff(u);
B = diff(v);
R = hypot(A,B);
P = [u(1)-R v(1)-R 2*R 2*R];


if get(handles.Quickmeasure,'value')
    position = [u(1) v(1) ; u(2) v(2)];
    h = plot(u,v,'r+',u,v,'bo','markersize',10);
    for k = 3:5
        set(handles.Status,'string',sprintf('Circle: Select Point %g / 5 on the Edge of the circle',k))
        if get(handles.ZoomSelect,'Value')
            [u v] = zoomselect(Data.gca,Data.options.zoomfactor);
        else
            [u v] = ginput(1);
        end
        h = [h plot(u,v,'or',u,v,'.b','markersize',10)];
        position(k,:) = [u v];
    end
    delete(h);
else
    % position a draggable circle
    set(handles.Status,'string','Circle: Adjust the Circle, double click the line when ready')
    h = imellipse(Data.gca,P);
    % fix the aspect ratio (so no ellipses are allowed)
    setFixedAspectRatioMode(h,true)
    position = wait(h);
    delete(h);
end
% use circlefit to obtain the radius
circ = circlefit(position(:,1),position(:,2));
xc = circ.xc;
yc = circ.yc;
Radius = circ.R;

% store points on the circle for later plotting
if get(handles.Quickmeasure,'value')
    phi = linspace(0,2*pi,30);
    X = circ.R*sin(phi) + circ.xc;
    Y = circ.R*cos(phi) + circ.yc;
else
    X = position(:,1);
    Y = position(:,2);
end

% create image space (for intensity)
[x y] = meshgrid(Data.x,Data.y);

% find all pixels inside the circle
incircle = inpolygon(x,y,X,Y);

% grayscale the image
im = grayscale(Data.Im);

% calculate the average intensity
intensity = mean(im(incircle));
```

```matlab
    % distance from center
    ti = hypot(x(incircle)-xc,y(incircle)-yc).';

    % profile
    profile = im(incircle).';



    if ~isfield(Data,'unit')
        Data.unit = 'pixels';
    end

    %Save the measurement in the structure
    if ~isfield(Data,'Mdata')
        n = 1;
    else
        n = length(Data.Mdata) + 1;
    end

    Data.Mdata(n).n         = n;
    Data.Mdata(n).type      = 'Circle (R)';
    Data.Mdata(n).value     = Radius;
    Data.Mdata(n).unit      = Data.unit;
    Data.Mdata(n).X         = X;
    Data.Mdata(n).Y         = Y;
    Data.Mdata(n).spline    = [];
    Data.Mdata(n).circ      = circ;
    Data.Mdata(n).filenum   = Data.cfilenum;
    Data.Mdata(n).file      = Data.cfile;
    Data.Mdata(n).intensity = intensity;
    Data.Mdata(n).profile   = [ti ; profile];

    % update the status
    set(handles.Status,'String',sprintf('Circle: %.2f %s stored to measurements',Radius,Data.unit));drawnow

    % put the tool again back on top
    figure(handles.figure1)

    % update the gui
    handles.Data = Data;
    guidata(hObject, handles);
    plotfun(hObject, eventdata, handles)


    function Angle_Callback(hObject, eventdata, handles)
    % initate the Angle measurement
    if ~isfield(handles.Data,'gcf')
        return
    end
    Data = handles.Data;
    buttons = findobj(handles.figure1,'Enable','on');
    buttons = setdiff(buttons,[handles.Status handles.Clear]);
    set(buttons,'Enable','off')

    figure(Data.gcf)
    set(handles.Status,'string','Angle: Select the Intersection')
    if get(handles.ZoomSelect,'Value')
        [u v] = zoomselect(Data.gca,Data.options.zoomfactor);
    else
        [u v] = ginput(1);
    end
    h = plot(u,v,'r+',u,v,'bo','markersize',10);
    set(handles.Status,'string','Angle: Select a Point to form a Line 1 with the Intersection')
    if get(handles.ZoomSelect,'Value')
        [u(2) v(2)] = zoomselect(Data.gca,Data.options.zoomfactor);
    else
        [u(2) v(2)] = ginput(1);
    end
    h(3:4) = plot(u,v,'r+',u,v,'bo','markersize',10);
    set(handles.Status,'string','Angle: Select a Point to form a Line 2 with the Intersection')
    if get(handles.ZoomSelect,'Value')
        [u(3) v(3)] = zoomselect(Data.gca,Data.options.zoomfactor);
    else
        [u(3) v(3)] = ginput(1);
    end
    h(5:6) = plot(u,v,'r+',u,v,'bo','markersize',10);
    delete(h);
```

231

```matlab
Anglefun(hObject, eventdata, handles,u,v)
set(buttons,'Enable','on')


function Anglefun(hObject, eventdata, handles,u,v)
% This function allows the measurement of an angle using three points
Data = handles.Data ;

if get(handles.Quickmeasure,'value')
    position = [u(2),v(2);u(1),v(1);u(3),v(3)];
else
    set(handles.Status,'string','Angle: Adjust the Polygon, double click the line when ready')
    h = impoly(Data.gca,[u(2),v(2);u(1),v(1);u(3),v(3)],'Closed',false);
    position = wait(h);
    delete(h);
end

% Create two vectors from the vertices.
v1 = [position(1,1)-position(2,1), position(1,2)-position(2,2)];
v2 = [position(3,1)-position(2,1), position(3,2)-position(2,2)];
phi = acos(dot(v1,v2)/(norm(v1)*norm(v2)));
Angle = (phi * (180/pi)); % radtodeg(phi)

X = position(:,1);
Y = position(:,2);

% create image space (for intensity)
[x y] = meshgrid(Data.x,Data.y);

% calculate a length vector
t = [ 0 ; hypot(diff(X),diff(Y)) ];
t = cumsum(t);

% discretize the measurement line
Ni = 200;
ti = linspace(0,max(t),Ni);
xi = interp1(t,X,ti);
yi = interp1(t,Y,ti);

% grayscale the image
im = grayscale(Data.Im);

% interpolate the intensity profile along the measurement line
profile = interp2(x,y,im,xi,yi);

% calculate the average intensity
intensity = mean(profile);

%Save the measurement in the structure
if ~isfield(Data,'Mdata')
    n = 1;
else
    n = length(Data.Mdata) + 1;
end

Data.Mdata(n).n         = n;
Data.Mdata(n).type      = 'Angle';
Data.Mdata(n).value     = Angle;
Data.Mdata(n).unit      = Data.degree;
Data.Mdata(n).X         = X;
Data.Mdata(n).Y         = Y;
Data.Mdata(n).spline    = [];
Data.Mdata(n).circ      = [];
Data.Mdata(n).filenum   = Data.cfilenum;
Data.Mdata(n).file      = Data.cfile;
Data.Mdata(n).intensity = intensity;
Data.Mdata(n).profile   = [ti ; profile];

% update the status
set(handles.Status,'String',sprintf('Angle: %.2f %s stored to measurements',Angle,Data.degree));drawnow

% put the tool again back on top
figure(handles.figure1)

% update the gui
```

232

```matlab
handles.Data = Data;
guidata(hObject, handles);
plotfun(hObject, eventdata, handles)


function Spline_Callback(hObject, eventdata, handles)
% % this function preselects the spline measurement
if ~isfield(handles.Data,'gcf')
    return
end
Data = handles.Data;
buttons = findobj(handles.figure1,'Enable','on');
buttons = setdiff(buttons,[handles.Status handles.Clear]);
set(buttons,'Enable','off')

prompt = 'Enter number of points:';
dlg_title = 'Select the number of Spline points';
num_lines = 1;
def = {'5'};
answer = inputdlg(prompt,dlg_title,num_lines,def);

% if cancel
if isempty(answer)
    set(handles.Status,'string','Spline: Canceled')
    return
end
n = eval(answer{1});

% set minimum to 2
n = max([2 n]);

figure(Data.gcf)
u = zeros(1,n);
v = zeros(1,n);
h = zeros(2,n);
for k = 1:n
    set(handles.Status,'string',sprintf('Spline: Select Point %g / %g',k,n))
    if get(handles.ZoomSelect,'Value')
        [u(k) v(k)] = zoomselect(Data.gca,Data.options.zoomfactor);
    else
        [u(k) v(k)] = ginput(1);
    end
    h(:,k) = plot(u(k),v(k),'r+',u(k),v(k),'bo');
end
delete(h);

% call the real distance measurement function
Splinefun(hObject, eventdata, handles,u,v)
set(buttons,'Enable','on')



function Splinefun(hObject, eventdata, handles,u,v)
% this function allows the measuring of a multi point spline length
Data = handles.Data;

if get(handles.Quickmeasure,'value')
    position = [u ; v ].';
else
    % place an imline using the two points
    set(handles.Status,'string','Spline: Adjust the Polygon, double click the line when ready')
    h = impoly(Data.gca,[u ; v ].','Closed',false);
    % wait for double click, and get position
    position = wait(h);
    % remove the line
    delete(h);
end

X = position(:,1);
Y = position(:,2);

% save for later plotting
spl.x = X;
spl.y = Y;

% calculate a length vector
t = [ 0 ; hypot(diff(X),diff(Y)) ];
t = cumsum(t);
```

233

```matlab
% testing for uniqueness
I = unique(t);
if length(I) ~= length(t)
    set(handles.Status,'string','Spline: error, points must be distict')
    return
end


% number of interpolation points
N = 50*length(X);

% interpolation method
method = Data.options.splinemethod;

% intepolate along the length vector
ti = linspace(0,max(t),N) ;
xi = interp1(t,X,ti,method);
yi = interp1(t,Y,ti,method);

% calculate the spline length
L = sum( hypot( diff(xi),diff(yi) ) );

% create image space (for intensity)
[x y] = meshgrid(Data.x,Data.y);

% grayscale the image
im = grayscale(Data.Im);

% interpolate the intensity profile along the measurement line
profile = interp2(x,y,im,xi,yi);

% calculate the average intensity
intensity = mean(profile);

% get the unit, or set it to pixels
if ~isfield(Data,'unit')
    Data.unit = 'pixels';
end

%Save the measurement in the structure
if ~isfield(Data,'Mdata')
    % if first measurement
    n = 1;
else
    % or open a new slot in the measurement data structure
    n = length(Data.Mdata) + 1;
end

% store the measurement
Data.Mdata(n).n         = n;
Data.Mdata(n).type      = 'Spline';
Data.Mdata(n).value     = L;
Data.Mdata(n).unit      = Data.unit;
Data.Mdata(n).X         = xi;
Data.Mdata(n).Y         = yi;
Data.Mdata(n).spline    = spl;
Data.Mdata(n).circ      = [];
Data.Mdata(n).filenum   = Data.cfilenum;
Data.Mdata(n).file      = Data.cfile;
Data.Mdata(n).intensity = intensity;
Data.Mdata(n).profile   = [ti ; profile];

% update the status
set(handles.Status,'String',sprintf('Spline: %.2f %s stored to measurements',L,Data.unit));drawnow

% put the tool again back on top
figure(handles.figure1)

% update the gui
handles.Data = Data;
guidata(hObject, handles);
plotfun(hObject, eventdata, handles)


function PlotPoints_Callback(hObject, eventdata, handles)
plotfun(hObject, eventdata, handles)
```

234

```matlab
function PlotLines_Callback(hObject, eventdata, handles)
plotfun(hObject, eventdata, handles)

function PlotText_Callback(hObject, eventdata, handles)
plotfun(hObject, eventdata, handles)

function Edit_Callback(hObject, eventdata, handles)
% This function allows the editing of a previous measurement
if ~isfield(handles.Data,'Mdata') || isempty(handles.Data.Mdata)
    set(handles.Status,'String','Edit: No measurements to edit');drawnow
    return
end
Data = handles.Data;
Mdata = Data.Mdata;
n = length(Mdata);

% build a list of previous measurements
for i = 1:n
    prompt{i} = [num2str(Mdata(i).n) ': ' Mdata(i).type ' ' sprintf('%.2f',Mdata(i).value) ' ' Mdata(i).unit];
end

% always ask which one (allows for abort)
[Selection,ok] = listdlg('Name','Select a measurement','PromptString','Select a
measurement:','SelectionMode','single','ListString',prompt);
if (ok == 0) || isempty(Selection)
    return
end
k = Selection;

type = Mdata(k).type;
set(handles.Status,'string',['Edit: ' type])

% create a list for each dataset
N = 1:n;
% select the not selected sets
C = setdiff(N,k);
Data.Mdata = Mdata(C);
handles.Data = Data;
guidata(hObject, handles);


buttons = findobj(handles.figure1,'Enable','on');
buttons = setdiff(buttons,[handles.Status handles.Clear]);


% repeat the measurement function above, except with the old
% points as input/base of the new measurement
switch type
    case 'Distance'
        figure(Data.gcf)
        if get(handles.Quickmeasure,'value')
            Distance_Callback(hObject, eventdata, handles)
        else
            set(buttons,'Enable','off')
            u = Mdata(k).X;
            v = Mdata(k).Y;
            Distancefun(hObject, eventdata, handles,u,v)
            set(buttons,'Enable','on')
        end
    case 'Caliper'
        figure(Data.gcf)
        if get(handles.Quickmeasure,'value')
            Caliper_Callback(hObject, eventdata, handles)
        else
            set(buttons,'Enable','off')
            u = Mdata(k).X;
            v = Mdata(k).Y;

            % position the line
            set(handles.Status,'string','Caliper: Adjust the Line, double click the line when ready')
            h = imline(Data.gca,[u(1) v(1) ; u(2) v(2)]);
            L = wait(h);
            delete(h);

            % when done plot the temporary line
            X = L(:,1);
            Y = L(:,2);
            h = plot(X,Y,'-+r',X,Y,'--ob');
```

235

```matlab
                % now position a point
                set(handles.Status,'string','Caliper: Adjust the Point, double click the line when ready')
                hp = impoint(Data.gca, u(3), v(3));
                P = wait(hp);
                delete(hp);
                delete(h);

                u = [X ; P(1)];
                v = [Y ; P(2)];

                Caliperfun(hObject, eventdata, handles,u,v)
                set(buttons,'Enable','on')
            end
    case 'Circle (R)'
            if get(handles.Quickmeasure,'value')
                Circle_Callback(hObject, eventdata, handles)
            else
                set(buttons,'Enable','off')
                u = Mdata(k).circ.xc;
                v = Mdata(k).circ.yc;
                u(2) = u + Mdata(k).circ.R;
                v(2) = v;
                Circlefun(hObject, eventdata, handles,u,v)
                set(buttons,'Enable','on')
            end
    case 'Angle'
            if get(handles.Quickmeasure,'value')
                Angle_Callback(hObject, eventdata, handles)
            else
                set(buttons,'Enable','off')
                figure(Data.gcf)
                u = Mdata(k).X([2 1 3]);
                v = Mdata(k).Y([2 1 3]);
                Anglefun(hObject, eventdata, handles,u,v)
                set(buttons,'Enable','on')
            end
    case 'Spline'
            if get(handles.Quickmeasure,'value')
                Spline_Callback(hObject, eventdata, handles)
            else
                set(buttons,'Enable','off')
                u = Mdata(k).spline.x.' ;
                v = Mdata(k).spline.y.' ;
                Splinefun(hObject, eventdata, handles,u,v)
                set(buttons,'Enable','on')
            end
    otherwise
            set(handles.Status,'string','Edit: unkown measurement type')
            return
end


function Delete_Callback(hObject, eventdata, handles)
% this function allows the removal of one or several previously made
% measurements.
if ~isfield(handles.Data,'Mdata') || isempty(handles.Data.Mdata)
    set(handles.Status,'String','Delete: No measurements to edit');drawnow
    return
end
Data = handles.Data;
Mdata = Data.Mdata;
n = length(Mdata);

% build a list of previously made measurements
for i = 1:n
    prompt{i} = [num2str(Mdata(i).n) ': ' Mdata(i).type ' ' sprintf('%.2f',Mdata(i).value) ' ' Mdata(i).unit];
end

% always ask which one (allows for abort)
[Selection,ok] = listdlg('Name','Select measurements','PromptString','Select
measurements:','SelectionMode','multiple','ListString',prompt);
if (ok == 0) || isempty(Selection)
    return
end

% create a list for each dataset
N = 1:n;
% select the not selected sets
C = setdiff(N,Selection);
```

236

```matlab
    Data.Mdata = Mdata(C);

    handles.Data = Data;
    guidata(hObject, handles);
    plotfun(hObject, eventdata, handles)


function guihelp(handles)
% this function prints this help to a temporary file and opens the file in
% a text editor.
txt = {;
    'This tool (measure tool) is intended to aid measuring on images.'
    'In order to do this the image needs to have some visual scale to calibrate the pixel to length ratio on,
e.g. scale bar, ruler.'
    ''
    'Updates can be found at:'
    'http://www.mathworks.nl/Matlab@central/fileexchange/25964-image-measurement-utility'
    ''
    'Quick Help'
    '============================='
    ' - Select an image using <Browse>'
    ' - Press <Calibrate> and select two points of which the distance is known'
    ' - Use the zoom function of the toolbar and correct your initial selection'
    ' - Double Click the line to confirm'
    ' - Enter the length of the selected distance in the calibration panel'
    ' - Calibration is ready:'
    ' - Use the <Distance>, <Spline>, <Caliper>, <Circle>, or <Angle> tools to measure'
    ' - Each measurement can be deleted using <Delete> or modified using <Edit>'
    ''
    'Image processing toolbox tools'
    '============================='
    'The tool is intended for high quality measurements, and is therefore build around tools like "imline" from
the image processing toolbox. These tools are powerful because they allow you to select, zoom, re-adjust, and
than confirm your selection. As a result, all measurements require several "clicks", the first set of clicks
can be quick, and allow you to place the measurement tool, where after the tool can be modified using its
control points, when ready double click on the tool to finalize the selection. Finally, it is important that
the full sequence of "clicks" is finished before a new measurement is started, otherwise the GUI will terminate
less gracefully. If the image processing toolbox is unavailable, or a Matlab® version older then 2009b (7.9.0)
is used, then the <Quick> option can be used (optionally with <Zoom Select>) to bypass the "imline" selection
tools.'
    ''
    'Listbox of images'
    '============================='
    'After selecting an image (using the <Browse...> button), a list of all images in the folder is loaded in
the tool, this allows the measurement on several files without the need to re-calibrate, which off coarse only
works if the images actually share the same scale, e.g. like in a movie.'
    ''
    'Status'
    '============================='
    'Status information is shown here.'
    ''
    'Calibrate'
    '============================='
    'It goes without saying that each measurement depends on the calibration, so it is worth spending some time
on getting it right. Furthermore, the calibration can be re-done at any time, all measurements will be updated
accordingly.'
    ''
    'Measure'
    '============================='
    '<Distance>: measure the distance between two points, first place two initial points, then correct and
confirm the selected distance by double clicking on the line.'
    '<Caliper>: measure the perpendicular distance between a line and a point, first place two initial points,
then correct and confirm (double click) the position of the line, now place a point at a distance perpendicular
to the line, again correct the position and confirm with a double click.'
    '<Spline>: measure the length of a multi-point spline. This tool is very similar to the "Distance" tool,
except it handles more than 2 points and interpolates them using the spline interpolation method of interp1
(tip: set the method to "linear" in the options menu to measure polygons).'
    '<Circle>: measure a radius by placing a circle, first select the center of the circle and then one point
on the circle, the position and size of the circle can be corrected, confirm with a double click on the circle.
The selection behavior changes slightly when the "Quick" option is selected, then five points need to be
selected through which a circle is fitted.'
    '<Angle>: measure an angle between two lines, first select the intersection and then two more points to one
for each line, the three point line can be moved and the position of the points can be moved by dragging them
with the mouse, double click on the line to confirm the measurement.'
    '<Edit>: Reposition the points of one measurement which can be selected from a list'
    '<Delete>: Delete one or multiple measurements using a list'
    ''
    'Plot'
    '============================='
```

```
    'In this panel a set of plotting options can be found, which switch on (or off) visual objects. <Points>,
<Lines>, and, <Text>, not quite unexpectedly, enable (or disable) to plotting of points, lines, and texts. When
<All> is enabled then measurements from all images in the "List" are shown simultaneously, when disabled then
only measurements from the current image are shown. <Intensity> switches the text from the spatial quantity to
the average intensity of the pixels underneath the measured object. For "Distance", "Angle", and "Spline" the
intensity is calculated by interpolating the pixel values on discretized points of the measured (and plotted)
line, and average those. For "Caliper" the intensity is calculated in the same way but only for the
"perpendicular" line, i.e., the line connecting the selected line and point. For "Circle" the average intensity
is calculated for all pixels inside the circle. Actually, for all measurement types except "Circle", the
intensity profiles are stored and can be found in the myname(k).profile matrix (see "save to workspace"), where
the first column is the distance along the measurement and the second column the corresponding intensity.'
    ''
    'Save'
    '=============================='
    '<Workspace>: A popup asks for a variable name, to which all measurements are stored to the base workspace
in the form of a structure. The measurement data can be found by typing myname(k) where k is an integer
selecting the specific measurement.'
    '<Text>: A popup asks for a .txt file name, after which all data is written to the file.'
    '<Image (png)>: A popup asks for a .png file name, after which the "measure window" is saved as a .png file
(note, the image is anti-aliased which takes some time)'
    '<Image (pdf)>: A popup asks for a .pdf file name, after which the "measure window" is saved as a .pdf
file'
    ''
    'Current Figure'
    '=============================='
    'Calling measuretool(gcf) will open the tool for use on the current figure, for instance one created with
imagesc(x,y,Z). In this mode all file selection tools are disabled. Typically, such figures have non-square
pixels for which the calibration process is not well defined, therefore, the axes are assumed to be calibrated
(i.e. have meaningful values) and the calibration options are also disabled.'
    ''
    'Changelog'
    '=============================='
    'version 1.13 by Jan Neggers, Jan,12,2012'
    '   - added feature to measure the intensity (as suggested by Jakub)'
    '   - included the "Plot" section in the help'
    '   - simplified the save to workspace structure'
    ''
    'version 1.12 by Jan Neggers, Dec,7,2011'
    '   - most GUI buttons are now disabled during measurements to prevent confusion'
    '   - added a "clear" button to reset the tool'
    '   - added more input checks for the "options" menu'
    ''
    'version 1.11 by Jan Neggers, Sept,29,2011'
    '   - minor update, added the possibility to use a figure window which is already open (e.g.
measuretool(gcf))'
    '   - changed the zoom select from absolute to relative'
    '   - all buttons are now disabled during measurement'
    ''
    'version 1.10 by Jan Neggers, Sept,27,2011'
    '   - entire overhaul of the gui, added quite a few features, some of which as proposed by Mark Hayworth'
    ''
    'version 1.00 by Jan Neggers, Sept,22,2011'
    '   - fixed some bugs related to the help'
    '   - improved displaying in micrometers'
    '   - added the four <Save> buttons'
    ''
    'version 0.92 by Jan Neggers, Apr,06,2010'
    '   - fixed grayscale images showing in color (after comment from Till)'
    '   - improved help file displaying'
    ''
    'version 0.91 by Jan Neggers, Nov,30,2009'
    '   - first version'
    };

% create a temporary file to hold the help.txt
tempfile = [tempdir 'measuretool_help.txt'];
fid = fopen(tempfile,'wt+');
for i = 1:length(txt)
    fprintf(fid,'%s\n',txt{i});
end
fclose(fid);

% open the file (in windows or unix)
try
    if ispc
        % windows
        winopen(tempfile)
    elseif isunix
        % unix (linux)
        % finding out which text editors are present
        [a b] = system('type gedit kate mousepad');
```

```matlab
            % converting to a 3x1 cell
            a = textscan(b,'%s','delimiter','\n');
            % searching for the words not found
            a = regexpi(a{1},'.not found');
            % opening the text file
            if isempty(a{1})
                command = ['! gedit ' tempfile ' &'];
                eval(command)
            elseif isempty(a{2})
                command = ['! kate ' tempfile ' &'];
                eval(command)
            elseif isempty(a{3})
                command = ['! mousepad ' tempfile ' &'];
                eval(command)
            else
                % if no editor is found then print to command window
                set(handles.Status,'string','Help: could not find a suitable text editor to show the help file, see
command window.')
                for i = 1:length(txt)
                    fprintf('%s \n',txt{i})
                end
            end

    end
catch ME
    set(handles.Status,'string','Help: Something went wrong, printing help to command screen.')
    for i = 1:length(txt)
        fprintf('%s \n',txt{i})
    end
%       rethrow(ME)
end


function Help_Callback(hObject, eventdata, handles)
guihelp(handles)


function SaveWorkspace_Callback(hObject, eventdata, handles)
Data = handles.Data ;
if ~isfield(Data,'Mdata')
    set(handles.Status,'string','Save: No data to save to workspace.')
    return
end

N = length(Data.Mdata);
for k = 1:N;
    % load one measurement
    M = Data.Mdata(k);

    % store coordinates
    if strcmp(M.type,'Circle (R)')
        X = M.circ.xc ;
        Y = M.circ.yc ;
    elseif strcmp(M.type,'Spline')
        X = M.spline.x ;
        Y = M.spline.y ;
    else
        X = M.X;
        Y = M.Y;
    end

    % prepare save structure
    D(k).filename  = M.file;
    D(k).type      = M.type;
    D(k).value     = M.value;
    D(k).intensity = M.intensity;
    D(k).profile   = M.profile;
    D(k).unit      = M.unit;
    D(k).x = X;
    D(k).y = Y;
end

% build the popup window
prompt={'Choose a Workspace variable name'};
name='Save to workspace';
numlines=1;
defaultanswer={'mt'};
% pop the menu
A = inputdlg(prompt,name,numlines,defaultanswer);

% if cancel
```

```matlab
if isempty(A)
    set(handles.Status,'string','Save: Canceled')
    return
end

% save to workspace
assignin('base',A{1},D);

set(handles.Status,'string',sprintf('Save: Data saved to variable %s',A{1}))

function SaveText_Callback(hObject, eventdata, handles)
Data = handles.Data ;
if ~isfield(Data,'Mdata')
    set(handles.Status,'string','Save: No data to save to file.')
    return
end
% prompt for a filename to save to
[file,path] = uiputfile('mt_data.txt','Save file name');
if file == 0
    set(handles.Status,'string','Save: to text aborted.')
    return
end

% open file for writing (and trunctate)
fid = fopen(fullfile(path,file),'wt+');

% Write the header
fprintf(fid,'Data file created by measuretool.m \r\n');
fprintf(fid,'========================================= \r\n');
fprintf(fid,'Filename:    %s \r\n',Data.cfile);
fprintf(fid,'Date:        %s \r\n',datestr(now));
[n m k] = size(Data.Im);
fprintf(fid,'Image Size:  (%gx%gx%g) \r\n',n,m,k);
% Calibration
if isfield(Data,'Lppx')
    fprintf(fid,'Calibration: %g %s per pixel \r\n',Data.Lppx,Data.unit);
else
    fprintf(fid,'Calibration: none \r\n');
end
fprintf(fid,'= End of Header =========================== \r\n');
fprintf(fid,'%3s, %12s, %5s, %10s, %12s, %s, %s, %s
\r\n','n','value','unit','type','intensity','[xcoords]','[ycoords]','filename');

% Write the Data
N = length(Data.Mdata);
for k = 1:N;
    % load one measurement
    M = Data.Mdata(k);

    % get the coordinates
    if strcmp(M.type,'Circle (R)')
        X = M.circ.xc ;
        Y = M.circ.yc ;
    elseif strcmp(M.type,'Spline')
        X = M.spline.x ;
        Y = M.spline.y ;
    else
        X = M.X;
        Y = M.Y;
    end

    % format to a string
    xstr = '[ ';
    ystr = '[ ';
    for kk = 1:length(X);
        if kk == 1
            xstr = [ xstr sprintf('%8.2e',X(kk)) ] ;
            ystr = [ ystr sprintf('%8.2e',Y(kk)) ] ;
        else
            xstr = [ xstr ' ; ' sprintf('%8.2e',X(kk)) ] ;
            ystr = [ ystr ' ; ' sprintf('%8.2e',Y(kk)) ] ;
        end
    end
    xstr = [ xstr ' ]' ];
    ystr = [ ystr ' ]' ];

    % write to file
    fprintf(fid,'%3d, %12.6e, %5s, %10s, %12s, %s, %s, %s
\r\n',k,M.value,M.unit,M.type,M.intensity,xstr,ystr,M.file);
```

```matlab
    end

    % close the file
    fprintf(fid,'= End of File ============================== \r\n');
    fclose(fid);

    set(handles.Status,'string',sprintf('Save: Data saved to file %s',file))


    function SavePNG_Callback(hObject, eventdata, handles)
    % this is an attempt to get anti-aliased png images, it works reasonably
    % well execpt for the font sizes, which change a bit between saving.
    Data = handles.Data;
    if ~isfield(Data,'gcf')
        set(handles.Status,'string','Save: No image to save')
        return
    end
    H = Data.gcf;

    % prompt for a filename to save to
    [file,path] = uiputfile('mt_data.png','Save file name');
    if file == 0
        set(handles.Status,'string','Save: to png aborted.')
        return
    end

    % set the status
    set(handles.Status,'string','Save: Writing png...')

    % fix the extention, to be always .png (small case)
    filename = fullfile(path,file);
    filename = [regexprep(filename,'.png$','','ignorecase') '.png'];

    % get the original figure position (and size)
    savepos = get(H,'Position');

    % set the paper position to 1 inch per 100 pixels
    set(H,'PaperUnits','inches','PaperPosition',savepos.*[0 0 1e-2 1e-2])

    % get the fontsize handles
    Hf = findobj(H,'-property','FontSize');

    % store the original fontsize
    fontsize = get(Hf(1),'FontSize');
    % double the font size (temporarily)
    set(Hf,'FontSize',fontsize*2);

    % get a temporary filename
    tmp = [tempname '.png'];

    % save png (2 times bigger than original)
    print(H,tmp,'-dpng','-r200')

    % restore the fontsize
    set(Hf,'FontSize',fontsize);


    % read the temporary image
    Im = imread(tmp,'PNG');

    % delete the temporary file
    delete(tmp);

    try
        I = imresize(Im, 0.5, 'bilinear');
    catch
        % workaround for missing Image Processing Toolbox

        % get the image size
        [n m k] = size(Im);
        % create the interpolation spacing
        xi = (1:2:m) + 0.5 ;
        yi = (1:2:n) + 0.5 ;

        % create a new image
```

241

```matlab
    mi = length(xi);
    ni = length(yi);
    I = zeros(ni,mi,k);

    % interpolate (per color)
    I(:,:,1) = interp2(double(Im(:,:,1)),xi,yi.','*linear');
    I(:,:,2) = interp2(double(Im(:,:,2)),xi,yi.','*linear');
    I(:,:,3) = interp2(double(Im(:,:,3)),xi,yi.','*linear');

    % convert back to integer
    I = uint8(round(I));
end
% write the real .png file
imwrite(I,filename,'PNG')

set(handles.Status,'string',sprintf('Save: PNG file %s saved',file))


function SavePDF_Callback(hObject, eventdata, handles)
Data = handles.Data;
if ~isfield(Data,'gcf')
    set(handles.Status,'string','Save: No image to save')
    return
end
H = Data.gcf;

% prompt for a filename to save to
[file,path] = uiputfile('mt_data.pdf','Save file name');
if file == 0
    set(handles.Status,'string','Save: to pdf aborted.')
    return
end

set(handles.Status,'string','Save: Writing pdf...')

filename = fullfile(path,file);

% fix the extention, to be always .png (small case)
filename = [regexprep(filename,'.pdf$','','ignorecase') '.pdf'];

% get the original figure position (and size)
savepos = get(H,'Position');

% set the paper position to 1 inch per 100 pixels
set(H,'PaperUnits','inches','PaperPosition',savepos.*[0 0 1e-2 1e-2])
set(H,'PaperSize',savepos(3:4).*[1e-2 1e-2])

% save png (3 times bigger than original)
print(H,filename,'-dpdf')

set(handles.Status,'string',sprintf('Save: PDF file %s saved',file))


% --- Executes on selection change in FileBox.
function FileBox_Callback(hObject, eventdata, handles)
Data = handles.Data;

cfilenum = get(handles.FileBox,'Value');
if ~isfield(Data,'ftypes')
    return
end

ctype = Data.ftypes{cfilenum};
cfile = Data.files{cfilenum};

set(handles.Status,'string','List: new file selected')

Data.cfile    = cfile ;
Data.ctype    = ctype ;
Data.cfilenum = cfilenum ;

% storing in the Data structure
handles.Data = Data;
% Update handles structure
guidata(hObject, handles);
```

```matlab
plotfun(hObject, eventdata, handles)


function FileBox_CreateFcn(hObject, eventdata, handles)
if ispc && isequal(get(hObject,'BackgroundColor'), get(0,'defaultUicontrolBackgroundColor'))
    set(hObject,'BackgroundColor','white');
end


function ShowAll_Callback(hObject, eventdata, handles)
plotfun(hObject, eventdata, handles)


function Quickmeasure_Callback(hObject, eventdata, handles)


function ZoomSelect_Callback(hObject, eventdata, handles)


function Clear_Callback(hObject, eventdata, handles)
Data = handles.Data;
if isfield(Data,'gcf')
    close(Data.gcf)
end
D.options  = Data.options;
D.degree = Data.degree;

Data = D;
handles = rmfield(handles,'Data');

% Enable the all buttons
buttons = findobj(handles.figure1,'Enable','off');
set(buttons,'Enable','on')

% select the current file from in the list
set(handles.FileBox,'String',{'...'});
set(handles.FileBox,'Value',1);

% set status
set(handles.Status,'string','measuretool reset')
```
```matlab
% storing in the Data structure
handles.Data = Data;
% Update handles structure
guidata(hObject, handles);

function Intensity_Callback(hObject, eventdata, handles)
plotfun(hObject, eventdata, handles)

function I = grayscale(I)
I = double(I);
if ndims(I) == 3
    I = 0.2989 * I(:,:,1) + 0.5870 * I(:,:,2) + 0.1140 * I(:,:,3);
end
```

This page intentionally left blank

Bibliography

1. Newell-McGloughlin, M. & E. R. *The evolution of biotechnology: From Natufians to Nanotechnology*; 2006.

2. Simopoulos, A. P. The importance of the omega-6/omega-3 fatty acid ratio in cardiovascular disease and other chronic diseases. *Exp. Biol. Med. (Maywood).* **2008**, *233*, 674–88.

3. Phinney, S. D.; Odin, R. S.; Johnson, S. B.; Holman, R. T. Reduced arachidonate in serum phospholipids and cholesteryl esters associated with vegetarian diets in humans. *Am. J. Clin. Nutr.* **1990**, *51*, 385–392.

4. Jacobs, M. N.; Coraci, M.; Gheorghe, A.; Schepens, A.; Covaci, A.; Schepens, P. Time trend investigation of PCBs, PBDEs, and organochlorine pesticides in selected n-3 polyunsaturated fatty acid rich dietary fish oil and vegetable oil supplements; nutritional relevance for human essential n-3 fatty acid requirements. *J. Agric. Food Chem.* **2004**, *52*, 1780–8.

5. Qi, B.; Fraser, T.; Mugford, S.; Dobson, G.; Sayanova, O.; Butler, J.; Napier, J. a; Stobart, a K.; Lazarus, C. M. Production of very long chain polyunsaturated omega-3 and omega-6 fatty acids in plants. *Nat. Biotechnol.* **2004**, *22*, 739–745.

6. Graham, I. a.; Larson, T.; Napier, J. a. Rational metabolic engineering of transgenic plants for biosynthesis of omega-3 polyunsaturates. *Curr. Opin. Biotechnol.* **2007**, *18*, 142–147.

7. Khozin-Goldberg, I.; Iskandarov, U.; Cohen, Z. LC-PUFA from photosynthetic microalgae: Occurrence, biosynthesis, and prospects in biotechnology. *Appl. Microbiol. Biotechnol.* **2011**, *91*, 905–915.

8. Abad, S.; Turon, X. Valorization of biodiesel derived glycerol as a carbon source to obtain added-value metabolites: Focus on polyunsaturated fatty acids. *Biotechnol. Adv.* **2012**, *30*, 733–41.

9. Rosa, S. M.; Soria, M. A.; Vélez, C. G.; Galvagno, M. A. Improvement of a two-stage fermentation process for docosahexaenoic acid production by Aurantiochytrium limacinum SR21 applying statistical experimental designs and data analysis. *Bioresour. Technol.* **2010**, *101*, 2367–74.

10. Jacobs, M.; Wyatt, C.; Santillo, D.; French, M. Organochlorine pesticide and PCB residues in pharmaceutical, industrial and food grade fish oils. *Int. J. EnViron. Pollut* **1997**, *8*, 74–93.

11. Nevado, J.; Martín-Doimeadiós, R. Multiresidue determination of organochlorines in fish oil by GC–MS: A new strategy in the sample preparation. *Talanta* **2010**.

12. Hussein, N. M.; Wilkinson, P. A.; Leach, C.; Burdge, G. C.; Wootton, S. A.; Griffin, B. A.; Millward, J. D. Relative rates of long chain conversion of^ 1^ 3C alpha-linolenic acid in adult men fed high alpha-linolenic acid or high linoleic acid diets. *PROCEEDINGS-NUTRITION Soc. LONDON* **2002**, *61*, 128A--128A.

13. Wen, Z.-Y.; Chen, F. Heterotrophic production of eicosapentaenoic acid by microalgae. *Biotechnol. Adv.* **2003**, *21*, 273–294.

14. Burja, A. M.; Radianingtyas, H.; Windust, A.; Barrow, C. J. Isolation and characterization of polyunsaturated fatty acid producing Thraustochytrium species : screening of strains and optimization of omega-3 production. *Appl. Microbiol. Biotechnol.* **2006**, *72*, 1161–1169.

15. Huang, J.; Aki, T.; Yokochi, T.; Nakahara, T.; Honda, D.; Kawamoto, S.; Shigeta, S.; Ono, K.; Suzuki, O. Grouping newly isolated docosahexaenoic acid-producing thraustochytrids based on their polyunsaturated fatty acid profiles and comparative analysis of 18S rRNA genes. *Mar. Biotechnol. (NY).* **2003**, *5*, 450–7.

16. Jakobsen, A. N.; Aasen, I. M.; Josefsen, K. D.; Strøm, A. R. Accumulation of docosahexaenoic acid-rich lipid in thraustochytrid Aurantiochytrium sp. strain T66: effects of N and P starvation and O2 limitation. *Appl. Microbiol. Biotechnol.* **2008**, *80*, 297–306.

17. Jakobsen, A. N.; Aasen, I. M.; Strøm, A. R. Endogenously synthesized (-)-proto-quercitol and glycine betaine are principal compatible solutes of Schizochytrium sp. strain S8 (ATCC 20889) and three new isolates of phylogenetically related thraustochytrids. *Appl. Environ. Microbiol.* **2007**, *73*, 5848–56.

18. Luque, R.; Lovett, J. C.; Datta, B.; Clancy, J.; Campelo, J. M.; Romero, A. a. Biodiesel as feasible petrol fuel replacement: a multidisciplinary overview. *Energy Environ. Sci.* **2010**, *3*, 1706.

19. Luque, R.; Herrero-Davila, L.; Campelo, J. M.; Clark, J. H.; Hidalgo, J. M.; Luna, D.; Marinas, J. M.; Romero, A. a. Biofuels: a technological perspective. *Energy Environ. Sci.* **2008**, *1*, 542.

20. Thompson, J.; He, B. Characterization of crude glycerol from biodiesel production from multiple feedstocks. *Appl. …* **2006**, *22*, 2006–2007.

21. Pyle, D. J. Use of Biodiesel-Derived Crude Glycerol for the Production of Omega-3 Polyunsaturated Fatty Acids by the Microalga Schizochytrium limacinum, 2008.

22. Johnson, D. T.; Taconi, K. A. The glycerin glut: Options for the value-added conversion of crude glycerol resulting from biodiesel production. *Environ. Prog.* **2007**, *26*, 338–348.

23. Prielipp, G. G.; Keller, H. H. Purification of crude glycerin by ion exclusion. *J. Am. Oil Chem. Soc.* **1956**, *33*, 103–108.

24. Yang, F.; Hanna, M. a; Sun, R. Value-added uses for crude glycerol--a byproduct of biodiesel production. *Biotechnol. Biofuels* **2012**, *5*, 13.

25. Himmi, E. H.; Bories, A.; Barbirato, F. Nutrient requirements for glycerol conversion to 1,3-propanediol by Clostridium butyricum. *Bioresour. Technol.* **1998**, *67*, 123–128.

26. Cardona, C.; Posada, J.; Montoya, M. Use of Glycerol from biodiesel production: Conversion to added value products. *Proc. Eur. Congr. Chem. Eng.* **2007**, *16*, 20.

27. Saxena, R. K.; Anand, P.; Saran, S.; Isar, J. Microbial production of 1,3-propanediol: Recent developments and emerging opportunities. *Biotechnol. Adv.* **2009**, *27*, 895–913.

28. Nabe, K.; Izuo, N.; Yamada, S.; Chibata, I. Conversion of Glycerol to Dihydroxyacetone by Immobilized Whole Cells of Acetobacter xylinum. *Appl. Environ. Microbiol.* **1979**, *38*, 1056–60.

29. Bauer, R.; Katsikis, N.; Varga, S.; Hekmat, D. Study of the inhibitory effect of the product dihydroxyacetone on Gluconobacter oxydans in a semi-continuous two-stage repeated-fed-batch process. *Bioprocess Biosyst. Eng.* **2005**, *28*, 37–43.

30. Bories, A.; Claret, C.; Soucaille, P. Kinetic study and optimisation of the production of dihydroxyacetone from glycerol using Gluconobacter oxydans. *Process Biochem.* **1994**, *26*, 243–248.

31. Lee, P. C.; Lee, W. G.; Lee, S. Y.; Chang, H. N. Succinic acid production with reduced by-product

formation in the fermentation of Anaerobiospirillum succiniciproducens using glycerol as a carbon source. *Biotechnol. Bioeng.* **2001**, *72*, 41–8.

32. Mantzouridou, F.; Naziri, E.; Tsimidou, M. Z. Industrial glycerol as a supplementary carbon source in the production of beta-carotene by Blakeslea trispora. *J. Agric. Food Chem.* **2008**, *56*, 2668–75.

33. Narayan, M. S.; Manoj, G. P.; Vatchravelu, K.; Bhagyalakshmi, N.; Mahadevaswamy, M. Utilization of glycerol as carbon source on the growth, pigment and lipid production in Spirulina platensis. *Int. J. Food Sci. Nutr.* **2005**, *56*, 521–528.

34. Barclay, W. R.; Meager, K. M.; Abril, J. R.; W. R. Barclay, K. M. M. A. J. R. A. Heterotrophic production of long chain omega-3 fatty acids utilizing algae and algae-like microorganisms. *J. Appl. Phycol.* **1994**, *6*, 123–129.

35. Pratima, B.; Bajpai, P. K. Eicosapentaenoic acid (EPA) production from microorganisms : a review. *J. Biotechnol.* **1992**, *30*, 161–183.

36. Yongmanitchai, W.; Ward, O. P. Growth of and omega-3 fatty acid production by Phaeodactylum tricornutum under different culture conditions. *Appl. Environ. Microbiol.* **1991**, *57*, 419–25.

37. Athalye, S. K. Production of Eicosapentaenoic acid from biodiesel derived crude glycerol using fungal culture., Virginia Polytechnic Institute and State University, 2008.

38. Athalye, S. K.; Garcia, R. a; Wen, Z. Use of biodiesel-derived crude glycerol for producing eicosapentaenoic acid (EPA) by the fungus Pythium irregulare. *J. Agric. Food Chem.* **2009**, *57*, 2739–44.

39. Berge, J.-P.; Gouygoy, J.-P.; Dubacq, J.-P.; Durand, P. Reassessment of lipid composition of the diatom, Skeletonema costatum. *Phytochemistry* **1995**, *39*, 1017–1021.

40. Blanchemain, A.; Grizeau, D. Increased production of eicosapentaenoic acid by Skeletonema costatum cells after decantation at low temperature. *Biotechnol. Tech.* **1999**, 497–501.

41. Dembitsky, V. M.; Rezankova, H.; Rezanka, T.; Hanus, L. O. Variability of the fatty acids of the marine green algae belonging to the genus Codium. *Biochem. Syst. Ecol.* **2003**, *31*, 1125–1145.

42. Gandhi, S. R.; Weete, J. D. Production of the polyunsaturated fatty acids arachidonic acid and eicosapentaenoic acid by the fungus Pythium ultimum. *J. Gen. Microbiol.* **1991**, *137*, 1825–30.

43. Goecke, F.; Hernández, V.; Bittner, M.; Hernandez, V.; Gonzalez, M.; Becerra, J.; Silva, M. Fatty acid composition of three species of Codium (Bryopsidales, Chlorophyta) in Chile. *Rev Biol Mar …* **2010**, *45*, 325–330.

44. Vazhappilly, R.; Chen, F. Eicosapentaenoic acid and docosahexaenoic acid production potential of microalgae and their heterotrophic growth. *J. Am. Oil Chem. Soc.* **1998**, *75*, 393–397.

45. Ellenbogen, B. B.; Aaronson, S.; Goldstein, S.; Belsky, M. Polyunsaturated fatty acids of aquatic fungi: Possible phylogenetic significance. *Comp. Biochem. Physiol.* **1969**, *29*, 805–811.

46. Lewis, T. E.; Nichols, P. D.; McMeekin, T. A. The Biotechnological Potential of Thraustochytrids. *Mar. Biotechnol.* **1999**, *1*, 580–587.

47. Quilodran, B.; Himzpeter, I.; Hormazabal, E.; Quiroz, A.; Shene, C.; Quilodrán, B.; Hinzpeter, I. Docosahexaenoic acid (C22:6n - 3, DHA) and astaxanthin production by Thraustochytriidae sp. AS4-A1 a native strain with high similitude to Ulkenia sp.: Evaluation of liquid residues from food industry as

nutrient sources. *Enzyme Microb. Technol.* **2010**, *47*, 24–30.

48. Ward, O. P.; Singh, A. Omega-3/6 fatty acids : Alternative sources of production. *Process Biochem.* **2005**, *40*, 3627–3652.

49. Singh, A.; Wilson, S.; Ward, O. P. Docosahexaenoic Thraustochytrium sp. ATCC 20892, acid (DHA) production. *Microbiology* **1996**, *1*.

50. Singh, A.; Ward, O. P. Production of high yields of docosahexaenoic acid by Thraustochytrium roseum ATCC 28210. *J. Ind. Microbiol.* **1996**, *16*, 370–373.

51. Bajpai, P. K.; Ward, O. P. Optimization of Production of Docosahexaenoic Acid (DHA) by by*Thraustochytrium aureum* ATCC 34304. *J. Am. Oil Chem. Soc.* **1991**, *68*, 3–8.

52. Ethier, S.; Woisard, K.; Vaughan, D.; Wen, Z. Continuous culture of the microalgae Schizochytrium limacinum on biodiesel-derived crude glycerol for producing docosahexaenoic acid. *Bioresour. Technol.* **2010**, *102*, 88–93.

53. Li, Z. yi; Ward, O. P. Production of docosahexaenoic acid by<i>Thraustochytrium roseum</i> *J. Ind. Microbiol. & Biotechnol.* **1994**, *13*, 238–241.

54. Zhu, L.; Zhang, X.; Ji, L.; Song, X.; Kuang, C. Changes of lipid content and fatty acid composition of Schizochytrium limacinum in response to different temperatures and salinities. *Process Biochem.* **2007**, *42*, 210–214.

55. Raghukumar, S. Thraustochytrid Marine Protists: production of PUFAs and Other Emerging Technologies. *Mar. Biotechnol. (NY).* **2008**, *10*, 631–40.

56. Honda, D.; Yokochi, T.; Nakahara, T.; Erata, M.; Higashihara, T. Schizochytrium limacinum sp. nov., a new thraustochytrid from a mangrove area in the west Pacific Ocean. *Mycol. Res.* **1998**, *102*, 439–448.

57. Koller, M.; Bona, R.; Braunegg, G. Production of polyhydroxyalkanoates from agricultural waste and surplus materials. … **2005**, 561–565.

58. Muir, D.; Wagemann, R.; Hargrave, B. T.; Thomas, D. J.; Peakall, D. B.; Norstrom, R. J. Arctic marine ecosystem contamination. *Sci. Total Environ.* **1992**, *122*, 75–134.

59. Řezanka, T.; Sigler, K. Odd-numbered very-long-chain fatty acids from the microbial, animal and plant kingdoms. *Prog. Lipid Res.* **2009**, *48*, 206–238.

60. Huang, J.; Aki, T.; Hachida, K. Profile of polyunsaturated fatty acids produced by Thraustochytrium sp. KK17-3. *J. Am. …* **2001**, 1–4.

61. Horrocks, L. A.; Yeo, Y. K. Health benefits of docosahexaenoic acid (DHA). *Pharmacol. Res.* **1999**, *40*, 211–225.

62. Holman, R. T. The slow discovery of the importance of omega 3 essential fatty acids in human health. *J. Nutr.* **1998**, *128*, 427S–433S.

63. Hazel, J. R. Thermal adaptation in biological membranes: is homeoviscous adaptation the explanation? *Annu. Rev. Physiol.* **1995**, *57*, 19–42.

64. Lipid, A. Insect lipids a n d lipoproteins, a n d their role in physiological processes. *Lipids* **1972**, *24*, 19–67.

65. Simopoulos, a P. Omega-3 fatty acids in health and disease and in growth and development. *Am. J. Clin. Nutr.* **1991**, *54*, 438–63.

66. Hansen-Krone, I. J.; Enga, K. F.; Südduth-Klinger, J. M.; Mathiesen, E. B.; Njølstad, I.; Wilsgaard, T.; Watkins, S.; Brækkan, S. K.; Hansen, J.-B. High fish plus fish oil intake is associated with slightly reduced risk of venous thromboembolism: the Tromsø Study. *J. Nutr.* **2014**, *144*, 861–7.

67. Major, R.; Kostapanos, M. S. Association Between Omega-3 Fatty Acid. **2012**.

68. Group, T. R. and P. S. C. n–3 Fatty Acids in Patients with Multiple Cardiovascular Risk Factors. *N. Engl. J. Med.* **2013**, *368*, 1800–1808.

69. Hospital, H. G. n–3 Fatty Acids and Cardiovascular Outcomes in Patients with Dysglycemia. *N. Engl. J. Med.* **2012**, *367*, 309–318.

70. Hu, F. B.; Manson, J. E. Omega-3 Fatty Acids and Secondary Prevention of Cardiovascular Disease—Is It Just a Fish Tale? *Arch Intern Med* **2012**, *172*, 9–11.

71. Kwak, S. M.; Myung, S.-K.; Lee, Y. J.; Seo, H. G. Efficacy of Omega-3 Fatty Acid Supplements (Eicosapentaenoic Acid and Docosahexaenoic Acid) in the Secondary Prevention of Cardiovascular Disease: A Meta-analysis of Randomized, Double-blind, Placebo-Controlled Trials. *Arch. Intern. Med.* **2012**, *172*, 686–694.

72. Study, a C. Cause-Specific Mortality in Older Adults. **2013**.

73. Tjonneland, A.; Overvad, K.; Bergmann, M. M.; Nagel, G.; Linseisen, J.; Hallmans, G.; Palmqvist, R.; Sjodin, H.; Hagglund, G.; Berglund, G.; Lindgren, S.; Grip, O.; Palli, D.; Day, N. E.; Khaw, K.-T.; Bingham, S.; Riboli, E.; Kennedy, H.; Hart, A. Linoleic acid, a dietary n-6 polyunsaturated fatty acid, and the aetiology of ulcerative colitis: a nested case-control study within a European prospective cohort study. *Gut* **2009**, *58*, 1606–1611.

74. Brasky, T. M.; Lampe, J. W.; Potter, J. D.; Patterson, R. E.; White, E. Specialty Supplements and Breast Cancer Risk in the VITamins And Lifestyle (VITAL) Cohort Specialty Supplements and Breast Cancer Risk in the VITamins And Lifestyle (VITAL) Cohort. **2010**, *2*, 1696–1708.

75. Daenen, L. G. M.; Cirkel, G. a.; Houthuijzen, J. M.; Gerrits, J.; Oosterom, I.; Roodhart, J. M. L.; van Tinteren, H.; Ishihara, K.; Huitema, A. D. R.; Verhoeven-Duif, N. M.; Voest, E. E. Increased Plasma Levels of Chemoresistance-Inducing Fatty Acid 16:4(n-3) After Consumption of Fish and Fish Oil. *JAMA Oncol.* **2015**, *di*, 1–12.

76. Meleth, a D.; Reed, G. F.; Sperduto, R. D.; Clemons, T. E.; Sangiovanni, J. P.; Agro, E. Omega-3 long-chain polyunsaturated fatty acid intake and 12-y incidence of neovascular age-related macular degeneration and central geographic atrophy : AREDS report 30 , a prospective cohort study from the Age-Related Eye Disease Study 1 – 4. **2009**, 1601–1607.

77. Rondanelli, M.; Giacosa, A.; Opizzi, A.; Pelucchi, C.; La Vecchia, C.; Montorfano, G.; Negroni, M.; Berra, B.; Politi, P.; Rizzo, A. M. Effect of omega-3 fatty acids supplementation on depressive symptoms and on health-related quality of life in the treatment of elderly women with depression: a double-blind, placebo-controlled, randomized clinical trial. *J. Am. Coll. Nutr.* **2010**, *29*, 55–64.

78. Rizzo, A. M.; Corsetto, P. a; Montorfano, G.; Opizzi, A.; Faliva, M.; Giacosa, A.; Ricevuti, G.; Berra, B.; Rondanelli, M.; Pelucchi, C. Comparison between the AA/EPA ratio in depressed and non depressed elderly females: omega-3 fatty acid supplementation correlates with improved symptoms but does not

change immunological parameters. *Nutr. J.* **2012**, *11*, 82.

79. Lewis, M. D.; Hibbeln, J. R.; Johnson, J. E.; Hong, Y. L.; Hyun, D. Y.; Loewke, J. D. Suicide Deaths of Active Duty U.S. Military and Omega-3 Fatty Acid Status: A Case Control Comparison. **2012**, *72*, 1585–1590.

80. Leaf, a; Weber, P. C. A new era for science in nutrition. *Am. J. Clin. Nutr.* **1987**, *45*, 1048–1053.

81. Braune, B. M.; Outridge, P. M.; Fisk, A. T.; Muir, D. C. G.; Helm, P. A.; Hobbs, K.; Hoekstra, P. F.; Kuzyk, Z. A.; Kwan, M.; Letcher, R. J.; Lockhart, W. L.; Norstrom, R. J.; Stern, G. A.; Stirling, I. Persistent organic pollutants and mercury in marine biota of the Canadian Arctic: an overview of spatial and temporal trends. *Sci. Total Environ.* **2005**, *351–352*, 4–56.

82. Muir, D.; Braune, B.; Demarch, B.; Norstrom, R.; Wagemann, R.; Lockhart, L.; Hargrave, B.; Bright, D.; Addison, R.; Payne, J.; Reimer, K. Spatial and temporal trends and effects of contaminants in the Canadian Arctic marine ecosystem : a review. *Sci. Total Environ.* **2005**, *230*, 83–144.

83. Joint report of the Scientific Advisory Committee on Nutrition (SACN) and the Committee on Toxicity (COT) on the consumption of fish. Advice on fish consumption: benefits & risks 2004. *Advice fish Consum. benefits risks* **2004**.

84. Sunderland, E. M.; Schoeny, R. NIH Public Access. **2012**, *69*, 493–508.

85. van Larebeke, N.; Hens, L.; Schepens, P.; Covaci, a; Baeyens, J.; Everaert, K.; Bernheim, J. L.; Vlietinck, R.; De Poorter, G. The Belgian PCB and dioxin incident of January-June 1999: exposure data and potential impact on health. *Environ. Health Perspect.* **2001**, *109*, 265–73.

86. Idowu, S. O. *Encyclopedia of Corporate Social Responsibility*; 2013.

87. Secretariat of the Stockholm Convention Ridding the World of POPs: A Guide to the Stockholm Convention. **2010**, 20.

88. Besselink, H. T.; Denison, M. S.; Hahn, M. E.; Karchner, S. I.; Vethaak, A. D.; Koeman, J. H.; Brouwer, A. Low inducibility of CYP1A activity by polychlorinated biphenyls (PCBs) in flounder (Platichthys flesus): characterization of the Ah receptor and the role of CYP1A inhibition. *Toxicol. Sci.* **1998**, *43*, 161–71.

89. Bandiera, S.; Safe, S.; Okey, A. B. Binding of polychlorinated biphenyls classified as either phenobarbitone-, 3-methylcholanthrene- or mixed-type inducers to cytosolic Ah receptor. *Chem. Biol. Interact.* **1982**, *39*, 259–277.

90. McKinney, J. D.; Darden, T.; Lyerly, M. A.; Pedersen, L. G. PCB and Related Compound Binding to the Ah Receptor(s). Theoretical Model Based on Molecular Parameters and Molecular Mechanics. *Quant. Struct.-Act. Relat.* **1985**, *4*, 166–172.

91. Schecter, A.; Birnbaum, L.; Ryan, J. J.; Constable, J. D. Dioxins: an overview. *Env. Res* **2006**, *101*, 419–428.

92. Unagul, P.; Assantachai, C.; Phadungruengluij, S.; Suphantharika, M. C. V.; Verduyn, C. Properties of the docosahexaenoic acid-producer Schizochytrium mangrovei Sk-02: effects of glucose, temperature and salinity and their interaction. *Bot. Mar.* **2005**, *48*, 387–394.

93. Chi, Z.; Pyle, D.; Wen, Z.; Frear, C.; Chen, S.; Zhiyou, W.; Shulin, C. A laboratory study of producing docosahexaenoic acid from biodiesel-waste glycerol by microalgal fermentation. *Process Biochem.* **2007**, *42*, 1537–1545.

94. Carvalho, A. P.; Malcata, F. X. Optimization of omega-3 fatty acid production by microalgae: crossover effects of CO2 and light intensity under batch and continuous cultivation modes. *Mar. Biotechnol. (NY).* **2005**, *7*, 381–8.

95. Ryu, B.-G.; Kim, K.; Kim, J.; Han, J.-I.; Yang, J.-W. Use of organic waste from the brewery industry for high-density cultivation of the docosahexaenoic acid-rich microalga, Aurantiochytrium sp. KRS101. *Bioresour. Technol.* **2013**, *129*, 351–9.

96. Burgess, J. G.; Iwamoto, K.; Miura, Y.; Takano, H.; Matsunaga, T. B edmology AppC l Microbiology An optical fibre photobioreactor for enhanced production of the marine unicellular alga Isochrysis aft . galbana T-Iso (UTEX LB 2307) rich in docosahexaenoic acid. *Appl. Microbiol. Biotechnol.* **1993**, *39*, 456–459.

97. Jang, H.-D.; Lin, Y.-Y.; Yang, S.-S. Effect of culture media and conditions on polyunsaturated fatty acids production by Mortierella alpina. *Bioresour. Technol.* **2005**, *96*, 1633–44.

98. Mendes, A.; Guerra, P.; Madeira, V.; Ruano, F.; Lopes da Silva, T.; Reis, A. Study of docosahexaenoic acid production by the heterotrophic microalga Crypthecodinium cohnii CCMP 316 using carob pulp as a promising carbon source. *World J. Microbiol. Biotechnol.* **2007**, *23*, 1209–1215.

99. Zeng, Y.; Ji, X.-J.; Lian, M.; Ren, L.-J.; Jin, L.-J.; Ouyang, P.-K.; Huang, H. Development of a temperature shift strategy for efficient docosahexaenoic acid production by a marine fungoid protist, Schizochytrium sp. HX-308. *Appl. Biochem. Biotechnol.* **2011**, *164*, 249–55.

100. De Swaaf, M. E.; Sijtsma, L.; Pronk, J. T. High-cell-density fed-batch cultivation of the docosahexaenoic acid producing marine alga Crypthecodinium cohnii. *Biotechnol. Bioeng.* **2003**, *81*, 666–72.

101. Kautharapu, K. B.; Rathmacher, J.; Jarboe, L. R. Growth condition optimization for docosahexaenoic acid (DHA) production by Moritella marina MP-1. *Appl. Microbiol. Biotechnol.* **2012**, 2859–2866.

102. Wen, Z. Y.; Chen, F. Application of statistically-based experimental designs for the optimization of eicosapentaenoic acid production by the diatom Nitzschia laevis. *Biotechnol. Bioeng.* **2001**, *75*, 159–69.

103. Martins, D. A.; Custódio, L.; Barreira, L.; Pereira, H.; Ben-Hamadou, R.; Varela, J.; Abu-Salah, K. M. Alternative sources of n-3 long-chain polyunsaturated fatty acids in marine microalgae. *Mar. Drugs* **2013**, *11*, 2259–81.

104. Jiang, H.; Gao, K. Effects of Lowering Temperature During Culture on the Production of Polyunsaturated Fatty Acids in the Marine Diatom Phaeodactylum Tricornutum (Bacillariophyceae)1. *J. Phycol.* **2004**, *40*, 651–654.

105. Thepenier, C.; Gudin, C.; Sarrobert, B. Process for the selective production of polyunsaturated fatty acids from a culture of microalgae of the pophytidium cruentum. *US Pat. 5338673A* **1994**.

106. Giménez, A.; González, M.; Medina, A. Downstream processing and purification of eicosapentaenoic (20: 5n-3) and arachidonic acids (20: 4n-6) from the microalga Porphyridium cruentum. *Bioseparation* **1998**, 89–99.

107. Brown, M. R. Nutritional Value and Uses of Microalgae in Aquaculture. *Av. en Nutr. Acuícola VI. Memorias …* **2002**, 281–292.

108. Nakahara, T.; Yokochi, T. Production of docosahexaenoic and docosapentaenoic acids

251

bySchizochytrium sp. isolated from Yap Islands. *J. Am. …* **1996**.

109. Yokochi, T.; Honda, D.; Higashihara, T.; Nakahara, T. Optimization of docosahexaenoic acid production by Schizochytrium limacinum SR21. *Appl. Microbiol. Biotechnol.* **1997**, *49*, 72–76.

110. Yokoyama, R.; Salleh, B.; Honda, D. Taxonomic rearrangement of the genus Ulkenia sensu lato based on morphology, chemotaxonomical characteristics, and 18S rRNA gene phylogeny (Thraustochytriaceae, Labyrinthulomycetes): Emendation for Ulkenia and erection of Botryochytrium, Parietichytrium, . *Mycoscience* **2007**, *48*, 329–341.

111. Nagano, N.; Sakaguchi, K.; Taoka, Y.; Okita, Y.; Honda, D.; Ito, M.; Hayashi, M. Detection of genes involved in Fatty Acid elongation and desaturation in thraustochytrid marine eukaryotes. *J. Oleo Sci.* **2011**, *60*, 475–481.

112. Matsuda, T.; Sakaguchi, K.; Hamaguchi, R. The analysis of {Delta} 12-fatty acid desaturase function revealed that two distinct pathways are active for the synthesis of polyunsaturated fatty acids in. *J. lipid* **2012**, 6–10.

113. SPARROW Jr, K.; others Aquatic Phycomycetes exclusive of the Saprolegniaceae and Pythium. *Aquat. Phycomycetes Exclus. Saprolegniaceae Pythium.* **1943**.

114. Leander, C. A. C.; Porter, D. The Labyrinthulomycota Is Comprised of Three Distinct Lineages. *Mycologia* **2001**, *93*, 459–464.

115. Tsui, C. K. M.; Marshall, W.; Yokoyama, R.; Honda, D.; Lippmeier, J. C.; Craven, K. D.; Peterson, P. D.; Berbee, M. L. Labyrinthulomycetes phylogeny and its implications for the evolutionary loss of chloroplasts and gain of ectoplasmic gliding. *Mol. Phylogenet. Evol.* **2009**, *50*, 129–40.

116. Aki, T.; Hachida, K.; Yoshinaga, M.; Katai, Y.; Yamasaki, T.; Kawamoto, S.; KAKIZONO, T.; MAOKA, T.; SHIGETA, S.; SUZUKI, O.; ONO, K. Thraustochytrid as a potential source of carotenoids. *J. Am. Oil Chem. Soc.* **2003**, *80*, 789–794.

117. Chatdumrong, W. Optimization of docosahexaenoic acid (DHA) production and improvement of astaxanthin content in a mutant Schizochytrium limacinum isolated from mangrove. *Mar. …* **2006**, *334*, 324–334.

118. Nakazawa, A.; Matsuura, H.; Kose, R.; Kato, S.; Honda, D.; Inouye, I.; Kaya, K.; Watanabe, M. M. Optimization of culture conditions of the thraustochytrid Aurantiochytrium sp. strain 18W-13a for squalene production. *Bioresour. Technol.* **2012**, *109*, 287–91.

119. Li, Q.; Chen, G.-Q.; Fan, K.-W.; Lu, F.-P.; Aki, T.; Jiang, Y. Screening and characterization of squalene-producing thraustochytrids from Hong Kong mangroves. *J. Agric. Food Chem.* **2009**, *57*, 4267–72.

120. Baldauf, S. L.; Roger, A. J.; Wenk-Siefert, I.; Doolittle, W. F. A kingdom-level phylogeny of eukaryotes based on combined protein data. *Science* **2000**, *290*, 972–977.

121. Cavalier-Smith, T.; Chao, E. E.-Y. Phylogeny and megasystematics of phagotrophic heterokonts (kingdom Chromista). *J. Mol. Evol.* **2006**, *62*, 388–420.

122. Harper, J. T.; Waanders, E.; Keeling, P. J. On the monophyly of chromalveolates using a six-protein phylogeny of eukaryotes. *Int. J. Syst. Evol. Microbiol.* **2005**, *55*, 487–496.

123. Tyler, B. M.; Tripathy, S.; Zhang, X.; Dehal, P.; Jiang, R. H. Y.; Aerts, A.; Arredondo, F. D.; Baxter, L.; Bensasson, D.; Beynon, J. L.; Chapman, J.; Damasceno, C. M. B.; Dorrance, A. E.; Dou, D.; Dickerman, A.

W.; Dubchak, I. L.; Garbelotto, M.; Gijzen, M.; Gordon, S. G.; Govers, F.; Grunwald, N. J.; Huang, W.; Ivors, K. L.; Jones, R. W.; Kamoun, S.; Krampis, K.; Lamour, K. H.; Lee, M.-K.; McDonald, W. H.; Medina, M.; Meijer, H. J. G.; Nordberg, E. K.; Maclean, D. J.; Ospina-Giraldo, M. D.; Morris, P. F.; Phuntumart, V.; Putnam, N. H.; Rash, S.; Rose, J. K. C.; Sakihama, Y.; Salamov, A. A.; Savidor, A.; Scheuring, C. F.; Smith, B. M.; Sobral, B. W. S.; Terry, A.; Torto-Alalibo, T. A.; Win, J.; Xu, Z.; Zhang, H.; Grigoriev, I. V; Rokhsar, D. S.; Boore, J. L. Phytophthora genome sequences uncover evolutionary origins and mechanisms of pathogenesis. *Science* **2006**, *313*, 1261–1266.

124. Amon, J. P.; French, K. H. Photoresponses of the marine protist Ulkenia sp. zoospores to ambient, artificial and bioluminescent light. *Mycologia* **2004**, *96*, 463–9.

125. Tsui, C.; Vrijmoed, L. A Re-Visit to the Evolution and Ecophysiology of the Labyrinthulomycetes. *cdn.intechweb.org* **2009**.

126. Tsu, C. C. K. M.; Fan, K. W. K. W.; Chow, R. K. K. K. R.; Jones, E. B. G.; Vrijmoed, L. L. P. P.; Tsui, C. K. M.; Fan, K. W. K. W.; Chow, R. K. K. K. R.; Jones, E. B. G.; Vrijmoed, L. L. P. P. Zoospore production and motility of mangrove thraustochytrids from Hong Kong under various salinities. *Mycoscience* **2012**, *53*, 1–9.

127. Yokoyama, R.; Honda, D. Taxonomic rearrangement of the genus Schizochytrium sensu lato based on morphology, chemotaxonomic characteristics, and 18S rRNA gene phylogeny (Thraustochytriaceae, Labyrinthulomycetes): emendation for Schizochytrium and erection of Aurantiochytrium and . *Mycoscience* **2007**, *48*, 199–211.

128. Raghukumar, S. Ecology of the marine protists, the Labyrinthulomycetes (Thraustochytrids and Labyrinthulids). *Eur. J. Protistol.* **2002**, *38*, 127–145.

129. Porter, D. Phylum labyrinthulomycota. In *Handbook of Protoctista*; 1990; pp. 388–398.

130. Pooksawang, N.; Nangtharat, S.; Yunchalard, S. Batch fermentation of marine microalgae using glycerol obtained from biodiesel plant for docosahexaenoic acid (DHA) production. *3rd Int. Conf. Ferment. Technol. Value-Added Agric. Prod.* **2009**, *Fer4 P26*, 1–7.

131. Pyle, D. J.; Garcia, R. a; Wen, Z. Producing docosahexaenoic acid (DHA)-rich algae from biodiesel-derived crude glycerol: effects of impurities on DHA production and algal biomass composition. *J. Agric. Food Chem.* **2008**, *56*, 3933–9.

132. Fan, K. W.; Vrijmoed, L. L. P.; Jones, E. B. G. Physiological Studies of Subtropical Mangrove Thraustochytrids. *Bot. Mar.* **2002**, *45*, 50–57.

133. Shabala, L.; McMeekin, T.; Shabala, S. Osmotic adjustment and requirement for sodium in marine protist thraustochytrid. *Environ. Microbiol.* **2009**, *11*, 1835–43.

134. Liu, B.; Zhao, Z. K. Biodiesel production by direct methanolysis of oleaginous microbial biomass. *Chem. Technol.* **2007**, *780*, 775–780.

135. Lotero, E.; Liu, Y.; Lopez, D. E.; Suwannakarn, K.; Bruce, D. a.; Goodwin, J. G. Synthesis of Biodiesel via Acid Catalysis. *Ind. Eng. Chem. Res.* **2005**, *44*, 5353–5363.

136. Samul, D.; Leja, K.; Grajek, W. Impurities of crude glycerol and their effect on metabolite production. *Ann. Microbiol.* **2014**, *64*, 891–898.

137. Khozin, I.; Adlerstein, D.; Bigogno, C.; Cohen, Z. Elucidation of the biosynthesis of eicosapentaenoic

253

acid (EPA) in the microalga Porphyridium cruentum. *Physiol. Biochem. …* **1997**, 223–230.

138. Pereira, S. L.; Leonard, A. E.; Huang, Y.-S.; Chuang, L.-T.; Mukerji, P. Identification of two novel microalgal enzymes involved in the conversion of the omega3-fatty acid, eicosapentaenoic acid, into docosahexaenoic acid. *Biochem. J.* **2004**, *384*, 357–66.

139. de Swaaf, M. E. Docosahexaenoic acid production by the marine alga Crypthecodiunium cohnii, 2003.

140. Iida, I.; Nakahara, T.; Yokochi, T.; Kamisaka, Y.; Yagi, H.; Yamaoka, M.; Suzuki, O. Improvement of docosahexaenoic acid production in a culture of Thraustochytrium aureum by medium optimization. *J. Ferment. Bioeng.* **1996**, *81*, 76–78.

141. Hong, W.-K.; Kim, C. H.; Rairakhwada, D.; Kim, S.; Hur, B.-K.; Kondo, A.; Seo, J.-W. Growth of the oleaginous microalga Aurantiochytrium sp. KRS101 on cellulosic biomass and the production of lipids containing high levels of docosahexaenoic acid. *Bioprocess Biosyst. Eng.* **2012**, *35*, 129–33.

142. Jiang, Y.; Fan, K.-W.; Wong, R. T.-Y.; Chen, F. Fatty acid composition and squalene content of the marine microalga Schizochytrium mangrovei. *J. Agric. Food Chem.* **2004**, *52*, 1196–200.

143. Bowles, R.; Hunt, A.; Bremer, G. 3 polyunsaturated fatty acid production by members of the marine protistan group the thraustochytrids: screening of isolates and optimisation of docosahexaenoic acid. *Prog. Ind. …* **1999**, *1656*.

144. Taha, A. I. B. H. M.; Kimoto, T.; Kanada, T.; Okuyama, H. Growth optimization of thraustochytrid strain 12B for the commercial production of docosahexaenoic acid. *Food Sci. Biotechnol.* **2013**, *22*, 53–58.

145. Jakobsen, A. N. Anita Nordeng Jakobsen Compatible solutes and docosahexaenoic acid accumulation of thraustochytrids of the Aurantiochytrium group. **2008**.

146. Chin, H. J.; Shen, T. F.; Su, H. P.; Ding, S. T. Schizochytrium limacinum SR-21 as a source of docosahexaenoic acid: optimal growth and use as a dietary supplement for laying hens. *Aust. J. Agric. Res.* **2006**, *57*, 13.

147. Abad, S.; Pérez, X.; Planas, A.; Turon, X. Rapid monitoring of glycerol in fermentation growth media: Facilitating crude glycerol bioprocess development. *Talanta* **2014**, *121*, 210–4.

148. Liang, Y.; Cui, Y.; Trushenski, J.; Blackburn, J. W. Converting crude glycerol derived from yellow grease to lipids through yeast fermentation. *Bioresour. Technol.* **2010**, *101*, 7581–7586.

149. IUPAC Standard Methods for the Analysis of Oils. Fats and Derivatives Section III. Glycerines. *Pure Appl. Chem.* **1982**, *54*, 1257–1295.

150. Bansal, K.; McCrady, J.; Hansen, A.; Bhalerao, K. Thin layer chromatography and image analysis to detect glycerol in biodiesel. *Fuel* **2008**, *87*, 3369–3372.

151. Bligh, E. G.; Dyer, W. J. A rapid method of total lipid extraction and purification. *Can. J. Biochem. Physiol.* **1959**, *37*, 911–917.

152. Indarti, E.; Majid, M. I. A.; Hashim, R.; Chong, A. Direct FAME synthesis for rapid total lipid analysis from fish oil and cod liver oil. *J. Food Compos. Anal.* **2005**, *18*, 161–170.

153. Dessì, M. A.; Deiana, M.; Day, B. W.; Rosa, A.; Banni, S.; Corongiu, F. P. Oxidative stability of

polyunsaturated fatty acids : effect of squalene * Research Paper. *Eur. J. Lipid Sci. Technol.* **2002**, *104*, 506–512.

154. Bubrick, P. Production of astaxanthin from Haematococcus. *Bioresour. Technol.* **1991**, *38*, 237–239.

155. Guerin, M. Haematococcus astaxanthin: applications for human health and nutrition. *Trends Biotechnol.* **2003**, *21*, 210–216.

156. Aliano, N. P.; Ellis, M. D. Oxalic acid: a prospective tool for reducing Varroa mite populations in package bees. *Exp. Appl. Acarol.* **2009**, *48*, 303–9.

157. Strasser, H.; Burgstaller, W.; Schinner, F. High-yield production of oxalic acid for metal leaching processes by Aspergillus niger. *FEMS Microbiol. Lett.* **1994**, *119*, 365–70.

158. Mathupala, S. P.; Ko, Y. H.; Pedersen, P. L. The pivotal roles of mitochondria in cancer: Warburg and beyond and encouraging prospects for effective therapies. *Biochim. Biophys. Acta* **2010**, *1797*, 1225–30.

159. Perkins, F. O. The ultrastructure of Holdfasts, "Rhizoids", and "Slime Tracks" in Thraustochytriaceous Fungi and Labyrinthyla spp. **1972**, *118*.

160. Kathiresan, K.; Saravanakumar, K.; Anburaj, R.; Gomathi, V.; Abirami, G.; Sahu, S. K.; Anandhan, S. MICROBIAL ENZYME ACTIVITY IN DECOMPOSING LEAVES OF MANGROVES. *bipublication.com* **2011**, *2*, 382–389.

161. Morita, E.; Kumon, Y.; Nakahara, T.; Kagiwada, S.; Noguchi, T. Docosahexaenoic acid production and lipid-body formation in Schizochytrium limacinum SR21. *Mar. Biotechnol.* **2006**, *8*, 319–327.

162. Ashford, a; Barclay, W. R.; Weaver, C. a; Giddings, T. H.; Zeller, S. Electron microscopy may reveal structure of docosahexaenoic acid-rich oil within Schizochytrium sp. *Lipids* **2000**, *35*, 1377–86.

163. Bongiorni, L.; Jain, R.; Raghukumar, S.; Aggarwal, R. K. Thraustochytrium gaertnerium sp. nov.: A new thraustochytrid stramenopilan protist from mangroves of Goa, India. *Protist* **2005**, *156*, 303–315.

164. Raghukumar, S. Bacterivory: a novel dual role for thraustochytrids in the sea. *Mar. Biol.* **1992**, *113*, 165–169.

165. Raghukumar, S.; Ramaiah, N.; Raghukumar, C. Dynamics of thraustochytrid protists in the water column of the Arabian Sea. *Aquat. Microb. Ecol.* **2001**, *24*, 175–186.

166. Rao, C. V; Newmark, H. L.; Reddy, B. S. Chemopreventive effect of squalene on colon cancer. *Carcinogenesis* **1998**, *19*, 287–90.

167. Fan, K. W.; Aki, T.; Chen, F.; Jiang, Y. Enhanced production of squalene in the thraustochytrid Aurantiochytrium mangrovei by medium optimization and treatment with terbinafine. *World J. Microbiol. Biotechnol.* **2010**, *26*, 1303–1309.

168. Chen, G.; Fan, K. W.; Lu, F. P.; Li, Q.; Aki, T.; Chen, F.; Jiang, Y. Optimization of nitrogen source for enhanced production of squalene from thraustochytrid Aurantiochytrium sp. *N. Biotechnol.* **2010**, *27*, 382–389.

169. Lewis, T. E.; Nichols, P. D.; McMeekin, T. a Sterol and squalene content of a docosahexaenoic-acid-producing thraustochytrid: influence of culture age, temperature, and dissolved oxygen. *Mar. Biotechnol. (NY).* **2001**, *3*, 439–47.

170. Mendes-Pinto, M. M.; Raposo, M. F. J.; Bowen, J.; Young, A. J.; Morais, R. Evaluation of different cell

disruption processes on encysted cells of Haematococcus pluvialis: Effects on astaxanthin recovery and implications for bio-availability. *J. Appl. Phycol.* **2001**, *13*, 19–24.

171. Yokoyama, R.; Salleh, B.; Honda, D. Taxonomic rearrangement of the genus Ulkenia sensu lato based on morphology, chemotaxonomical characteristics, and 18S rRNA gene phylogeny (Thraustochytriaceae, Labyrinthulomycetes): Emendation for Ulkenia and erection of Botryochytrium, Parietichytrium, . *Mycoscience* **2007**, *48*, 329–341.

172. Andersen, R. A. *Algal Culturing Techniques*; 2004.

173. Provasoli, L.; McLaughlin, J. J. a; Droop, M. R. The development of artificial media for marine algae. *Arch. f??r Mikrobiol.* **1957**, *25*, 392–428.

174. Allen, E. J.; Nelson, E. W. On the artificial culture of marine plankton organisms. **1910**.

175. Provasoli, L.; Pintner, I. J. Artificial media for freshwater algae: problems and suggestions. In *The Ecology of Algae. Tryon, C.A. & Hartman, R.T. [Eds.] Special Publication No. 2. Pymatuning Laboratory of Field Biol. University Pittsburgh*; 1959; pp. 84–96.

176. Allen, E. J. On the culture of the plankton diatom Thalassiosira gravida Cleve, in artificial sea-water. **1914**.

177. Vishniac, H. S. The nutritional requirements of isolates of Labyrinthula spp. *J. Gen. Microbiol.* **1955**, *12*, 455–463.

178. Starr, R. C.; Zeikus, J. A.; Zeikus, A.; Zeikus, J. A. The culture collection of algae at the university of Texas at Austin. *J. Phycol.* **1993**, *29*, 1–106.

179. Chen, G.; Fan, K.-W.; Lu, F.-P.; Li, Q.; Aki, T.; Chen, F.; Jiang, Y. Optimization of nitrogen source for enhanced production of squalene from thraustochytrid Aurantiochytrium sp. *N. Biotechnol.* **2010**, *27*, 382–389.

180. Wu, S.-T.; Yu, S.-T.; Lin, L.-P. Effect of culture conditions on docosahexaenoic acid production by Schizochytrium sp. S31. *Process Biochem.* **2005**, *40*, 3103–3108.

181. Hutner, S. . H. .; Provasoli, L. .; Schatz, A.; Haskins, C. . P. . Some Approaches to the Study of the Role of Metals in the Metabolism of Microorganisms. *Proc. Am. Philos. Soc.* **1950**, *94*, 152–170.

182. Loeblich, A. R. A seawater medium for dinoflagellates and the nutrition of cahonina niei. *J.Phycol.* **1975**, *11*, 80–86.

183. da Silva, G. P.; Mack, M.; Contiero, J. Glycerol: A promising and abundant carbon source for industrial microbiology. *Biotechnol. Adv.* **2009**, *27*, 30–39.

184. Qu, L.; Ji, X.-J.; Ren, L.-J.; Nie, Z.-K.; Feng, Y.; Wu, W.-J.; Ouyang, P.-K.; Huang, H. Enhancement of docosahexaenoic acid production by Schizochytrium sp. using a two-stage oxygen supply control strategy based on oxygen transfer coefficient. *Lett. Appl. Microbiol.* **2010**, *52*, 22–7.

185. Unagul, P.; Assantachai, C.; Phadungruengluij, S.; Suphantharika, M.; Tanticharoen, M.; Verduyn, C. Coconut water as a medium additive for the production of docosahexaenoic acid (C22:6 n3) by Schizochytrium mangrovei Sk-02. *Bioresour. Technol.* **2007**, *98*, 281–7.

186. Perveen, Z.; Ando, H.; Ueno, A.; Ito, Y.; Yamamoto, Y.; Yamada, Y.; Takagi, T.; Kaneko, T.; Kogame, K.; Okuyama, H. Isolation and characterization of a novel thraustochytrid-like microorganism that

efficiently produces docosahexaenoic acid. *Biotechnol. Lett.* **2006**, *28*, 197–202.

187. Yaguchi, T.; Tanaka, S.; Yokochi, T.; Nakahara, T.; Higashihara, T. Production of high yields of docosahexaenoic acid by Schizochytrium sp. strain SR21. *J. Am. Oil Chem. Soc.* **1997**, *74*, 1431–1434.

188. Abad, S.; Turon, X. Biotechnological production of docosahexaenoic acid using aurantiochytrium limacinum: Carbon sources comparison and growth characterization. *Mar. Drugs* **2015**, *13*, 7275–7284.

189. Huang, T. Y.; Lu, W. C.; Chu, I. M. A fermentation strategy for producing docosahexaenoic acid in Aurantiochytrium limacinum SR21 and increasing C22:6 proportions in total fatty acid. *Bioresour. Technol.* **2012**, *123*, 8–14.

190. Zhou, L.; Lu, Y.; Zhou, M.; Zhao, X. Enhanced production of docosahexaenoic acid using Schizochytrium sp. by optimization of medium components. *J. Chem. Eng. Japan* **2007**, *40*, 1093–1100.

191. Song, X.; Zhang, X.; Kuang, C.; Zhu, L.; Guo, N. Optimization of fermentation parameters for the biomass and DHA production of Schizochytrium limacinum OUC88 using response surface methodology. *Process Biochem.* **2007**, *42*, 1391–1397.

192. Kim, K.; Jung Kim, E.; Ryu, B.-G.; Park, S.; Choi, Y.-E.; Yang, J.-W. A novel fed-batch process based on the biology of Aurantiochytrium sp. KRS101 for the production of biodiesel and docosahexaenoic acid. *Bioresour. Technol.* **2012**, *135*, 269–274.

193. Chaung, K.-C.; Chu, C.-Y.; Su, Y.-M.; Chen, Y.-M. Effect of culture conditions on growth, lipid content, and fatty acid composition of Aurantiochytrium mangrovei strain BL10. *AMB Express* **2012**, *2*, 42.

194. Shabala, L.; McMeekin, T.; Shabala, S. Thraustochytrids Can Be Grown in Low-Salt Media Without Affecting PUFA Production. *Mar. Biotechnol. (NY).* **2013**.

195. Zhu, L.; Zhang, X.; Ren, X.; Zhu, Q. Effects of culture conditions on growth and docosahexaenoic acid production from Schizochytrium limacinum. *J. Ocean Univ. China* **2008**, *7*, 83–88.

196. Wethered, J. M.; Jennings, D. H. Major solutes contributing to solute potential of Thraustochytrium aureum and T. roseum after growth in media of different salinities. *Trans. Br. Mycol. Soc.* **1985**, *85*, 439–446.

197. Nagano, N.; Taoka, Y.; Honda, D.; Hayashi, M. Optimization of culture conditions for growth and docosahexaenoic acid production by a marine thraustochytrid, Aurantiochytrium limacinum mh0186. *J. Oleo Sci.* **2009**, *58*, 623–8.

198. Shuler, M. L.; Kargi, F. *Bioprocess Engineering: Basic Concepts*; 2006.

199. Tchobanoglous, G.; Burton, F. L.; Stensel, H. D. *Wastewater Engineering, Treatment, and Reuse*; 2003.

200. Chi, Z.; Liu, Y.; Frear, C.; Chen, S. Study of a two-stage growth of DHA-producing marine algae Schizochytrium limacinum SR21 with shifting dissolved oxygen level. *Appl. Microbiol. Biotechnol.* **2009**, *81*, 1141–8.

201. Prabu, R. Effect of sodium sulphate salinity for production of docosahexaenoic acid (DHA) by Thraustochytrids aureum RAK-21. *Asian Biomed. (Research Rev. …* **2012**, *6*, 693–701.

202. Qu, L.; Ren, L.-J.; Sun, G.-N.; Ji, X.-J.; Nie, Z.-K.; Huang, H. Batch, fed-batch and repeated fed-batch

fermentation processes of the marine thraustochytrid Schizochytrium sp. for producing docosahexaenoic acid. *Bioprocess Biosyst. Eng.* **2013**.

203. Ren, L.-J.; Ji, X.-J.; Huang, H.; Qu, L.; Feng, Y.; Tong, Q.-Q.; Ouyang, P.-K. Development of a stepwise aeration control strategy for efficient docosahexaenoic acid production by Schizochytrium sp. *Appl. Microbiol. Biotechnol.* **2010**, *87*, 1649–1656.

204. Ren, L.-J.; Feng, Y.; Li, J.; Qu, L.; Huang, H. Impact of phosphate concentration on docosahexaenoic acid production and related enzyme activities in fermentation of Schizochytrium sp. *Bioprocess Biosyst. Eng.* **2012**.

205. Ren, L. J.; Sun, G. nan; Ji, X. J.; Hu, X. chao; Huang, H. Compositional shift in lipid fractions during lipid accumulation and turnover in Schizochytrium sp. *Bioresour. Technol.* **2014**, *157*, 107–113.

206. Ganuza, E.; Anderson, a J.; Ratledge, C. High-cell-density cultivation of Schizochytrium sp. in an ammonium/pH-auxostat fed-batch system. *Biotechnol. Lett.* **2008**, *30*, 1559–64.

207. Hong, W.-K.; Rairakhwada, D.; Seo, P.-S.; Park, S.-Y.; Hur, B.-K.; Kim, C. H.; Seo, J.-W. Production of lipids containing high levels of docosahexaenoic acid by a newly isolated microalga, Aurantiochytrium sp. KRS101. *Appl. Biochem. Biotechnol.* **2011**, *164*, 1468–80.

208. Chang, K. J. L.; Dumsday, G.; Nichols, P. D.; Dunstan, G. A.; Blackburn, S. I.; Koutoulis, A. High cell density cultivation of a novel Aurantiochytrium sp. strain TC 20 in a fed-batch system using glycerol to produce feedstock for biodiesel and omega-3 oils. *Appl. Microbiol. Biotechnol.* **2013**, *97*, 6907–6918.

209. Taoka, Y.; Nagano, N.; Okita, Y.; Izumida, H.; Sugimoto, S.; Hayashi, M. Influences of culture temperature on the growth, lipid content and fatty acid composition of Aurantiochytrium sp. Strain mh0186. *Mar. Biotechnol. (NY).* **2009**, *11*, 368–74.

210. Arafiles, K.; Alcantara, J.; Batoon, J. Cultural optimization of thraustochytrids for biomass and fatty acid production. … **2011**, 521–531.

211. Taoka, Y.; Nagano, N.; Okita, Y.; Izumida, H.; Sugimoto, S.; Hayashi, M. Effects of cold shock treatment on total lipid content and fatty acid composition of Aurantiochytrium limacinum strain mh0186. *J. Oleo Sci.* **2011**, *60*, 217–20.

212. Li, J.; Ren, L.-J.; Sun, G.-N.; Qu, L.; Huang, H. Comparative metabolomics analysis of docosahexaenoic acid fermentation processes by Schizochytrium sp. under different oxygen availability conditions. *OMICS* **2013**, *17*, 269–81.

213. Ganuza, E.; Izquierdo, M. S. Lipid accumulation in Schizochytrium G13/2S produced in continuous culture. *Appl. Microbiol. Biotechnol.* **2007**, *76*, 985–990.

214. Yokochi, T. Novel microorganisms capable of producing highly unsaturated fatty acids and process for producing highly unsaturated fatty acids by using the microorganisms. *WO Pat. 96/33263* **1996**, 32.

215. Olaizola, M. Commercial production of astaxanthin from Haematococcus pluvialis using 25,000-liter outdoor photobioreactors. *J. Appl. Phycol.* **2000**, *12*, 499–506.

216. Borowitzka, M. a.; Huisman, J. M.; Osborn, A. Culture of the astaxanthin-producing green algaHaematococcus pluvialis 1. Effects of nutrients on growth and cell type. *J. Appl. Phycol.* **1991**, *3*, 295–304.

217. Kobayashi, M. In vivo antioxidant role of astaxanthin under oxidative stress in the green alga

Haematococcus pluvialis. *Appl. Microbiol. Biotechnol.* **2000**, *54*, 550–5.

218. Benefits, H.; Methods, P. Health Benefits and Production Methods of Natural Astaxanthin.

219. Yamasaki, T.; Aki, T.; Shinozaki, M.; Taguchi, M.; Kawamoto, S.; Ono, K. Utilization of Shochu distillery wastewater for production of polyunsaturated fatty acids and xanthophylls using thraustochytrid. *J. Biosci. Bioeng.* **2006**, *102*, 323–7.

220. Hong, W.-K.; Yu, A.; Heo, S.-Y.; Oh, B.-R.; Kim, C. H.; Sohn, J.-H.; Yang, J.-W.; Kondo, A.; Seo, J.-W. Production of lipids containing high levels of docosahexaenoic acid from empty palm fruit bunches by Aurantiochytrium sp. KRS101. *Bioprocess Biosyst. Eng.* **2013**, *36*, 959–63.

221. Li, J.; Liu, R.; Chang, G.; Li, X.; Chang, M.; Liu, Y.; Jin, Q.; Wang, X. A strategy for the highly efficient production of docosahexaenoic acid by Aurantiochytrium limacinum SR21 using glucose and glycerol as the mixed carbon sources. *Bioresour. Technol.* **2015**, *177*, 51–57.

222. Buchgraber, M.; Ulberth, F.; Emons, H.; Anklam, E. Triacylglycerol profiling by using chromatographic techniques. *Eur. J. Lipid Sci. Technol.* **2004**, *106*, 621–648.

223. Fauconnot, L.; Hau, J.; Aeschlimann, J.-M.; Fay, L.-B.; Dionisi, F. Quantitative analysis of triacylglycerol regioisomers in fats and oils using reversed-phase high-performance liquid chromatography and atmospheric pressure chemical ionization mass spectrometry. *Rapid Commun. Mass Spectrom.* **2004**, *18*, 218–24.

224. Jessop, P. G.; Phan, L.; Carrier, A.; Robinson, S.; Dürr, C. J.; Harjani, J. R. A solvent having switchable hydrophilicity. *Green Chem.* **2010**, *12*, 809.

225. Hellweg, S.; Fischer, U.; Scheringer, M.; Hungerb hler, K. Environmental assessment of chemicals: methods and application to a case study of organic solvents. *Green Chem.* **2004**, *6*, 418.

226. Chemat, F.; Vian, M. A.; Cravotto, G. Green extraction of natural products: Concept and principles. *Int. J. Mol. Sci.* 2012, *13*, 8615–8627.

227. Capello, C.; Fischer, U.; Hungerbühler, K. What is a green solvent? A comprehensive framework for the environmental assessment of solvents. *Green Chem.* **2007**, *9*, 927.

228. Roy, R. *A primer on the Taguchi Method*; 2010.

229. Gross, M.; Klein, S. Fish Oil Triglycerides vs . Ethyl Esters. **2009**.

230. Nordøy, A.; Barstad, L.; Connor, W. E.; Hatcher, L. Absorption of the n-3 eicosapentaenoic and docosahexaenoic acids as ethyl esters and triglycerides by humans. *Am. J. Clin. Nutr.* **1991**, *53*, 1185–1190.

231. BHAGAT, P. An introduction to neural nets. *Chem. Eng. Prog. 86*, 55–60.

232. Moss, G. P.; Smith, P. a S.; Tavernier, D. Glossary of Class Names of Organic Compounds and Reactive Intermediates Based on Structure. *Pure Appl. Chem.* **1995**, *67*, 1307–1375.

233. Wallis, J. G.; Watts, J. L.; Browse, J. Polyunsaturated fatty acid synthesis: What will they think of next? *Trends Biochem. Sci.* **2002**, *27*, 467–473.

234. Hester, R. .; Harisson, R. M. Chlorinated Organic Micropollutants. *R. Soc. Chem.* **1996**, 56–59.

235. Harun, R.; Singh, M.; Forde, G. M.; Danquah, M. K. Bioprocess engineering of microalgae to produce

a variety of consumer products. *Renew. Sustain. Energy Rev.* **2010**, *14*, 1037–1047.

236. Riisberg, I.; Orr, R. J. S.; Kluge, R.; Shalchian-Tabrizi, K.; Bowers, H. A.; Patil, V.; Edvardsen, B.; Jakobsen, K. S. Seven Gene Phylogeny of Heterokonts. *Protist* **2009**, *160*, 191–204.

237. Cavalier-Smith, T.; Allsopp, M. T. E. P.; Chao, E. E. Thraustochytrids are chromists, not Fungi: 18s rRNA signatures of Heterokonta. *Philos. Trans. R. Soc. B Biol. Sci.* **1994**, *346*, 387–397.

238. Mo, C.; Douek, J.; Rinkevich, B.; J., D.; B., R. Development of a PCR strategy for thraustochytrid identification based on 18S rDNA sequence. *Mar. Biol.* **2002**, *140*, 883–889.

239. Fischer, E.; Speier, A. Darstellung der ester. *Berichte der Dtsch. Chem. Gesellschaft* **1895**, *10*, 3252–3258.

240. Lee, Y. K. Bioprocess Technology. **2006**, 23–71.

241. Liu, S. *Bioprocess Engineering: Kinetics, Biosystems, Sustainability, and Reactor Design*; 2012.